Identification and characterisation of MOB proteins as regulators of innate immunity in *Arabidopsis thaliana*

Jeoffrey George

Thesis submitted to the University of East Anglia for the degree of Doctor of Philosophy

The Sainsbury Laboratory
John Innes Centre
Norwich, United Kingdom

September, 2020

Abstract

Cell-surface pattern recognition receptors sense invading pathogens by perceiving elicitors such as microbial patterns, and activate innate immunity. These responses are often under tight control to avoid excessive or untimely activation of cellular responses, which may otherwise be detrimental to host cells, but how this fine-tuning is accomplished remains mostly unknown. A forward genetics suppressor screen was performed to identify *Arabidopsis thaliana* mutants that regained immune signalling in the immunodeficient genetic background *bak1-5*. This screen led to the identification of 10 *modifier of bak1-5* (*mob*) mutants. Here, I report that *bak1-5 mob7*, *8*, *9* and *10* restore elicitor-induced signalling, with some specificities in their responses to the different elicitors tested. Through map-based cloning and next-generation mapping, the *mob7* causative mutation was mapped to the gene *CONSERVED BINDING OF EIF4E1* (*CBE1*) encoding a plant-specific RNA-binding protein (RBP). CBE1 represents a novel RBP involved in immune signalling, regulating elicitor-induced reactive oxygen species production potentially by controlling the protein level of the NADPH oxidase RESPIRATORY BURST OXIDASE HOMOLOG D. Furthermore, various mRNA decapping and translation initiation factors co-localised with CBE1 and regulate immune signalling, similarly as CBE1. The results of this project led to the current working model in which, by analogy to mammalian translational regulation, CBE1 acts as a translation repressor within processing-bodies by controlling mRNA turnover. This study thus identified a novel regulator of immune signalling and provides new insights into the regulation of translation in plants.

List of contents

List of figures

List of tables

Abbreviations

4E-BP	EIF4E-BINDING PROTEIN
4E-BS	EIF4E-BINDING SITE
4E-HP	4E HOMOLOGOUS PROTEIN
4E-T	EIF4E-TRANSPORTER
ABA	Abscisic acid
ABI1	ABA-INSENSITIVE 1
ACS	1-AMINOCYCLOPROPANE-1-CARBOXYLIC ACID SYNTHASE
ADF	ACTIN DEPOLYMERIZING FACTOR
AGGIE	ARABIDOPSIS GENES GOVERNING IMMUNE GENE EXPRESSION
AHA	H(+)-ATPASE
ANX	ANXUR
Arabidopsis	*Arabidopsis thaliana*
AS	Alternative splicing
ASR3	ARABIDOPSIS SH4-RELATED3
Avr	Avirulence protein
BAK1	BRI1-ASSOCIATED KINASE 1
BES1	BRI1-EMS-SUPPRESSOR 1
bHLH	Basic helix-loop-helix
BIK1	BOTRYTIS-INDUCED KINASE 1
BIR	BAK1-INTERACTING RECEPTOR-LIKE KINASE
BKK1	BAK1-LIKE 1
BR	Brassinosteroid
BRI1	BRASSINOSTEROID INSENSITIVE 1
BSA	Bovine serum albumin
BSK	BRASSINOSTEROID-SIGNALING KINASE
bZIP	Basic leucine zipper domain
BZR1	BRASSINAZOLE-RESISTANT 1
CAD1	CONSTITUTIVE ACTIVE CELL DEATH 1
CALS8	CALLOSE SYNTHASE 8
CaM	Calmodulin
CAMTA	CAM-BINDING TRANSCRIPTION ACTIVATOR
CaMV	Cauliflower mosaic virus
CAPE1	CAP-DERIVED PEPTIDE 1
CAPS	Cleaved amplified Polymorphic Sequences
CASPL	CASPARIAN STRIP MEMBRANE DOMAIN PROTEIN(CASP)-LIKE PROTEIN
CBB	Coomassie brilliant blue
CBC	Cap-binding complex
CBE1	CONSERVED BINDING OF EIF4E1
CBP	CAP BINDING PROTEIN
CBP60G	CAM-BINDING PROTEIN 60-LIKE G
CC	COILED-COIL
CCE	CHANGED CALCIUM ELEVATION
CCR4-NOT	CARBON CATABOLITE REPRESSOR4-NEGATIVE ON TATA
CDKC	CYCLIN –DEPENDENT KINASE C
cDNA	complementary DNA

CDPK	CALCIUM-DEPENDENT PROTEIN KINASE
CEBiP	CHITIN OLIGOSACCHARIDE ELICITOR-BINDING PROTEIN
CERK1	CHITIN ELICITOR RECEPTOR KINASE 1
CFU	Colony Forming Unit
CIPK	CALCINEURIN B-LIKE KINASE
CIPP1	CERK1-INTERACTING PROTEIN PHOSPHATASE 1
CML	CALMODULIN-LIKE PROTEIN
CMV	Cucumber mosaic virus
CNGC	CYCLIC NUCLEOTIDE-GATED CHANNEL
CNL	CC-NLR
Col-0	Columbia-0
COR	Coronatine
CPK	CALCIUM-DEPENDENT KINASE
CPL	CTD PHOSPHATASE-LIKE
CRK	CYSTEINE-RICH RLK
CrRLK1L	*Catharanthus roseus* RLK1-like
CTD	C-terminal domain
CUM1	CUCUMO- VIRUS MULTIPLICATION 1
Da	Dalton(s)
DAG	Diacylglycerol
dCAPS	derived CAPS
DCP1	DECAPPING PROTEIN 1
DDX6	DEAD BOX PROTEIN6
DGK	Diacylglycerol kinase
DGPP	Diacylglycerol pyrophosphate
DNA	Deoxyribonucleic acid
dNTP	Deoxynucleoside triphosphate
DORN1	DOES NOT RESPOND TO NUCLEOTIDES 1
dpi	Days post-infiltration/inoculation
DRP2B	DYNAMIN RELATED PROTEIN 2B
DTT	Dithiothreitol
DUF	DOMAIN OF UNKNOWN FUNCTION
DUSP	Dual-specificity protein phosphatases
EDS1	ENHANCED DISEASE SUSCEPTIBILITY 1
EFR	EF-TU RECEPTOR
EF-Tu	Elongation factor Tu
EGF	Epidermal growth factor
EIF	EUKARYOTIC TRANSLATION INITIATION FACTOR
EIF(ISO)	Isoform of EIF
EIN	ETHYLENE INSENSITIVE
EIX	ETHYLENE-INDUCING XYLANASE
elf18	18 amino acid peptide derived from Escherichia coli
ELFIN	ELF18-INSENSITIVE
EMS	Ethyl methanesulfonate
EPS1	EPSIN1
ER	Endoplasmic reticulum /ERECTA
ERF	ETHYLENE-RESPONSIVE FACTOR
ERL1	ER-LIKE1
ET	Ethylene

ETR	ETHYLENE RESPONSE
FER	FERONIA
FIB2	FIBRILLARIN 2
FIN	FLG22-INSENSITIVE
FIR	FLS2-INTERACTING FACTOR
flg22	22 amino acid peptide derived from Pseudomonas aeruginosa
FLS2	FLAGELLIN-SENSING 2
FRK1	FLG22-INDUCED RECEPTOR-LIKE KINASE
F_x	Refers to the X generation following crosses between two different genotypes
GA	Gibberellic acid
GFP	GREEN FLUORESCENT PROTEIN
GPI	Glycosylphosphatidylinositol
GRP7	GLYCINE-RICH RNA-BINDING PROTEIN 7
HAE	HAESA
HAK5	HIGH-AFFINITY K(+) TRANSPORTER 5
HBI1	HOMOLOG OF BEE2 INTERACTING WITH IBH1
HMGB	HIGH MOBILITY GROUP BOX
HPCA1	HYDROGEN-PEROXIDE-INDUCED Ca2+ INCREASES 1
HR	Hypersensitive Response
HRP	Horseradish peroxidase
HSL2	HAE-LIKE2
ICS1	ISOCHORISMATE SYNTHASE 1
ILK1	INTEGRIN-LINKED KINASE 1
InDel	Insertion/deletion marker
IOS1	IMPAIRED OOMYCETE SUSCEPTIBILITY 1
IP	Immunoprecipitate
IRR	IMMUNOREGULATORY RNA-BINDING PROTEIN
JA	Jasmonic acid
KAPP	KINASE-ASSOCIATED PROTEIN PHOSPHATASE
KUODA1	KUA1
La*er*	Landsberg *erecta*
LLG	LORELEI-LIKE-GPI-ANCHORED PROTEIN
LPS	Lipopolysaccharides
LRR	Leucine-rich repeat
LYK	LYSM-CONTAINING RECEPTOR-LIKE KINASE
LYM	LYSM DOMAIN- CONTAINING GPI-ANCHORED PROTEIN
LYP	LYSM-CONTAINING RECEPTOR PROTEIN
LysM	Lysine motif
MAMP	MICROBE-ASSOCIATED MOLECULAR PATTERN
MAPK	MITOGEN-ACTIVATED PROTEIN KINASE
MC	METACASPASE
MEKK	MAPKK-KINASE
miRNA	micro RNA
MKK	MAPK KINASE
MKP	MAPK PHOSPHATASE
MKS1	MAPK SUBSTRATE1
MOB	MODIFIER OF BAK1-5
mRNA	messengerRNA

mRNP	mRNA ribonucleoprotein
MS	Mass spectrometry / Murashige and Skoog
MT	Microtubule
MTSF1	MITOCHONDRIAL STABILITY FACTOR 1
MVQ	MPK3/MPK6-TARGETED VQ-MOTIF-CONTAINING PROTEIN
M_x	refers to the X generation following EMS mutagenesis
NAC	NAM, ATAF and CUC
NAD(P)	Nicotinamide adenine dinucleotide (phosphate)
NDR1	NON-RACE-SPECIFIC DISEASE RESISTANCE 1
NF-Y	NUCLEAR FACTOR Y
NGD	No-go decay
NGM	Next-generation EMS mutation mapping
NIK	NUCLEAR-SHUTTLE PROTEIN-INTERACTING KINASES
NIS	NECROSIS-INDUCING SECRETED PROTEIN
NLP	NEP1-LIKE PROTEIN
NLR	Nucleotide-binding domain leucine-rich repeat
NLS	Nuclear localisation sequence
NMD	Nonsense-mediated RNA decay
NO	Nitric oxide
NOS	NO SYNTHASE
NSD	Non-stop decay
OD	Optical density
OG	Oligogalacturonides
OST1	OPEN STOMATA 1
PA	Phosphatidic acid
PAB2	POLY(A) BINDING PROTEIN 2
PAD4	PHYTOALEXIN-DEFICIENT 4
PAMP	Pathogen-associated molecular pattern
PARG	PAR GLYCOSYLHYDROLASES
PARN	POLY(A) RIBONUCLEASE
Parylation	poly(ADP-ribosyl)ation
PAT1	ARABIDOPSIS HOMOLOG OF YEAST PAT1
PATL1	PAT1-LIKE PROTEIN 1
PBL	PBS1-LIKE
p-bodies	processing-bodies
PCC	Pearson's correlation coefficient
PCD	Programmed cell death
PCR	Polymerase Chain Reaction
PCRK	PTI COMPROMISED RECEPTOR-LIKE CYTOPLASMIC KINASE
PD	Plasmodesmata
PDLP	PD-LOCATED PROTEIN
PEP	PLANT ELICITOR PEPTIDE
PEPR	PEP-RECEPTOR
PGN	Peptidoglycan
PIF	PHYTOCHROME INTERACTING FACTOR
PIP	PAMP-INDUCED PEPTIDE
PIRE	PBL13-INTERACTING RING-TYPE E3 UBIQUITIN LIGASE
PLC	PHOSPHOLIPASE C

PLL	POLTERGEIST-LIKE
PM	Plasma membrane
PMR	POWDERY MILDEW RESISTANT
PMSF	Phenylmethylsulfonyl fluoride
POX	PEROXIDASE
PP2C	PROTEIN PHOSPHATASES TYPE 2C
PPT	Phosphinothricin
PR	PATHOGENESIS-RELATED
PRR	Pattern-recognition receptor
PSK	Phytosulfokines
PSKR	PSK RECEPTOR
PSL	PRIORITY IN SWEET LIFE
PTI	PRR-triggered immunity
Pto	*Pseudomonas syringae* pathovar *tomato*
PTP	PROTEIN- TYROSINE-PHOSPHATASE
PUB	PLANT U-BOX
PVDF	Polyvinyldifluoride
R	Resistance
RALF	RAPID ALKALINIZATION FACTOR
RBOH	RESPIRATORY BURST OXIDASE HOMOLOG
RBP	RNA-BINDING PROTEIN
RFP	RED FLUORESCENT PROTEIN
RGS1	REGULATOR OF G PROTEIN SIGNALLING PROTEIN 1
RH	RNA HELICASE
RHA3	RING-H2 FINGER A3
RIP	Ribosome-inactivating proteins
RK	Receptor kinase
RLCK	Receptor-like cytoplasmic kinase
RLP	RECEPTOR-LIKE PROTEIN
RLU	Relative Light Units
RNA	Ribonucleic acid
RNAPII	RNA POLYMERASE II
ROI	Region of interest
ROS	Reactive oxygen species
RPL	RIBOSOMAL PROTEIN L
RPM1	RESISTANCE TO P. SYRINGAE PV MACULICOLA 1
RPP1	RECOGNITION OF PERONOSPORA PARASITICA 1
RPS	RESISTANT TO P. SYRINGAE
RRS1	RESISTANT TO RALSTONIA SOLANACEARUM 1
RT-qPCR	Real-time-quantitative PCR
S1P	SITE-1 PROTEASE
SA	Salicylic acid
SAG101	SENESCENCE-ASSOCIATED GENE 101
SARD1	SAR DEFICIENT 1
SCOOP	SERINE-RICH ENDOGENOUS PEPTIDE
SDS	Sodium dodecyl sulfate
SERK	SOMATIC EMBRYOGENESIS RELATED KINASE
SFI5	SUPPRESSOR OF EARLY FLG22-INDUCED IMMUNE RESPONSE 5

SG	Stress granules
SGI	Seedling growth inhibition
SIF	STRESS INDUCED FACTOR
SIK1	SERINE-THREONINE KINASE 1
siRNA	Small interfering RNA
SLAC	SLOW ANION CHANNEL
SLAH	SLAC1 HOMOLOG
SNC	SUPPRESSOR OF NPR1-1, CONSTITUTIVE
SNP	Single nucleotide polymorphism
SOBIR1	SUPPRESSOR OF BIR1 1
SPL	SQUAMOSA PROMOTER BINDING PROTEIN-LIKE
SR45	SERINE/ARGININE-RICH 45
SSLP	Simple sequence length polymorphisms
SUMM2	SUPPRESSOR OF MKK1 MKK2
SYR1	SYSTEMIN RECEPTPOR 1
TBS	Tris-buffered saline
TBST	TBS Tween
TCV	Turnip crinkle virus
TF	Transcription factor
TGN	Trans-Golgi network
TIR	TOLL-INTERLEUKIN 1 RECEPTOR
TLR	TOLL-LIKE RECEPTOR
TM	Transmembrane
TNL	TIR-NLR
TNRC6B	TRINUCLEOTIDE REPEAT- CONTAINING GENE 6B
TOE	TARGET OF EARLY ACTIVATION TAGGED
TOR	TARGET OF RAPAMYCIN
TRAP	Translating Ribosome Affinity Purification
T_x	Refers to the X generation following Agrobacterium transformation
TZF9	TANDEM ZINC FINGER PROTEIN 9
UBI10 / UBQ10	UBIQUITIN 10
UBP	OLIGOURIDYLATE-BINDING PROTEIN
UPF	UP-FRAMESHIFT
v/v	Volume per volume
VAP1	VENOM ALLERGEN-LIKE PROTEIN 1
VCS	VARICOSE
w/v	weight per volume
WAK	WALL-ASSOCIATED KINASE
WB	Western blotting
wpg	Weeks post-germination
WT	Wild-type
XB	XA21-mediated immune responses
XLG2	EXTRA-LARGE GTP-BINDING PROTEIN 2
XRN4	EXORIBONUCLEASE 4
YFP	Yellow Fluorescent protein
ZAR1	HOPZ-ACTIVATED RESISTANCE 1

Acknowledgments

First, I would like to thank my main supervisor Cyril Zipfel for giving me this opportunity and for his supports and guidance throughout the years. Thank you as well for having made possible the move to Zürich, it has been an enriching scientific journey. I am also very grateful to my other PhD committee members Jonathan Jones and Martin Stegmann for their valued insights on the project. Thanks to Marta Bjornson, Julien Gronnier, Jack Rhodes and Cyril Zipfel for proof-reading my thesis but also for being always present to discuss ideas. I want to thank as well Martin Stegmann and Jacqueline Monaghan for initiating the project and the *mob* screen. It has been a real pleasure to work on the *mob* mutants, which led me to new topics of interest. I want to thank as well all the support and facilities associated with TSL and IPMB.

I am very grateful to my friends Sebastian Pfeilmeier, Jack Rhodes and Julien Gronnier but also Alicia Abarca Cifuentes, Henning Mühlenbeck and Laura Herold that I met during these years. We have shared great moments together that I will not forget.
I want to thank as well, all other past and current members of CZL, especially Florian, Freddy, Isabel, Kathrin, Kyle, Maria, Marta, Philipp, Priya and Tamaryn. It has been very fun and enriching to work with you. I also want to thank specific people I met during my time in Norwich and Zürich, particularly Anna, Azhara, Baptiste, Bruno, Cécilia, Erin, Helen, Jan, Janina, Joanna, Michele, Ola, Sam and Yan. You made my life in Norwich and Zürich very enjoyable. Thanks to Adrien Demilly, Gautier Jacquinet and Laure Ginger for always being present and supportive.

I want to give my special thanks to Lucie Rackelboom for her support and I am grateful for the concessions she made in order to be part of my journey in Norwich and now in Switzerland.

Lastly, I thank my family and especially my parents and my brothers for being always present and having visited me during this time.

1. Introduction

1.1. Plants and microbes

Plants live in constant contact with a myriad of microorganisms, known as the microbiome. The microbiome is composed of fungi, bacteria, oomycetes, and archaea that can be either pathogenic or beneficial for plant health and fitness (Müller et al., 2016). Beneficial associations can be either mutualistic, generally termed symbiosis, where organisms benefit from each other, or commensalistic in which one benefits without affecting the other. In the case of detrimental associations, one organism benefits at the expense of another. Interestingly, beneficial microbes can protect plants against pathogens, through antagonism and competition or by stimulating the plant's immune system (Pieterse et al., 2014; Schlaeppi and Bulgarelli, 2015; Zipfel and Oldroyd, 2017). Well-studied examples of beneficial microbes include rhizobial bacteria living in symbiosis with legumes and mycorrhizal fungi associated with most terrestrial plants (Smith and Smith, 2011; Udvardi and Poole, 2013). Plants can recognise microbial molecules, which ultimately leads to symbiosis or immunity (Zipfel and Oldroyd, 2017). The restriction of invading organisms is governed by a passive and active defence, which is effective against all types of plant pathogens and pests, including viruses, insects, nematodes and even parasitic plants (Gust et al., 2017).

1.2. Preformed defences in plants

1.2.1. Mechanical defences

To prevent pathogen attachment or penetration, plant tissues are reinforced with structural barriers. Plant cells are surrounded by a rigid layer, the cell wall, composed of cellulose, hemicellulose, and pectin, which provides some protection against microbes (Hückelhoven, 2007; Houston et al., 2016). Often, other polymers such as lignin, suberin or cutin are anchored to or embedded in plant cell walls. Lignin is a polymer of phenolic compounds, and provides rigidity to cells, forming a primary component in wood. Besides, cutin, suberin and waxes create fatty deposits in cell walls (Schreiber, 2010), preventing pathogens from contacting the epidermis (Reina-Pinto and Yephremov, 2009). Whilst the mechanical defence provided by the cell wall is preformed, it can be actively modified in response to microbial perception. For example, reactive oxygen species (ROS) released in response to pathogen perception catalyse cross-linking of cell wall polymers strengthening this barrier (Passardi et al., 2004).

1.2.2. Chemical defences

Plants rely heavily on chemical defences to protect themselves against microbial and herbivore attacks (Chezem and Clay, 2016). These compounds are either phytoanticipins, which are preformed antimicrobial compounds or phytoalexins, which are antimicrobial compounds produced by plants in

response to biotic and abiotic stresses (VanEtten et al., 1994). Phytoanticipins include mostly saponins, cyanogenic glycosides, glucosinolates, phenols, phenolic glycosides, unsaturated lactones and sulfur compounds. Phytoanticipins can accumulate in dead cells or are excreted into the external environment (*e.g.* rhizosphere) or may be stored in vacuoles in an inactive form (Tiku, 2020).

1.3. The immune system

In comparison to animals, plants do not have a circulating immune system and, as such, each cell has to be able to respond independently against pathogenic microorganisms. These responses are related to the innate immune system in animals (Ausubel, 2005); however, plants deploy an expanded recognition repertoire to compensate for their lack of an adaptive immune system (Cui et al., 2015; Boutrot and Zipfel, 2017). Plants possess two strategies to detect pathogens (Figure 1.1) (Chisholm et al., 2006; Jones and Dangl, 2006). On the external surface of the plant cell, conserved microbial elicitors called pathogen- or microbe-associated molecular patterns (PAMPs/MAMPs; hereafter, referred to as PAMPs) are recognised by receptor proteins called pattern recognition receptors (PRRs) (Boller and Felix, 2009; Boutrot and Zipfel, 2017). PAMPs are typically important components of whole classes of microbes, such as bacterial flagellin or fungal chitin. PRRs can also recognise endogenous molecules released during pathogen invasions, such as cell wall or cuticular fragments. Stimulation of PRRs leads to PRR-triggered immunity (alternately known as PAMP-, pattern-triggered immunity; PTI; surface immunity) (Boutrot and Zipfel, 2017; Hou et al., 2019). Pathogens can secrete effector proteins into the host apoplast and cytoplasm to interfere with recognition and immune signalling (Cui et al., 2015). However, in resistant plants, these effectors are often recognised by intracellular nucleotide-binding domain leucine-rich repeat (NLR)-type immune sensors, leading to NLR-triggered immunity (NTI; also known as intracellular immunity) (Cui et al., 2015). Traditionally, plant immunity has been described in terms of PTI or effector-triggered immunity (ETI); nevertheless, PTI and ETI share signalling components and responses; thus it is more accurate to define plant immunity based on the receptors involved (Win et al., 2012; Wang et al., 2019d). Generally, NTI involves a form of localised cell death called the hypersensitive response (HR) (Win et al., 2012; Cui et al., 2015) but several PAMPs (*e.g.* bacterial flagellin and oomycete elicitins) can also induce HR (Ricci et al., 1989; Taguchi et al., 2003). In comparison to PAMPs, effectors are characteristically variable and dispensable for microbes (Win et al., 2012). Historically, effectors were also known as avirulence proteins (Avr), because when they are recognised by an NLR encoded by a specific resistance (R) gene, NTI leads to a loss of pathogen virulence. This interaction has been characterised as race-specific gene-for-gene resistance (Flor, 1942; Flor, 1971). The mode of pathogen recognition by plants leads to co-evolutionary dynamics between the plant and pathogen (Thompson and Burdon, 1992). As a result, there is an extreme diversification of NTI receptors and pathogen effectors both within and between species, whereas PRR functions are

generally conserved widely across families (Dievart et al., 2020; Tamborski and Krasileva, 2020). However, it is now clear that specific patterns/epitopes recognised as PAMPs within otherwise conserved molecules are under selective pressure and are thus more polymorphic than previously thought (Cook, Hughes and Morris, 2015). PTI is generally effective against non-adapted pathogens in a phenomenon called non-host resistance whereas NTI is active against adapted pathogens (Boller and Felix, 2009; Win et al., 2012; Böhm et al., 2014; Couto and Zipfel, 2016). However, these relationships are not exclusive and depend on the elicitor molecules present in each infection.

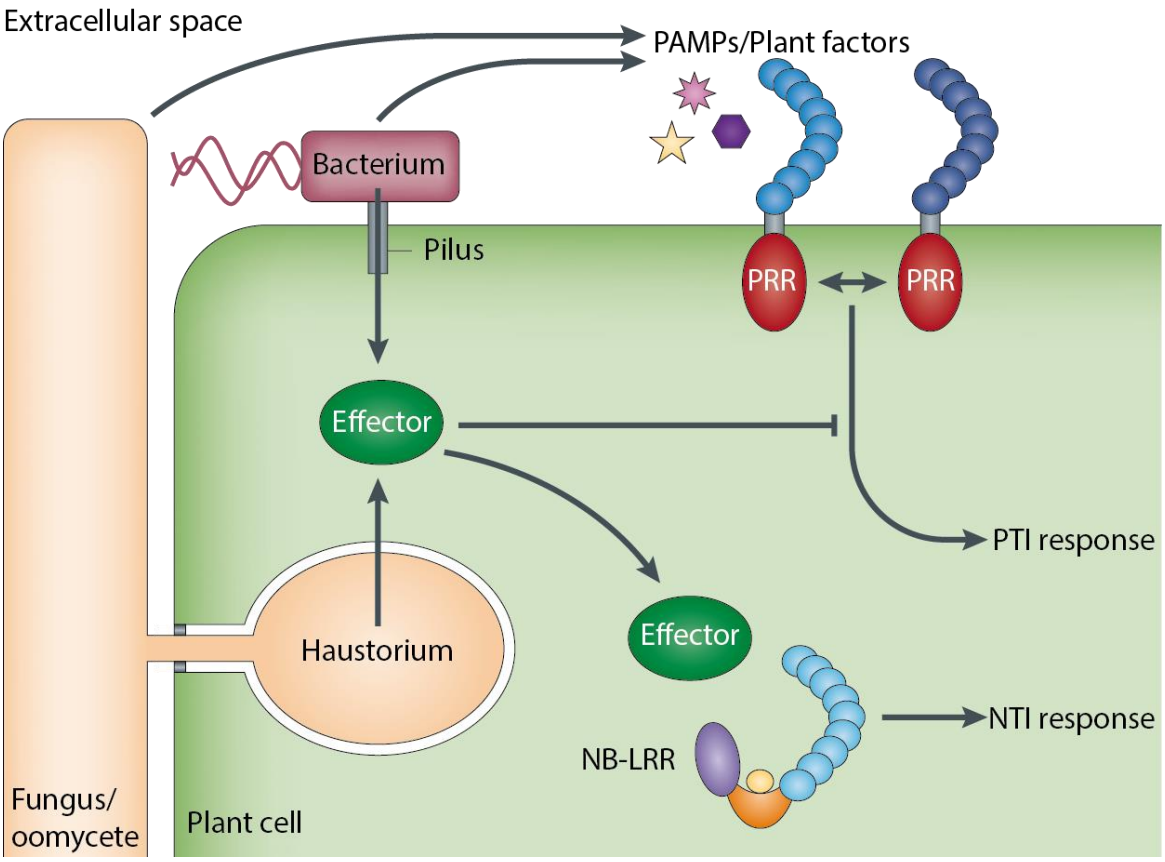

Figure 1.1 The principles of plant immunity.
Bacterial plant pathogens propagate mostly in the extracellular spaces of plant tissues. Most fungal and oomycete pathogens also extend their hyphae into this space, although many also form specialised feeding structures, known as haustoria, that penetrate host cell walls but not the plasma membrane. Pathogen associated molecular patterns (PAMPs) or immunogenic plant factors are recognised by cell surface pattern recognition receptors (PRRs) and elicit PRR-triggered immunity (PTI). Many PRRs interact with a receptor-associated kinase to initiate defence signalling. Bacterial pathogens deliver effector proteins into the host cell by a type-III secretion pilus. In contrast, fungi and oomycetes deliver effectors from haustoria or other intracellular structures by an unknown mechanism. These intracellular effectors often act to suppress PTI. However, many are recognised by intracellular nucleotide-binding-leucine-rich repeat (NB-LRR) receptors, which induces NLR-triggered immunity (NTI). This figure has been adapted with permission from one published by Dodds and Rathjen, 2010.

1.4. Pathogen perception in plants

1.4.1. Pattern recognition receptors

Plant PRRs are either plasma membrane (PM)-localised receptor kinases (RKs) or receptor-like proteins (RLPs) (Boutrot and Zipfel, 2017). RKs contain a ligand-binding ectodomain, a single-pass transmembrane domain, and an intracellular kinase domain, whereas RLPs lack any obvious intracellular signalling domains (Fritz-Laylin et al., 2005; Wang et al., 2008a). Historically, RKs were named receptor-like kinase (RLK) as it was unclear if they were *bona fide* ligand-binding receptors. In *Arabidopsis thaliana* (hereafter Arabidopsis), there are around 410 RKs and 170 RLPs (Shiu and Bleecker, 2003; Shiu et al., 2004; Li et al., 2016d).

1.4.1.1. PRR extracellular domains

PRR ectodomains are diverse and as such, recognise ligand of different biochemical natures. The ectodomain of PRRs can contain leucine-rich repeats (LRRs), lectin motifs, lysine motifs (LysMs), malectin-like domains, epidermal growth factor (EGF)-like domains, cysteine-rich domains of unknown function (DUF26), or thaumatin domains (Shiu and Bleecker, 2003; Dievart et al., 2020). LRR-type PRRs mostly recognise proteins or peptides. However, likely due to their variability, LRRs have been observed to bind a wide range of ligands, including sterols, lipids, sugars, peptides, lipopeptides and nucleic acids, although these recognition specificities have not necessarily been demonstrated for plant PRRs (Jamieson et al., 2018). There are 239 LRR-RKs and 109 LRR-RLPs in Arabidopsis, accounting for well over half the total PRRs currently known (Shiu and Bleecker, 2003; Shiu et al., 2004; Li et al., 2016d; Man et al., 2020). In contrast to bacterial and animal LRR proteins, which form a horseshoe-shaped structure, plant LRRs usually form a twisted or superhelical assembly (Hohmann et al., 2017). PRRs with plant lectin or lectin-like domains represent the second largest group (56 RKs and 15 RLPs in Arabidopsis), and are usually involved in the perception of carbohydrates and glycans (Lannoo and Van Damme, 2014; Li et al., 2016d). LysMs, named for their similarity to bacterial autolysins, are considered a distinct plant lectin subfamily and found in both plant RKs and RLPs (Shiu and Bleecker, 2003; Desaki et al., 2018). Malectin-like ectodomains were originally found in the *Catharanthus roseus* RLK1-like (CrRLK1L) subfamily of RKs (Lindner et al., 2012; Li et al., 2016b; Nissen et al., 2016). Malectin domains bear similarity to the animal carbohydrate-binding malectin proteins involved in the endoplasmic reticulum (ER) quality control (Schallus et al., 2008). Interestingly, some RKs such as IMPAIRED OOMYCETE SUSCEPTIBILITY 1 (IOS1) contain both LRR and malectin-like domains, and are thus named malectin-like/LRR-RKs (Shiu and Bleecker, 2001b; Hok et al., 2011). The FLG22-INDUCED RECEPTOR-LIKE KINASE (FRK1), whose expression level is often used as an indicator of early defence (Asai et al., 2002; Li et al., 2014a), also belongs to the malectin-like/LRR-RK subfamily.

Furthermore, although most PRRs seem to perceive their ligands directly, examples of indirect recognition also exist. For example, tomato immune receptor Cf-2 does not interact directly with the apoplastic elicitor Avr2 from *Cladosporium fulvum* or with the nematode elicitor VENOM ALLERGEN-LIKE PROTEIN 1 (VAP1) from *Globodera rostochiensis* (Lozano-Torres et al., 2012) but rather senses the inhibition imposed by these elicitor proteins on the host protease RCR3 (Dixon et al., 2000; Rooney et al., 2005; Lozano-Torres et al., 2012).

1.4.1.2. Receptor kinases

RKs comprise more than 60 % of all kinases in *Arabidopsis* (Shiu and Bleecker, 2001b; Lehti-Shiu et al., 2009). Most RKs are serine/threonine kinases, although several have tyrosine kinase activity (Shiu and Bleecker, 2001b; Oh et al., 2009; Lin et al., 2014; Macho et al., 2015). Among various kinase regulation strategies, autophosphorylation of a regulatory region termed the activation loop is critical to most kinases (Adams, 2003). The activation loop typically resides close to the kinase active site and generally blocks substrate access to the active site in the kinase-inactive state and, upon phosphorylation, conformational changes expose the active site (Adams, 2003). Kinases that are regulated by activation loop phosphorylation typically carry a conserved arginine (R) immediately preceding the invariant aspartate (D) in subdomain VI required for catalytic activity (Johnson et al., 1996). The combination of these 2 residues allows charge neutralisation, which is essential for proper orientation of the subdomain that facilitates phosphotransfer (Krupa et al., 2004). Kinases that are regulated through this mechanism are commonly referred to as RD kinases. Among various types of RKs, predominantly non-RD RKs are involved in immunity (Dardick et al., 2012). LRR-RKs are not only the most common but also the most studied RKs in plants (Shiu and Bleecker, 2001a; Fischer et al., 2016). Interestingly, in LRR-RKs, the intracellular kinase domain exhibits more conservation than the extracellular LRR domain (Shiu et al., 2004).

1.4.1.3. Receptor-like proteins

Generally, RLPs are single-pass transmembrane proteins (Shiu and Bleecker, 2001b; Fritz-Laylin et al., 2005; Wang et al., 2008a). However, some proteins without transmembrane domains might be considered as RLPs by their attachment to the extracellular face of the PM using a glycosylphosphatidylinositol (GPI) anchor (Borner et al., 2002; Gong et al., 2017). Besides, RLPs traditionally contain an N-terminal signal peptide. The most common extracellular ligand-binding domain found in RLPs is the LRRs type (Shiu and Bleecker, 2003; Li et al., 2016d). Without a kinase domain, RLPs likely act as receptors or regulators and transduce signals by associating with RKs and other transmembrane- and membrane-associated proteins (Gust and Felix, 2014; Liebrand et al., 2014).

1.4.1.4. Receptor-associated kinases

The best-characterised receptor associated-kinases for PRR are members of LRR subfamily II of the RK superfamily (Hosseini et al., 2020). This family is represented by 13 members in the Arabidopsis genome, which can be divided into three closely related clusters: one includes SOMATIC EMBRYOGENESIS RECEPTOR KINASE1-5 (SERK1-5); the second, a cluster of NUCLEAR-SHUTTLE PROTEIN-INTERACTING KINASES (NIK1-3); and a cluster of LRR-RKs of unknown function (Zhang et al., 2006; Sakamoto et al., 2012; Hosseini et al., 2020). The SERKs are shared co-receptors for multiple LRR-RKs and LRR-RLPs, and usually heterodimerise with the cognate receptor upon corresponding ligand perception (Ma et al., 2016). SERK3, also named BRI1-ASSOCIATED RECEPTOR KINASE 1 (BAK1) is the best-characterised subfamily member and plays a major role in plant immunity (Chinchilla et al., 2007; Heese et al., 2007; Wang et al., 2014). SERK4, also called BAK1-LIKE 1 (BKK1), contributes to immunity only in the absence of BAK1, whereas SERK1 and SERK2 have no contribution to immunity (Roux et al., 2011). NIKs have been proposed to act similarly as co-receptors. NIK1 plays a negative role in plant antibacterial immunity and a positive role in antiviral defence (Machado et al., 2015), which may be dependent on the phosphorylation status of the protein (Li et al., 2019). Emerging evidence has indicated that NIK1 exhibits a role in modulating PTI (Ahmed et al., 2018). NIK1 associates with BAK1 and FLAGELLIN SENSING 2 (FLS2) and the NIK1 interaction is strengthened upon flagellin-derived flg22 treatment (Li et al., 2019). Another well-characterised receptor associated-kinase for RLPs is the LRR-RK SUPPRESSOR OF BIR1-1 (SOBIR1), which has been found in complex with multiple LRR-RLPs (Gao et al., 2009). The function of several SOBIR1-associated RLPs requires the formation of this complex, including tomato Ve1 and Cf proteins, and Arabidopsis RLP23 (Liebrand et al., 2014; Albert et al., 2015). In addition, these LRR-RLPs associate with and functionally require BAK1. Some RLPs constitutively complex with SOBIR1, and subsequently recruit BAK1 upon ligand perception, forming a tripartite BAK1-SOBIR1-RLP complex (Albert et al., 2015; Du et al., 2015; Postma et al., 2016; Tang et al., 2017). SOBIR1 can stabilise LRR-RLPs, which may lead to enhanced kinase activity of SOBIR1 and/or BAK1 for signal transduction (Liebrand et al., 2013; Postma et al., 2016). CHITIN ELICITOR RECEPTOR KINASE 1 (CERK1) is a RK, which forms a receptor complex with LysM-type PRRs. In rice and Arabidopsis, CERK1 is an essential receptor for chitin-induced defence signalling and also known to be important for the activation of defence signalling by peptidoglycan (PGN) (Desaki et al., 2019). Besides being involved as co-receptors in ligand binding, additional RKs seem to have regulatory functions during cell-surface signalling. For example, BAK1-INTERACTING RECEPTOR KINASES (BIRs) interact with different ligand-binding receptors to inhibit or attenuate the signalling pathway (Imkampe et al., 2017; Hohmann et al., 2018). In addition, the LRR-RK APEX associates with PRR and APEX serve as regulatory scaffold proteins for different PRR complexes (Smakowska-Luzan et al., 2018).

1.4.2. Examples of bacterial perception by PRRs

1.4.2.1. Flagellin perception

Most motile bacteria possess protruding filaments called flagella, which contribute to the virulence of pathogenic bacteria through chemotaxis, adhesion to and invasion of the host surface (Ramos et al., 2004). Flagella are up to 15 µm long and composed mainly of the structural protein, flagellin (Ramos et al., 2004). Many organisms have evolved the capacity to recognise flagellin and elicit defence. Indeed, flagellin was discovered as the first general bacterial elicitor (Felix et al., 1999). In humans, TOLL-LIKE RECEPTOR 5 (TLR5) recognises flagellin (Hayashi et al., 2001) and interacts with different domains of flagellin formed by an N-terminal and a C-terminal part of the peptide chain (Smith et al., 2003). A synthetic 15- or 22-amino acid minimal motif based on *Pseudomonas aeruginosa* flagellin is sufficient to elicit defence responses in tomato (flg15) and Arabidopsis (flg22) respectively (Felix et al., 1999). In Arabidopsis, FLS2 recognises flagellin (Gómez-Gómez and Boller, 2000) and binds flg22 (Chinchilla et al., 2006). FLS2 is a non-RD kinase from subfamily LRR-RK XII with 28 extracellular LRRs, a transmembrane domain, and a cytoplasmic serine/threonine kinase domain (Gómez-Gómez and Boller, 2000; Shiu et al., 2004). In tomato, in addition to FLS2, FLS3 recognises an unrelated flagellin epitope, flgII-28 (Hind et al., 2016). While in Arabidopsis, FLS2 recognises the N-terminal of flagellin, rice possesses a yet unknown receptor to sense the C-terminal epitope of *Acidovorax avenae* flagellin (Katsuragi et al., 2015). Moreover, an allelic FLS2 receptor, named $FLS2^{XL}$, from wild grape confers resistance to the crown-gall pathogen *Agrobacterium tumefaciens* when expressed in tobacco (Fürst et al., 2020). Some bacteria might avoid host flagellin perception, either through the production of unrecognised flagellins or using alternative infection strategies (Felix et al., 1999; Pfund et al., 2004; Sun et al., 2006). For example, pathogens can evade flg22 recognition by either modifying the glycan moieties that cover their flagellum or by inhibiting plant glycosidases (Schäffer and Messner, 2017; Buscaill et al., 2019).

1.4.2.2. EF-Tu perception

Elongation factor thermo unstable (EF-Tu, also known as EF1A) is a G protein that transports aminoacylated tRNAs to the ribosome in eubacteria and eukaryotes (Sprinzl, 1994). EF-Tu is one of the most abundant proteins in bacteria constituting 5 to 10 % of bacterial cellular proteins (Bosch et al., 1983). Beside its cytoplasmic canonical role in translation, EF-Tu is exposed on the surface of bacteria where it fulfils secondary functions including adherence and immune regulation (Harvey et al., 2019). In animals, bacterial EF-Tu was shown to dampen the host immune response (Harvey et al., 2019). Brassicaceae species specifically recognise an N-acetylated peptide comprising the N-terminal 18 amino acids of EF-Tu from *Escherichia coli*, termed elf18, and induce defence responses (Kunze et al., 2004).

By contrast, the shorter peptide elf12, comprising the acetyl group and the first 12 N-terminal amino acids, is inactive as a PAMP but acts as a specific antagonist of elf18 (Kunze et al., 2004). EF-Tu is recognised by the Brassicaceae-specific PRR from LRR-RK subfamily XII, ELONGATION FACTOR TU RECEPTOR (EFR) (Shiu et al., 2004; Zipfel et al., 2006). EFR is a non-RD kinase that contains an extracellular domain with 21 LRRs, a transmembrane domain, and a cytoplasmic serine/threonine kinase domain (Zipfel et al., 2006). In rice, it has been shown that elf18 did not elicit any immune responses, whereas an EF-Tu middle region comprising Lys176 to Gly225, termed EFa50, is fully active as a PAMP (Furukawa et al., 2014). Interestingly, ectopic expression of EFR in species lacking this receptor, such as Solanaceae and legumes, conferred responsivity to EF-Tu and increase resistance to bacterial pathogens, suggesting that downstream components are conserved between families (Zipfel et al., 2006; Lacombe et al., 2010; Lu et al., 2015; Schoonbeek et al., 2015; Schwessinger et al., 2015; Boschi et al., 2017; Kunwar et al., 2018; Pfeilmeier et al., 2019).

1.4.3. Chitin perception from fungi

Chitin is a polymer of N-Acetyl-D-glucosamine found in fungal cell walls, insect exoskeletons, and crustacean shells. Despite not having chitin, plants possess chitin-degrading enzymes, chitinases, to directly affect the viability of the invading fungal pathogen and to release short chitin fragments (chitooligosaccharides) (Wan et al., 2008). Chitooligosaccharides induce defence responses in a wide range of plant cells, including both monocotyledons and dicotyledons (Shibuya and Minami, 2001). Chitooligosaccharides were reported to induce defence responses also in mammalian and insect cells (Furukawa et al., 1999; Shibuya and Minami, 2001). Interestingly, derivatives of chitooligosaccharides are used by some microbes, such as rhizobial bacteria and mycorrhizal fungi to induce symbiotic interaction (Truchet et al., 1991; Gough and Cullimore, 2011). Different mechanisms are employed by Arabidopsis and rice (*Oryza sativa*) for the perception of chitooligosaccharides. In rice, chitin perception requires a hetero-oligomeric receptor complex formed by dimers of CHITIN OLIGOSACCHARIDE ELICITOR-BINDING PROTEIN (OsCEBiP) and OsCERK1, which form a sandwich-type receptor for chitin oligomers (Kaku et al., 2006; Shimizu et al., 2010; Shinya et al., 2012; Hayafune et al., 2014). In addition to OsCEBiP, the LysM-RLPs LYSM-CONTAINING RECEPTOR PROTEIN 4 (OsLYP4) and OsLYP6 also bind chitin and are involved in chitin responsiveness (Liu et al., 2012a). LYP4 and LYP6 act as dual-specificity receptors for both chitin and peptidoglycan, associating with OsCERK1 in a ligand-dependent manner (Liu et al., 2012b; Ao et al., 2014). In Arabidopsis, CERK1 was thought to be the unique chitin receptor, as it homodimerises upon direct chitin-binding (Miya et al., 2007; Petutschnig et al., 2010; Liu et al., 2012a). However, LYSM-CONTAINING RECEPTOR-LIKE KINASE 5 (LYK5) displays higher chitin-binding affinity than CERK1 (Cao et al., 2014a). In addition, LYK5 and to a lesser extent its closest homologue LYK4, are genetically required for chitin responsiveness and form a chitin-

dependent complex with CERK1 (Wan et al., 2012; Cao et al., 2014a) indicating that LYK5 may form a receptor complex with CERK1 to facilitate chitin perception. Arabidopsis CERK1 is also recruited by the orthologues of rice LYP4 and LYP6, LYSM DOMAIN-CONTAINING GPI-ANCHORED PROTEIN 1 (LYM1) and LYM3 during peptidoglycan recognition to mediate antibacterial immune responses (Gimenez-Ibanez et al., 2009a; Gimenez-Ibanez et al., 2009b; Willmann et al., 2011). LYM1 and LYM3 do not seem to have a role in commonly measured chitin-induced responses (Willmann et al., 2011), but the paralogous LYM2 protein contributes with LYK4 and LYK5 to chitin-triggered plasmodesmata (PD) closure, thus controlling symplastic communication between plant cells and contributing to anti-fungal immunity (Faulkner et al., 2013; Cheval et al., 2020). Interestingly, chitin and chitosan oligosaccharides with varying degrees of polymerisation or acetylation induce different responses. Inhibition of chito-octamer-induced immunity has been shown by a chitosan octamer consisting of alternating GlcN and GlcNAc (Hayafune et al., 2014). To explain these differences, a new model has been proposed in which a heterotetramer is formed from each homodimer of AtLYK5 and AtCERK1 (Gubaeva et al., 2018).

1.4.4. Perception of plant factors

In addition to microbial molecules, PRRs perceive immunogenic plant factors, allowing plant cells to indirectly monitor a greater diversity of pathogens and to amplify responses beyond those triggered solely by PAMP perception (Heil and Land, 2014; Yamada et al., 2016b). Immunogenic plant factors are divided into two categories (Gust et al., 2017). Primary or constitutive danger signals are named damage-associated molecular patterns (DAMPs) and can be derived from pre-existing structures or molecules, including breakdown products of the extracellular matrix, or can be passively released intracellular molecules. Secondary or inducible danger signals are called phytocytokines through analogy with metazoan cytokines. Phytocytokines are actively processed and released upon tissue damage or other stimuli.

1.4.4.1. DAMPs

Herbivory, mechanical damage, or microbial infections result in the breakdown of plant tissue and subsequent release of cell wall-associated or intracellular molecules into the apoplastic space (Choi and Klessig, 2016; Duran-Flores and Heil, 2016). While herbivores destroy plant tissues during feeding either mechanically and/or by chemical modification, microbial infection-induced plant damage is often due to deleterious activities of microbial hydrolytic enzymes or toxins (D'Ovidio et al., 2004; Horbach et al., 2011).

During fungal infections, oligomeric fragments of the primary plant cell-wall pectin, termed oligogalacturonides (OGs) are produced through enzymatic hydrolysis by secreted fungal

polygalacturonases (Côté and Hahn, 1994; De Lorenzo et al., 2001; Horbach et al., 2011; Ferrari et al., 2013; Kohorn, 2016). WALL-ASSOCIATED KINASE 1 (WAK1) is implicated in OG sensing (Brutus et al., 2010) and more recently the ortholog in tomato SlWAK1 has been proposed to act in a complex with SlFLS2 and SlFLS3 (Zhang et al., 2020).

Breakdown of cellulose from the cell wall by microbial or plant glucosidases leads to the generation of cellooligomers, including cellobiose, cellotriose, and cellotetraose, and other short-chain β-1,4-linked D-glucoses. Cellobiose and cellotriose have been reported to trigger plant immunity responses, although cellotriose but not cellobiose can induce reactive oxygen species (ROS) production (Souza et al., 2017; Johnson et al., 2018). In addition, the POLY(A) RIBONUCLEASE (PARN) positively regulates responses induced by cellotriose and other cellooligomers, suggesting a post-transcriptional control of signalling component involved in cellooligomers-triggered immune activation (Johnson et al., 2018).

Intracellular ATP can be released into the extracellular matrix, where it is referred to as extracellular ATP (eATP). ATP is released not only upon cell rupture but has been proposed to be also exported by vesicle fusion with the PM and transporter-mediated ATP export (Kim et al., 2006; Rieder and Neuhaus, 2011; Cao et al., 2014b). In Arabidopsis, the L-type lectin RKs DOES NOT RESPOND TO NUCLEOTIDES 1 (DORN1), recently renamed P2K1, and P2K2 perceive eATP and contribute to plant immunity (Choi et al., 2014; Pham et al., 2020). P2K1 appears to be the primary eATP receptor in Arabidopsis, while the expression of P2K2 is induced upon addition of ATP or pathogen treatment (Pham et al., 2020).

Plant extracellular nicotinamide adenine dinucleotide ($eNAD^+$) triggers immune activation in Arabidopsis, suggesting that plants have evolved sensing systems for dinucleotide danger signals (Zhang and Mou, 2009). LecRK-I.8 has been suggested as a putative $eNAD^+$ receptor in Arabidopsis (Wang et al., 2017). In addition, LecRK-VI.2, which associates constitutively with BAK1, is potentially the receptor for $eNAD(P)^+$ (Wang et al., 2019a).

Finally, extracellular Arabidopsis HIGH MOBILITY GROUP BOX 3 (HMGB3), has been characterised as immunogenic danger signals, triggering immune activation (Choi et al., 2016). HMGB3 belongs to a family of highly conserved nuclear proteins expressed in most eukaryotic cells. HMGBs participate in the organisation, stabilisation and repair of genomic DNA, and transcription regulation (Klune et al., 2008).

1.4.4.2. Phytocytokines

Phytocytokines are typically produced as larger pro-proteins that are processed by proteolytic cleavage and secreted upon wounding, PAMP treatment, or microbial infection (Yamaguchi and Huffaker, 2011; Segonzac and Monaghan, 2019). The first phytocytokines identified were systemins in tomato. Systemin is an 18-amino acid polypeptide that is released from the prosystemin precursor upon wounding or

herbivore attack (Pearce et al., 1991; McGurl et al., 1992). Exogenous application of systemin activates defence-related responses (Schilmiller and Howe, 2005). In tomato, the LRR-RK SYSTEMIN RECEPTPOR 1 (SYR1) was identified as the systemin receptor (Wang et al., 2018c).

PLANT ELICITOR PEPTIDE (PEP), originally identified in Arabidopsis (AtPEP1–8) and later in maize (*Zea mays*) (ZmPEP1), constitute small peptide families that are derived from the C-terminal end of larger PROPEP precursors (Huffaker et al., 2006; Yamaguchi et al., 2006; Bartels and Boller, 2015). PROPEP1 is sequestered at the vacuolar membrane in the absence of damage, but it is processed by METACASPASE 4 (MC4) and released only in damaged cells (Hander et al., 2019). AtPEPs are recognised by two closely related LRR-RKs, PEP RECEPTOR 1 (PEPR1) and PEPR2 (Yamaguchi et al., 2006; Krol et al., 2010; Yamaguchi et al., 2010). Once perceived, Pep1 activates various PTI responses (Huffaker et al., 2006; Ranf et al., 2011; Ma et al., 2012; Bartels et al., 2013; Liu et al., 2013; Ma et al., 2013).

Arabidopsis PAMP-INDUCED PEPTIDEs (PIPs) represent another family of plant immunogenic peptides from C-terminal of 11 pre-proproteins precursors (PROPIPs) (Hou et al., 2014). PIP1, PIP2 trigger immune responses similarly as AtPep1 or flg22 and PIP1 is recognised by the LRR-RK, RLK7 (Hou et al., 2014).

RAPID ALKALINIZATION FACTORs (RALFs) are a family of cysteine-rich peptides, which are generated from pre-proproteins (Pearce et al., 2001; Pearce et al., 2010). Several of them, including RALF1 and RALF23, were confirmed to be perceived by LORELEI-LIKE-GPI-ANCHORED PROTEIN 1 (LLG1) in complex with FERONIA (FER) (Haruta et al., 2014; Stegmann et al., 2017; Xiao et al., 2019). RALFs have been shown to positively and negatively regulate plant immunity (Stegmann et al., 2017). Some RALF propeptides have been suggested to be cleaved at an RRXL site by the serine protease SITE-1 PROTEASE (S1P), leading to the generation of mature peptides (Srivastava et al., 2009; Stegmann et al., 2017).

Phytosulfokines (PSKs) are pentapeptides containing a sulfated tyrosine residue, which are processed from pre-propeptides by post-translational sulfation and proteolytic cleavage (Matsubayashi and Sakagami, 1996; Yang et al., 1999; Yang et al., 2001; Komori et al., 2009; Srivastava et al., 2009). In tomato, PSKs have been shown to contribute to the immunity to necrotrophic fungal pathogen *Botrytis cinerea* (Zhang et al., 2018a). In Arabidopsis, two LRR-RKs PSK RECEPTOR 1 (PSKR1) and PSKR2 perceive PSKs (Matsubayashi et al., 2006; Amano et al., 2007). PSKR1 acts as a positive regulator of immunity to the necrotrophic fungal pathogen, *Alternaria brassicicola,* and as a negative regulator to the biotrophic bacterial pathogen, *Pseudomonas syringae* (Igarashi et al., 2012; Mosher et al., 2013). SERINE-RICH ENDOGENOUS PEPTIDES (SCOOPs) constitute a new family of phytocytokines from C-terminal of 14 pre-proproteins precursors (PROSCOOPs) (Gully et al., 2019). It has been shown as well that application of SCOOP12 peptide induces various defence responses in Arabidopsis (Gully et al., 2019).

1.4.5. Defence signalling induced by PRRs

Upon PRR activation by ligand perception, a series of intertwined cellular and physiological responses are triggered in the plant cell (Figure 1.2).

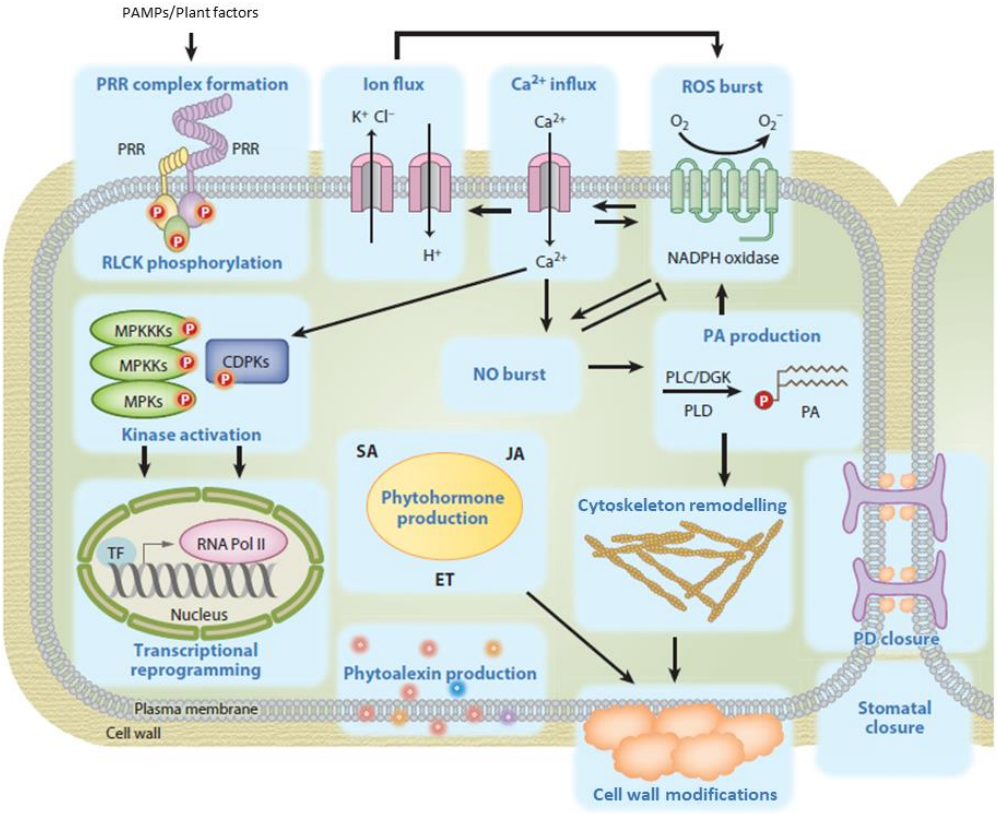

Figure 1.2 Cellular and physiological responses triggered by patterns in plants.
Upon ligand perception, pattern-recognition receptors (PRRs) complex formation is accompanied by rapid transphosphorylation in the complex and phosphorylation of receptor-like cytoplasmic kinases (RLCKs). Activation of PRR complexes activates MITOGEN-ACTIVATED PROTEIN KINASE (MAPK) cascades and CALCIUM-DEPENDENT PROTEIN KINASES (CDPKs), which regulate gene transcriptional changes and other cellular responses. The hallmarks of PRR-triggered immunity (PTI) responses include calcium influx, ion fluxes, actin filament remodelling, plasmodesmata (PD) and stomatal closure, callose deposition, and production of reactive oxygen species (ROS), nitric oxide (NO), phosphatidic acid (PA), phytoalexins, and phytohormones. Collectively, these responses contribute to plant resistance against a variety of pathogens. The potential connections among different responses are indicated with an arrowed line for positive regulation and a T-shaped line for negative regulation. Abbreviations: DGK, diacylglycerol kinase; ET, ethylene; JA, jasmonic acid; PLC, phospholipase C; PLD, phospholipase D; SA, salicylic acid; TF, transcription factor. This figure has been adapted with permission from one published by Yu et al., 2017.

1.4.5.1. PRR complex formation and transphosphorylation

Ligand perception induces stabilisation and formation of PRR complex at the PM, which leads to activation of the PRRs and transduction of the signal from the apoplast to the cytoplasm. For LRR-RK

and LRR-RLP PRRs, ligand perception induces PRR-BAK1 heterodimerisation. For example, FLS2 forms a complex with the receptor-associated kinase BAK1 quasi-instantaneously upon flg22 perception (Chinchilla et al., 2007; Heese et al., 2007; Schulze et al., 2010). flg22 stabilises FLS2-BAK1 dimerisation by acting as ‘‘molecular glue’’ between the two ectodomains (Sun et al., 2013). This interaction occurs independently of kinase activity and the presence of intracellular domains (Schwessinger et al., 2011; Sun et al., 2013). Similarly, BAK1 heterodimerises with EFR and PEPR1 in the presence of the cognate ligand (Heese et al., 2007; Chinchilla et al., 2009; Schulze et al., 2010; Tang et al., 2015). Concerning some LRR-RLPs, which constitutively complex with SOBIR; upon ligand perception, BAK1 associates and forms a tripartite BAK1-SOBIR1-RLP complex (Liu et al., 2020). Whilst not required for complex formation, conserved phosphosites are required for the induction of downstream immune responses (Macho et al., 2014; Suzuki et al., 2016; Liu et al., 2018; Perraki et al., 2018). In the case of chitin, it has been shown that PRRs homodimerise and also multimerise. The current model suggests that chitin first binds to the existing LYK5 homodimer, which would then recruit the chitin-induced CERK1 homodimer to form a heterotetrameric receptor complex (Gubaeva et al., 2018). This complex will bring together CERK1 cytoplasmic domains, which contain an active kinase, enabling intermolecular transphosphorylation (Petutschnig et al., 2010).

In addition, several PM proteins have been shown to regulate complex formation. IOS1 associates with PRRs including FLS2, EFR, CERK1, as well as with BAK1, and promotes FLS2-BAK1 complex formation upon flg22 perception (Yeh et al., 2016). FER was also found to regulate PRR-triggered signalling by several PAMPs and associates with both FLS2 and BAK1 (Stegmann et al., 2017). LRR-RK FLS2-INTERACTING FACTOR (FIR) promotes FLS2-BAK1 complex formation and is required for flg22 response activation and immunity to microbial infection (Smakowska-Luzan et al., 2018). In addition, NIK1 associates with FLS2 or BAK1 at the resting state and becomes phosphorylated upon flg22 perception, which leads to suppression of translational machinery activation (Li et al., 2019). The LRR-RK APEX associates with PEPR1/2 and has been found as a regulatory scaffold critical for signalling network integrity (Smakowska-Luzan et al., 2018). The induced proximity of the cytoplasmic domains upon ligand binding induces complex activation and a series of trans- and auto-phosphorylation events rendering the complex competent to regulate the activity of cytoplasmic signalling cascades

1.4.5.2. RLCK phosphorylation

PRRs directly interact with and activate downstream immune signalling through a class of related receptor-like cytoplasmic kinases (RLCKs). They are cytoplasmic proteins that contain a RK-homologous kinase domain but lack the transmembrane and extracellular domains. In Arabidopsis, multiple members from subfamilies 1, 4, 5, 7, and 8 of RLCK-VIIs play roles in immunity with diverse function in responses to various elicitors (Rao et al., 2018; Liu et al., 2019). In most cases, RLCK-VII

single mutants do not show significant defects in immunity, likely due to overlapping functions. BOTRYTIS-INDUCED KINASE1 (BIK1) and the closely related PBS1-Like1 (PBL1), belonging to subfamily VII-8 of the RLCKs, mediate pattern-triggered immunity by associating directly with FLS2, EFR, CERK1, and PEPR1 (Lu et al., 2010; Zhang et al., 2010a; Liu et al., 2013). BIK1 and PBL1 are required for the elicitor-triggered ROS production, calcium influx, and callose deposition (Lu et al., 2010; Zhang et al., 2010a; Kadota et al., 2014; Li et al., 2014b; Ranf et al., 2014; Tian et al., 2019) but not MAPK activation (Feng et al., 2012). In rice, the members of the RLCK family VII, RLCK176 and RLCK185, interact with CERK1 and positively regulate responses to peptidoglycan and chitin (Yamaguchi et al., 2013; Ao et al., 2014). Mechanistically, BIK1 dissociates from the receptor complex and phosphorylates multiple downstream targets including REGULATOR OF G PROTEIN SIGNALLING PROTEIN 1 (RGS1), which regulates heterotrimeric G proteins (Liang et al., 2018); RESPIRATORY BURST OXIDASE HOMOLOG D (RBOHD), the NADPH oxidase responsible for PRR-mediated ROS burst (Kadota et al., 2014; Li et al., 2014b); and CYCLIC NUCLEOTIDE-GATED CHANNEL 2 (CNGC2) and CNGC4 as well as OSCA1.3, which are nonselective cation channels mediating PAMP-induced calcium influx in the cytosol (Tian et al., 2019; Thor et al., 2020) (Figure 1.3). Intriguingly, although BIK1 is a positive regulator of flg22- and elf18-triggered immunity, it acts as a negative regulator of immunity induced by the conserved 20-amino-acid fragment (nlp20) found in most NEP1-LIKE PROTEINS (NLPs), which is recognised by the LRR-RLP RECEPTOR LIKE PROTEIN 23 (RPL23), suggesting an opposing regulatory role of BIK1 in LRR-RLP and LRR-RK signalling (Wan et al., 2019b). PBL27, from the RLCK-VII-1 subfamily, was shown to promote chitin-induced stomatal closure by phosphorylating the S-type anion channel SLAH3 (Liu et al., 2019). PBL27 was also reported to phosphorylate MAPKKK5, initiating a MAP kinase signalling cascade (Yamada et al., 2016a). However, a subsequent report claims that RLCK-VII-4 subfamily members, but not PBL27, mediate this process (Bi et al., 2018). Besides, the RLCK-VII-4 subfamily is important for ROS production in response to chitin but not flg22 or elf18 (Rao et al., 2018). PTI COMPROMISED RECEPTOR-LIKE CYTOPLASMIC KINASE 1 (PCRK1) and PCRK2 from the RLCK-VII-4 are required for ROS production, callose deposition, and salicylic acid (SA) accumulation in response to various elicitations (Sreekanta et al., 2015; Kong et al., 2016). It remains unclear whether different RLCK VII members are differentially coopted for distinct PRRs and whether different RLCK VII members regulate different downstream responses. In addition to the family RLCK-VII, the 12-member RLCK-XII family also play important roles in immune and developmental signalling. BRASSINOSTEROID-SIGNALING KINASE1 (BSK1), a member of the RLCK XII subfamily associates with FLS2 and is critical for several immune responses, including flg22-induced ROS (Shi et al., 2013). Like PBL27 and RLCK-VII-4s, BSK1 was also reported to phosphorylate MAPKKK5 and thereby initiate MAPK signalling (Yan et al., 2018). The related BSK5 was recently shown to be involved in FLS2-, EFR-, and PEPR- mediated responses (Majhi et al., 2019).

In addition to RLCK-VII and XII, other kinases are important for early signalling including calcium-dependent kinases (CPKs) such as CPK5 (Yip Delormel and Boudsocq, 2019), the MAP4Ks SERINE-THREONINE KINASE 1 (SIK1) and MAP4K4 (Zhang et al., 2018b; Jiang et al., 2019), and CYS-RICH RECEPTOR-LIKE KINASES (CRKs) such as CRK2 (Kimura et al., 2020).

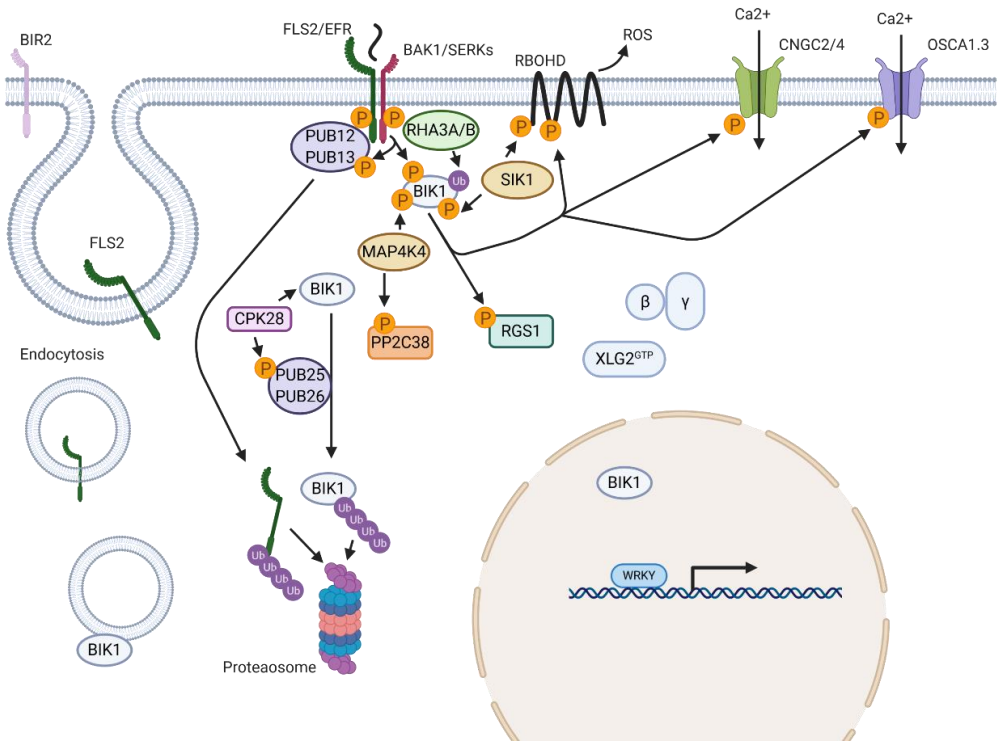

Figure 1.3 The RLCK BIK1 is an important mediator of transmembrane signal transduction that regulates immune signalling.
Upon flg22 perception, FLAGELLIN-SENSING 2 (FLS2) associates with BRI1-ASSOCIATED KINASE 1 (BAK1), which triggers transphosphorylation of the receptors and dissociation from BAK1-INTERACTING RECEPTOR-LIKE KINASE 2 (BIR2). Once phosphorylated, BAK1 phosphorylates BOTRYTIS-INDUCED KINASE 1 (BIK1) and PLANT U-BOX 12 (PUB12)/PUB13 which lead to polyubiquitination of FLS2. BIK1 is further regulated by post-translational regulation. BIK1 is mono-ubiquitylated by E3 ligase RING-H2 FINGER A3A (RHA3A)/B and phosphorylated by MAP4K4 and SERINE-THREONINE KINASE 1 (SIK1). Activated BIK1 phosphorylate RESPIRATORY BURST OXIDASE HOMOLOG D (RBOHD), calcium channels CYCLIC NUCLEOTIDE-GATED CHANNEL 2 (CNGC2)/4 and OSCA1.3, and REGULATOR OF G PROTEIN SIGNALLING PROTEIN 1 (RGS1). BIK1 localises as well in the nucleus and regulate WRKY transcription factors. RBOHD is also phosphorylated by SIK1 and leads to ROS production. RGS1 phosphorylation leads to dissociation of the heterotrimeric G-protein from RGS1, GDP-to-GTP exchange by EXTRA-LARGE GTP-BINDING PROTEIN 2 (XLG2) and G-protein activation. MAP4K4 phosphorylates PROTEIN PHOSPHATASES TYPE 2C 38 (PP2C38), which is then released of BIK1. CALCIUM-DEPENDENT KINASE 28 (CPK28) phosphorylates PUB25 and PUB26 which enhances the E3 ligase activity of PUB25 and PUB26 and accelerates the degradation of nonactivated BIK1. Polyubiquitinated BIK1 and FLS2 are then degraded by the proteasome. FLS2 and BIK1 are also endocytosed from the plasma membrane. Circled P represents phosphorylation of proteins and Ub, ubiquitination. Figure created with Biorender.com.

1.4.5.3. Calcium influx

Calcium (Ca^{2+}) is a universal second messenger in eukaryotic signalling pathways by which many fundamental biological phenomena are controlled (Berridge et al., 2000). Unstimulated cells have a relatively low concentration of free Ca^{2+} in the cytosol ($[Ca^{2+}]_{cyt}$) (*i.e.*100-200 nM), which is 10,000–20,000 times lower than outside of the cell, to avoid its cytotoxicity and to generate a steep $[Ca^{2+}]$ membrane potential which can be rapidly depolarised in response to various stimuli (Berridge et al., 2000; Ranf et al., 2011; Seybold et al., 2014). A Ca^{2+} signal is generated by a combination of various channels, pumps and transporters using extracellular and intracellular Ca^{2+} stores. Prominent Ca^{2+} sensors are CALMODULIN (CaM), CALMODULIN-LIKE PROTEINS (CMLs), CALCIUM-DEPENDENT PROTEIN KINASES (CDPKs/CPKs), CALCINEURIN B-LIKE proteins (CBLs) and their interacting kinases CALCINEURIN B-LIKE KINASE (CIPKs) (DeFalco et al., 2010; Edel and Kudla, 2015; Zhu et al., 2015). Furthermore, plants also have two major extra-cytoplasmic compartments, the vacuole and the apoplast, which leads to the complex regulation of Ca^{2+} signalling (Seybold et al., 2014). In immunity, the Ca^{2+} influx is important for transcriptional activation (Boudsocq et al., 2010; Lenzoni et al., 2018), stomata-mediated immunity (Underwood et al., 2007), and cell-cell and systemic signals (Choi et al., 2017). The rapid increase of $[Ca^{2+}]_{cyt}$ is among the earliest cellular responses with an increase of $[Ca^{2+}]_{cyt}$ with a delay of ∼30–40 sec and a peak at ∼2–6 min after elicitation (Ranf et al., 2011; Seybold et al., 2014). Interestingly, different elicitors induce different patterns of $[Ca^{2+}]_{cyt}$ oscillations (Keinath et al., 2015). An initial apoplastic Ca^{2+} influx is often necessary for Ca^{2+}-induced Ca^{2+} release from internal stores either directly or mediated by second messengers, that stimulate ligand-gated channels at internal stores, such as the vacuole and the ER (Bewell et al., 1999; Navazio et al., 2000; Ng et al., 2001; Lemtiri-Chlieh et al., 2003). Phosphorylation of CNGC2/4 by BIK1 is critical for calcium spiking in response to immune elicitors only under specific calcium concentrations (Tian et al., 2019). The related channel proteins CNGC19 and 20 were recently identified as positive regulators of cell death in *bak1*/*bkk1* and to positively regulate the defence against spodoptera herbivory but also to be important for the colonisation by the endosymbiont *Piriformospora indica* in Arabidopsis (Meena et al., 2019; Yu et al., 2019b; Jogawat et al., 2020). However, it is not yet known if BIK1 also has a role in activating CNGC19 and CNGC20. Arabidopsis CPK4, CPK5, CPK6, and CPK11 are transiently activated in response to flg22 treatment and redundantly regulate expression of a subset of PAMP-responsive genes distinct from or overlapping with those controlled by MAPKs (Boudsocq et al., 2010). In addition, CPK5 positively regulates the flg22-induced ROS burst via direct phosphorylation of RBOHD at specific residues different from those phosphorylated by BIK1 (Dubiella et al., 2013; Kadota et al., 2014). Recently, the calcium-permeable channel OSCA1.3 was shown to be rapidly phosphorylated upon perception of elicitors and to control stomatal closure (Thor et al., 2020).

1.4.5.4. Ion flux and extracellular alkalinisation

Elicitor perception induces rapid Cl^-, NO_3^-, and K^+ effluxes, as well as H^+ influx across the PM, which often leads to membrane depolarisation and extracellular alkalinisation (Felix et al., 1993; Jeworutzki et al., 2010). This strong membrane potential depolarisation and extracellular alkalinisation was recorded 1 min after flg22 or elf18 treatment in Arabidopsis mesophyll cells (Jeworutzki et al., 2010). Recovery of flg22-induced membrane potential to the resting state takes more than 1 h, a long-lasting process compared with that triggered by abiotic stresses (Jeworutzki et al., 2010). PM-resident H^+-ATPASES (AHAs) are considered the primary pumps to transfer protons from cytosol to the extracellular matrix to establish the PM potential (Elmore and Coaker, 2011) but their function in immune responses remains elusive. Upon PAMP perception, H^+ influx is accompanied by effluxes of Cl^- and K^+. Interestingly, flg22 treatment triggers a considerably higher peak value of Cl^- efflux than of H^+ influx, suggesting the involvement of anion channels in establishing PM depolarisation (Jeworutzki et al., 2010). INTEGRIN-LINKED KINASE 1 (ILK1), which interacts with the HIGH-AFFINITY K^+ TRANSPORTER 5 (HAK5), positively regulates flg22-induced PM depolarisation, implicating the involvement of K^+ efflux in PM depolarisation (Brauer et al., 2016).

1.4.5.5. ROS burst

ROS can act as a toxin barrier against subsequent pathogen infections and are involved in strengthening plant cell, but also act as secondary signalling molecules (Torres et al., 2006; Scheler et al., 2013). ROS include partially reduced forms of oxygen such as superoxide (O_2^-), hydrogen peroxide (H_2O_2), and hydroxyl radicals ($^{\bullet}OH$). Transient and rapid generation of apoplastic ROS referred to as a ROS burst, is a hallmark of the early response to PAMP treatment (Torres et al., 2006). However, the specific role and direct molecular targets of ROS during elicitor-recognition have remained elusive (Qi et al., 2017). Typically, a ROS burst is initiated within ∼4–6 min, reaches its peak ∼10– 15 min, then gradually declines to the resting state ∼30 min after PAMP treatments in various plant species (Jabs et al., 1997). Both PM-localised NADPH oxidases and cell wall-associated peroxidases are involved in a PAMP-induced ROS burst (Daudi et al., 2012). NADPH oxidases transfer electrons from cytosolic NADPH or NADH to apoplastic oxygen, leading to the production of O_2^-, which is then converted to H_2O_2 by unknown superoxide dismutase (Torres et al., 2006). Among 10 *RESPIRATORY BURST OXIDASE HOMOLOG A-J* (*RBOHA-J*) genes encoding NADPH oxidases in Arabidopsis, RBOHD is the major enzyme in PAMP-induced ROS production (Torres et al., 2002; Nühse et al., 2007).

PAMP perception induces the phosphorylation of RBOHD at multiple residues (Benschop et al., 2007; Nühse et al., 2007; Dubiella et al., 2013; Kadota et al., 2014; Li et al., 2014b). During PTI, BIK1 and CPK5 activate RBOHD by phosphorylating the N-terminal of RBOHD (Kadota et al., 2014; Li et al., 2014b; Ma, 2014; Lee et al., 2020). In addition, CYSTEINE-RICH RLK2 (CRK2) phosphorylates the C

terminus of RBOHD, which positively regulates flg22-induced ROS production and defence against *Pseudomonas syringae* pathovar *tomato* (*Pto*) DC3000 (Kimura et al., 2020). Furthermore, SIK1 phosphorylates, and stabilises BIK1 to enhance BIK1 activity and SIK1 also directly interacts with and phosphorylates the N-terminal of RBOHD to increase ROS production independent of BIK1 (Zhang et al., 2018b).To avoid constitutive activation of RBOHD at the resting state, PBL13 phosphorylates the C-terminal of RBOHD, which promotes ubiquitination by PBL13-INTERACTING RING-TYPE E3 UBIQUITIN LIGASE (PIRE) (Lee et al., 2020). Flagellin perception induces the dissociation of PBL13 from RBOHD, leading to the release of RBOHD from PBL13-mediated negative regulation (Lee et al., 2020).

Interestingly, feedback regulation of $[Ca^{2+}]_{cyt}$ by ROS likely exists because $[Ca^{2+}]_{cyt}$ increases in response to H_2O_2 treatment and PAMP-induced ROS burst is important for inducing the second peak or prolonged plateau of $[Ca^{2+}]_{cyt}$ (Ranf et al., 2011; Segonzac et al., 2011). Moreover, in response to abiotic stress, ROS and calcium have been shown to interact cooperatively to promote long-distance calcium signalling (Evans et al., 2016). Interestingly, the RK HYDROGEN-PEROXIDE-INDUCED Ca^{2+} INCREASES 1 (HPCA1) has recently been identified as an apoplastic ROS sensor, and this receptor induces cytoplasmic calcium influx in response to apoplastic ROS, strengthening the interconnection between ROS and calcium (Wu et al., 2020).

1.4.5.6. Nitric oxide production

A rapid burst of the free radical gas nitric oxide (NO), is a hallmark of animal innate immune responses (Scheler et al., 2013). An NO burst is detected within a few minutes upon treatment with cryptogein, xylanase, flg22, PGN, Lipopolysaccharides (LPS), eATP and AtPEPs in various plant species (Foresi et al., 2007; Ma et al., 2013; Scheler et al., 2013). NO has also been suggested to act as an important secondary messenger and antimicrobial agent in plant defence (Scheler et al., 2013). In animals, NO is synthesized by NO synthases (NOS) by converting L-arginine to NO and L-citrulline. However, the exact sources and enzymes mediating PAMP-induced NO biosynthesis remain elusive in plants (Scheler et al., 2013). In Arabidopsis, NOS1 has been shown to play a positive role in LPS-induced NO production and gene expression (Zeidler et al., 2004). Interestingly, CNGC2 and CML24 have a positive effect on LPS-induced NO production suggesting a link between Ca^{2+} signalling and NO production (Ma et al., 2008; Albert et al., 2015). NO was also shown to be linked with ROS production during PAMP-triggered stomatal closure (Arnaud and Hwang, 2015).

1.4.5.7. Phosphatidic acid production

Phosphatidic acid (PA), an important intermediate in lipid biosynthesis, is also considered to be a key signalling molecule regulating various cellular activities and environmental responses. During immunity,

PA is potentially involved in the regulation of ROS production, MAPK activation, defence gene induction, and actin remodelling (Testerink and Munnik, 2011). The levels of PA and its phosphorylated derivative diacylglycerol pyrophosphate (DGPP) are elevated in suspension cells after elicitation. The accumulation of PA occurs in 2 min and reaches its peak approximately 8 min after treatment (van der Luit et al., 2000; Yamaguchi et al., 2003). The combined actions of phospholipase C (PLC) and diacylglycerol kinase (DGK) to phosphorylate diacylglycerol (DAG) to PA was suggested to be the predominant biosynthetic pathway in immunity (van der Luit et al., 2000; Laxalt et al., 2007).

1.4.5.8. MAPK activation

The activation of MAPK cascades is of profound importance in disease resistance (Asai et al., 2002; Meng et al., 2013; Meng and Zhang, 2013). In Arabidopsis stimulated with flg22, a transient increase in MPK6 activity was observed, starting with a lag phase of ∼1–2 min and peaking after 5–10 min (Nühse et al., 2000). A MAPK cascade typically contains at least three sequentially activated kinases of a MAPK kinase kinase (MAPKKK or MEKK), a MAPK kinase (MAPKK or MKK), and a MAPK (MPK). At least two canonical MAPK cascades consisting of MAPKKK3/MAPKKK5-MKK4/MKK5-MPK3/MPK6 and MEKK1-MKK1/MKK2-MPK4/MPK11 in Arabidopsis have been indicated to exert opposing roles in plant defence (Mithoe and Menke, 2018). The MPK3/MPK6 cascade was shown to have a positive role. For instance, MPK3 and MPK6 regulate flg22-triggered ET production through phosphorylation of 1-AMINOCYCLOPROPANE-1-CARBOXYLIC ACID SYNTHASE 2 (ACS2) and ACS6, the rate-limiting enzymes in ET biosynthesis (Liu and Zhang, 2004). Besides, flg22-activated MPK3 and MPK6 phosphorylate TANDEM ZINC FINGER PROTEIN 9 (TZF9), residing in cytoplasmic processing bodies (hereafter, p-bodies), the sites for mRNA storage and decay, where TZF9 may sequester and inhibit the translation of subsets of mRNAs in the absence of stress (Tabassum et al., 2019). On the other side, MPK4 cascade has a negative role in immunity (Asai et al., 2002; Kong et al., 2012; Meng et al., 2013). Flg22-activated MPK4 phosphorylates ARABIDOPSIS HOMOLOG OF YEAST PAT1 (PAT1), a key component in mRNA decay, leading to its accumulation in p-bodies and contributing to post-transcriptional regulation of gene expression (Roux et al., 2015). In addition, MAPK cascade is monitored during plant defence by the NLR, SUPPRESSOR OF MKK1 MKK2 (SUMM2), which guards PAT1 (Zhang et al., 2012; Roux et al., 2015). The activation mechanism of MAPKKKs remains contentious as it was shown that PBL27 or BSK1 phosphorylate MAPKKK5 (Yamada et al., 2016a; Rao et al., 2018; Yan et al., 2018) however another report claimed that RLCK-VII-4 subfamily members, but not PBL27, mediate this process (Bi et al., 2018).

1.4.5.9. Plasmodesmata closure

Plasmodesmata (PD) are cytoplasmic channels that bridge the cell wall and directly connect the cytoplasm of neighbouring cells (Tilsner et al., 2016). PD directly connect the PM, ER and cytoplasm forming symplastic junctions between cells that allow for direct molecular exchange between cells and tissues (Tilsner et al., 2016). Besides, PD are dynamic structures regulated by callose deposition in a variety of stress and developmental contexts (Lee et al., 2011; Lee and Lu, 2011; Cheval and Faulkner, 2018). Chitin and flg22 induce PD closure by stimulating PD callose deposition in Arabidopsis (Felix and Boller, 2003) and CML41 is required for flg22-induced callose deposition at PD (Xu et al., 2017a). Chitin responses in PD require the RLP LYM2 as well as LYK4 and LYK5 (Cheval et al., 2020). In addition, PD-LOCATED PROTEIN (PDLP1) and PDLP5 have been implicated in immune responses in Arabidopsis (Wang et al., 2013; Caillaud et al., 2014). Interestingly, CALLOSE SYNTHASE 8 (CALS8) is required for ROS-dependent PD closure but not essential for PD responses during infection, (Cui and Lee, 2016).

1.4.5.10. Cytoskeleton remodelling

Two major classes of the plant cytoskeletal network are found in most eukaryotes. The first, microfilaments, commonly referred to as the actin cytoskeleton, is responsible for functions ranging from cytoplasmic streaming (*e.g.*, movement of organelles) and cell division to trafficking and endocytosis. The second, microtubules (MTs), are composed of a complex array of α/β-tubulin heterodimers, a network that is typically associated with cell growth and long-distance intercellular movement and communication (Brandizzi and Wasteneys, 2013; Li and Day, 2019). The cytoskeleton is important for immune responses by establishing and maintaining signalling-competent microenvironments and also for cellular trafficking of organelles, proteins and small molecules (Li and Day, 2019). The MT network is important for distinct complex formation and specific signalling, through interaction with PRRs localising to nanodomains within the PM (Bucherl et al., 2017). By contrast, actin filaments may be important for negative regulation of immunity as disruption of actin filament organisation leads to the generation of a relatively enhanced ROS burst response following flg22 elicitation (Sun et al., 2018).

In addition to regulation of immunity by the cytoskeleton, perception of PAMPs has been shown to trigger the re-organisation of actin in Arabidopsis (Henty-Ridilla et al., 2013; Henty-Ridilla et al., 2014; Shimono et al., 2016). Pathogens can also alter actin cytoskeletal structures during infection to evade immunity and promote infection. *Pseudomonas syringae* induces a change in host actin 20 h post-inoculation (Lee et al., 2012; Henty-Ridilla et al., 2013) and other virulent pathogens show similar effect (Kobayashi et al., 1992; Opalski et al., 2005; Miklis et al., 2007). Among the first regulators of actin cytoskeletal organisation revealed to play an important role in immunity, the ACTIN DEPOLYMERIZING FACTOR (ADF) or cofilin family of proteins regulate actin cytoskeletal

organisation via filament severing and depolymerisation (Kanellos and Frame, 2016; Li and Day, 2019) and actin or MT-associated proteins such as capping proteins (Li et al., 2015b; Li et al., 2017).

1.4.5.11. Defence gene expression

PTI elicitation induces rapid, dynamic, and global changes in the transcription of plant genes involved in a broad range of biological functions (Navarro et al., 2004; Zipfel et al., 2004; Zipfel et al., 2006; Li et al., 2016a). Differential expression analysis over 60 minutes of flg22 treatment in leaf discs of adult Arabidopsis revealed 763 genes downregulated and 1218 genes upregulated (False Discovery Rate<0.01 and log2 fold change < or >1) (Rallapalli et al., 2014). Transcription reprogramming is conferred by the concerted action of myriad transcription (co)factors that function directly or indirectly to recruit or release RNA POLYMERASE II (RPII) (Moore et al., 2011). Several TFs from the families of WRKY, APETALA2/ETHYLENE RESPONSIVE FACTOR (AP2/ERF), NAM, ATAF and CUC (NAC), MYB, basic leucine zipper domain (bZIP), basic helix-loop-helix (bHLH), NUCLEAR FACTOR Y (NF-Y) and CaM-BINDING TRANSCRIPTION ACTIVATOR (CAMTA) play crucial roles in immune responses against pathogens (Nuruzzaman et al., 2013; Buscaill and Rivas, 2014; Huang et al., 2016; Phukan et al., 2016; Noman et al., 2017; Zanetti et al., 2017). Specific transcription factors directly phosphorylated by MAPKs or acting downstream of Ca^{2+} signalling have been shown to play a role in regulating PAMP-responsive gene expression. The Arabidopsis transcription factors ETHYLENE-RESPONSIVE FACTOR 104 (ERF104) and BRI1-EMS-SUPPRESSOR 1 (BES1) phosphorylated by MPK6 play positive roles in PAMP-responsive gene expression (Bethke et al., 2012; Kang et al., 2015), whereas the trihelix transcription factor ARABIDOPSIS SH4-RELATED3 (ASR3) phosphorylated by MPK4 negatively regulates expression of a subset of PAMP-responsive genes (Li et al., 2015a). In other cases, TFs are not the direct targets of MAPKs, but instead, their activation is monitored by MAPK phosphorylation substrates. MPK3 and MPK6 phosphorylate a subset of MPK3/MPK6-TARGETED VQ-MOTIF-CONTAINING PROTEINS (MVQs), which interact with plant-specific WRKYs transcription factors (Pecher et al., 2014). WRKY have been particularly associated with plant immunity. For example, Arabidopsis WRKY33 is responsible for PAMP-induced production of camalexin (Tsuda and Somssich, 2015). WRKY33 is maintained in an inhibitory complex by MPK4 and the MVQ protein, MAPK SUBSTRATE1 (MKS1) (Qiu et al., 2008) and upon flg22 perception, MPK4 phosphorylates MKS1 and releases the MKS1–WRKY33 complex, allowing WRKY33 to be phosphorylated and activated by MPK3 and MPK6 (Mao et al., 2011; Rasmussen et al., 2012). BIK1 has also been shown to partially localise to the nucleus, where it can phosphorylate several WRKY TFs involved in transcriptional reprogramming (Lal et al., 2018).The transcription factors CAM-BINDING PROTEIN 60-LIKE G (CBP60G) and its homolog SAR DEFICIENT 1 (SARD1) bind to the promoters of genes encoding PRR complexes or signalling components, including *BAK1*, *BIK1*, and *MPK3* as well as of the

SA biosynthetic gene *ISOCHORISMATE SYNTHASE 1* (*ICS1*), which modulate their expression (Zhang et al., 2010b; Wang et al., 2011; Sun et al., 2015).

During plant defence, the general transcription machinery is also affected. PAMP treatments induce rapid and transient phosphorylation of RNAPII C-terminal domain (CTD) via CYCLIN–DEPENDENT KINASE Cs (CDKCs), which are phosphorylated and activated by MPK3 and MPK6 (Li et al., 2014a). The MEDIATOR multiprotein complex, which functions as a transcriptional coactivator in all eukaryotes was reported to be implicated in plant defence (Li et al., 2016a). Flg22 treatment induces poly(ADP-ribosyl)ation (PARylation), to regulate some of late PTI responses potentially via chromatin remodelling (Feng et al., 2015; Feng et al., 2016). Finally, translation has also been shown to be tightly regulated and poorly correlated with transcription during plant defence (Xu et al., 2017b). Interestingly, genes with increased translational efficiency show in their messenger RNA sequences, a highly enriched consensus sequence, R-motif, consisting of mostly purines, which regulates translation through interaction with poly(A)-binding proteins during defence (Xu et al., 2017b). In addition, flg22 induced various changes among RNA-binding proteins (RBPs) (Bach-Pages et al., 2020).

1.4.5.12. Stomatal closure

Stomata are the openings formed by two guard cells on the leaf surface for gas exchange and water transpiration. As the major routes for pathogen entry, stomatal opening and closure are regulated during pathogen infection. PRR activation induces stomatal closure within 1 h, which serves as an important mechanism to limit pathogen entry (Melotto et al., 2006). PAMP-induced stomatal closure is regulated by early signalling molecules, such as NO and ROS, as well as ethylene and several oxylipin molecules, which are metabolites from fatty acid oxidation (Arnaud and Hwang, 2015). For example, the enzyme ASPARTATE OXIDASE is required for the PAMP-induced RBOHD-dependent ROS burst and stomatal closure (Macho et al., 2012). flg22-induced stomatal closure shares common regulators with abscisic acid (ABA)-mediated stomatal closure, the key regulator of stomatal closure in abiotic stresses (Deger et al., 2015). For example, the kinase OPEN STOMATA 1 (OST1) regulates both ABA- and flg22-induced stomatal closure (Melotto et al., 2006). The S-type anion channel SLOW ANION CHANNEL1 (SLAC1) and its homolog SLAC1 HOMOLOG 3 (SLAH3) are also required for flg22-induced stomatal closure (Deger et al., 2015). These ion channels contribute to efflux of Cl^-, a major contributor of stomatal closure. STRESS INDUCED FACTOR 2 (SIF2) physically associates with the FLS2-BAK1 PRR complex and interacts with and phosphorylates SLAC1 leading to its activation upon flg22 perception (Chan et al., 2020). PBL27 promotes chitin-induced stomatal closure by phosphorylating SLAH3 (Liu et al., 2019). In addition, flg22 inhibits inward K^+ channel and H^+-ATPase activity that regulates stomatal reopening (Zhang et al., 2008). Recently, the Ca^{2+} channels, OSCA1.3 was reported to be phosphorylated by BIK1 and to regulate stomatal immunity (Thor et al., 2020).

1.4.5.13. Cell wall modifications

Callose is a high molecular weight β-1,3 glucan polymer that strengthens weak or compromised sections of plant cell walls (Luna et al., 2011). Callose deposits form a prominent physical barrier for pathogen attacks and often lead to the formation of papillae. Various elicitors induce callose deposits (Luna et al., 2011). POWDERY MILDEW RESISTANT 4 (PMR4), a glucan synthase-like protein, is involved in callose synthesis and plays an important role in plant resistance against fungal infections (Clay et al., 2009; Luna et al., 2011). Callose deposition is regulated at multiple levels. NADPH oxidase- and peroxidase-produced ROS are required for PAMP-induced callose biosynthesis (Galletti et al., 2008; Daudi et al., 2012). In addition to callose deposition, lignification of the cell wall and expression of lignin biosynthetic genes are also induced upon pathogen infection (Bhuiyan et al., 2009; Miedes et al., 2014; Chezem et al., 2017). Defence-induced lignification is a conserved basal defence mechanism in the plant immune response against (hemi)-biotrophic pathogens in a wide range of plant species (Miedes et al., 2014; Lee et al., 2019). In particular, the SG2-type R2R3-MYB transcription factor MYB15 and CASPARIAN STRIP MEMBRANE DOMAIN PROTEIN(CASP)-LIKE PROTEINS (CASPLs) have been shown to regulate defence-induced lignification (Chezem et al., 2017; Lee et al., 2019).

1.4.5.14. Production of antimicrobial compounds and proteins

Phytoalexins act as toxins for the attacking pathogens as they can delay maturation, disrupt metabolism, and prevent the reproduction of the pathogen and also puncture the cell walls (Ahuja et al., 2012; Tiku, 2020). Camalexin (3-thiazol-2'yl-indole), is the major phytoalexin that accumulates in Arabidopsis in response to fungal and bacterial pathogens (Tsuji et al., 1992; Thomma et al., 1999; Ferrari et al., 2003) and microbial elicitors (Qutob et al., 2006; Gust et al., 2007; Millet et al., 2010; SCHENKE et al., 2011). Camalexin provides resistance to several necrotrophic fungi (Thomma et al., 1999; Kliebenstein et al., 2005; Nafisi et al., 2007) and has also been reported to play a defensive role against the hemibiotrophic fungus *Leptosphaeria maculans* (Bohman et al., 2004; Staal et al., 2006) and the oomycete *Phytophthora brassicae* (Schlaeppi et al., 2010). Indole-glucosinolates, another group of tryptophan-derived secondary metabolites, also participate in Arabidopsis defence against bacteria and fungi and are required for flg22-induced callose deposition (Clay et al., 2009). The tryptophan-derived cyanogenic compound, 4-hydroxyindole-3-carbonyl nitrile, is induced by flg22 treatment and contributes to defence responses in Arabidopsis (Rajniak et al., 2015). In rice, chitin elicits accumulation of terpenoids, the major phytoalexins in monocotyledons (Schmelz et al., 2014). Phenolic compounds, such as phenylamides, are another type of phytoalexins that accumulate in response to PAMP treatment and mainly participate in cell wall reinforcement upon pathogen attacks in rice (Cho and Lee, 2015).

In addition to secondary metabolites, plants produced a variety of proteins with antimicrobial properties. PATHOGENESIS-RELATED (PR) proteins comprise several classes of proteins and peptides induced by microbe, insect or herbivore attack (van Loon et al., 2006). Defensins (PR-12 family), first identified in barley and wheat, are small cysteine-rich proteins with broad antimicrobial activity, especially against fungal infection (Stotz et al., 2011). The defensin *PDF1.2a* gene is induced by pathogens and jasmonic acid (JA)/ET application and is used as a marker for defence against necrotrophic fungal pathogens (Penninckx et al., 1998). Thionins (PR-13 family) are also cysteine-rich peptides, with broad antifungal and antibacterial activities (Epple et al., 1995). Protease inhibitors (PR-6 family), commonly induced by herbivore attack, inhibit digestive enzymes such as chymotrypsin (Sels et al., 2008). Interestingly, PR-1 protein accumulation, used as a marker for defence activation, is associated with systemic acquired resistance (SAR) (van Loon et al., 2006). PR-1 binds and sequestrates sterol from pathogens, which negatively affect pathogen growth such as the sterol-auxotroph oomycete Phytophthora (Gamir et al., 2017). Moreover, a PR1-derived peptide, named CAP-DERIVED PEPTIDE 1 (CAPE 1), was isolated from apoplastic fluids of tomato leaves suggesting that it might act as a DAMP or phytocytokines (Chen et al., 2014). Other enzymes may also directly target pathogens, for example by the degradation of fungal or oomycete cell walls by chitinases or glucanases, respectively, which have both been shown to possess antimicrobial properties (van Loon et al., 2006).

1.4.5.15. Production of phytohormones and systemic resistance

Plant defence hormones, including SA, ET, and JA, have been implicated in PTI responses (Glazebrook, 2005; Pieterse et al., 2012). Consistently, the biosynthesis of these hormones is induced upon PAMP treatment (Felix et al., 1999; Mishina and Zeier, 2007; Flury et al., 2013b). Flg22 induces ET production at 1 h and peaks at 4 h in Arabidopsis seedlings (Liu and Zhang, 2004). It has been shown as well that the 22-kDa fungal protein ETHYLENE-INDUCING XYLANASE (EIX) induces ethylene biosynthesis and defence responses in specific plant species and/or varieties (Ron and Avni, 2004; Van Der Hoorn et al., 2005). Moderate accumulation of SA was detected upon flg22 or LPS treatment in Arabidopsis (Tsuda et al., 2008). In addition, JA production, which is usually induced by necrotrophic pathogen infections, is elevated upon oomycete-derived Pep-13 treatment in potato (Halim et al., 2009). SA, JA, and ET act positively in flg22- and elf18-mediated PTI and mainly contribute to some of the late PTI responses (Tsuda et al., 2009). Additionally, other plant hormones including brassinosteroids (BRs), auxins, ABA, cytokinins, and gibberellins, are also implicated in plant immunity (Couto and Zipfel, 2016). The hormones also regulate systemic resistance, including SAR and induced systemic resistance (ISR) (Durrant and Dong, 2004; Pieterse et al., 2014). SAR and ISR are two forms of induced resistance wherein the plant immune system is primed by a prior localised infection that results in resistance throughout the plant against subsequent challenge by a broad spectrum of pathogens. However, induction

of the two forms of systemic resistance is mechanistically distinct. SAR depends on SA, whereas ISR relies on the signalling pathways activated by JA and ET (Durrant and Dong, 2004; Pieterse et al., 2014). Interestingly, pipecolic acid accumulates upon pathogen infection and confers SAR by increasing levels of the free radicals, NO and ROS (Wang et al., 2018a). SA and ET positively regulate FLS2 expression and consequently flg22-triggered responses (Boutrot et al., 2010; Tintor et al., 2013; Tateda et al., 2014; Yi et al., 2014). Conversely, JA has a negative effect on FLS2-mediated responses, such as ROS burst and callose deposition (Yi et al., 2014). Whether this effect is due to perturbation of FLS2 accumulation and/or a reflection of the JA–SA antagonism remains unknown. Remarkably, several pathogenic *P. syringae* strains produce the phytotoxin coronatine (COR), a structural mimic of a bioactive JA conjugate, as well as effector proteins that directly activate JA signalling (Geng et al., 2014). Consequently, this suppresses SA signalling and inhibits typical PTI responses, such as stomatal closure and cell wall reinforcement (Geng et al., 2014). ET, induced by pathogens, plays both antagonistic and synergistic roles in its relationship with SA, while mostly being synergistic to JA (Yi et al., 2014). ETHYLENE RESPONSE 1 (ETR1) or ETHYLENE INSENSITIVE 2 (EIN2), which are involved in ET perception and signalling, respectively, have been shown to play a critical role in PAMP-induced callose deposition (Clay et al., 2009). JA production seems to be required for flg22-dependent, induction of the AtPep1, PEPR1 and PEPR2 pathway (Flury et al., 2013b; Holmes et al., 2018), which further strengthens PTI responses. In turn, this pathway is synergistically activated by ET and SA during elf18-triggered responses (Felix et al., 1999). Several growth-promoting hormones have been associated with plant immunity. For example, auxin is known to antagonise SA signalling, and some plant pathogens have evolved to hijack auxin signalling and use it to their advantage (Robert-Seilaniantz et al., 2011). Importantly, BRs can inhibit PTI responses (Albrecht et al., 2012; Belkhadir et al., 2012), in a process that is mainly mediated by the TF BRASSINAZOLE-RESISTANT 1 (BZR1) (Lozano-Durán et al., 2013). Among transcriptional target of BZR1, the TF HOMOLOG OF BEE2 INTERACTING WITH IBH1 (HBI1) negatively regulate PTI signalling, while being a positive regulator of BR signalling (Fan et al., 2014; Malinovsky et al., 2014). The current model proposes that BZR1 integrates BR and gibberellin signalling, as well as environmental cues, such as light or darkness, to inhibit PTI via activation of a set of WRKY transcription factors that negatively regulate immunity (Lozano-Durán et al., 2013; Lozano-Durán and Zipfel, 2015). Interestingly, the expression of BR biosynthetic genes is rapidly inhibited following PAMP perception (Jiménez-Góngora et al., 2015), revealing a complex bidirectional negative crosstalk between PTI and BR signalling. Plant hormones make up a flexible and robust system that feeds back either positively or negatively, on immune signalling, and is capable of responding to pathogenic threats, while maintaining homeostasis.

1.4.5.16. Growth inhibition

The activation of defence responses occurs at the expense of growth, a phenomenon, which is commonly known as the growth-defence trade-off (Huot et al., 2014). In Arabidopsis, elicitors such as flg22, elf18 or AtPep1 induce seedling growth inhibition. This growth penalty upon defence activation has long been attributed to resource limitations, whereby energy for growth is allocated to adaptation responses (Lozano-Durán and Zipfel, 2015; Smakowska et al., 2016). However, studies indicate that growth inhibition because of activation of defence responses is not a default program (Eichmann and Schäfer, 2015); instead, the antagonistic relation between growth and defence appears to be the result of incompatible molecular pathways or sharing of signalling components between the programs (Kliebenstein, 2016). A complex network of plant hormones regulates plant growth and development and also exerts direct or indirect effects on plant immunity. Among them, JA, gibberellic acid, BR and SA, have been proposed to modulate the trade-off between growth and immunity (Huot et al., 2014; Lozano-Durán and Zipfel, 2015). There is also a link between apoplastic reactive oxygen species (ROS) homeostasis and cell expansion during leaf growth (Lu et al., 2014; Schmidt et al., 2016). Specifically, the transcription factor KUODA1 (KUA1) promotes cell expansion by repressing the expression of apoplast-targeted PEROXIDASES (POXs) (Lu et al., 2014) to prevent the accumulation of H_2O_2, which stiffens the cell wall and restricts growth (Schöpfer, 1996; Schmidt et al., 2016). The TF HBI1 acts also as a major hub in the central growth regulation circuit of plants that mediates the trade-off between growth and immunity (Bai et al., 2012; Fan et al., 2014; Malinovsky et al., 2014) through transcriptional regulation of ROS homeostasis (Neuser et al., 2019). Growth inhibition also may be connected to the induction of a miRNA that negatively regulates auxin-responsive genes (Navarro et al., 2006). Some of the endogenous RALF peptides similarly cause growth inhibition in seedlings (Pearce et al., 2001; Stegmann et al., 2017). Finally, the transcription factor PHYTOCHROME INTERACTING FACTOR 4 (PIF4) which coordinates thermosensory growth and immunity, acts as a negative regulator of plant immunity, and modulation of its function alters the balance between growth and defence. Importantly, natural variation of PIF4 signalling underlies growth-defence balance in Arabidopsis natural strains (Gangappa et al., 2017)

1.4.6. Negative regulation of PRR signalling in plants

To maintain immune homeostasis, plants use many different strategies to adjust the amplitude and duration of PTI responses (Couto and Zipfel, 2016). These include limiting the ability of PRRs to recruit their cognate co-receptors, regulation of signalling initiation and amplitude at the level of PRR complexes, monitoring of cytoplasmic signal-transducing pathways, and control of transcriptional reprogramming (Couto and Zipfel, 2016).

1.4.6.1. Regulation of the receptor complex formation

Pseudokinases account for at least 10 % of all human and Arabidopsis kinases (Castells and Casacuberta, 2007; Zeqiraj and van Aalten, 2010) and in plants they remain, for the most part, enigmatic. Pseudokinases may be important signalling regulators, by acting as allosteric activators of other kinases, or by promoting or preventing protein-protein interactions (Shaw et al., 2014). In Arabidopsis, the LRR-receptor kinases BIRs have been proposed as general negative regulators of SERK co-receptor mediated LRR-RK signalling pathways (Moussu and Santiago, 2019). BIR2-4 are pseudokinases and BIR2-3 have been shown to dynamically associates with BAK1 (Gao et al., 2009; Blaum et al., 2014; Halter et al., 2014; Imkampe et al., 2017; Ma et al., 2017; Moussu and Santiago, 2019) and negatively regulate BAK1–FLS2 complex formation (Gao et al., 2009; Halter et al., 2014; Imkampe et al., 2017). Upon activation, BAK1 phosphorylates BIR2/3, which promotes their dissociation from the receptor complex, facilitating the formation of an active complex (Halter et al., 2014; Imkampe et al., 2017). Interestingly, BRI1 and BIRs compete for binding of SERKs (Hohmann et al., 2018). Emerging evidence has indicated that NIK1 exhibits a role in modulating PTI (Ahmed et al., 2018). At the resting stage, NIK1 associates with FLS2 or BAK1 to prevent autoimmunity without pathogen invasion. Upon bacterial infection, NIK1 is phosphorylated and leads to activation of an antiviral signal through RPL10 phosphorylation and phosphorylated NIK1 exhibits higher affinity to FLS2 and BAK1, which may lead to receptor complex instability or disassembly, followed by FLS2 ubiquitination and degradation (Li et al., 2019). Two malectin-like-domain RKs ANXUR 1 (ANX1) and ANX2 also associate with FLS2 and BAK1 and negatively regulate FLS2-BAK1 complex formation (Mang et al., 2017). In addition, RALF23 negatively regulates FER and thereby the complex formation between FLS2 and BAK1 (Stegmann et al., 2017; Xiao et al., 2019). APEX associates with PEPR1 and PEPR2 in a ligand-independent manner and negatively regulates PEPR1/PEPR2-mediated and FLS2-mediated immune responses to AtPep1 or flg22.

1.4.6.2. Regulation of receptor complex phosphorylation status

The prominence of kinases within PRR complexes suggests that their phosphorylation status must be kept under tight regulation, especially by protein phosphatases. The reversible nature of this regulation allows plant cells not only to prevent unintended signalling activation but also to modulate signalling amplitude and fine-tune immune responses. It has long been suspected that protein phosphatases were important regulators of plant immunity, as treatment of cell cultures with phosphatase inhibitors was sufficient to initiate responses similar to those triggered by PAMPs (Felix et al., 1994; Chandra and Low, 1995). PRRs are negatively regulated by PROTEIN PHOSPHATASES TYPE 2C (PP2Cs). For example, the rice PP2C XA21-BINDING PROTEIN 15 (XB15) dephosphorylates XA21 *in vitro* and negatively regulates XA21-mediated immune responses (Park et al., 2008). The XB15 orthologues in Arabidopsis

POLTERGEIST-LIKE 4 (PLL4) and PLL5 associate with EFR and have a negative role in EFR-mediated responses (Holton et al., 2015). Another Arabidopsis PP2C, KINASE-ASSOCIATED PROTEIN PHOSPHATASE (KAPP), might negatively regulate FLS2 signalling and other PRRs (Gómez-Gómez et al., 2001; Ding et al., 2007). In addition PP2A, the most abundant protein phosphatase in eukaryotic cells constitutively associates with and negatively regulates BAK1 activity (Segonzac et al., 2014). The activity of the BAK1-associated PP2A is reduced following PAMP perception (Segonzac et al., 2014), suggesting that PP2A itself is negatively regulated to allow PRR complex activation. This demonstrates that tight regulation of PRRs is crucial to prevent unintended activation of downstream RLCKs in the absence of PAMPs. BIK1 phosphorylation is also under dynamic regulation. The protein phosphatase PP2C38 dynamically associates with BIK1, controls its phosphorylation, and negatively regulates BIK1-mediated responses. Notably, PP2C38 is phosphorylated upon PAMP perception, presumably by BIK1, which is required for dissociation of the PP2C38–BIK1 complex, and is likely to enable full BIK1 activation (Couto et al., 2016). Phosphatases are also important for PRRs to return to unstimulated state. CERK1 is autophosphorylated at resting state and upon chitin activation, CERK1-INTERACTING PROTEIN PHOSPHATASE 1 (CIPP1) dephosphorylates CERK1 and dampen signalling (Liu et al., 2018). CIPP1 subsequently dissociates from dephosphorylated CERK1, allowing CERK1 to regain autophosphorylation and return to a standby state (Liu et al., 2018).

1.4.6.3. Regulation of receptor complex protein turnover

Attachment of K48-linked polyubiquitin chains is a universally conserved mechanism among eukaryotes to selectively mark proteins for proteasomal degradation, and an effective way to control the levels of signalling components in the cell (Kondo et al., 2012; Heride et al., 2014). Members of the Arabidopsis Plant U-box (PUB) family of ubiquitin E3 ligases are known to negatively regulate PTI responses. PUB22, PUB23 and PUB24 are negative regulators of ROS production and immune marker gene expression (Trujillo et al., 2008). PUB22 is stabilised upon flg22 perception and mediates proteasomal degradation of Exo70B2, a subunit of the exocyst complex that is required for PTI responses (Stegmann et al., 2012). Other partially redundant members of the same E3 ligase family, PUB12 and PUB13, have been implicated in the degradation of FLS2. Upon flg22 treatment, BAK1 phosphorylates PUB12 and PUB13, promoting their transfer to FLS2, which is then ubiquitylated (Lu et al., 2011). Similarly, modulation of PTI signalling amplitude in Arabidopsis can be achieved by fine-tuning BIK1 protein levels. Arabidopsis CPK28 constitutively associates with BIK1 to control its proteasome-dependent turnover (Monaghan et al., 2014). Under elicitation, CPK28 phosphorylates PUB25 and PUB26 which enhances the E3 ligase activity of PUB25 and PUB26 and accelerates the degradation of nonactivated BIK1 (Wang et al., 2018b). Degradation of PM proteins typically follows the endocytic route, which can also be regulated in an ubiquitin-dependent manner. FLS2, EFR and other PRRs undergo ligand-

dependent endocytosis (Robatzek et al., 2006; Ben Khaled et al., 2015; Mbengue et al., 2016). DYNAMIN 2B (DRP2B), a dynamin required for scission and release of clathrin-coated vesicles during endocytosis, and EPSIN1 (EPS1), a clathrin adaptor implicated in clathrin-coated vesicle formation at the trans-Golgi network (TGN), are required for flg22-induced FLS2 endocytosis (Smith et al., 2014; Collins et al., 2020). Other components of the endocytic machinery have been shown to negatively regulate plant defence (Ben Khaled et al., 2015).

1.4.6.4. Regulation of MAPK cascades

MAPKs are instrumental for transcriptional reprogramming by directly or indirectly controlling the activity of transcription factors following PAMP perception (Arthur and Ley, 2013; Meng and Zhang, 2013; Lee et al., 2015; Tsuda and Somssich, 2015). Thus, the actions of MAPKs must be also controlled. The MAP3K MKKK7 associates with FLS2 and is phosphorylated upon flg22 treatment, negatively regulating flg22-triggered MPK6 activation and the ROS burst through unknown mechanisms (Mithoe et al., 2016). Phosphorylation of both Tyr and Thr residues in the activation loop of MAPK is crucial for activation; consequently, dephosphorylation of any of these residues renders them inactive (Caunt and Keyse, 2013). Dual-specificity protein phosphatases (DUSPs; also known as MAPK PHOSPHATASES (MKPs)) dephosphorylate both these residues and are important modulators of MAPK activity during innate immunity in mammals (Arthur and Ley, 2013; Caunt and Keyse, 2013). In Arabidopsis, DUSPs, as well as PROTEIN TYR PHOSPHATASES (PTPs) and protein Ser/Thr phosphatases (in particular PP2Cs) also target PRR-activated MAPKs. The closely related PP2Cs PP2C-type phosphatase AP2C1 and PP2C5 regulate PRR-dependent MPK3 and MPK6 activation (Brock et al., 2010; Galletti et al., 2011). In addition to its effects on MPK3 and MPK6, AP2C1 was shown to inactivate MPK4 (Schweighofer et al., 2007). The DUSPs MKP1 and PTP1 regulate MPK3 and MPK6 in a partially redundant manner. MPK1 negatively regulates elf26-dependent responses and MPK3 and MPK6 activation (Anderson et al., 2011). In addition, MAPK activation is guarded indirectly by the NLRs SUPPRESSOR OF NPR1-1, CONSTITUTIVE 1 (SNC1) (Bartels et al., 2009) and SUMM2 (Zhang et al., 2012; Roux et al., 2015). MPK2 dephosphorylate both MPK3 and possibly MPK6, during the early stages of *B. cinerea* infection (Lumbreras et al., 2010). Together, this demonstrates the importance of the regulation of MAPKs and immune responses.

1.4.6.5. Transcriptional and translational regulation

Several mechanisms are in place that negatively regulate activation of immune-related genes, at the levels of transcription, mRNA stability, splicing, and translation. First, at the level of transcription factors, ARABIDOPSIS SH4- RELATED 3 (ASR3) is a plant-specific trihelix transcription factor that acts as a transcriptional repressor during PTI (Li et al., 2015a). Phosphorylation of ASR3 by MPK4 upon

flg22 elicitation enhances its DNA affinity. With this action, MPK4 promotes binding of ASR3 to the promoter regions of flg22-upregulated genes, such as FRK1, initiating a negative feedback mechanism to fine-tune immune gene expression (Li et al., 2015a). Interestingly, while MED19a promotes expression of *PR1*, FIBRILLARIN 2 (FIB2) directly interacts with MED19a and acts as a negative transcriptional regulator for immune responsive genes, including *PR1* (Seo et al., 2017; Seo et al., 2019). Acting on transcription more generally, CTD PHOSPHATASE-LIKE 3 (CPL3) was also shown to dephosphorylate PAMP-activated CTD phosphorylation of RPII and negatively regulates expression of a large portion of PAMP-responsive genes (Li et al., 2014a). At the level of mRNA stability, the positive role of PARylation in PTI signalling can be reversed by the action of PAR GLYCOSYLHYDROLASES (PARGs). PARG1 was found to negatively regulate PAMP-induced gene transcription (Feng et al., 2015). Furthermore, mRNA with an enriched-purine sequence are translationally regulated through interaction with poly(A)-binding proteins (Xu et al., 2017b). In addition, alternative splicing (AS) of pre-mRNAs in plants is an important mechanism of gene regulation. MPK4 was found to be a key regulator of PAMP-induced differentially AS events as the AS of several splicing factors and immunity-related protein kinases are affected, such as the calcium-dependent protein kinase CPK28, the CYSTEINE-RICH RLK 13 (CRK13) and CRK29 or the FLS2 co-receptor SERK4/BKK1 (Bazin et al., 2020). Besides, PRRs RK, SNC4 and CERK1 were shown to undergo AS in responses to PAMPs (Zhang et al., 2014; Sanabria and Dubery, 2016). Upon bacterial infection, NIK1-induced RIBOSOMAL PROTEIN L10 (RPL10) phosphorylation leads to suppression of translational machinery-related gene expression (Li et al., 2019). DECAPPING PROTEIN 1 (DCP1) phosphorylation by immune-activated MAPKs contributes to P-body disassembly and mRNA decay on a subset of immune-regulated genes, revealing mRNA-decay-mediated posttranscriptional regulation (Yu et al., 2019a). In addition, RHs function to limit the accumulation and translation of stress-responsive mRNAs associated with autoimmunity to maintain the growth-defence balance in plants (Chantarachot et al., 2020).

1.4.6.6. Pathogen effectors

Plant-adapted pathogens suppress or evade plant immunity through the use of secreted protein effectors, many of which directly target the PRR complexes (Albert et al., 2020). Bacterial pathogens utilise a type-III secretion system to transport effectors that suppress the catalytic activity of RKs (Göhre et al., 2008; Shan et al., 2008; Macho et al., 2014), degrade PRRs (Göhre et al., 2008; Gimenez-Ibanez et al., 2009a; Li et al., 2016c), or inhibit phosphorylation of PRRs and RLCKs (Zhang et al., 2010a; Feng et al., 2012; Yamaguchi et al., 2013). No bacterial effectors have been found to target the extracellular domain of PRRs.

Typical examples include the *avrPto* gene of *Pto*, which can target multiple LRR-RKs (*e.g*. FLS2, EFR, and BAK1) (Shan et al., 2008; Xiang et al., 2008); AvrPtoB, which can target both LRR-RKs (*e.g.* FLS2

and BAK1) and LysM-RK CERK1 (Göhre et al., 2008; Gimenez-Ibanez et al., 2009a); the tyrosine phosphatase HopAO1, which can target FLS2 and EFR (Macho et al., 2014); and the cysteine protease AvrPphB, which degrades RLCKs; and the 59-monophosphate transferase AvrAC that uridylates RLCKs (Zhang et al., 2010a; Feng et al., 2012). Effectors do not act solely through degrading host immune signalling components, they also inhibit or modulate immune signalling. The *Pto* DC3000 T3SE HopU1 is a mono-ADP-ribosyltransferase (mono-ADP-RT) required for full virulence in Arabidopsis (Fu et al., 2007). HopU1 targets at least five different Arabidopsis RBPs, including GLYCINE-RICH PROTEIN 7 (GRP7) and GRP8 (Fu et al., 2007). HopU1 modulates EFR and FLS2 levels by blocking the interaction of their mRNAs with GRP7 (Nicaise et al., 2007). Interestingly, thus far, no oomycete effectors have been definitively shown to target PRRs. However, some *Phytophthora infestans* RxLR effectors suppress plant early immune responses (Zheng et al., 2014). The RxLR effector SUPPRESSOR OF EARLY FLG22-INDUCED IMMUNE RESPONSE 5 (SFI5) suppresses ROS accumulation and MAPK activation triggered by flg22 in a Calcium/calmodulin- dependent manner in both Arabidopsis and tomato (Zheng et al., 2018). The eATP receptor LecRK- I.9/DORN1 is implicated as a possible target of the *P. infestans* RxLR effector IPI-O (Bouwmeester et al., 2011). Unlike bacterial and oomycete effectors, a limited number of fungal effectors have been functionally characterised. The vascular fungal pathogen *Fusarium oxysporum* produces small secreted peptides homologous to plant RALFs (F-RALFs). F-RALFs induce host alkalinisation, which is required for the infection of some hemi-biotrophic fungi (Masachis et al., 2016). F-RALFs negatively regulate the host ROS accumulation, callose deposition, and PR gene expression during fungal infection. F-RALF-mediated immune suppression was hypothesized to act via mimicking endogenous FER-targeting RALF peptides (Masachis et al., 2016). Interestingly, many other phytopathogenic fungi produce RALF-like peptides with functions (Thynne et al., 2017). Another conserved fungal effector named NECROSIS-INDUCING SECRETED PROTEIN 1 (NIS1) from *Colletotrichum spp.* and *Magnaporthe oryzae* was found to inhibit autophosphorylation of BAK1 and BIK1 (Irieda et al., 2019). NIS1 also disrupts BIK1 association with RBOHD upon flg22 treatment. Interestingly, NIS1 not only suppresses immune responses triggered by the extracellular patterns flg22, INF1, and chitin, but also responses triggered upon recognition of the *P. infestans* effector Avr3a (Irieda et al., 2019). In addition, insects or nematodes produce numerous effectors that suppress immunity (Hogenhout and Bos, 2011; Mejias et al., 2019), and nematodes are known to manipulate RKs in other signalling pathways through ligand mimicry (Hu and Hewezi, 2018).

1.4.7. Roles of intracellular immune receptors

In both plant and animal innate immunity systems, specific intracellular immune receptors, NLRs, protect the organisms against pathogen invasion by activating immunity upon detection of pathogen invasion-associated molecules (Duxbury et al., 2016; Mermigka et al., 2020). Pathogen perception by

NLRs can lead to activation of localised programmed cell death (PCD) (Danial and Korsmeyer, 2004), known in plants as the hypersensitive response (HR), whose main role is to restrict pathogens from spreading in host tissues and typically leads to the prevention of the disease development (Van Der Biezen and Jones, 1998; Duxbury et al., 2016; Jones et al., 2016). NLR proteins are divided into two major subclasses that have distinct N-terminal domains (Cui et al., 2015). NLR with a toll-interleukin 1 receptor (TIR) domain are called TNLs, and those with a coiled-coil (CC) domain are called CNLs (Maekawa et al., 2011; Griebel et al., 2014). NLRs operate as molecular switches that cycle between a closed, ADP-bound "off" (autoinhibited) state and an open, ATP-bound "on" (activated) state (Takken and Goverse, 2012; Hu et al., 2013; Griebel et al., 2014). The N-terminal TIR or CC and C-terminal LRR domains cooperate to inhibit the nucleotide-binding (NB) domain from ATP/ADP exchange (Takken and Goverse, 2012; Griebel et al., 2014). A sequence of conformational transitions from the off to the on state opens up the molecule to expose the N-terminal domains for interaction with signalling components (Takken and Goverse, 2012; Griebel et al., 2014). Most NLRs require downstream signalling components for HR activation. Multiple CNLs recruit PM-anchored integrin-like protein NON-RACE-SPECIFIC DISEASE RESISTANCE 1 (NDR1) (Day et al., 2006; Knepper et al., 2011) whereas TNLs require the nucleocytoplasmic lipase-like protein ENHANCED DISEASE SUSCEPTIBILITY 1 (EDS1); this protein, generally dispensable for CNL resistance (Wiermer et al., 2005). Both are important junctions at which NLRs engage the basal resistance machinery. The mechanisms by which the NDR1 and EDS1 proteins function in ETI are also different (Cui et al., 2015). NDR1 anchors RIN4, which is guarded by the CNLs RESISTANCE TO P. SYRINGAE PV MACULICOLA 1 (RPM1) and RESISTANT TO P. SYRINGAE 2 (RPS2), at the PM (Day et al., 2006; Knepper et al., 2011). By contrast, Arabidopsis EDS1 forms soluble nucleocytoplasmic and nuclear signalling complexes with two sequence-related signalling partners, PHYTOALEXIN-DEFICIENT 4 (PAD4) and SENESCENCE-ASSOCIATED GENE 101 (SAG101), respectively (Feys et al., 2005; Rietz et al., 2011). Besides, NLR signalling rapidly augments the transcript and protein levels of key components of PRR signalling at an early stage and in a SA-independent manner (Ngou et al., 2020; Yuan et al., 2020). Plant NLRs can also act as pairs and can exhibit head-to-head chromosomal orientation to facilitate co-expression (Le Roux et al., 2015; Sarris et al., 2015; Lolle et al., 2020). Most NLR pairs consist of a canonical signalling NLR, such as RPS4, and a sensor NLR carrying an integrated domain that interacts with an effector target, such as RESISTANT TO RALSTONIA SOLANACEARUM 1 (RRS1)-R with a WRKY domain (Le Roux et al., 2015; Sarris et al., 2015). Some sensor NLRs can rely on a partially redundant network of helper NLRs to form a functional unit for disease resistance (Wu et al., 2017a). For some plant NLRs, pathogen recognition occurs via the direct interaction between NLR and specific pathogen effectors. For example, the LRR domains of the plant RECOGNITION OF PERONOSPORA PARASITICA 1 (RPP1) and Pi-ta NLR receptors interact with their cognate ligands (Jia et al., 2000; Krasileva et al., 2010). For several plant NLRs, pathogen

recognition occurs indirectly (Duxbury et al., 2016). To explain this indirect recognition, "guard/decoy" models have been proposed. According to these models, some plant NLRs guard specific host components involved in plant immunity (guardee), or proteins with no obvious role in plant immunity (decoy) that have been proposed to function as pathogen "effector baits", and detect modifications triggered by pathogen effectors during host colonisation (Duxbury et al., 2016; Lolle et al., 2020). Both the guard and decoy recognition models propose efficient mechanisms by which a host plant can use a limited number of NLR receptors to recognise different pathogens through the specific guarding of a limited number of host proteins (Lolle et al., 2020).

Despite their importance, how intracellular immune receptors confer disease resistance is still unknown. Recent insights in the activation mechanism of the plant CNL-type HOPZ-ACTIVATED RESISTANCE 1 (ZAR1) suggest that CNLs form a pentameric complex termed resistosome, which might form a pore at the PM (Wang et al., 2019b; Wang et al., 2019c). However, the mechanism of TNL activation remains elusive, as there is no structural evidence for TNL resistosome formation. Recently, TIR domains of both plant and animal NLRs were reported to possess an NADase activity that requires TIR domain oligomerisation and leads to immune response activation (Horsefield et al., 2019; Wan et al., 2019a). However further investigation will be required to understand whether the NADase activity of TIR domain is fully responsible for NTI activation, and why NAD^+ cleaving only happens in the presence of TIR self-association.

1.5. Aim of the thesis

Plant immunity is a signalling pathway which is tightly regulated to prevent excessive or untimely activation of immune responses. Immune homeostasis is thus maintained at different levels through regulatory mechanisms. Despite recent advances, our knowledge of the molecular events occurring downstream of PRR activation is still limited, especially about negative regulation of immune signalling (Couto and Zipfel, 2016; Albert et al., 2020). In order to identify novel components playing a key role in the early signalling events leading to the establishment of PTI and especially in the regulation of ROS production, a forward genetic was performed in the immunodeficient allele *bak1-5*. From this screen, 10 suppressor mutants named *modifier of bak1-5 1* to *10* (*mob1-10*) were isolated and regained elicitor-induced ROS production. Four *mob* mutants have already been characterised and revealed roles in the negative regulation of PTI (Monaghan et al., 2014; Monaghan et al., unpublished; Stegmann et al., 2017). The central question of the thesis is thus: What are the *MOBs* and how they regulate elicitor-induced ROS production. This project will focus on the uncharacterised mutants *mob7*, *mob8*, *mob9* and *mob10*. Depending on the mutation two main hypotheses are plausible on the role of the MOBs. The first hypothesis is that the MOBs are negative regulators of ROS production in the case of loss-of-function mutations. On the other hand, MOBs could be positive regulator if the mutation leads to a gain-of-

function. The first objective will be to define the phenotypes of these mutants upon various immune elicitors and pathogen. Mutations within *mob* mutants will be then mapped and confirmed through different approaches in order to identify the mutations responsible for *mob* phenotypes. Afterwards, the functional characterisation of MOB proteins will be performed to understand mechanistically their function and involvement in immune signalling. Biochemical assays will be accomplished to further investigate the spectrum of proteins regulated by MOBs. In addition, cell biological studies will be conducted to analyse the subcellular localisation of the respective proteins. This project aims thereby to contribute to unravelling the complexity of the regulatory network in immune signalling.

2. Materials and methods

2.1. Plant material and growth conditions

2.1.1. *Arabidopsis thaliana*

2.1.1.1. Growth conditions

Arabidopsis thaliana plants were grown on soil as one to four plants per pot (7 x 7 cm) in controlled environment rooms maintained at 20°C with a 10-hour photoperiod and 60 % humidity, or as seedlings on sterile Murashige and Skoog (MS) media supplemented with vitamins and 1 % sucrose (Duchefa) with a 16-hour photoperiod. Assays using soil-grown plants were performed at 4 to 6 weeks post germination (wpg), before the reproductive transition. Assays using plate-grown seedlings were performed at 2 wpg. *A. thaliana* ecotype Columbia-0 (Col-0) was used as a wild-type control for all plant assays and was the background for all mutants and transgenic lines used in this study, except otherwise stated (Table 2.1).

Allele/Line	Details	Gene	Source	Description	Reference
Col-0			Zipfel lab stock	Columbia 0, wild-type reference line.	
Col-0 *35S-eGFP-cCBE1*		*AT4G01290*		Transgenic line overexpressing tagged-CBE1	
Col-0 *35S-cCBE1-eGFP*		*AT4G01290*		Transgenic line overexpressing tagged-CBE1	
Col-0 *pCBE1-gCBE1-eGFP*		*AT4G01290*		Transgenic line overexpressing tagged-CBE1	
Col-0 *pUBI10-cCBE1-eGFP*		*AT4G01290*		Transgenic line overexpressing tagged-CBE1	
La-*er*			Zipfel lab stock	Landsberg *erecta* ecotype, parental mapping line.	
bak1-4	SALK_ 116202	*AT4G33430*	Zipfel lab stock	Knock-out mutant.	(Chinchilla et al., 2007)
bak1-5		*AT4G33430*	Zipfel lab stock	EMS-induced missense substitution mutant, three times back-crossed to Col-0. Semi-dominant mutant.	(Schwessinger et al., 2011)
bak1-5 mob7				EMS-induced mutant. M_5 generation	
bak1-5 mob7 x bak1-5				F_3 generation from the backcross, used for whole-genome sequencing	
bak1-5 mob7 x a-La-*er*				F_2 generation from the outcross, used for map-based cloning	
bak1-5 mob7 35S-cCBE1-eGFP		*AT4G01290*		Complementation line overexpressing tagged-CBE1	
bak1-5 mob7 35S-eGFP-cCBE1		*AT4G01290*		Complementation line overexpressing tagged-CBE1	

bak1-5 mob7 35S-cCBE1-eGFP		*AT4G01290*		Complementation line overexpressing tagged-CBE1	
bak1-5 mob7 pCBE1-gCBE1-eGFP		*AT4G01290*		Complementation line expressing tagged-CBE1	
bak1-5 mob7 pCBE1-gCBE1(S473A)-eGFP		*AT4G01290*		Complementation line expressing phosphomimetic variant of tagged-CBE1	
bak1-5 mob7 pCBE1-gCBE1(S473D)-eGFP		*AT4G01290*		Complementation line expressing phosphodead variant of tagged-CBE1	
bak1-5 mob7 pUBI10-cCBE1-eGFP		*AT4G01290*		Complementation line overexpressing tagged-CBE1	
bak1-5 mob8				EMS-induced mutant. M_5 generation	
bak1-5 mob9				EMS-induced mutant. M_5 generation	
bak1-5 mob10				EMS-induced mutant. M_5 generation	
bik1 pbl1	SALK_005291 ; SAIL_1236_D07	*AT3G55450 ; AT2G39660*	Zipfel lab stock	Double knock-out mutant	(Zhang et al., 2010a)
cbe1-1	WiscDsLoxHs188_10F	*AT4G01290*	Karen Browning	Knock-out mutant	(Patrick et al., 2018)
cbe1-1 35S-eGFP-cCBE1		*AT4G01290*		Complementation line overexpressing tagged-CBE1	
cbe1-1 35S-cCBE1-eGFP		*AT4G01290*		Complementation line overexpressing tagged-CBE1	
cbe1-1 pCBE1-gCBE1-eGFP		*AT4G01290*		Complementation line expressing tagged-CBE1	
cbe1-1 pCBE1-gCBE1(S473A)-eGFP		*AT4G01290*		Complementation line expressing phosphomimetic variant of tagged-CBE1	
cbe1-1 pCBE1-gCBE1(S473D)-eGFP		*AT4G01290*		Complementation line expressing phosphodead variant of tagged-CBE1	
cbe1-1 pUBI10-cCBE1-eGFP		*AT4G01290*		Complementation line overexpressing tagged-CBE1	
ceres-1	SALK_129709	*AT4G23840*	Mar Castellano	Knock-out mutant	(Toribio et al., 2019)
ceres-2	SALK_054336	*AT4G23840*	Mar Castellano	Knock-out mutant	(Toribio et al., 2019)
cum1-1		*AT4G18040*	Karen Browning	EMS-induced mutant in EIF4E1. Knock-out mutant	(Yoshii et al., 1998)
eif4g	SALK_80031	*AT3G60240*	Karen Browning	Knock-out mutant	(Patrick et al., 2018)
eifiso4e	SLAT line	*AT5G35620*	Karen Browning, Christophe Robaglia	Knock-out mutant	(Duprat et al., 2002)
eifiso4g1	SALK_009905	*AT5G57870*	Sylvie German-Retana	Knock-out mutant	(Nicaise et al., 2007)

eifiso4g2	SALK_ 076633	*AT2G24050*	Sylvie German-Retana	Knock-out mutant	(Nicaise et al., 2007)
eifiso4g1 eifiso4g2	SALK_ 009905; SALK_ 076633	*AT5G57870; AT2G24050*	Karen Browning	Double knock-out mutant	(Nicaise et al., 2007)
GK_150_H09 (WT)	GK_150_ H09	*AT4G01290*		Wild-type derived from segregation of GK_150_H09	
GK_150_H09 (HOM)	GK_150_ H09	*AT4G01290*		Knock-out mutant	
mob7				F_3 from cross *bak1-5 mob7* x Col-0	
pat1-1	SALK_ 040660	*AT1G79090*	Morten Petersen	Knock-out mutant	(Roux et al., 2015)
pat1-1 summ2-8	SALK_ 040660; SAIL_ 1152A06	*AT1G79090; AT1G12280*	Morten Petersen	Double knock-out mutant	(Roux et al., 2015)
rbohd	SLAT line	*AT5G47910*	Zipfel lab stock	Knock-out mutant	(Torres et al., 2002)
SALK_038452 (WT)	SALK_03 8452	*AT4G01290*		Wild-type derived from segregation of SALK_038452	
SALK_038452 (HOM)	SALK_03 8452	*AT4G01290*		Knock-out mutant	
summ2-8	SAIL_ 1152A06	*AT1G12280*	Morten Petersen	Knock-out mutant	(Roux et al., 2015)
upf1-5	SALK_ 112922	*AT5G47010*	Nottingham Arabidopsis Stock Centre	Knock-down mutant	(Arciga-Reyes et al., 2006)

Table 2.1 List of *Arabidopsis thaliana* lines used in this study.
c[GENE] refers to the cDNA of the gene obtained from its transcripts and g[GENE] refers to the genomic sequence of the gene.

2.1.1.2. Stable transformation of Arabidopsis

Transgenic Arabidopsis plants were generated using floral dip method (Clough and Bent, 1998). Briefly, flowering Arabidopsis plants were dipped into suspension culture of *Agrobacterium tumefaciens* GV3101 carrying the indicated plasmid. Plants carrying a T-DNA insertion event were selected either on MS medium containing the appropriate selection or as soil-grown seedlings by spray application of Basta (Bayer Crop Science). Plants containing multiple transgenes were generated through crosses.

2.1.1.3. Arabidopsis seed sterilisation

Arabidopsis seeds were sterilized in 1.5-mL tubes by either chlorine gas or bleach. For chlorine gas, 75 mL of 5 % sodium hypochlorite solution was combined with 3 mL of 37 % HCl in a closed container with the seeds and left closed for 4-8 h. After the sterilisation period, the seeds were aired in the flow hood for at least 1 h. For sterilisation using bleach, seeds were first washed with 70 % ethanol, before adding a solution containing 6 % sodium hypochlorite, 0.005 % Triton X-100 (AppliChem). After 5 min, seeds were centrifuged at 7,500 x*g* and washed four times with sterile water. After both methods of sterilisation, seeds were stratified at 4 °C for 2 d in the dark.

2.1.1.4. Generation of Arabidopsis progeny

Fine tweezers were used to emasculate individual flowers. To prevent self-pollination, only flowers that had a well-developed stigma but immature stamens were used for crossing. Fresh pollen from three to four independent donor stamens was dabbed onto individual stigma. Mature siliques containing F_1 seeds were harvested and approximately five F_1 seeds per cross were grown and allowed to self-pollinate.

2.1.2. *Nicotiana benthamiana*

2.1.2.1. Growth conditions

Nicotiana benthamiana plants were grown on soil as one plant per pot (8 x 8 cm) at 25 °C during the day with 16 h light and at 22 °C during the night (8 h). Relative humidity was maintained at 60 %.

2.1.2.2. Transient expression

N. benthamiana plants were used for transient transformation at 4 to 5 wpg. *Agrobacterium tumefaciens* GV3101 overnight cultures grown at 28 °C in low-salt LB were harvested by centrifugation at 2,500 x*g* and resuspended in buffer containing 10 mM $MgCl_2$, 10 mM MES for 3 h at room temperature. *A. tumefaciens*-mediated transient transformation of *N. benthamiana* was performed by infiltrating leaves with OD_{600}=0.2 of each construct together with P19 construct in a 1:1 ratio. Samples were collected 2-3 d after infiltration.

2.2. Elicitor assays

2.2.1. Elicitors

The following elicitors were used in this study: chitin (Nacosy) , flg22 peptide (CKANSFREDRNEDREV) (Felix et al., 1999), elf18 peptide (ac-SKEKFERTKPHVNVGTIG) (Kunze et al., 2004) and AtPep1 peptide (ATKWKAKQRGKEKVSSGRPGQHN) (Huffaker et al., 2006). All peptides were synthesized by SciLight-peptide, China with a purity above 95% and dissolved in water.

2.2.2. Seedling growth inhibition

Seedling growth inhibition was performed as previously described (Schwessinger et al., 2011). Sterilised and stratified seeds were sown on MS media and grown in controlled environment rooms. Five-day-old seedlings were transferred into liquid MS with or without the indicated amount of peptide. Ten to twelve days later, individual seedlings were gently blotted-dry and weighed using a precision scale (Sartorius).

2.2.3. ROS burst assays

Reactive oxygen species (ROS) production was measured as previously described (Schwessinger et al., 2011). For the assay, either adult plants (4-to-6-week-old plants) or seedlings (2-week-old) were used. For adult plants, leaf discs (4 mm diameter) were collected using a biopsy punch and floated overnight on distilled, deionised water in a white 96-well plate to recover. For ROS assays on whole seedlings, seedlings were grown on MS agar plates for 5 d before being transferred to MS liquid medium in transparent 96-well plates. After 8 d or when the seedling was almost the size of the well, seedlings were transferred to a white 96-well plate and allowed to recover overnight in sterile water. The water was then removed and replaced with an eliciting solution containing 17 µg/mL luminol (Sigma-Aldrich), 100 µg/mL horseradish peroxidase (Sigma-Aldrich), and an appropriate concentration of the desired PAMP. For seedlings, luminol was replaced by 0.5 µM L-012 (Fujifilm). Luminescence was recorded over a 40-to-60-minute period using a charge-coupled device camera (Photek Ltd., East Sussex UK).

2.2.4. MAP kinase phosphorylation assay

Phosphorylation of mitogen-activated protein kinases (MAP Kinases) was measured as previously described (Flury et al., 2013a). Either adult plants (4-to-6-week-old plants) or seedlings (2-week-old) were used. Arabidopsis seedlings were grown for 5 d on MS agar plates and then transferred to liquid MS in 24-well plates. After 9 d, liquid MS was replaced with distilled, deionised water. For adult plants, leaf discs were cut in the evening and left overnight, floating in 6-well plates on distilled, deionized water. In the morning, the elicitor peptide was added to the desired concentration and tissue was blotted dry and flash-frozen in liquid nitrogen for protein extraction at the indicated time points. MAP kinase phosphorylation was measured via western blot using an antibody specific to the active phosphorylated form of the proteins (phospho-p44/42 MAPK). Two seedlings or 15 leaf discs were used per condition.

2.2.5. PAMP-induced defence gene induction

Either adult plants (4-to-6-week-old) or seedlings (2-week-old) were used. Arabidopsis seedlings were grown for five days on MS agar plates and then transferred to liquid MS in 24-well plates. After 9 d, liquid MS was replaced with distilled, deionized water. For adult plants, leaf discs were cut in the evening and left overnight, floating in 6-well plates on distilled, deionized water. In the morning, the elicitor was added. Two seedlings or 15 leaf discs were used per condition. Tissue was flash frozen for RNA extraction.

The expression of each marker gene was normalised to the internal reference gene *AT4G05320* (*MUSE3/UBOX*) or *AT3G18780* (*ACTIN 2*).

2.3. Pathogen assays

2.3.1. Bacterial spray inoculation of Arabidopsis

Spray inoculations were performed as previously described (Katagiri et al., 2002). *Pseudomonas syringae* pv. *tomato* (*Pto*) DC3000 *COR*$^-$ (defective in production of the phytotoxin coronatine) strain (Melotto et al., 2006) was grown in overnight culture in King's B medium supplemented with 50 µg/mL rifampicin, 50 µg/mL kanamycin and 100 µg/mL spectinomycin and incubated at 28°C. Cells were harvested by centrifugation and pellets resuspended in 10 mM $MgCl_2$ to an OD_{600} of 0.2, corresponding to $1x10^8$ CFU/mL. Immediately before spraying, Silwet L-77 (Sigma Aldrich) was added to a final concentration of 0.04 %. Four-to-five-week-old plants were uniformly sprayed with the suspension and covered with a clear plastic lid for 3 d. Three leaf discs (4 mm) were taken using a biopsy punch from three respective leaves of one plant and ground in collection microtubes (Qiagen), containing one glass bead (3 mm) and 200 µL water each, using a 2010 Geno/Grinder (SPEX) at 1,500 rpm for 1.5 min. Ten microliters of serial dilutions from the extracts were plated on L agar medium containing antibiotics and 25 µg/mL nystatin (Melford). Colonies were counted after incubation at 28 °C for 1.5 to 2 d.

2.4. Mapping

2.4.1. Genetic analysis of *mob* mutants

To determine inheritance, *bak1-5 mob7*, *bak1-5 mob8*, *bak1-5 mob9* and *bak1-5 mob10* were back-crossed to *bak1-5*. Segregating F_2 plants were scored, based on PAMP-induced ROS or PAMP-induced seedling growth inhibition.

2.4.2. Map-based cloning

The *bak1-5 mob7* mutant (in Col-0) was crossed to La*er*. Fifty six F_2 segregants were genotyped for *bak1-5* using a dCAPS marker. Homozygous *bak1-5* segregants were phenotyped for PAMP-induced ROS production similar to *mob7*. Linkage analysis was performed using genome-wide markers designed in-house or by the Arabidopsis Mapping Platform (Hou et al., 2010) (Table 2.4).

2.4.3. Whole-genome resequencing

Four hundred forty F_2 plants from the cross *bak1-5 mob7* with *bak1-5* were scored for chitin-induced ROS production. One hundred thirty-three plants showed moderately increased and 93 plants highly increased ROS production. Out of these 93 plants, 70 were tested in the F_3 generation, and only 15 showed a confirmed phenotype to restore AtPep1-induced -seedling growth inhibition in 3 experiments. Thirty seedlings from each of the positive F_3 parents were bulked and ground to a fine powder in liquid nitrogen and gDNA extracted. Ground tissues was equilibrated in buffer containing 50 mM Tris-HCl

(pH 8.0), 200 mM NaCl, 2 mM EDTA for 30 min at 37 °C with occasional mixing, and a further 20 min at 37 °C with 0.2 mg/mL RNase. Roughly 10 ng of genomic DNA was then extracted using a standard chloroform/phenol method and resuspended in TE buffer (10 mM Tris HCl pH 7.5;1 mM EDTA pH 8). Prepared gDNA of pooled *bak1-5 mob7* F3s as well as *bak1-5* as a reference was submitted to The Beijing Genomics Institute (Hong Kong) for Illumina-adapted library preparation and paired-end sequencing using the High-Seq 2000 platform. Average coverage from Illumina sequencing of *bak1-5 mob7* over the nuclear chromosomes was 15.79. Paired-end reads were aligned to the TAIR10 reference assembly using BWA v 0.6.1 with default settings (Li and Durbin, 2009). BAM files were generated using SAMTools v 0.1.8 (Li and Durbin, 2009) and single-nucleotide polymorphisms (SNPs) were called using the mpileup command. High quality SNPs were obtained using the filters (1) Reads with mapping quality less than 20 were ignored; (2) SNP position had a minimum coverage of 6 and a maximum of 250; (3) the reference base must be known; and (4) SNPs were present in *bak1-5 mob7* but not *bak1-5* control. Resulting pileup files contained a list of SNPs and their genomic positions. SNPs unique to *bak1-5 mob7* and not present in the *bak1-5* control were identified. SNPs passing filters were analysed on CandiSNP (Etherington et al., 2014). Relevant SNPs were confirmed in the original *bak1-5 mob7* mutant and backcrossed lines by Sanger sequencing of PCR amplicons. All primers used are listed in Table 2.4.

2.5. Molecular biology

2.5.1. DNA methods

2.5.1.1. Isolation of genomic DNA from Arabidopsis

DNA extractions were performed based on previously described protocol (Edwards et al., 1991). Small leaf samples from young tissue were collected with a pair of tweezers into either 2-mL tubes or collection microtubes (Qiagen) containing two or one glass beads (3 mm) respectively. Tissue was ground to a fine powder using a 2010 Geno/grinder (SPEX) at 1,500 rpm for 1.5 min. Three hundred microliters (tubes) or 200 µL (microtubes) of DNA extraction buffer [0.2 M Tris-HCl pH 7.5; 0.25 M NaCl; 0.025 M EDTA; 0.5 % (w/v) SDS] were added. The solution was centrifuged at 16,000 x*g* (tubes) or 2,500 x*g* (microtubes) for 10 min and 250 µL (tubes) or 100 µL (microtubes) of the supernatant was transferred to a fresh tube or 96-well PCR plate. One volume of isopropanol was added to precipitate DNA and centrifuged for 30-40 min at 12,000 x*g* (tubes) or 2,500 x*g* (plate). The supernatant was discarded carefully. The pellet was washed with 70 % ethanol and dried. Finally, the pellet was dissolved in 100 µL TE buffer (10 mM Tris HCl pH 7.5;1 mM EDTA pH 8) and 1 µL of the DNA solution was used for a 20 µL PCR reaction mixture. Genomic DNA was stored at 4 °C or -20 °C for long-term storage.

2.5.1.2. PCR methods

2.5.1.2.1. Standard PCR

This method was used when sequence accuracy was not required (*e.g.* genotyping, colony PCR). Briefly, a PCR reaction master mix [1X buffer; 0.2 mM of each dNTP; 0.25 µM of each primer; 0.2 pg–20 ng/µL of template DNA; 0.0125 U/µL polymerase] was prepared per primer set. Cycling conditions were as follows: one pre-incubation cycle (95 °C, 3 min), 35 amplification cycles [(denaturation: 95 °C, 30 s), (annealing: Tm-5 °C of the primers, 30 s), (elongation: 72 °C, 1 min/kb)], one final elongation (72 °C, 10 min).

2.5.1.2.2. Colony PCR

The previously described PCR conditions were used with slight adjustments. A small pipette tip, dipped into colonies showing antibiotic resistance, was added to 20 µL dH2O and 2 µL of this solution was used per 20 µL PCR reaction.

2.5.1.2.3. High-fidelity PCR

This method was used when sequence accuracy was required (*e.g.* cloning, sequencing). Briefly, a PCR reaction master mix [1X buffer; 0.2 mM of each dNTP; 0.25 µM of each primer; 0.5-1 ng/µL of template DNA; 0.02 U/µL Phusion polymerase (New England Biolabs)] was prepared per primer set. Cycling conditions were as follows: one pre-incubation cycle (98°C, 30 s), 35 amplification cycles [(denaturation: 98 °C, 10 s), (annealing: Tm-5 °C of the primers, 30 s), (elongation: 72 °C, 30 s/kb)], one final elongation (72 °C, 10 min).

2.5.1.2.4. Targeted mutagenesis PCR

This method was used to introduce the desired mutation within a DNA sequence. Briefly, a PCR reaction master mix (1X GC-rich buffer; 0.2 mM of each dNTP; 0.25 µM of each primer; 0.5-1 ng/µL of template DNA; 0.04 U/µL Phusion polymerase) was prepared per primer set. Primers were designed between 30 and 45 bases in length with a melting temperature above 78 °C and harbouring the desired mutation in the middle of the primers. Cycling conditions were as follows: one pre-incubation cycle (98 °C, 30 s), 20 amplification cycles [(denaturation: 98 °C, 10 s), (annealing: Tm-5 °C of the primers, 30 s), (elongation: 72 °C, 30 s/kb)], one final elongation (72 °C, 15 min).

One µL DpnI (New England Biolabs) was added to each 50 µL PCR reaction and incubated for several hours at 37 °C. Five µL were then used directly to transform *E. coli* DH10β.

2.5.1.2.5. Fusion PCR

This method was used when one-step amplification of long DNA fragment was unsuccessful (*e.g. CBE1* genomic sequence with its promoter). Briefly, this method consists of three steps, amplification of the different fragments, overlap PCR and then purification PCR. First, a PCR reaction master mix (1X GC-rich buffer; 0.2 mM of each dNTP; 0.25 µM of each primer; 0.5-5 ng/µL of template DNA; 0.02 U/µL Phusion polymerase) was prepared per primer set for amplification of the different fragments. Primers for the parts to assemble were designed between 25 and 50 bases in length with a melting temperature above 78 °C. Cycling conditions were as follows: one pre-incubation cycle (98 °C, 30 s), 25 amplification cycles [(denaturation: 98 °C, 10 s), (annealing: Tm-5 °C of the primers, 30 s), (elongation: 72 °C, 30 s/kb)], one final elongation (72 °C, 10 min). The specificity of each reaction was checked on an agarose gel and then PCR fragments were purified using the E.Z.N.A. Cycle Pure Kit (Omega). A second PCR reaction master mix (1X GC-rich buffer; 0.2 mM of each dNTP; 2-3 ng/µL of each fragment; 0.02 U/µL Phusion polymerase) was prepared as joining PCR. Cycling conditions were as follows: one pre-incubation cycle (98 °C, 30 s), 9 amplification cycles [(denaturation: 98 °C, 10 s), (annealing: Tm-5 °C of the primers, 30 s), (elongation: 72 °C, 30 s/kb)]. Primers from the extremity were then added (0.4 µM of each primer) for the purification PCR and cycling continue as follows: one pre-incubation cycle (98 °C, 30 s), 30 amplification cycles [(denaturation: 98 °C, 10 s), (annealing: Tm-5 °C of the primers, 30 s), (elongation: 72 °C, 30 s/kb)], one final elongation (72 °C, 10 min). Specificity was checked by size on agarose gel at each step and by Sanger sequencing at final step.

2.5.1.2.6. DNA sequence verification

Sanger sequencing (dideoxy sequencing) reactions were carried out in a final volume of 10 µL containing 75-150 ng template DNA, 1 µM primer, 2 µL 5x buffer and 0.8 µL ABI BigDye Terminator Ready Reaction Mix (Nimagen). The PCR cycle conditions were: initial denaturation (96 °C, 1 min), 13 amplification cycles [(denaturation: 96 °C, 10 s), (annealing: 50 °C, 5 s), (elongation: 60 °C, 1 min 15 s)], 17 amplification cycles [(denaturation: 96 °C, 10 s), (annealing: 50 °C, 5 s), (elongation: 60 °C, 1 min 15 s with 4 additional seconds per cycle)], and then kept at 12 °C. Sequencing was carried out on a 3730 ABI DNA Analyser (Applied Biosystems).

2.5.1.2.7. Agarose gel electrophoresis

DNA fragments were separated by electrophoresis in horizontal agarose gels. The gels were prepared in 1 x TAE (40 mM Tris, 20 mM AcOH, 1 mM EDTA) including 0.2 µg/mL ethidium bromide (Sigma) for visualization purposes. Depending on the sizes of the DNA fragments to be separated, the concentration of agarose varied between 1 - 2 % (w/v) with 1 % (w/v) gels most commonly used for analytical purposes. DNA samples were prepared by adding 0.1 vol of 6 x loading buffer [30 % (v/v)

glycerol, 0.25 % (w/v) bromophenol blue]. Gels were run at 100-200 V until the desired separation was achieved. Analytical gels were photographed on a short wavelength UV transilluminator (GelDoc XR, BioRad).

2.5.1.2.8. DNA purification from agarose gel pieces

DNA was visualised on a long wavelength UV transilluminator and the desired fragment was excised using a razor blade. Fragments were purified using E.Z.N.A. gel extraction kit (Omega Bio-Tek) following the manufacturer's instructions.

2.5.1.2.9. DNA purification from PCR reaction

Two methods were used depending on the consecutive use of DNA. For cloning purposes, DNA was purified using E.Z.N.A Cycle Pure Kit (Omega Bio-Tek) following the manufacturer's instructions. For sequencing, DNA was purified using CL-6B sepharose (Sigma). Holes were made using a syringe needle into the bottom of PCR strips. Slurry sepharose was then added to PCR strips with holes and centrifuged at 1,500 x*g* for 1 min. PCR reaction solution was then added to the dry sepharose and centrifuged at 1,500 x*g* for 1 min. Purified DNA was collected into clean PCR strips.

2.5.1.2.10. *bak1-5* genotyping

For *bak1-5* homozygous mutant identification, a dCAPS marker was designed using dCAPS Finder 2.0 (Neff et al., 2002) (Table 2.4 List of primers used in this study. Standard PCR was carried out using dCAPS primers and the PCR product was then digested using NruI (New England Biolabs). The corresponding products were then resolved on a 2% (w/v) agarose gel.

2.5.1.3. Cloning

2.5.1.3.1. Gateway entry vector cloning

DNA fragments were amplified by high-fidelity PCR with primers carrying the following extension: attB1 5'- GGGGACAAGTTTGTACAAAAAAGCAGGCTNN - for the forward primer and attB2 5'- GGGGACCACTTTGTACAAGAAAGCTGGGTN - for the reverse primer. After DNA purification from PCR reaction, a 5 µL BP reaction mix [4-10 fmol/µL attB-PCR product; 15 ng/µL pDONR vector; 20% (v/v) Gateway BP Clonase II (Invitrogen)] was incubated overnight at room temperature. The whole reaction volume was used to transform *E. coli* DH10β.

2.5.1.3.2. Gateway LR reaction

LR Gateway reaction was used to introduce the insertion of the entry vector into a destination vector. A 5 µL LR reaction mix [5-15 ng/µL entry clone; 15 ng/µL destination vector; 20% (v/v) Gateway LR Clonase (Invitrogen)] was incubated overnight at room temperature. One µL was used to transform *Escherichia coli* DH10β.

2.5.1.3.3. Transformation of *Escherichia coli* by heat shock

For transformation, 50 µL *E. coli* DH10β cells were mixed with 1-5 µL of plasmid solution and left on ice for 30 min. The cells were heat-shocked at 42 °C for 30-45 s and immediately chilled on ice for 2 min. The cells were re-suspended in 1 mL of liquid LB and incubated while shaking at 225 rpm at 37°C for 1 h. The solution was plated on LB-agar plates containing the appropriate antibiotic selection.

2.5.1.3.4. Transformation of *Agrobacterium tumefaciens* by electroporation

Two strains of *A. tumefaciens* were used, GV3101::pMP90 and GV3101::pMP90RK. 30 ng of plasmid was added to 50 µL electrocompetent cells. Cells were transferred to a chilled (20 min at -20 °C) electroporation cuvette. After electroporation (2.40 V, 200 Ω, capacitance extender 250 µFD, capacitance 25 µFD), cells were immediately resuspended in 1 mL of liquid LB and incubated while shaking at 225 rpm at 28 °C for 2-3 h. The bacterial solution was plated on LB-agar plates containing the appropriate antibiotic selection.

2.5.1.3.5. Plasmid purification

Single colonies corresponding to positive colony PCR results were incubated overnight in 5 mL LB containing the appropriate antibiotics and spun down for 5 min at 2,500 x*g*. Plasmids were extracted from the bacterial cell pellet using E.Z.N.A. Plasmid Mini Kit I (Omega Bio-Tek) following the manufacturer's protocol.

2.5.1.3.6. Restriction analysis

Restriction reaction mixes were assembled with 50 ng/µL of plasmid, 1X reaction buffer, and 0.05 U/µL of each of the cutting enzymes, and incubated for 1.5 h at optimal enzyme temperature. Products were analysed by agarose gel electrophoresis.

2.5.1.3.7. Plasmids used in this study

Name	Insert	Promoter	Insert sequence	Tag	Backbone	Reference
p35S-eGFP	GFP	CaMV 35S			pK7WGF2.0	
p35S-mRFP1	RFP	CaMV 35S			pB7WGR2.0	
p35S-cCBE1-eGFP	CBE1 (*AT4G01290*)	CaMV 35S	cDNA	eGFP C-terminus	pK7FWG2.0	
p35S-eGFP-cCBE1	CBE1 (*AT4G01290*)	CaMV 35S	cDNA	eGFP N-terminus	pK7WGF2.0	
p35S-cCBE1-mRFP1	CBE1 (*AT4G01290*)	CaMV 35S	cDNA	mRFP1 C-terminus	pB7RWG2.0	
p35S-mRFP1-cCBE1	CBE1 (*AT4G01290*)	CaMV 35S	cDNA	mRFP1 N-terminus	pB7WGR2.0	
pUBI10-cCBE1-eGFP	CBE1 (*AT4G01290*)	Ubiquitin promoter	cDNA	eGFP C-terminus	pUBC-GFP-Dest	
pCBE1-gCBE1-eGFP	CBE1 (*AT4G01290*)	CBE1 promoter (1.5 kb)	gDNA	eGFP C-terminus	pGWB604	
pCBE1-gCBE1(S473A)-sGFP	CBE1 (*AT4G01290*)	CBE1 promoter (1.5 kb)	gDNA Phosphomimetic	sGFP C-terminus	pGWB604	
pCBE1-gCBE1(S473D)-sGFP	CBE1 (*AT4G01290*)	CBE1 promoter (1.5 kb)	gDNA Phosphodead	sGFP C-terminus	pGWB604	
p35S-mRFP1-UPF1	UPF1 (*AT5G47010*)	CaMV 35S	cDNA	mRFP1 N-terminus	pB7WGR2.0	(Moreno et al., 2013)
p35S-mRFP1-DCP1	DCP1 (*AT1G08370*)	CaMV 35S	cDNA	mRFP1 N-terminus	pB7WGR2.0	(Moreno et al., 2013)
p35S-mCherry-PAB2	PAB2 (*AT4G34110*)	CaMV 35S	cDNA	mCherry N-terminus	pAMARENA	(Bhasin and Hülskamp, 2017)
p35S-YFP-UBP1B	UBP1B (*AT1G17370*)	CaMV 35S	cDNA	YFP N-terminus	pENS-G-YFP	(Bhasin and Hülskamp, 2017)
p35S-YFP-EIF4E1	EIF4E1 (*AT4G18040*)	CaMV 35S	cDNA	YFP N-terminus	pENS-G-YFP	(Bhasin and Hülskamp, 2017)
p35S-YFP-RBP47C	RBP47C (*AT1G47490*)	CaMV 35S	cDNA	YFP N-terminus	pENS-G-YFP	(Bhasin and Hülskamp, 2017)

Table 2.2 List of plasmids used in this study

2.5.2. RNA methods

2.5.2.1. Translating ribosome affinity purification (TRAP)

For this assay, whole rosettes from 5-week-old Arabidopsis were used. A day before the treatment, rosettes were cut and permeabilised by vacuum infiltration in water for 3 min and let them recovered overnight in 15 cm petri dishes containing water. The next day, elicitor or water was added to the solution within petri dishes and homogenized for 1 min by gently swirling. After incubation, tissue was frozen in liquid nitrogen. TRAP of polysomes was performed as described previously (Mustroph et al., 2009; Reynoso et al., 2015). Briefly, pulverised tissue was added to polysome extraction buffer in ratio 1:5 (PEB: 200 mM Tris, pH 9.0, 200 mM KCl, 25 mM EGTA, 35 mM $MgCl_2$, 1% PTE, 1 mM DTT, 1 mM PMSF, 100 µg/mL cycloheximide, 50 µg/mL chloramphenicol) and 1 % detergent mix [20 % (w/v)

polyoxyethylene(23)lauryl ether, 20 % (v/v) Triton X-100, 20 % (v/v) Octylphenyl-polyethylene glycol, 20 % (v/v) Polyoxyethylene sorbitan monolaurate 20] and incubated until thawed on ice. The homogenized mixture was incubated on ice for 10 min and centrifuged at 16,000 x*g* at 4ºC for 15 min. After centrifugation, the supernatant was filtered through sterilized Miracloth (Millipore) to produce a clarified extract (input). The clarified extract was added to Anti-FLAG M2 Affinity Gel beads that were pre-washed twice with wash buffer [WB; 200 mM Tris (pH 9.0), 200 mM KCl, 25 mM EGTA, 35 mM MgCl2, 1 mM DTT, 1 mM PMSF, 100 µg/mL cycloheximide, 50 µg/mL chloramphenicol]. Binding of FLAG epitope-tagged ribosome-mRNA complexes was accomplished by incubation at 4°C for 2 h with gentle rocking. The beads were precipitated by centrifugation at 8,200 ×*g* for 2 min at 4°C, the supernatant was removed, and the beads were gently resuspended in 6 mL WB for 2 min at 4ºC with rocking. This step was repeated two additional times before the beads were resuspended in 300 µL elution buffer (WB containing 200 ng/µL 3× FLAG peptide) and incubated 30 min at 4ºC with rocking. After centrifugation at 8,200 ×*g* for 2 min at 4°C, the supernatants were stored at −80°C.

2.5.2.2. Isolation of total RNA from Arabidopsis

RNA extractions were performed based on previously described protocol (Shi and Bressan, 2006). Total RNA was extracted at 4 ºC from seedlings or leaf discs. Thirty-to-fifty mg of tissue was ground in 2 mL tubes containing 2 glass beads (3 mm) using pre-cooled racks at -80 °C and 2010 Geno/grinder (SPEX) at 1,500 rpm for 1.5 min. Ground tissue was resuspended, homogenised in 900 µL TRI reagent (Ambion) and incubated 5 min at room temperature. Two hundreds µL chloroform was added, shaken by hand for 15 s, and incubated at room temperature for 3 min. Samples were centrifuged at 12,000 x*g* for 15 min. Four hundreds µL of the upper phase was transferred to a new tube, homogenised with 500 µL isopropanol and incubated at room temperature for 10 min. Samples were centrifuged at 15,000 x*g* for 20 min. The pellet was then washed twice with 500 µL and 1 mL 70 % ethanol, respectively, with intermediate centrifuge at 12,000 x*g* for 10 min. After the last centrifuge at 7,500 x*g* for 5 min, all the supernatant was removed and the pellet was dried for 5 min at room temperature under flow hood. The pellet was then dissolved in 30 µL RNase-free water, and RNA was quantified with a Nanodrop spectrophotometer (Thermo Scientific).

2.5.2.3. DNase treatment of RNA

DNase treatment was performed using TURBO DNA-free (Ambion). A 10 µL DNase reaction mix (175 ng/ µL RNA, 1X reaction buffer, 0.04 U/ µL TURBO DNase) was incubated at 37 °C for 30 min. The reaction was then inactivated by adding 1 µL inactivation reagent and incubated at room temperature for 5 min with regular shaking. After centrifugation at 2,500 x*g*, the supernatant was transferred to a new tube and RNA was quantified with a Nanodrop spectrophotometer (Thermo Scientific).

2.5.2.4. Control of genomic DNA contamination

Genomic DNA contamination was checked by standard PCR on RNA post-DNAse treatment and concentration normalization. Primers aligning specifically to introns were used for the PCR and the product was analysed by agarose gel electrophoresis.

2.5.2.5. Control of RNA integrity

RNA integrity was checked visually by analysis on agarose gel electrophoresis of the two primary ribosomal bands.

2.5.2.6. cDNA synthesis

Reverse transcription was performed using RevertAid First Strand cDNA Synthesis (Thermo Scientific) on RNA post-DNAse treatment and concentration normalization. A 10 µL RT reaction mix [5 pg-250 ng/µL RNA; 5 µM Oligo$(dT)_{18}$ primer; 1X reaction buffer; 1U/µL RiboLock RNase inhibitor (Thermo Scientific); 1 mM dNTP mix; 20 U/µL RevertAid] was incubated for 60 min at 42 °C, followed by 5 min at 70 °C to terminate the reaction.

2.5.2.7. RT-qPCR

For RT-qPCR, PowerUp SYBR Green Master Mix (Applied Biosystems) was used with cDNA diluted 1:20. A 10 µL PCR reaction mix (5 µL SYBR Green, 0.5 mM each primer, 1:20 diluted cDNA) was prepared per primer set. Cycling conditions were as follows: one pre-incubation cycle (95 °C, 4 min), 39 amplification cycles [(denaturation: 94 °C, 10 s), (annealing: 60 °C, 15 s), (elongation: 72 °C, 10 s)], two final steps (65 °C, 1 s) and then (95 °C, 10 min). Quantitative PCRs were conducted on 96-well plates using a 7500 Real-Time PCR System (Applied Biosystems). The *UBOX/MUSE3* transcripts (*AT5G15400*) or *ACTIN 2* transcripts (*AT3G18780*) were used as internal standards for sample comparisons. The specificity and efficiency of the amplification were verified by analyses of melting curves and standard curves, respectively. The $2^{-\Delta Ct}$ method (Livak and Schmittgen, 2001) was used for the calculation of relative expression.

2.5.3. Protein methods

2.5.3.1. General protein methods

2.5.3.1.1. SDS-polyacrylamide gel electrophoresis

The reagents and SDS-polyacrylamide gel preparation methods were followed according to Laemmli, 1970 (Laemmli, 1970). Gels were run in Mini PROTEAN Tetra gel tanks (Bio-Rad) filled with SDS-

running buffer [25 mM Tris; 193 mM glycine; 1 % (w/v) SDS]. The gel electrophoresis was performed in a continuous buffer system at 100-150 V. All gels included the molecular size marker 10 to 180 kDa, PageRuler Prestained Protein Ladder (Thermo Scientific).

2.5.3.1.2. Electroblotting

Two Whatman papers and sponges per gel were equilibrated for 5 min in transfer buffer [25 mM Tris; 192 mM glycine; 20 % (v/v) methanol]. The PVDF membrane was activated for 1 min in methanol. Transfer was conducted at 4 °C, either overnight at 30 V or for 1 h at 100 V.

2.5.3.1.3. Coomassie staining

The proteins on the membrane were visualized by Coomassie staining. The membrane was transferred to a tray containing Coomassie stain solution [0.5 % (w/v) Coomassie brilliant blue G-250 (AppliChem); 50 % (v/v) methanol; 7.5 % (v/v) glacial acetic acid), agitated at RT for 1 min, and de-stained three times under agitation for 30 min with de-stain solution [20 % (v/v) methanol; 5 % (v/v) acetic acid].

2.5.3.1.4. Immunodetection

PVDF transfer membranes with immobilised, denatured proteins were blocked for 1 h at room temperature with TBST buffer [150 mM NaCl; 20 mM Tris-HCl; 0.1 % (v/v) Tween-20; pH 7.4] containing 5 % (w/v) dried skimmed milk powder with gentle agitation on a platform shaker. Membranes were then incubated with the primary antibodies directed against the selected target protein with TBST buffer containing 5 % (w/v) dried skimmed milk powder or BSA for 1 h at RT or overnight at 4 °C. Following primary antibody incubation, membranes were washed three times for 5-10 min each with TBST buffer, and then incubated for 1 h at RT with TBST buffer containing 5 % (w/v) dried skimmed milk powder and secondary antibodies directed against the anti-immunoglobulin of the primary antibody covalently coupled to horseradish peroxidase (HRP). Finally, after secondary antibody incubation membranes were washed two times for 5-10 min each with TBST buffer and finally washed 5-10 min with TBS buffer (150 mM NaCl, 20 mM Tris-HCl, pH 7.4). Detection of the peroxidase signal of the secondary antibody HRP-conjugated was performed with SuperSignal West Pico Plus Chemiluminescent Substrate (Thermo Scientific), or SuperSignal West Femto Maximum Sensitivity Substrate (Thermo Scientific). Membranes were imaged using the ChemiDoc Touch Imaging System (Bio-rad) with exposures that ranged from 10 s to 10 min.

2.5.3.1.5. Antibodies

Antibodies used in western blots are listed below (Table 2.3).

Antibody	Origin	Clonality	Dilutions	Source / Reference
Anti-BAK1	Rabbit		1:2 000	CZL
Anti-GFP	Mouse	Monoclonal	1:5 000	Santa Cruz sc-9996
Anti-phospho-MAPK	Rabbit	Polyclonal	1:1 000	Cell Signaling Technology #9101
Anti-RBOHD	Rabbit	Polyclonal	1:1 000	Agrisera AS152962
Anti-RFP (HRP)	Rabbit	Polyclonal	1:5 000	Abcam AB34767
Anti-BIK1	Rabbit	Polyclonal	1:3 000	Agrisera AS16 4030
Anti-mouse (HRP)	Goat		1:15 000	Sigma A0168
Anti-rabbit (HRP)	Goat		1:10 000	Sigma A0545

Table 2.3 List of antibodies used in this study

2.5.3.2. *In-vivo* protein analysis

2.5.3.2.1. Protein extraction

Flash frozen tissue was ground to a fine powder using pre-cooled racks at -80 °C and a 2010 Geno/grinder (SPEX) at 1,500 rpm for 1.5 min. Samples were solubilised in extraction buffer [375 mM Tris-HCl pH 6.8; 50 % (v/v) glycerol; 9 % (w/v) SDS; 0.03 % (w/v) bromophenol blue; 100 mM DTT] relative to weight. Samples were boiled at 95 °C for 5-10 min and centrifuged at 11,000 x*g* for 5 min.

2.6. Cellular biological methods

2.6.1. Confocal laser scanning microscopy

N. benthamiana leaf discs (4 mm) transiently over-expressing indicated proteins were sampled at 2-3 dpi with water as the imaging medium. Live-cell imaging employed a laser-scanning confocal microscope Leica SP5 Confocal Microscope (Leica Microsystems, Wetzlar, Germany) and 63x (glycerol immersion) objective. GFP was excited at 488 nm and collected between 496–536 nm (shown in green), YFP excited at 514 nm and collected between 524–551 nm (shown in yellow), RFP derivatives (mRFP, mCherry, tag-RFP) excited at 561 nm and collected between 571-635 nm (shown in magenta). Co-localisation was performed using sequential channels analysis was performed by calculating Pearson's coefficient (Adler and Parmryd, 2010; Dunn et al., 2011) using the coloc 2 plugin of ImageJ. Image analysis was performed with Fiji.

2.7. Statistical analysis

Statistical analysis was performed using R or GraphPad Prism. Based on Gaussian distribution parametric or nonparametric tests were chosen and when n ≥30, normal distribution was assumed. Prior

to multiple comparisons, ANOVA or Kruskal-Wallis test were performed to look for a difference across groups. For multiple comparisons, Dunnett's and Dunn's tests were favoured to compare multiple groups to one control group. Tests were realised on the overall set of replicates and replicates were included only when positive and negative controls showed the expected results.

2.8. Antibiotics used in this study

Final concentrations of 100 µg/mL carbenicillin (Apollo Scientific), 20 µg/mL gentamycin (Roth), 50 µg/mL hygromycin (sigma), 50 µg/mL kanamycin (Fluorochem), 50 µg/mL rifampicin (Apollo Scientific), 100 µg/mL spectinomycin (Apollo Scientific), 25 µg/mL zeocin (Invitrogen) were used for bacterial cultures. For the selection of Arabidopsis transgenic lines, 50 µg/mL kanamycin (Fluorochem), 40 µg/mL hygromycin or 10 µg/mL phosphinothricin (Duchefa) were used. All antibiotic solutions were filter-sterilised using a 22-µm syringe filter.

2.9. Media used in this study

King's B [1 % (w/v) proteose peptone #3 (Difco); 0.15 % (w/v) dipotassium hydrogenphosphate; 1.5 % (w/v) glycerol; 5 mM magnesium sulfate; 1 % (w/v) agar for solid medium; pH7.0].
LB [1 % (w/v) bacto tryptone; 0.5 % (w/v) bacto yeast extract; 0.5 % (w/v) NaCl; 1.5 % (w/v) agar for solid medium].
MS [0.228 % (w/v) MS-Medium (Duchefa Mod. # M0221); 1 % (w/v) sucrose; 0.9 % (w/v) phytoagar for solid medium; pH5.8].

2.10. Primers used in this study

Name	Sequence (5'-3')	Purpose	Locus	Project
T10O24.F	ATCAAAACTACGTCGTTTTA	Map-based cloning		General
T10O24.R	TTCAAAATCAATCGAACATA	Map-based cloning		General
F19G10.F	ATGTCACCGTGAACGACATC	Map-based cloning		General
F19G10.R	TGCGAGTTAAGACCTAGGAG	Map-based cloning		General
T3F24-2.F	TCCACACACGCAACTTCATGGCAT	Map-based cloning		General
T3F24-2.R	TTACTTAGGTGACACGTGTGATGT	Map-based cloning		General
T2E12.F	CGACTAGCCAGTCCGATACA	Map-based cloning		General
T2E12.R	CGTTTTGGGAGCCACGTTTC	Map-based cloning		General
F24J13-2.F	CTTGTAAAACCTCGATATTATCTC	Map-based cloning		General
F24J13-2.R	ACTAAGATACTAGTAGGCTCGGCT	Map-based cloning		General
T23K3.F	CGTGTTTACCGGGTCGGA	Map-based cloning		General
T23K3.R	AAAACCCTTGAAGAATACG	Map-based cloning		General
T4D8.F	ATTAACCCCAATGATGCTGA	Map-based cloning		General
T4D8.R	AGCGGATAGATAATGGTCAA	Map-based cloning		General
F2G1.F	CGTCGTCGGAAGTTTCAGAG	Map-based cloning		General
F2G1.R	GAATAAGAAGAACACATGCGTC	Map-based cloning		General
T8O18.F	GATATGGATGTAACGACCCAA	Map-based cloning		General
T8O18.R	CAGCTTCGAGTGGATTCTAC	Map-based cloning		General
T6A23.F	ATGTCCAAATTGACCAACCG	Map-based cloning		General
T6A23.R	CAAAATAAACACCCCCAACT	Map-based cloning		General
T251P5.F	CATCCGAATGCCATTGTTC	Map-based cloning		General
T251P5.R	AGCTGCTTCCTTATAGCGTCC	Map-based cloning		General
MIE1.F	CTAAGTTCTTCCACCATCTG	Map-based cloning		General
MIE1.R	CAAGGAGCATCTAGCCAGAG	Map-based cloning		General
K13N2-3.F	ATTAAATCTAAAATCGAGTGATT	Map-based cloning		General
K13N2-3.R	AACAAACATTACTCGGTATCCAGT	Map-based cloning		General
F18B3.F	GTTCATTAAACTTGCGTGTGT	Map-based cloning		General
F18B3.R	TACGGTCAGATTGAGTGATTC	Map-based cloning		General
F24B22.F	CTGGGAACAAAGGTGTCATC	Map-based cloning		General
F24B22.R	CAAGGTCTCCAGAACACAAAC	Map-based cloning		General
CIW5.F	GGTTAAAAATTAGGGTTACGA	Map-based cloning		General
CIW5.R	AGATTTACGTGGAAGCAAT	Map-based cloning		General
T419.F	TTATAGCAAACGTACAAGTC	Map-based cloning		General
T419.R	CTGCATACACGTCGTCTC	Map-based cloning		General
F24G24.F	GCCAAACCCAAAATTGTAAAAC	Map-based cloning		General
F24G24.R	TAGAGGGAACAATCGGATGC	Map-based cloning		General
T4C9.F	CAAAGGTTTCGTGTCGGAGC	Map-based cloning		General
T4C9.R	CGTTGACGGGATACTCGGTG	Map-based cloning		General
T13J8.F	ATGTTCCCAGGCTCCTTCCA	Map-based cloning		General
T13J8.R	GAGATGTGGGACAAGTGACC	Map-based cloning		General

F20M13.F	TCTCGTAAGCAAATCAACGAATAG	Map-based cloning	General
F20M13.R	AAGATGCGTGCGTTGATGGACCAA	Map-based cloning	General
K18J17-2.F	GGTCCGAATCTAAACTCGGTTAAT	Map-based cloning	General
K18J17-2.R	AGTGTTCGAGCAATAAGAGTGATT	Map-based cloning	General
MQJ16.F	TAGTGAAACCTTTCTCAGAT	Map-based cloning	General
MQJ16.R	TTATGTTTTCTTCAATCAGTT	Map-based cloning	General
MYJ24.F	CTAATCCCAAGCTGAATCAC	Map-based cloning	General
MYJ24.R	TGACAGAGAATCCGACTGTG	Map-based cloning	General
K15E6.F	GGCTGCTTCACTGAGTTG	Map-based cloning	General
K15E6.R	AAAAGCCCATTTAAAACG	Map-based cloning	General
K19E20.F	GACAAGAACCACATGAGAGC	Map-based cloning	General
K19E20.R	GTTATGTGTACACTTCAGGTC	Map-based cloning	General
MQJ2.F	ATTCTCCGTAGACCACAG	Map-based cloning	General
MQJ2.R	TCAACAGACTCCGCATACT	Map-based cloning	General
K9I9-1.F	TGGACTTGAATAGTTAGGCTGTCT	Map-based cloning	General
K9I9-1.R	ATTACCAGTACTTAATAAAATGAT	Map-based cloning	General
K1.19642942.F	GCATTCCACTGTAAGCTACTG	Mapping	MOB7
K1.19642942.R	AAGAACTCCAAACTGCACCT	Mapping	MOB7
K1.21074737.F	CAAACCGGGAACTGGAATGTC	Mapping	MOB7
K1.21074737.R	CAGAAGCAAATCTATTACAGCTCC	Mapping	MOB7
K1.22016665.F	GTTTCACGTAGTTCCTTGGT	Mapping	MOB7
K1.22016665.R	TTGAATCTTTCCCATCTTCTCC	Mapping	MOB7
K1.22569512.F	CTCCAGTCAGAGTAATGCCT	Mapping	MOB7
K1.22569512.R	CGAAGAGGTCCTAAGTGGTC	Mapping	MOB7
K1.22639584.F	CAGTGGAATAGGATGTTTGGTGTG	Mapping	MOB7
K1.22639584.R	GATTGTAAATCACTCTTCCAAGCG	Mapping	MOB7
K1.22860256.F	GTGGAACGTGTTGAAGAAGCTC	Mapping	MOB7
K1.22860256.R	GTCTCCATCCAAGAGAAGGAC	Mapping	MOB7
K1.24671295.F	GTTTCGTAACAGCGCATCCC	Mapping	MOB7
K1.24671295.R	AGCTGTTATACATCCAACTTCCC	Mapping	MOB7
K1.25925409.F	CTTTGAACAAATGGGATGTCGG	Mapping	MOB7
K1.25925409.R	ATGTTGATTCAGGTATGGACTGC	Mapping	MOB7
K1.26941401.F	TTTAAGATCCTTTGGCCGTC	Mapping	MOB7
K1.26941401.R	TTGTTTATCAGGTGGAGCAG	Mapping	MOB7
K1.29730343.F	TTCCCTCCTCTGTATGTTGCTG	Mapping	MOB7
K1.29730343.R	GCCTACTCATATTACCTTCTTCCT	Mapping	MOB7
K1.29743251.F	GTCGTGTCACATCAGTAGAG	Mapping	MOB7
K1.29743251.R	GCATCATTTCCGAAACACAG	Mapping	MOB7
K2.2593.F	CGCATGATATTACCGAGATGTCC	Mapping	MOB7
K2.2593.R	TTTGCTACCCGTCTCGTTCC	Mapping	MOB7
K4.5727143.F	CAAGTGGCATGAAATTTACTGTGG	Mapping	MOB7
K4.5727143.R	GCCCAGCAGAGATTATAACTGAG	Mapping	MOB7
K4.8227310.F	TATATCGTTCATTCTGCAGGTAGC	Mapping	MOB7
K4.8227310.R	GGGAGAACTTAGTTGTTGCATGG	Mapping	MOB7
K5.376938.F	CGTAACTCCTGCCCACTCTG	Mapping	MOB7

K5.376938.R	TTTCAACTAATGAGCACTCCCT	Mapping		MOB7
K5.6700137.F	AGGAGAGTACACGTCATCTTGC	Mapping		MOB7
K5.6700137.R	AACCATTGACACCACTTGGTC	Mapping		MOB7
K5.6704873.F	TGTGTCAGACCGTAGTATCTACC	Mapping		MOB7
K5.6704873.R	TTCCACATTGAACAATCTCCAG	Mapping		MOB7
K5.14327194.F	AGTTAATGTTACGTGTTTCACAC	Mapping		MOB7
K5.14327194.R	CTCTTGAACATTGTTCCTTTAGC	Mapping		MOB7
K5.21318563.F	GCAGAAGTTCAACAAGGCGT	Mapping		MOB7
K5.21318563.R	CAGCAAATTCTTCAGCAGGCA	Mapping		MOB7
K5.21319329.F	CCTCAACAGAAAGACCAAAGGA	Mapping		MOB7
K5.21319329.R	TCAAGATTCCCTTCTCAGAACC	Mapping		MOB7
K5.21320023.F	TGTAAACATGAGCGATTCACATCC	Mapping		MOB7
K5.21320023.R	CATCTGGGAATCTCTTAAACCGA	Mapping		MOB7
K5.21320578.F	GGCCCATACACTGATACAAACC	Mapping		MOB7
K5.21320578.R	GTTGTTGTCGTTGGCTACCAC	Mapping		MOB7
K5.26227168.F	CTGGTTCTTCATCTCGTCCT	Mapping		MOB7
K5.26227168.R	AGCCATCTTCTTGTAGTTCGT	Mapping		MOB7
K5.1823996.F	ATCGTTGGTTGCCTTTCTCTG	Mapping		MOB7
K5.1823996.R	GGACAATGGTTAGTTTAGTTGGGA	Mapping		MOB7
K1.19188293.F	CCGATTGATCTTGATTTCTGAC	Mapping		MOB7
K1.19188293.R	GAACTGCAAGACAAATTGAGAG	Mapping		MOB7
K4.542701.F	TGTTGCTGTGAGACTCTATCC	Mapping		MOB7
K4.542701.R	TAGACAAGCAGACTTCATGCC	Mapping		MOB7
K4.433442.F	GGATCAGAGTTCTAAGCCGT	Mapping		MOB7
K4.433442.R	GATTCAGCACCAATCTTCGCT	Mapping		MOB7
AT4G01290.pro.attB1	GGGGACAAGTTTGTACAAAAAAGCAGGCTCAACCTCTTGGGATTGCTGTCAC	Cloning Gateway	*AT4G01290*	MOB7
AT4G01290.ATG.attB1	GGGGACAAGTTTGTACAAAAAAGCAGGCTGTATGATGAGTATAGCAAATGAAC	Cloning Gateway	*AT4G01290*	MOB7
AT4G01290.stop.attB2	GGGGACCACTTTGTACAAGAAAGCTGGGTGTTACCTGTAGCCAAACCCAAGG	Cloning Gateway	*AT4G01290*	MOB7
AT4G01290.nostop.attB2	GGGGACCACTTTGTACAAGAAAGCTGGGTGTGACCTGTAGCCAAACCCAAGG	Cloning Gateway	*AT4G01290*	MOB7
AT4G01290.GWY.frgmt1.R	AGACCTCCGAGATGGCATACCAGAACGCCTTCCAGGCTCTCC	Cloning Gateway	*AT4G01290*	MOB7
AT4G01290.GWY.frgmt2.F	GTATGCCATCTCGGAGGTCTTGGCAAGCACCTGAGCATGATGGAC	Cloning Gateway	*AT4G01290*	MOB7
AT4G01290.GWY.frgmt3.R	GGATTTATTAATGGTCTGAGGGCTTCGTATTTCTTCTACttttttCG	Cloning Gateway	*AT4G01290*	MOB7
AT4G01290.GWY.frgmt4.F	CGaaaaaGTAGAAGAAATACGAAGCCCTCAGACCATTAATAAATCC	Cloning Gateway	*AT4G01290*	MOB7
AT4G01290.S473A.F	ATTAATGGTCTGAGGAGCTCGTATTTCTTCTACttttttCG	Cloning SDM	*AT4G01290*	MOB7
AT4G01290.S473A.R	aGTAGAAGAAATACGAGCTCCTCAGACCATTAATAAATCC	Cloning SDM	*AT4G01290*	MOB7
AT4G01290.S473D.F	ATTAATGGTCTGAGGATCTCGTATTTCTTCTACttttttCG	Cloning SDM	*AT4G01290*	MOB7
AT4G01290.S473D.R	aGTAGAAGAAATACGAGATCCTCAGACCATTAATAAATCC	Cloning SDM	*AT4G01290*	MOB7
MTSF1-3	CCTAACTCCTCAAGCGCAATA	Genotyping	*AT1G06710*	MOB7
MTSF1-5	TTTCACCTGTAGCCGTTATCT	Genotyping	*AT1G06710*	MOB7
MTSF1-8	CATATCCTGGCATGTGACC	Genotyping	*AT1G06710*	MOB7

MTSF1-7	ATAATTGTTTGATTCAGGC	Genotyping	*AT1G06710*	MOB7
summ2-8.F	TACGCCATTCTTGTACCATCC	Genotyping	*AT1G12280*	MOB7
summ2-8.R	CCACTAATGACGCTGAGCTTC	Genotyping	*AT1G12280*	MOB7
upf3-1.F	ACTTCTATTGTTGATCTCTGG	Genotyping	*AT1G33980*	MOB7
upf3-1.R	ATGCTGTTCCGGTTGTGGTGG	Genotyping	*AT1G33980*	MOB7
pat1-1.F	GGTTCCTTTCTCTTCAATCCG	Genotyping	*AT1G79090*	MOB7
pat1-1.R	CGGAAGCTCTGTCGAGTATTG	Genotyping	*AT1G79090*	MOB7
eIF(iso)4G-2.F	AATGCAACAACAAGGTGAACC	Genotyping	*AT2G24050*	MOB7
eIF(iso)4G-2.R	AAGAAGCTCGTACTTCTCCGG	Genotyping	*AT2G24050*	MOB7
vcs-6.F	TTGAAGGGTATTTGCTGTTGG	Genotyping	*AT3G13300*	MOB7
vcs-6.R	TCGGTACACGAATAGGACCTG	Genotyping	*AT3G13300*	MOB7
ACT2pro.F	ATGGATCGATGCCAAAAGTCCC	Genotyping	*AT3G18780*	General
ACT2pro.R	TGGCTACTACTACATCCGAACTCG	Genotyping	*AT3G18780*	General
eIF4Gmut.F	AGGTTCATGTTGATCAATGCC	Genotyping	*AT3G60240*	MOB7
eIF4Gmut.R	GAACGCACCAGAGTGCTTATC	Genotyping	*AT3G60240*	MOB7
cum1-1.F	AAGCCTAATTCAATAGAGAATCCGA	Genotyping	*AT4G18040*	MOB7
cum1-1.R	GTCGGAAATAAAATAAAATCAAAAACCTAAGCT	Genotyping	*AT4G18040*	MOB7
CERES.+540.F	GGCAAAAGCTCAGTTAACGC	Genotyping	*AT4G23840*	MOB7
CERES.+1639.R	GACAAGGACTCTGTCTCGGC	Genotyping	*AT4G23840*	MOB7
dCAPS.F.bak1-5.NruI	AAGAGGGCTTGCGTATTTACATGATCATC	Genotyping	*AT4G33430*	General
dCAPS.R.bak1-5.NruI	GACCAATTGTCCCACGCACTG	Genotyping	*AT4G33430*	General
smg7-1.F	GACCTTGGTAGCTGGTCC TGAG	Genotyping	*AT5G19400*	MOB7
smg7-1.R	GGACAACAGGCCAACCATTCAAC	Genotyping	*AT5G19400*	MOB7
eIFiso4E-1.F	TTGACCCAATAGAGTCCAGAAAT	Genotyping	*AT5G35620*	MOB7
eIFiso4E-1.R	CTCTCCAATCAAAGCCATCAACTA	Genotyping	*AT5G35620*	MOB7
eIFiso4E-1.insert	GGTGCAGCAAAACCCACACTTTTACT	Genotyping	*AT5G35620*	MOB7
upf1-5.F	ATTATGCCACACAAGGAGCAC	Genotyping	*AT5G47010*	MOB7
upf1-5.R	AGGGACAACAAAATCATGTCG	Genotyping	*AT5G47010*	MOB7
eIF(iso)4G-1.F	TGATTGGTGAGCTTTTGAAGC	Genotyping	*AT5G57870*	MOB7
eIF(iso)4G-1.R	CCAAGCTCCTCTACACACTGC	Genotyping	*AT5G57870*	MOB7
Kan.F	GAACAAGATGGATTGCACGC	Genotyping		General
Kan.R	GATGTTTCGCTTGGTGGTC	Genotyping		General
35S-HF-RPL18.F	AGGATGATGATGATAAGGGAGG	Genotyping		MOB7
GK_LB_o8474	ATAATAACGCTGCGGACATCTACATTTT	Genotyping		General
SAIL_LB1	GCCTTTTCAGAAATGGATAAATAGCCTTGCTTCC	Genotyping		General
SALK_LBb1.3	ATTTTGCCGATTTCGGAAC	Genotyping		MOB7
L4.WiscDsLoxHs.LB	TGATCCATGTAGATTTCCCGGACATGAAG	Genotyping		General
CBE1.cbe1mut2.R	AACGTCCGCAATGTGTTATTAAGTTGTC	Genotyping		General
35S-HF-RPL18.R	TAAGAAGAACCGTGTTCTGG	Genotyping		MOB7
GK-150H09_F'	AGTATTCCATCCGTTCGATTCAC	Genotyping GK-150H09	*AT4G01290*	MOB7
GK-150H09_R	AGAAACGAGAGTCCATAGAGAC	Genotyping GK-150H09	*AT4G01290*	MOB7

SAIL_859_E09_F'	TATTTTGGCTGTTGATTTGGC	Genotyping SAIL_859_E09	*AT4G01000*	MOB7
SAIL_859_E09_R'	ATCATTGCGAAAGCGATAATG	Genotyping SAIL_859_E09	*AT4G01000*	MOB7
SALK_038452_F'	GAAATACGAAGCCCTCAGACC	Genotyping SALK_038452	*AT4G01290*	MOB7
SALK_038452_R'	GTATTGTTGGGGATGTTGGTG	Genotyping SALK_038452	*AT4G01290*	MOB7
SALK_114391_F'	GAAGGATGGTGAAGAAGGGAG	Genotyping SALK_114391	*AT4G01000*	MOB7
SALK_114391_R'	GGCCAGTAATTTCTTTGGGAG	Genotyping SALK_114391	*AT4G01000*	MOB7
cbe1mut.F	ATGTACATTTGTAGGCGCCAC	Genotyping WiscDsLoxHs188_10F	*AT4G01290*	MOB7
cbe1mut.R	CTTAATTCCCAACGGTTTTCC	Genotyping WiscDsLoxHs188_10F	*AT4G01290*	MOB7
BPS1.qF	CTTCTCTCGTCTTTCCTGG	RT-qPCR	*AT1G01550*	MOB7
BPS1.qR	CCGCGTTCTTCGAAGATA	RT-qPCR	*AT1G01550*	MOB7
PP2AA3.qF	CGATAGTCGACCAAGCGGTT	RT-qPCR	*AT1G13320*	General
PP2AA3.qR	TACCGAACATCAACATCTGG	RT-qPCR	*AT1G13320*	General
UPF3.qF	GGGAGGTTGATCAAGGGAAT	RT-qPCR	*AT1G33980*	General
UPF3.qR	TCTTTCCCTGCTCGAGTGTT	RT-qPCR	*AT1G33980*	General
CPuORF19.qF	AAGATGCCGAGGATGATGAC	RT-qPCR	*AT1G36730*	MOB7
CPuORF19.qR	AAGTGTCATGAGCCCCATTC	RT-qPCR	*AT1G36730*	MOB7
DRP4Das.qF	ACACGGTTGACCGTCTAAGG	RT-qPCR	*AT1G60510*	General
DRP4Das.qR	TGAAGTCGCATGACAAGAGG	RT-qPCR	*AT1G60510*	General
RBOHF.qF	AAGAAGGTGATGCTCGTTCTGC	RT-qPCR	*AT1G64060*	General
RBOHF.qR	AGTGTGTTCTGACCCTAGTGCC	RT-qPCR	*AT1G64060*	General
NPR1.qF	GAAGCACACCTGCAGCAATA	RT-qPCR	*AT1G64280*	General
NPR1.qR	TCGGTGAGACTCTTGCCTCT	RT-qPCR	*AT1G64280*	General
SARD1.qF	CCTCAACCAGCCCTACGTTA	RT-qPCR	*AT1G73805*	General
SARD1.qR	TAGTGGCTCGCAGCATATTG	RT-qPCR	*AT1G73805*	General
SID2.qF	TCCGTGACCTTGATCCTTTC	RT-qPCR	*AT1G74710*	General
SID2.qR	ACAGCGATCTTGCCATTAGG	RT-qPCR	*AT1G74710*	General
PR1.qF	GTAGGTGCTCTTGTTCTTCCC	RT-qPCR	*AT2G14610*	General
PR1.qR	CACATAATTCCCACGAGGATC	RT-qPCR	*AT2G14610*	General
BIK1.qF	ACCGTCTTCTAGTCTACGAG	RT-qPCR	*AT2G39660*	General
BIK1.qR	ATTGGACCGTCTCTAGCTAG	RT-qPCR	*AT2G39660*	General
BIK1.qF	ACATGTCATCAGGTCACTTGAATGC	RT-qPCR	*AT2G39660*	General
BIK1.qR	CCGGTCTGTTATGATCCAACGC	RT-qPCR	*AT2G39660*	General
PTC+.qF	AAGGGATGTAAATACAGAGAAAAGCTTC	RT-qPCR	*AT2G45670*	MOB7
PTC+.qR	AGGGTAACCAGGGATGAAAGC	RT-qPCR	*AT2G45670*	MOB7
Actin2.qF	CTTGTTCCAGCCCTCGTTTGTG	RT-qPCR	*AT3G18780*	General
Actin2.qF	CCTTGGAGATCCACATCTGCTG	RT-qPCR	*AT3G18780*	General
PBL1.qF	TACTGGACTCGGACTTCAACGC	RT-qPCR	*AT3G55450*	General
PBL1.qR	ACATACTCAGGAGCTGCGTACC	RT-qPCR	*AT3G55450*	General
At4g01000_qPCR_F	ACCCATCGGTTGTTTGGTTTCAGG	RT-qPCR	*AT4G01000*	MOB7

At4g01000_qPCR_R	GCCTCGCAGCTCGCTCTCG	RT-qPCR	*AT4G01000*	MOB7
At4g01000_qPCR_F_2	CAGCAGACATGGAGGTTTTGGG	RT-qPCR	*AT4G01000*	MOB7
At4g01000_qPCR_R_2	TAAAAATAGCCTCGCAGCTCGC	RT-qPCR	*AT4G01000*	MOB7
At4g01000_qPCR_F_3	CGAAGATTGGTGCTGAATCTGAG	RT-qPCR	*AT4G01000*	MOB7
At4g01000_qPCR_R_3	CGTCGTCGCTATCATCACTG	RT-qPCR	*AT4G01000*	MOB7
At4g01290_qPCR_F	CGGCTGCTCTAGGGAGCCAGG	RT-qPCR	*AT4G01290*	MOB7
At4g01290_qPCR_R	CACCGGCTTGACCCACTGCC	RT-qPCR	*AT4G01290*	MOB7
At4g01290_qPCR_F_2	TTGGGGATTCAGCAGAGGATGG	RT-qPCR	*AT4G01290*	MOB7
At4g01290_qPCR_R_2	ACCCAAGGTCGAGTTCATGACC	RT-qPCR	*AT4G01290*	MOB7
At4g01290_qPCR_F_3	AGCACTGTTGCTTGACTTCG	RT-qPCR	*AT4G01290*	MOB7
At4g01290_qPCR_R_3	GGCGATGAACTATAGTCATTCCG	RT-qPCR	*AT4G01290*	MOB7
BAK1.qF	TGTTACTAGACTGGGTGAAAGGG	RT-qPCR	*AT4G33430*	General
BAK1.qR	AGCCACTTGGATTAGCTGCTCC	RT-qPCR	*AT4G33430*	General
CPK5.qF	TTTGATGAACTCAAAGCTGGGC	RT-qPCR	*AT4G35310*	General
CPK5.qR	CACTGTTGTCTACATCAGCCGC	RT-qPCR	*AT4G35310*	General
SFC.qF	GACTCTCCCATGTTCCGCAA	RT-qPCR	*AT5G13300*	MOB7
SFC.qR	CTCGCCTAGTCCTTCAGTGTATTT	RT-qPCR	*AT5G13300*	MOB7
Ubox.qF	TGCGCTGCCAGATAATACACTATT	RT-qPCR	*AT5G15400*	General
Ubox.qR	TGCTGCCCAACATCAGGTT	RT-qPCR	*AT5G15400*	General
SMG7.qF	TCCTAGTGGAGGCTTCAGGA	RT-qPCR	*AT5G19400*	General
SMG7.qR	TGCAGGCACTTGAATACTCG	RT-qPCR	*AT5G19400*	General
CBP60g.qF	CGGGCGTAACACTTCTCTTC	RT-qPCR	*AT5G26920*	General
CBP60g.qR	AGCTTCGGCCTTTAATTGGT	RT-qPCR	*AT5G26920*	General
UPF1.qF	GTTAAGGTCCCATCAGAGCAA	RT-qPCR	*AT5G47010*	MOB7
UPF1.qR	GCCTCAACTTCATGTCCCAAT	RT-qPCR	*AT5G47010*	MOB7
RbohD.qF	CGAATGGCATCCTTTCTCAATC	RT-qPCR	*AT5G47910*	General
RbohD.qR	GTCACCGAGAGTGCGGATATG	RT-qPCR	*AT5G47910*	General
RBOHD.qF	TCGTTGCAACACGCTAAGAACG	RT-qPCR	*AT5G47910*	General
RBOHD.qR	GAAGACTCCTATTCTTTTGCCGGG	RT-qPCR	*AT5G47910*	General
RBOHD.2.qF	ATGATCAAGGTGGCTGTTTACCC	RT-qPCR	*AT5G47910*	General
RBOHD.2.qR	GCAGTTCACCAACATGAACTGTCC	RT-qPCR	*AT5G47910*	General
18s.rRNA.qF	AAACGGCTACCACATCCAAG	RT-qPCR		MOB7
18s.rRNA.qR	CCTCCAATGGATCCTCGTTA	RT-qPCR		MOB7
AT4G01000_a	TGAGTATCTGAAGAAGCAATCC	Sequencing	*AT4G01000*	MOB7
AT4G01000_b	GATTTACCTGTTTCTGTTGCTG	Sequencing	*AT4G01000*	MOB7
AT4G01290_a	CACTAGACGTGACGCTAGAG	Sequencing	*AT4G01290*	MOB7
AT4G01290_b	AAAGCTTTCCTCGATCTCGA	Sequencing	*AT4G01290*	MOB7
AT4G01290_c	CTGTTGATGACCAGGCTTCG	Sequencing	*AT4G01290*	MOB7
AT4G01290_d	CGTCTCACTTGAATGGTTCAG	Sequencing	*AT4G01290*	MOB7
AT4G01290.-1327	CGAGATTTCCAAGGTGTGAGTCC	Sequencing	*AT4G01290*	MOB7

AT4G01290.-355	TTCATCTTTTCCCGATTTGAGG	Sequencing	*AT4G01290*	MOB7
AT4G01290.+138	GCAGTTGCAATTGTTTTCAGGAAACC	Sequencing	*AT4G01290*	MOB7
AT4G01290.+647	GTGGACTAGTATTCTGAATAGTTACC	Sequencing	*AT4G01290*	MOB7
AT4G01290.+1174	TCTTGAATACTGCTCCATCACG	Sequencing	*AT4G01290*	MOB7
AT4G01290.+1671	ATCACGCTCCAACAATTCCTGG	Sequencing	*AT4G01290*	MOB7
AT4G01290.+2657	AGCTTTCCTCGATCTCGACTCC	Sequencing	*AT4G01290*	MOB7
AT4G01290.+3653	TCGGTGACAGCTATCATCCACC	Sequencing	*AT4G01290*	MOB7
AT4G01290.+4154	ACCCATCAAAATACATGTCTTTTCC	Sequencing	*AT4G01290*	MOB7
AT4G01290.+4643	ATGTAAACAACCAGATGCCGGG	Sequencing	*AT4G01290*	MOB7
AT4G01290.-1106	GTTGGTTGGTTTATTACACTCTAGG	Sequencing	*AT4G01290*	MOB7
AT4G01290.-679	TCAATTTTACCTTCCCCTTTGAGAG	Sequencing	*AT4G01290*	MOB7
AT4G01290.+2114	GAGTAAGAGAATTTGGGAATAGAGG	Sequencing	*AT4G01290*	MOB7
AT4G01290.+3132	ACGACTTGTTTGGGAAATGATAGGG	Sequencing	*AT4G01290*	MOB7
bak1-5_F	CAGTTCCAGACAGAGGTTGAG	Sequencing	*AT4G33430*	General
bak1-5_R	CTCCATACCCAAAGACATCGG	Sequencing	*AT4G33430*	General
BAK1_A_F	CTTCCAGAAAGCCACGTGCC	Sequencing	*AT4G33430*	General
BAK1_B_F	AGTGGGACTTTTAGATGGTTGG	Sequencing	*AT4G33430*	General
BAK1_C_F	GGATGATACACAATCGGTCACGG	Sequencing	*AT4G33430*	General
BAK1_D_F	CGAACTTGCTATTAAGACCAAGCCC	Sequencing	*AT4G33430*	General
BAK1_E_F	AGCATTAAGTAGTCAACGGTCAGC	Sequencing	*AT4G33430*	General
BAK1_F_F	GGGTTACATCTGTTTCGACTGATTCC	Sequencing	*AT4G33430*	General
BAK1_G_F	AAGAATGGTAATGACAGGGAGC	Sequencing	*AT4G33430*	General
BAK1_H_F	TGTATGAAATCGATTTGGTTCTGG	Sequencing	*AT4G33430*	General
BAK1_I_F	TCTCAAACAATCCTCTCACCGG	Sequencing	*AT4G33430*	General
BAK1_J_F	TCATTGCGTGAACTACAAGTTGC	Sequencing	*AT4G33430*	General
BAK1_K_F	AAGAGTTTGAAGCCGTGGTTGG	Sequencing	*AT4G33430*	General
BAK1_L_F	TGGGAAGAGTGGCAAAAGGAGG	Sequencing	*AT4G33430*	General
BAK1_M_R	CGGCTATGCACTTAACCAAGCC	Sequencing	*AT4G33430*	General
BAK1_D'_R	ATCATCATAATCCTAATTACCGGCCC	Sequencing	*AT4G33430*	General
BAK1_G'_R	AGATCCAAGCTCACCAATTCCG	Sequencing	*AT4G33430*	General
BAK1_J'_R	AAGTACCATCAGCTAACCGTCC	Sequencing	*AT4G33430*	General
AT5G66210_a	AAAGTGGGAAAGTGAGAAGG	Sequencing	*AT5G66210*	General
AT5G66210_b	CATTTGCAACATTGTTCTGTGG	Sequencing	*AT5G66210*	General
AT5G66210_c	CCTCCTCCAATTTCTTGCAG	Sequencing	*AT5G66210*	General
AT5G66210_d	GCGGATTCTTTGACTAATGCT	Sequencing	*AT5G66210*	General
AT5G66210_e	CAGATTGATAGCAACACTGATGGG	Sequencing	*AT5G66210*	General

Table 2.4 List of primers used in this study

3. Phenotypic characterisation of *bak1-5 mob7, 8, 9* and *10*

3.1. Introduction

Despite increasing knowledge of PTI signalling, how immune homeostasis is maintained remains largely unknown. To identify novel factors involved in this regulation different strategies could be applied.

3.1.1. Approaches to identify novel regulators of immunity

One approach to identify a new component of a signalling pathway is to seek genes co-expressed with known genes involved in this pathway (Stuart et al., 2003; USADEL et al., 2009; Okamura et al., 2015). With accumulating transcriptomic data under different conditions and developmental stages, several platforms (*e.g.* Genevestigator, ATTED-II) integrate these different datasets to generate a gene expression profile, allowing inferences regarding gene function to be made (Hruz et al., 2008; USADEL et al., 2009; Obayashi et al., 2018). For example, in *Arabidopsis thaliana* (hereafter Arabidopsis) the Ca^{2+} permeable channel CYCLIC NUCLEOTIDE-GATED CHANNEL 19 (CNGC19) has recently been shown to be implicated in Arabidopsis defence against Spodoptera herbivory as *CNGC19* coexpresses with *PEP-RECEPTOR 1* (*PEPR1*) and *PEPR2* (Meena et al., 2019). Despite an increasing number of transcriptomics datasets, certain conditions or developmental stage remain insufficiently studied. In addition, co-expression does not necessarily correlate with protein level and involvement of the protein in a certain pathway (Zander et al., 2020).

Another approach is to explore direct protein interactions or components of protein complexes. Platforms such as STRING integrate published datasets and predicted interactions to build association networks (Szklarczyk et al., 2019). Protein interaction can be also investigated by immunoprecipitation of a known protein followed by mass spectrometry to identify new components. In addition, various novel proteins have been found though interaction screens in orthologous systems such as yeast two-hybrid screens (Brückner et al., 2009). In addition to *in vivo* screens, *in vitro* screens can also be used to identify interacting partners. An example relevant to pattern recognition receptors (PRR)-signalling is the leucine-rich repeat (LRR)-based cell surface interaction network (Smakowska-Luzan et al., 2018). This screen used extracellular domains of 200 LRR-RKs from Arabidopsis into bait and prey expression vectors for recombinant protein production in Drosophila and identified 567 pairwise interactions (Smakowska-Luzan et al., 2018). Proteins can be involved in various pathways which limit the identification of new proteins in a certain pathway. For example, BRASSINOSTEROID INSENSITIVE 1-ASSOCIATED RECEPTOR KINASE 1 (BAK1) interacts with the brassinosteroid receptor BRASSINOSTEROID INSENSITIVE1 (BRI1) (Li and Chory, 1997; Li et al., 2002; Nam and Li, 2002) and receptors involved in immunity such as FLAGELLIN SENSING2 (FLS2) and EF-TU RECEPTOR (EFR) (Gómez-Gómez and Boller, 2000; Zipfel et al., 2006; Chinchilla et al., 2007). All the proteins are

not suited for orthologous expression. For example, some proteins may become toxic or adopt different folding when expressed in orthologous systems (Xing et al., 2016).

Genetics can also be used to seek novel regulators. Natural variation is a great source of phenotype diversity in immune responses. In addition, forward genetic approaches have been extensively used to explore this diversity and identify PTI signalling components (Kato et al., 2020). A forward genetic screen aimed at the discovery of proteins involved in the biogenesis and function of EFR resulted in the identification of *elf18-insensitive* (*elfin*) mutants, which included mutants of proteins involved in endoplasmic reticulum (ER) quality control (Li et al., 2009; Nekrasov et al., 2009). Similarly, the genetic screen for *flagellin-insensitive* (*fin*) mutants showing alterations in flg22-induced ROS burst, led to the identification of various proteins involved in flagellin response such as FLS2, BAK1 and the enzyme ASPARTATE OXIDASE (Boutrot et al., 2010; Macho et al., 2012). Mutants with "changed Ca^{2+} elevation" (cce) after flg22 treatment were also screened using forward genetic and several alleles of receptor complex components were identified including BAK1 and FLS2 (Ranf et al., 2014). In Arabidopsis seedlings, the *priority in sweet life* (*psl*) mutant screens showed mutants with de-repressed anthocyanin accumulation in the presence of elf18 (Saijo et al., 2009; Serrano et al., 2012). Among these mutants, several genes involved in ER quality control were isolated (Lu et al., 2009; Saijo et al., 2009). To elucidate the signalling networks regulating immune gene activation, a genetic screen was performed in Arabidopsis transgenic plants carrying a luciferase reporter gene under the control of the *FLG22-INDUCED RECEPTOR-LIKE KINASE* (*FRK1*) promoter. Various mutants with altered luciferase activity upon flg22 treatment were identified and named as *arabidopsis genes governing immune gene expression* (*aggie*). This screen identified *aggie1*, a mutant of *RNA POLYMERASE II C-TERMINAL DOMAIN PHOSPHATASE-LIKE 3* (Li et al., 2014b) and *aggie2*, a mutant of *POLY(ADP-RIBOSE) GLYCOHYDROLASE 1*, revealing that protein poly ADP-ribosylation plays a role in defence gene expression (Feng et al., 2015).

Genetic screens require phenotypes that can be easily and robustly distinguishable which leads predominantly to the identification of major players in the pathway. With the increasing number of genetic screens, the identified genes are predominantly already known in the pathway. In addition, genetic screens are mainly conducted in a wild-type background to identify major, nonredundant factors. However, such screens often fail to identify regulatory genes that have overlapping functions with other genes. To circumvent this genetic redundancy, genetic screens can be conducted in a mutant background. Genetic modifier screens usually use a weak allele in a major player of a biological process, in order to isolate other genes in that biological pathway. The second-site mutations resulting from this screen can either lead to an enhancement or to a suppression of the phenotype of the mutant plants that are being mutagenized (Dinh et al., 2014). More recently, a transient RNA interference (RNAi)-based screen of

Arabidopsis T-DNA insertion lines, identified suppressors of *MAPK kinase kinase 1(MEKK1)*-mediated cell death (Yang et al., 2020). From this screen, MEKK2, SUPPRESSOR OF MKK1 MKK2 2 (SUMM2), and CALMODULIN-BINDING RECEPTOR-LIKE CYTOPLASMIC KINASE 3 (CRCK3) were identified as specific regulators of RNAi *MEKK1*, while they have been previously identified components in the *mekk1-mkk1/2-mpk4* cell death pathway (Kong et al., 2012; Zhang et al., 2012; Su et al., 2013; Zhang et al., 2017b).

3.1.2. *bak1-5* allele, a useful tool to study immunity

The LRR-type receptor kinase (LRR-RK) BAK1 and related SOMATIC EMBRYOGENESIS RECEPTOR KINASEs (SERKs) function as receptor-associated kinases that form stable complexes with multiple receptors at the PM (Ma et al., 2016). SERK3/BAK1 is involved in diverse processes and displays a developmental and PTI phenotype upon mutation in Arabidopsis (Kumar and Van Staden, 2019; Liu et al., 2020). BAK1 was initially identified as a regulator of brassinosteroid (BR) signalling and BRI1-interacting protein (Li et al., 2002; Nam and Li, 2002). BAK1 functions also in ABA-mediated stomatal closure in guard cells through OPEN STOMATA1 (OST1) phosphorylation, which is inhibited by the interaction of ABA-INSENSITIVE1 (ABI1) with BAK1 (Shang et al., 2016). In addition, BAK1 acts as co-receptor in stomatal patterning by interacting with the receptors ERECTA (ER) and ER-LIKE 1 (ERL1) in a ligand-dependent manner (Meng et al., 2015). Furthermore, BAK1 functions in PHYTOSULFOKINE alpha (PSK)-regulated root growth (Ladwig et al., 2015). Similar to other SERKs, BAK1 regulates floral organ abscission by association with HAESA (HAE) and HAE-LIKE2 (HSL2) in a ligand-dependent manner (Meng et al., 2016; Santiago et al., 2016). BAK1 might also play an essential role in regulating various types of programmed cell death (PCD) (Gao et al., 2018). *bak1* knock-out mutants have a spreading lesion phenotype upon pathogen infection and premature senescence (Kemmerling et al., 2007; Jeong et al., 2010), which is aggravated in double-mutant combinations with its closest paralog BKK1/SERK4 (He et al., 2007; Jeong et al., 2010). BAK1 is an important regulator of immune responses by forming ligand-dependent heteromers with PRRs (Yasuda et al., 2017). For example, BAK1 forms a complex with FLS2, which recognises the flagellin epitope, flg22 (Chinchilla et al., 2007; Heese et al., 2007; Schulze et al., 2010). BAK1 associates as well with EFR upon elf18 perception (Schulze et al., 2010; Roux et al., 2011) and PEP RECEPTORS (PEPRs) upon AtPep perception (Tang et al., 2015). In *bak1* null allele, *bak1-4*, only a delayed and slightly reduced reactive oxygen species (ROS) burst is observed upon flg22 and elf18 treatment while hyposensitive to brassinolide (Nam and Li, 2002; Chinchilla et al., 2007; Heese et al., 2007; Schwessinger et al., 2011). In addition, higher-order mutants with the absence of BAK1 and BKK1 trigger constitutive cell death and seedling lethality (Wang et al., 2008b).

Interestingly, another allele of BAK1, *bak1-5* was identified to be severely compromised in immune signalling but not impaired in BR signalling or cell death control (Schwessinger et al., 2011). The *bak1-5* allele was identified as an *elfin* mutant using a Col-0 EMS mutagenized population (Schwessinger et al., 2011). Out of 167 elfin mutants, only one showed blocked or reduced responses to both flagellin and EF-Tu. In this mutant, BAK1 was found to have a single missense substitution in the 10th exon, which leads to a C408Y change in the cytoplasmic kinase domain. Importantly, this mutation is a dominant-negative mutation that is not caused by impaired BAK1 accumulation or FLS2–BAK1 association, but results from reduced phosphorylation at the tyrosine 403 (Schwessinger et al., 2011; Perraki et al., 2018).

3.1.3. *mob* screen

To identify loci involved in PTI, a forward genetic screen was designed in the immunodeficient mutant *bak1-5*, called *modifier of bak1-5* (*mob*) screen (Monaghan et al., 2014). *bak1-5* allele offers the opportunity to find negative regulators of immune signalling in case of loss-of-function mutation or positive regulator if gain-of-function mutation is observed.

The *mob* screen looked for suppressors of the *bak1-5* ROS phenotype (Monaghan et al., 2014). *bak1-5* seeds were mutagenised with EMS, and around 40,000 seedlings in the M_2 generation were screened for regained flg22- and elf18-induced ROS production (Figure 3.1 A) (Monaghan et al., 2014). From 100 mutants with a consistent phenotype during 2 tests in the M_2, only 10 mutants named *mob1* to *mob10* retained restored flg22, elf18 and AtPep1 response in the M_3 generation (Monaghan et al., 2014). All the mutants were sequenced at the *BAK1* locus and none of the *mob* mutants presented another mutation in the *BAK1* coding sequence. In addition, allelism tests were performed between each *mob* and only two presented a clear allelism (*mob1* and *mob2*) (Monaghan et al., 2014).

3.1.4. Identified *MOBs*

MOB1 and *MOB2* have been mapped and confirmed to encode the CALCIUM-DEPENDENT PROTEIN KINASE 28 (CPK28) (Monaghan et al., 2014). The mutations in *bak1-5 mob1* results in a CPK28 protein with amino acid substitutions S245L and A295V, while the mutation in *bak1-5 mob2* results in an early stop codon predicted to produce in a truncated protein. CPK28 acts as a negative regulator in PTI through phosphorylating BIK1, which influences the ubiquitination of BIK1 by the E3 ligase PUB25/26. Once poly-ubiquitinated, BIK1 is degraded by the proteasome (Monaghan et al., 2014; Monaghan et al., 2015; Wang et al., 2018b).

MOB4 has been mapped and identified to encode CONSTITUTIVE ACTIVE DEFENSE 1 (CAD1) (Monaghan *et al.*, unpublished results). The mutation in *bak1-5 mob4* results in an amino acid substitution C43Y (Monaghan *et al.*, unpublished results). Loss of CAD1 results in programmed cell death in the context of plant immunity (Morita-Yamamuro et al., 2005). Also, this protein is a component

of a large molecular framework that controls endophytic microbial abundance and diversity in the phyllosphere (Chen et al., 2020).

MOB6 encodes the subtilase SITE-1 PROTEASE (S1P) (Stegmann et al., 2017). The mutation in *bak1-5 mob6* is a missense mutation, which leads to the amino acid substitution P612S (Stegmann et al., 2017). S1P cleaves pro-RAPID ALKALINIZATION FACTOR 23/33 (PRORALF23/33) to RALF23/33 (Stegmann et al., 2017). Once cleaved, these peptides are perceived by LORELEI-LIKE-GPI-ANCHORED PROTEIN 1 (LLG1) in complex with FERONIA (FER) (Haruta et al., 2014; Stegmann et al., 2017; Xiao et al., 2019) and modulate FLS2-BAK1 complex formation (Stegmann et al., 2017).

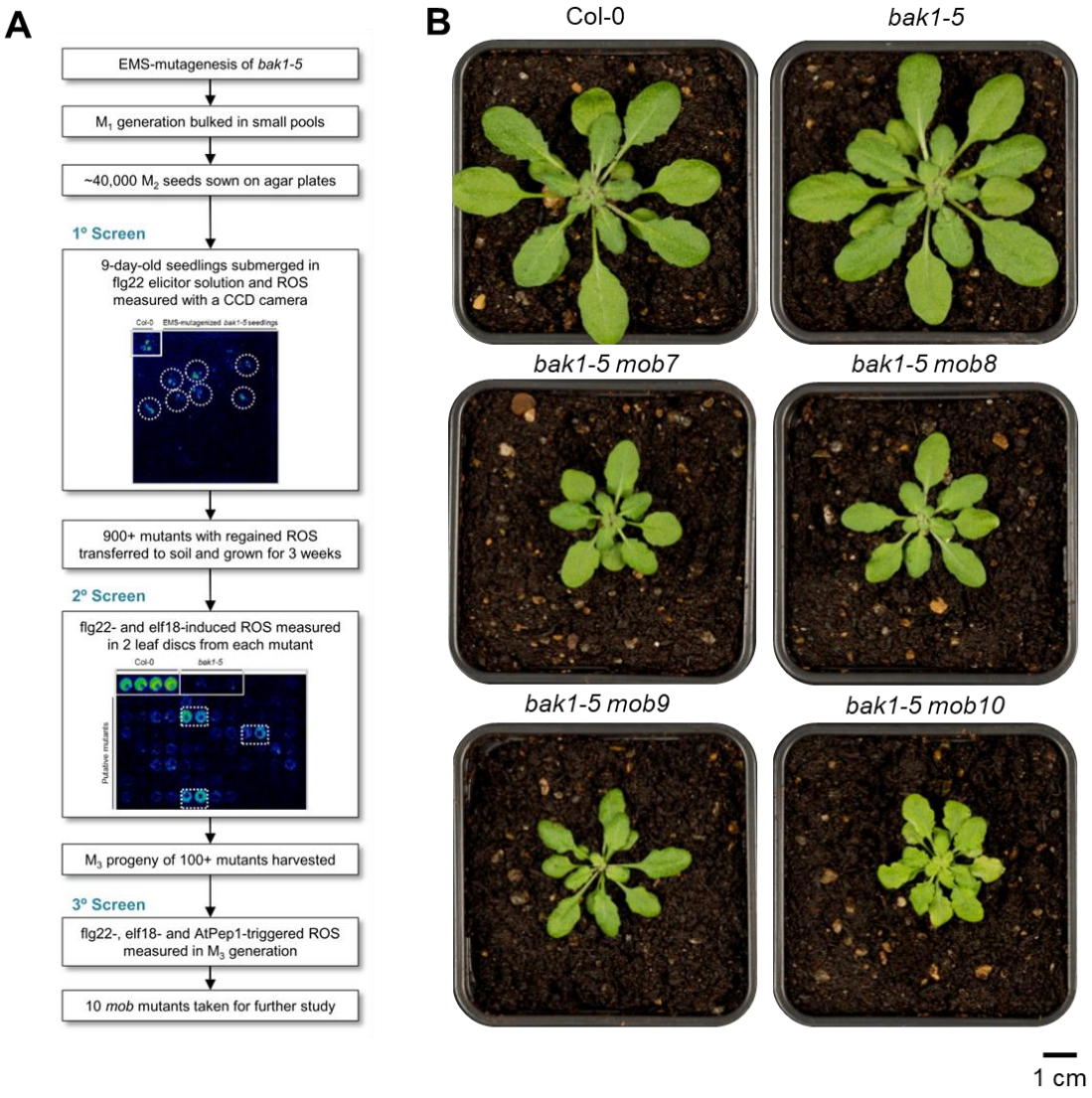

Figure 3.1 *mob* screen and growth phenotypes of *bak1-5 mob7, 8, 9* and *10*.
(A) Figure from previous article (Monaghan et al., 2014). Outline of the *mob* screen. (B) Rosette morphology of 5-week old plants of the corresponding genotype. Pictures were taken by Jacqueline Monaghan.

3.1.5. Objectives

As *bak1-5 mob7, 8, 9* and *10* were still uncharacterised and the causative mutations unidentified, one objective was to confirm previous phenotypes as found in the *mob* screen and characterise these mutants in immunity. Another objective was to determine the conditions in which *bak1-5 mob* mutants show the strongest difference in immune signalling compared to *bak1-5*; these conditions would be used to map the mutations.

3.2. Results

3.2.1. Restoration of elicitor-triggered ROS production in *bak1-5 mob7, 8, 9* and *10*

In order to corroborate the phenotype observed in the *mob* screen, ROS production was assayed in the different *mob* mutants. *bak1-5 mob7, 8, 9* and *10* at the M_5 generation partially restore elf18- and flg22-triggered ROS compared to *bak1-5* (Figure 3.2 A,C,D). Intriguingly, the intensity and the kinetics of the responses are different among the mutants (Figure 3.2 A). While maximum ROS production in Col-0 is generally observed at 10 min after elicitation with elf18, *bak1-5* shows a delay in this response with a peak at 17 min. Similar to *bak1-5*, the mutants *bak1-5 mob7, 8, 9* and *10* have a delayed ROS burst (Figure 3.2 B). All *bak1-5 mob* mutants have higher ROS production than *bak1-5* after elf18 treatment (Figure 3.2 C). With flg22, only *bak1-5 mob9* regained ROS production (Figure 3.2 D). Elicitation with the DAMP AtPep1 induced higher ROS production in *bak1-5 mob9* and *10*, and slightly higher in *bak1-5 mob7*, compared to *bak1-5* (Figure 3.2 E). For chitin-induced ROS production, which is independent of BAK1, only *bak1-5 mob7* shows higher ROS production than *bak1-5* (Figure 3.2 F). From the *bak1-5 mobs* tested, *bak1-5 mob9* has the strongest response to elicitors. Interestingly, differences are observed in *bak1-5 mobs* to the different elicitors. The mutant *bak1-5 mob7* shows higher ROS production than *bak1-5* after elf18 and chitin, and slightly higher with AtPep1. *bak1-5 mob8* only regained ROS production after elf18 treatment. From the *bak1-5 mob* mutants tested, *bak1-5 mob9* show the strongest response to elicitors. Intriguingly, restored ROS production in *bak1-5 mob10* seems to be specific to elf18 and AtPep1; the ROS production in response to flg22 and chitin is similar to that in *bak1-5*.

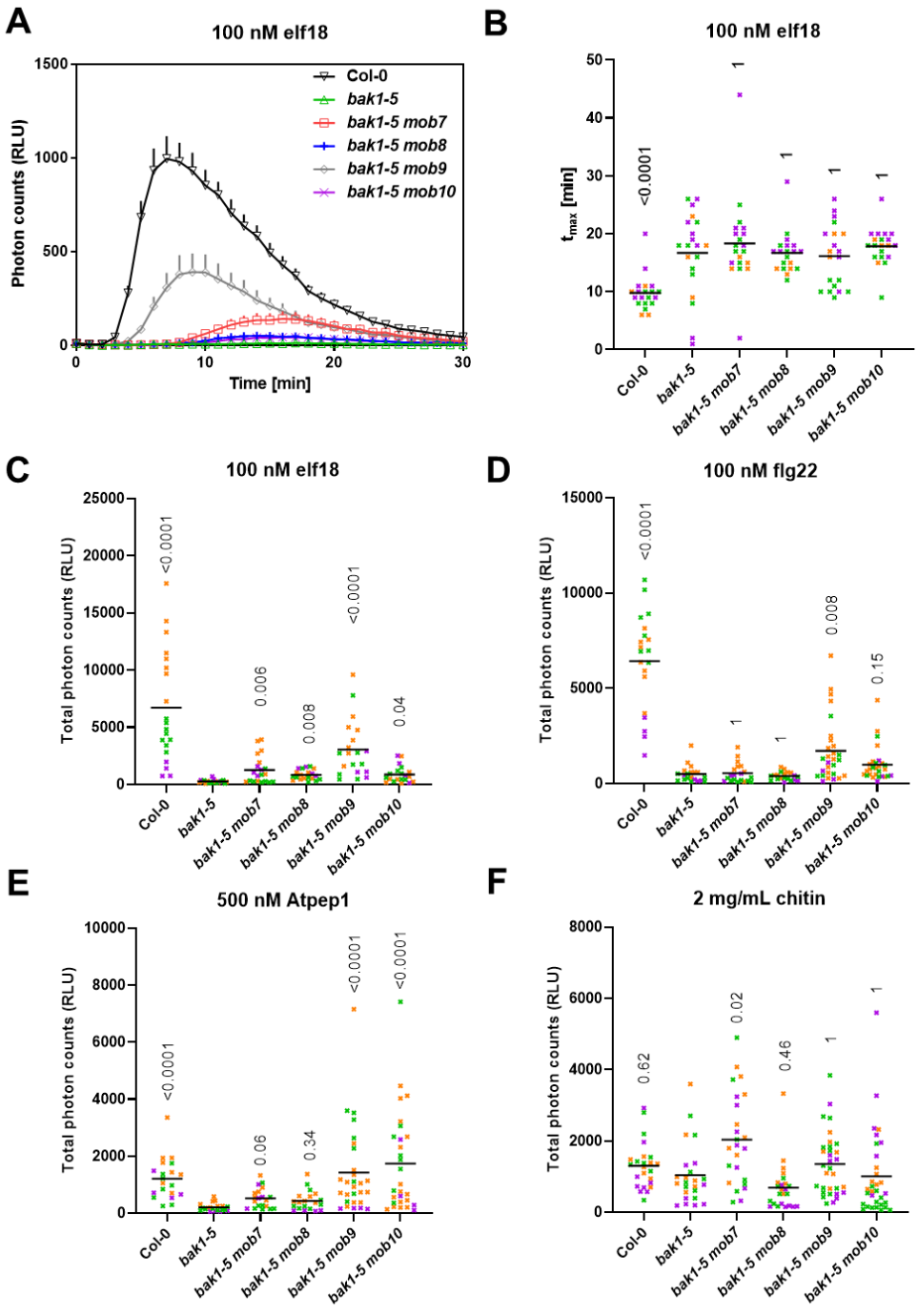

Figure 3.2 Restoration of elicitor-triggered ROS production in *bak1-5 mob7, 8, 9* and *10*.
(A) ROS burst kinetic expressed as relative light units (RLU), in leaf discs following treatment with 100 nM elf18. Values are means + standard errors (n=8). Experiment was repeated two times with similar results. (B-E) Total ROS accumulation over 60 min expressed as RLU after treatment with 100 nM elf18 (B) or 100 nM flg22 (C) or 500 nM Atpep1 (D) or 2 mg/mL chitin (E). (B-E) Horizontal lines represent the means from three independent experiments (n>3) and the symbol colours indicate the different experiments. Numbers above symbols are p-values from Dunn's multiple comparison test between corresponding genotype and *bak1-5*.

3.2.2. *mob7, 8, 9* and *10* restore signalling triggered by elicitors in *bak1-5*

Prolonged exposure to elicitors such as elf18, flg22 and AtPep1 leads to growth inhibition in wild-type seedlings (Gómez-Gómez et al., 1999; Zipfel et al., 2006; Krol et al., 2010); however, this effect is strongly impaired in *bak1-5* (Roux et al., 2011; Schwessinger et al., 2011). While *bak1-5 mob*s seedlings grow normally without elicitors, their growth is strongly affected by most elicitors tested (Figure 3.3 A). *bak1-5 mob7, 8* and *9*, unlike *bak1-5 mob10,* show a restoration of growth inhibition induced by elf18

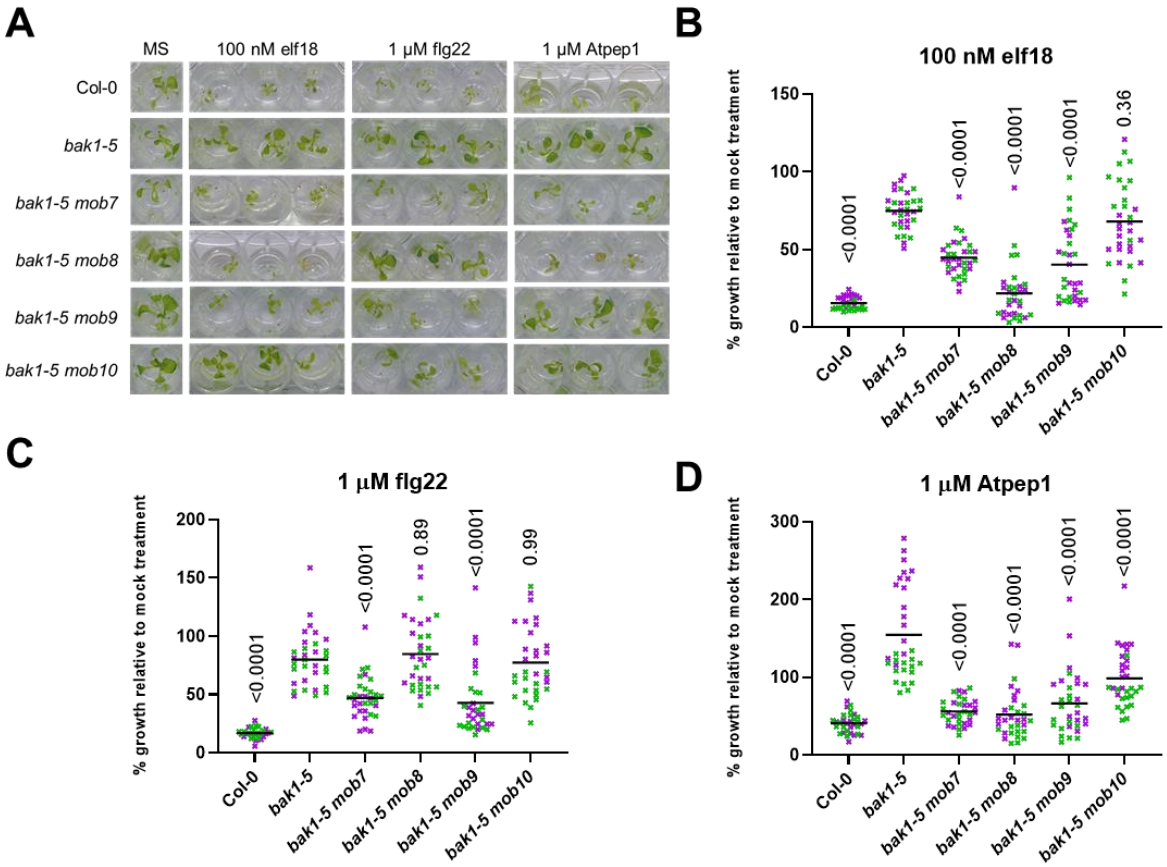

Figure 3.3 Restoration of growth inhibition in *bak1-5 mob7, 8, 9* and *10*.
(A) Images of 14-day-old seedlings grown in MS media or MS media containing 100nM elf18 or 1 µM flg22 or 1 µM AtPep1. Experiment was repeated once with similar results. (B-D) Growth inhibition represent as percentage of fresh weight in response to 100 nM elf18 (B) or 1 µM flg22 (C) or 1 µM AtPep1 (D) relative to untreated seedlings. (B-D) Horizontal lines represent the means from 2 independent experiments (n>14) and the symbol colours indicate the different experiments. Numbers above symbols are p-values from Dunnett's multiple comparison test between corresponding genotype and *bak1-5*.

treatment (Figure 3.3 B). While *bak1-5 mob8* and *10* still show insensitivity to flg22, the growth of *bak1-5 mob7* and *9* are impacted by this treatment (Figure 3.3 C). Growth inhibition in response to AtPep1 was restored in all *bak1-5 mob* mutants (Figure 3.3 D). In summary, the growth inhibition of *bak1-5 mob7* and *9* is restored in response to all elicitors tested relative to *bak1-5*. However, *mob8* only restores *bak1-5* growth inhibition in response to elf18 and AtPep1, while *bak1-5 mob10* is only affected by

AtPep1. Thus, *mob7, 8, 9* and *10* restore signalling triggered by immunogenic peptides in *bak1-5*. In addition, *bak1-5 mob7, 8, 9* and *10* might have constitutive activation of signalling as the mutants appear smaller than *bak1-5* at 5-week-old stage (Figure 3.1 A), although whether this phenotype is linked to the immune restoration phenotypes remains to be determined.

3.2.3. Antibacterial immunity in *bak1-5 mob7, 8, 9* and *10*

As PTI signalling results in resistance against pathogens and *bak1-5* is hyper-susceptible to the hypo-virulent bacterium *Pseudomonas syringae* pathovar *tomato* (*Pto*) DC3000 *coronatine-minus* (*COR*$^-$) strain, *bak1-5 mob*s were surface-inoculated with this pathogen. While *bak1-5 mob8, 9* and *10* show similar resistance as *bak1-5*, *bak1-5mob7* slightly regained resistance (Figure 3.4 A), which could be confirmed in 2 additional repeats (Figure 3.4 B).

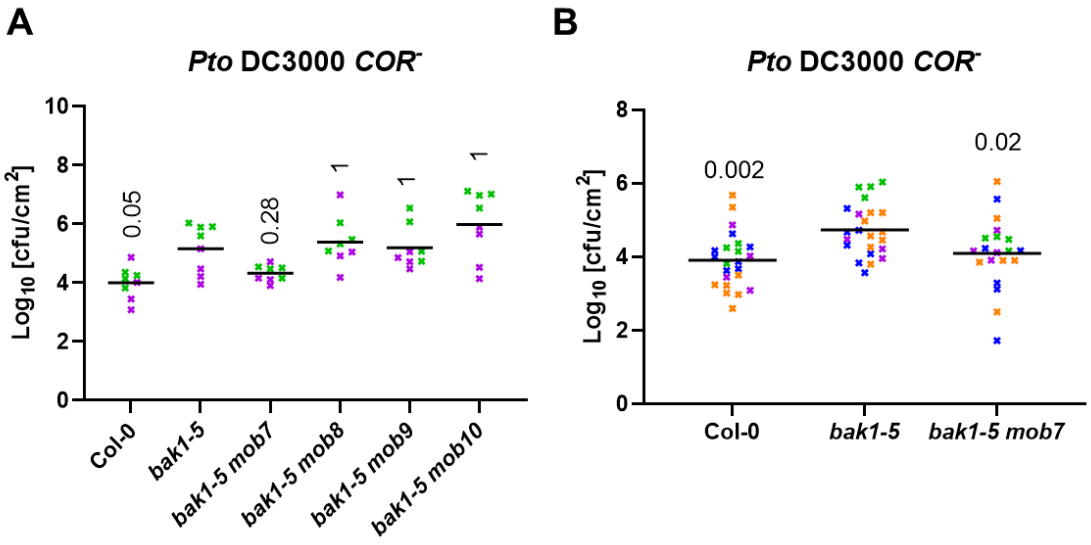

Figure 3.4 Antibacterial resistance of *bak1-5 mob* mutants.
(A-B) Bacterial growth (cfu/cm^2) in leaves spray inoculated with 10^7 cfu/mL (O.D. 0.2) *P. syringae* pv. *tomato* DC3000 *COR*$^-$ and sampled at 3 dpi. (A) Horizontal lines represent the means from 2 independent experiments (n>14) and the symbol colours indicate the different experiments. Numbers above symbols are p-values from Dunn's multiple comparison test between corresponding genotype and *bak1-5*. (B) Horizontal lines represent the means from 4 independent experiments (n>14) and the symbol colours indicate the different experiments. Numbers above symbols are p-values from Dunnett's multiple comparison test between corresponding genotype and *bak1-5*.

3.3. Discussion

bak1-5 mutant plants are strongly affected in PTI signalling; the *mob* mutants that restore PAMP response in this line thus represent potential negative regulators of PTI signalling. Similar to previously identified *mob* mutants (Monaghan et al., 2014; Stegmann et al., 2017), *bak1-5 mob7, 8, 9* and *10* show a restoration of elicitor-induced signalling. Interestingly *bak1-5 mob*s show some specificity in their

response to the different elicitors tested (Table 3.1). Varied assays allow a deeper understanding of the impact of *mob* mutations in PTI signalling.

	elf18		flg22		Atpep1		chitin	*Pto* DC3000 *COR*-
	ROS	SGI	ROS	SGI	ROS	SGI	ROS	
bak1-5 mob7	0.006	<0.0001	1	<0.0001	0.06	<0.0001	0.02	0.002
bak1-5 mob8	0.008	<0.0001	1	0.89	0.34	<0.0001	0.46	1
bak1-5 mob9	<0.0001	<0.0001	0.008	<0.0001	<0.0001	<0.0001	1	1
bak1-5 mob10	0.04	0.36	0.15	0.99	<0.0001	<0.0001	1	1

Table 3.1 Summary of restoration phenotypes in the different *bak1-5 mob* mutants.
Table summarising p-values from Figure 3.2, 3.3, 3.4. P-values are from different multiple comparison test between *bak1-5* and the corresponding *bak1-5 mob* mutants. P-values less than 5 % are highlighted in red.

3.3.1. *bak1-5 mob7*

bak1-5 mob7 showed restored responsiveness to all elicitors tested and is the only mutant to show a restoration of antibacterial resistance compared to *bak1-5*. Interestingly, even in *bak1-5 mob7*, not all elicitor responses were restored: the ROS response to both flg22 and AtPep1 remained low as in *bak1-5*. This is also a discrepancy with the strong effect of this mutation on growth inhibition induced by both these elicitors. This difference could be the result of the different elicitor concentration or developmental stage used for these two different assays. For example, it has been previously shown that FLS2 expression is differentially regulated during plant development (Hu and Yang, 2019). In 2-day-old seedlings, high levels of TARGET OF EARLY ACTIVATION TAGGED 1 and 2 (TOE1 and TOE2) proteins suppressed the transcription of *FLS2*. In 6-day-old seedlings, increased expression of *microRNA172* (*miR172*) repressed *TOE1/2* transcripts, thereby relieving the suppression of *FLS2* by TOE1/2 (Zou et al., 2018). In the transition from the juvenile to the adult vegetative phase, SQUAMOSA PROMOTER BINDING PROTEIN-LIKE 9 (SPL9) (Wu et al., 2009) and SPL15 (Hyun et al., 2016) directly bind to *miR172b* promoter and activate its expression. *bak1-5 mob7* is also the only *mob* to affect chitin responsiveness. Even though chitin is independent of BAK1, genes induced by chitin are highly similar to those induced by flg22 or elf26 (Wan et al., 2008). However, different receptor-like cytoplasmic kinase are recruited in response to flg22/elf18 in comparison to chitin (Shinya et al., 2015). MOB7 seems then to act downstream of PBLs. Despite recent findings suggesting that elicitor-induced seedling growth inhibition is caused by extracellular alkalinisation (Kesten et al., 2019) and that ROS impact plant growth (Mhamdi and Van Breusegem, 2018), underlying signalling events remains mostly unknown in comparison to elicitor-induced ROS production. Interestingly, flg22 induces seedling growth inhibition but not ROS production in *bak1-5 mob7*, thereby identification of *mob7* mutation could shed light on a mechanism responsible of flg22-induced seedling growth inhibition and independent of ROS production.

3.3.2. *bak1-5 mob8*

In *bak1-5 mob8*, responsiveness is specifically restored with elf18 and AtPep1 but not flg22 and chitin. As most the signalling components are common upon elicitation with elf18 and flg22 (Couto and Zipfel, 2016), identification of *mob8* mutation, could shed light on some differences between these elicitors. Among known differences, EFR accumulation depends on ER glycoprotein folding quality control (ERQC), while FLS2 and PEPR1/PEPR2 better tolerate dysfunction of ERQC (Tintor and Saijo, 2014). In addition, FLS2 strongly requires BAK1, in contrast to EFR or PEPR1/PEPR2 that can promiscuously function with different SERK members (Roux et al., 2011; Yamada et al., 2016b). MOB8 could be thereby involved in the regulation of some SERKs. Furthermore, the regained responsiveness is stronger for seedling growth inhibition than for ROS production, which could indicate a role of MOB8 either on the growth, or signalling independent of ROS production. Similar to *bak1-5 mob8*, *mob9* and *mob10*, restoration of immune signalling in these mutants does not impact bacterial resistance; thereby, it would be interesting to assay elicitor-induced resistance in these mutants to investigate how elicitor responses in these *mob*s functionally impact immune responses.

3.3.3. *bak1-5 mob9*

In *bak1-5 mob9*, responses are regained upon all elicitors tested but chitin. This difference of response between elf18, flg22, AtPep1 on one side and chitin in the other could be explained by the specificities of some downstream components such as BAK1, which is not required for chitin perception (Shan et al., 2008; Gimenez-Ibanez et al., 2009a; Couto and Zipfel, 2016).

3.3.4. *bak1-5 mob10*

Similar to *bak1-5 mob8*, responsiveness is specifically restored with elf18 and AtPep1 but not flg22 and chitin in *bak1-5 mob10*. Nevertheless, differences are observed between elicitor-induced seedling growth inhibition and ROS production, which suggest different mutations in *mob8* and *mob10*.

3.4. Future perspectives

In order to better understand the impact of *mob* mutants on immune signalling and their respective specificities, mapping of the *mob* mutations will be required. After identification and confirmation of the mutations responsible of the phenotypes, functional characterisation of MOB proteins will be performed to understand mechanistically their function and involvement in immune signalling.

4. *MOB7* encodes the RNA-binding protein CBE1

4.1. Introduction

4.1.1. Forward genetic screen

Forward genetic screenings is a powerful and unbiased technique to dissect biological processes and identify genes and mutations that underlie phenotypes of interest (Page and Grossniklaus, 2002). In order to perform successful forward genetic screens, the organism studied must have a defined genetic background to locate the mutation and the screening method must be simple to screen a large number of individuals. To ensure adequate coverage of the genome – meaning that one will get a mutation in every single gene – a large screening population must be obtained. Since natural allelic mutations are rare in a given Arabidopsis genotype (Ossowski et al., 2010), mutants with desired phenotypes are acquired by exposing a population of individuals to a known mutagen. It is then important to know the genome size and mutagen-dependent mutation rates. There are three main categories of agents used to alter the genome in forward genetic screens: physical mutagens (*e.g.* radiation with gamma-rays, fast neutrons or UV); chemical agents (*e.g.* ethyl-methane sulfonate (EMS)); and biological agents (*e.g.* T-DNA and transposons) (Siddique et al., 2020). The most commonly used mutagen for Arabidopsis is EMS, which predominantly introduces C to T and G to A changes (Krieg, 1963; James et al., 2013). EMS induces random point mutations at a high frequency and can produce viable, weak alleles in genes whose function is essential to the plant (Dinh et al., 2014). However, EMS mutagenesis tends to lead to plants containing more than one mutation (Dinh et al., 2014). Another common mode of mutagenesis is the use of Agrobacterium-mediated transformation, for which transfer DNA (T-DNA) is inserted within the genome (Clough and Bent, 1998). T-DNA mutagenesis often produces loss-of-function mutants as integration of the T-DNA usually perturbs the gene's function (Alonso and Ecker, 2006). An advantage of T-DNA mutagenesis compared to the use of EMS is that T-DNA insertion sites can often be readily identified using PCR-based approaches. However, multiple insertions and complex T-DNA loci may incur and T-DNA mutagenesis can result in chromosomal rearrangements, such as inversions or deletions (Wang and Wang, 2008). Similarly, physical mutagens can induce large DNA inversions and deletions that can prevent the identification of the genes underlying a mutant phenotype (Siddique et al., 2020). After mutagenesis and isolation of a mutant with the desired phenotype, the next step is to identify the mutation(s) responsible for the phenotype.

4.1.2. Identification of EMS mutation from forward genetic screens

Finding the genetic mutation, which is responsible for the observed phenotype, involves multiple steps and can be performed by different approaches (Schneeberger, 2014).

Map-based cloning, also called positional cloning is a technique to locate (map) the gene on its chromosome by crossbreeding with individuals that carry other unusual traits and collecting statistics on how frequently the two traits are inherited together. Hence, a high density of molecular markers is essential for high-resolution mapping. The Arabidopsis ecotypes Columbia (Col-0) and Landsberg *erecta* (La*er*), for example, show abundant divergent sequences that support the design of dense molecular markers (Hardtke et al., 1996; Lukowitz et al., 2000; Qu and Qin, 2014). The most commonly used molecular markers in Arabidopsis map-based cloning are insertion/deletion (InDel) markers based on simple sequence length polymorphisms (SSLP); cleaved amplified polymorphic sequences (CAPS) markers, and derived CAPS (dCAPS) markers based on single nucleotide polymorphisms (SNP) (Hou et al., 2010; Păcurar et al., 2012; Qu and Qin, 2014). These are all PCR-based markers and thus easy to use and affordable. However, if the phenotype studied is very sensitive to the genetic background or the mutation occurs in a region where the recombination rate is low, map-based cloning would not be suitable to identify mutations causing a phenotype.

Whole-genome resequencing is another method using high-throughput sequencing, which allows identification of EMS-induced mutations responsible for the observed phenotype, and which is now commonly being used. Two pipelines, SHOREMAP and next-generation EMS mutation mapping (NGM) have been predominantly used, which depend on bulk analysis of an F_2 mapping population (Schneeberger et al., 2009; Austin et al., 2011). Locating the position of the mutation responsible for the mutant phenotype relies on the fact that other EMS-generated mutations in the genome segregate according to their linkage or not with the mutation in question (Schneeberger and Weigel, 2011; Dinh et al., 2014). To reduce the number of SNPs, backcrossing to the original parent prior to sequencing reduce the number of non-causal mutations and sequencing the parental line from which the mutant was derived also helps to eliminate nonphenotype-causing mutations (James et al., 2013; Dinh et al., 2014). Whole-genome resequencing can be also applied to mutants derived from unsequenced accessions as long as the species has a sequenced-reference genome (Dinh et al., 2014).

4.1.3. Objectives

To identify loci involved in plant immunity, a forward genetic screen was designed in the immunodeficient mutant *bak1-5*, called *modifier of bak1-5* (*mob*) screen (Monaghan et al., 2014). This EMS-induced suppressor screen of the *bak1-5* phenotypes identified 10 mutants, named *mob1* to *mob10* with restored elicitor-induced reactive oxygen species (ROS) production (Monaghan et al., 2014). *MOB1* and *MOB2* have been mapped and confirmed to encode CALCIUM-DEPENDENT KINASE (CPK28) (Monaghan et al., 2014), while *MOB4* encodes CONSTITUTIVE ACTIVE DEFENSE 1 (CAD1) (Monaghan et al., unpublished results). In addition, *MOB6* has been mapped and identified to encode the subtilase SITE-1 PROTEASE (S1P) (Stegmann et al., 2017). However, mutations in *mob7, mob8, mob9*

and *mob10* still remained to be identified. *bak1-5 mob7*, *8*, *9* and *10* show a restoration of elicitor-induced signalling with some specificity in their response to the different elicitors tested (Chapter 3). In order to better understand *mob*s phenotypes, the causative mutations need to be identified. As *bak1-5 mob7* shows interesting phenotypes with an impact on bacterial immunity, mapping was performed to identify the *mob7* causative mutation.

4.2. Results

4.2.1. *mob7* mutation is mapped to *CBE1*

In order to identify the mutation(s) responsible for *mob7* phenotypes, different strategies were considered for mapping (Figure 4.1).

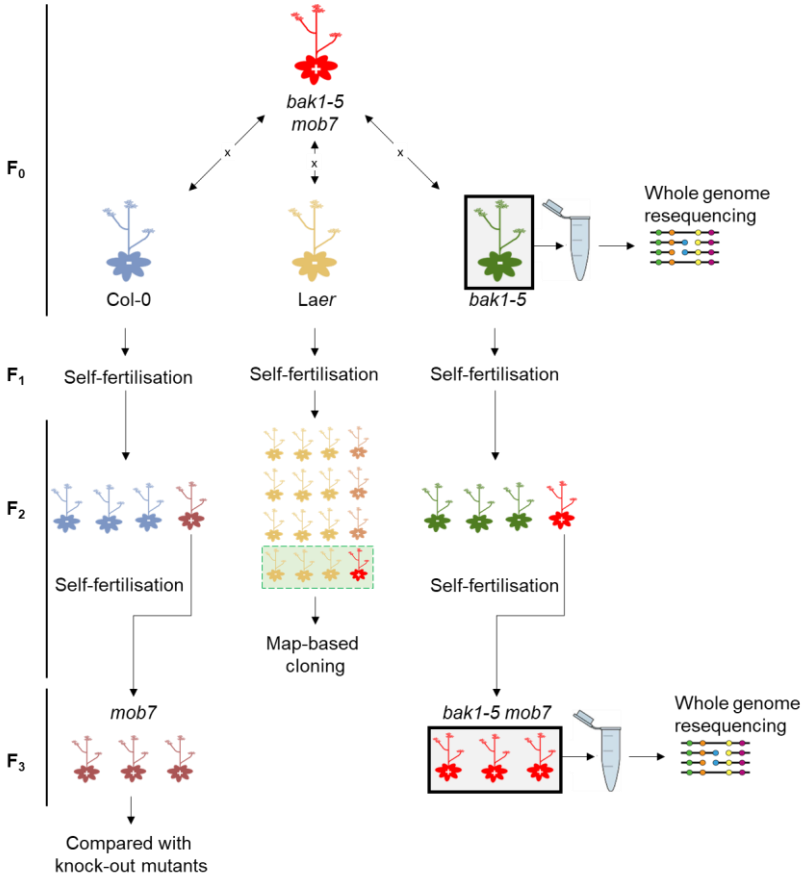

Figure 4.1 Crosses strategies to identify *mob7* mutation.
bak1-5 mob7 was crossed independently to Col-0, *Landsberg erecta* (La*er*) and *bak1-5* to identify *mob7* mutation. $F_{0\text{-}3}$, represents the different generation of the crosses. Within each plant, plus or minus sign indicates the homozygosity of *mob7* mutation. For *bak1-5 mob7* crossed with Col-0, F_2 plants with higher elicitor-induced responses were analysed at the F_3 generation and compared with knock-out mutants. For *bak1-5 mob7* crossed with La*er*, the green rectangle highlights the plants which were homozygous for *bak1-5* mutation and analysed for map-based cloning. For *bak1-5 mob7* crossed with *bak1-5*, F_2 plants with higher elicitor-induced responses were analysed at the F_3 generation. $F_{2:3}$ families were bulked and analysed by whole-genome resequencing and compared to *bak1-5*.

First, *mob7* inheritance was determined by crossing *bak1-5 mob7* to *bak1-5* (Figure 4.2). Analysis of elicitor-induced ROS production in F_1 progeny showed intermediate phenotypes of the F_1 plants compared to the two parents *bak1-5* and *bak1-5 mob7*, which indicates that *mob7* mutation is semi-dominant (back-cross was performed by Martin Stegmann and analysed by myself). F_2 plants were then analysed to determine whether one or multiple mutations were responsible for *mob7* phenotypes. As the assay to measure elicitor-induced ROS production can be quite variable, and the *mob7* mutation appears semi-dominant, different categories were considered depending on the response. Plants that showed high ROS production after chitin elicitation were denoted "ROS++" and plants with moderate ROS, "ROS+"

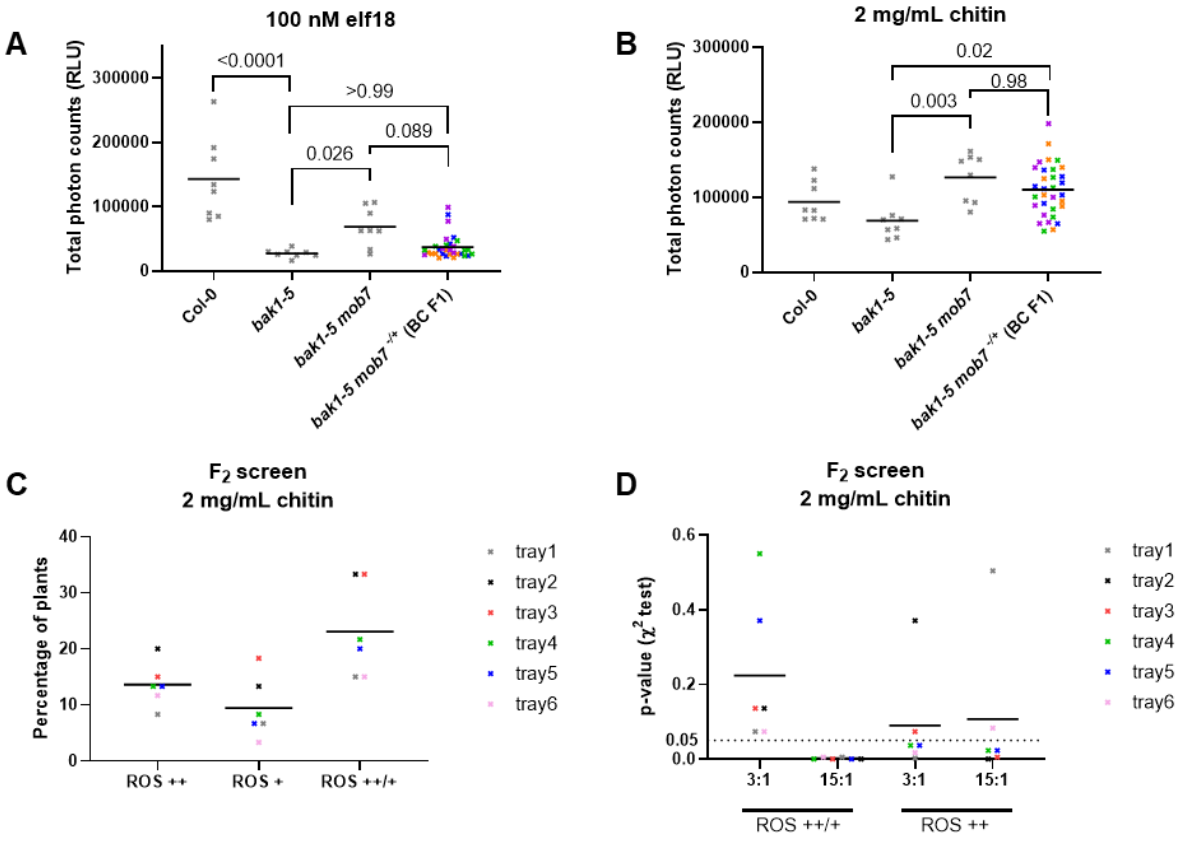

Figure 4.2 Segregation of *bak1-5 mob7* back-crossed to *bak1-5*.
(A-B) Total ROS accumulation over 60 min expressed as relative light unit (RLU) after treatment with 100 nM elf18 (A) or 2 mg/mL chitin (B). The different colours indicate independent F_1 plants. Horizontal lines represent the means from all leaf discs (n=8). Numbers above symbols are p-values from Dunn's multiple comparison test between corresponding genotype. (C-D) Analysis of F_2 plants with high ROS (ROS ++) or moderate/high ROS (ROS ++/+) after elicitation with 2 mg/mL chitin. The different colours indicate the different tray from which F_2 plants were grown and horizontal lines represent the means. (C) Percentage of plants per growing tray from F_2 screen with ROS ++ or ROS ++/+. (D) p-values from χ^2 test of the percentage of F_2 plants with different level of ROS per growing tray. Observed percentage were compared to different expected segregation percentages (3:1 for single

(Figure 4.4). From 360 F_2 plants analysed, divided in 6 trays, ROS++ represented 14 % of plants and ROS+ 9 %, which together (ROS+/++) represents 23 % (Figure 4.2C) (F_2 screen was performed by Martin Stegmann and analysed by myself). Statistical analysis with χ^2 test was performed on the percentage of individuals within trays in each category to determine whether the segregation was

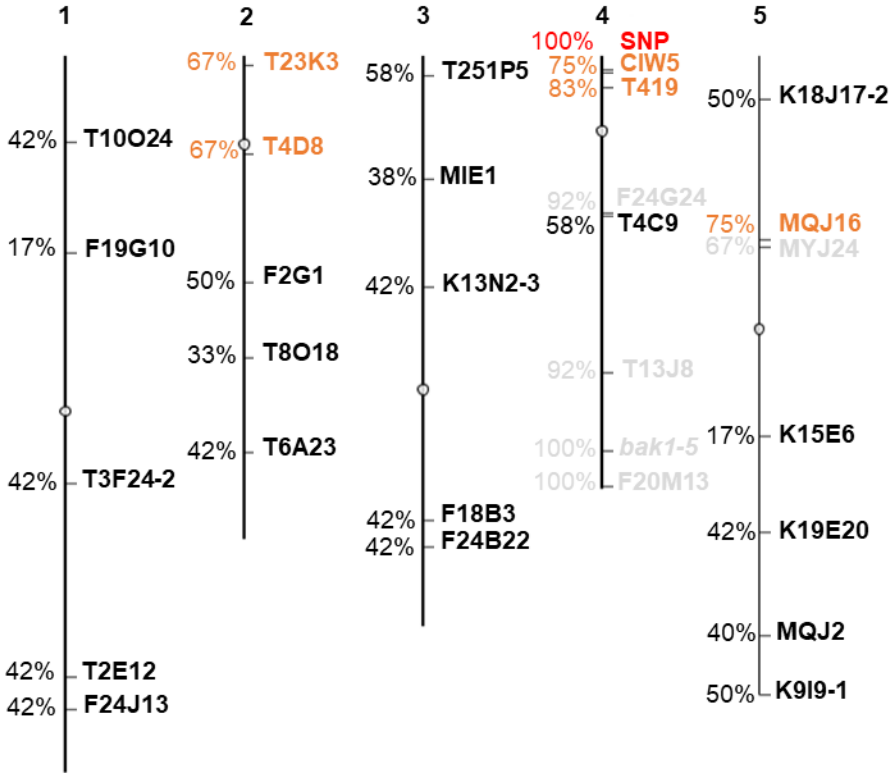

Figure 4.3 Map-based cloning of *bak1-5 mob7*.
Physical linkage map constructed using the F_2 population from *bak1-5 mob7*/La*er*. The SNP found in the gene *AT4G01290* is indicated in red (top arm of chromosome 4). All markers are InDels markers and analysed by PCR, except SNP which was analysed by Sanger-sequencing. The percentage represent the percentage of Col-0 alleles. Markers in grey are markers for which an increase of Col-0 alleles was also observed in plants with low elicitor-induced ROS production, thereby removed from further analysis. Markers in orange are markers with linkage statistically higher than 50 %. The marker in red is the only one with 100 % of Col-0 alleles. Circles represent centromeres. Significance was determined by χ^2 test. Figure based on results from table 4.1.

representative of one gene segregation (3:1) or 2 genes segregation (15:1). The highest p-value was obtained for the category gathering high and moderate ROS with one gene segregation (Figure 4.2D), suggesting one semi-dominant mutation is responsible of *mob7* phenotype.

To identify this mutation, the first strategy was to perform rough-mapping with map-based cloning to limit the causal mutation to a certain region. Hence, *bak1-5 mob7* in Col-0 ecotype was crossed to La*er* (Figure 4.3). F_2 plants were first genotyped for *bak1-5* mutation and only *bak1-5* homozygous F_2 lines were selected and analysed for elicitor-induced ROS production. Only 6 F_2 plants had restored elf18-triggered ROS comparable to or higher than *bak1-5 mob7*, and were taken for further analysis (group

named "+ROS") (Table 4.1). Fifteen plants with efl18-triggered ROS comparable to *bak1-5* were also analysed for counter selection (group noted "-ROS") (Table 4.1).

		+ ROS						- ROS												Percentage + ROS		Percentage - ROS		χ^2 (obs/exp) + ROS	χ^2 (obs/exp) - ROS
		#5	#8	#9	#13	#19	#145	#4	#20	#21	#26	#27	#35	#41	#42	#45	#48	#50	#103	#109	#137	#149	Col-0	Ler	Col-0	Ler		
Chromosome I	T10O24 (3.49)	L	H	H	C	L	H	H	L	L	H	H	H	L	H	H	H	H	H	H	H	H	42	58	40	61	0.096	0.038
	F19G10 (8)	L	L	L	C	L	L		L	L	L	C	H	L	C	L	L	H	H	L	H	H	17	83	32	68	3E-11	4E-04
	T3F24-2 (17.39)	H	H	L	C	H	L	C	H	H	H	C	H	L	C	H	H	L	H	C	H	H	42	58	57	46	0.096	0.285
	T2E12 (25.3)	H	H	L	C	H	L	H	H	H	H	C	H	L	C	L	H	C	C	H	C	H	42	58	60	39	0.096	0.038
	F24J13 (26.58)	H	H	L	C	H	L			H		H		H	L	H	L	H	C	H	H	C	H	42	58	50	50	0.096	1
Chromosome II	T23K3 (0.39)	H	H	C	C	L	C	L	L	H	C	H	H	L	L	L	L	C	L	L	H	L	67	33	27	71	9E-04	7E-06
	T4D8 (4)	H	H	C	C	L	C	L	L	H	C	C	H	L	H	L	H	C	L	L	H	L	67	33	37	61	9E-04	0.016
	F2G1 (9.2)	L	L	C	C	L	C	H	H		C	C	L	L	L	L	L	C	L	L	C	L	50	50	36	65	1	0.003
	T8O18 (12.3)	L	H	H	H	L	H	H	H	L	H	C	L	C	H	H	L	C	L	L	H	H	33	67	43	57	9E-04	0.167
	T6A23 (16.15)	L	H	H	C	L	H	H	H	H	H	H		H	H	H	L	C	L	H	H	H	42	58	46	54	0.096	0.458
Chromosome III	T251P5 (0.78)	H	H	C	H	C	L	C	C	C	C	C	C	C	C	H	C	H	L	H	H		58	42	80	21	0.096	5E-09
	MIE1 (5)		L	C	H		L	H	C	C	C	C	C	H	H	C	C	C	H	L	H	H	38	63	73	25	0.012	1E-06
	K13N2-3 (9.4)	H	L	C	L	C	L	H	H	C	H	H	H	H	H	C	H	C	H	L	C	H	42	58	60	39	0.096	0.038
	F18B3 (18.9)	L	C	H	L	H	H	H	L	C	C	H	H	C	C	C	H	C	L	H	H	L	42	58	60	39	0.096	0.038
	F24B22 (20)	H	C	H	L	L	H	H	L	C	C	H	H	C	C	H	H	L	L	H	H	H	42	58	53	46	0.096	0.49
Chromosome IV	SNP (0.54)	C	C	C	C	C	C	H	H	L	L	L	H	H	H	H	C	L	H	H	C	H	100	0	43	57	2E-23	0.167
	CIW5 (0.7)	H	H	H	C	C	C	H	H	L	L	L	H	H	H	H	C	L	H	C	C	H	75	25	47	54	6E-07	0.49
	T419 (1.3)	H	C	H	C	C	C	H	C	L	H	L	H	H	H	H	C	L	H	H	C	H	83	17	50	50	3E-11	1
	F24G24 (6.4)	C	H	C	C	C	C	C	C	L		H	C	H	H		C	L	H	C	C	H	92	8	65	38	8E-17	0.005
	T4C9 (6.5)	L	H	H	C	H	C	H	C	L	L	L	C	H	L	H	C	L	H	H	C	H	58	42	47	54	0.096	0.49
	T13J8 (12.9)	C	H	C	C	C	C	C	C	C	L	H	C	C	C	C	C	C	H	C	C	C	92	8	87	14	8E-17	5E-13
	F20M13 (18.04)	C	C	C	C	C	C	H	C	C		C		H	C	C	C		C	C	H	C	100	0	88	9	2E-23	4E-15
Chromosome V	K18J17-2 (1.78)	L	L	L	C	C	C	L	H	L	L	L	L	C	C	C	C			H	H	L	50	50	42	54	1	0.216
	MQJ16 (7.5)	H	H	H	C	C	C	H	H	H	C	H	L	H	H	C	C		C	H	L	H	75	25	57	42	6E-07	0.138
	MYJ24 (7.8)	H	L	H	C	C	C	H	H	H	C	H	H	H	H	C	C	C	C	H	L	H	67	33	63	36	9E-04	0.006
	K15E6 (15.5)	H	H	L	L	L	L	H	L	H	C	H	L	H	H	C	C	H	C	L	L	H	17	83	50	50	3E-11	1
	K19E20 (19.4)	H	H	H	H	L	H	H	L	H	C	H	H	H	L	C	C	H	C	L	L	L	42	58	47	54	0.096	0.49
	MQJ2 (23.6)	H	H	H	L	H		C		L	C	H	H	H	L	H	C	H					40	60	55	50	0.046	0.48
	K9I9-1 (27)	L	L	C	C	H	H			L	C	H	H	H	H	L	L	H	H	L	L	H	H	50	50	36	64	1	0.004

Table 4.1 Map-based cloning of *bak1-5 mob7*.

Linkage map constructed using the F_2 population from *bak1-5 mob7*/La*er*. SNP symbolised the SNP found in the gene *AT4G01290*. All markers are InDels markers and analysed by PCR, except SNP which was analysed by Sanger-sequencing The numbers below the markers name are the corresponding physical position on the chromosomes. The percentage represent the number of the corresponding alleles for the category of plants with high (+ ROS) and low (- ROS) ROS production. Percentages that are above 50 percent of Col-0 alleles for the category with high ROS and La*er* for low ROS are highlighted in red. χ^2 test was performed with an expected distribution of 50 % for each allele.

All markers that presented a statistically increase of Col-0 alleles for the category "-ROS" were removed for the analysis (Figure 4.3, Table 4.1). As expected, higher allele frequency was observed towards the ecotype Col-0 at the bottom arm of chromosome 4, around the locus of *bak1-5* (16 Mbp) (Figure 4.3). Three loci presented a statistically increase of Col-0 alleles only in the category "+ROS". The highest increase was observed at the top arm of chromosome 4 (Figure 4.3). Nevertheless, a statistical increase was also observed on chromosome 2 and the top arm of chromosome 5 (Figure 4.3). These regions were thus potential locations of the *mob7* causative mutation.

To narrow the region of interest and identify the causative SNP, a mapping-by-sequencing strategy was pursued in parallel. In this strategy, *bak1-5 mob7* was backcrossed to *bak1-5*, eliminating the need for selecting *bak1-5* homozygous plants in F_2 selection. F_2-derived F_3, named $F_{2:3}$ families with restored elicitor-induced ROS production from *bak1-5 mob7* backcrossed to *bak1-5* were bulked and sequenced using Illumina High-Seq (samples prepared by Martin Stegmann and analysed by myself). SNPs in the *bak1-5 mob7* genome were identified by comparing the mutant genome to the parental *bak1-5* genome that was previously sequenced (Monaghan et al., 2014). To further filter identified polymorphisms, SNPs identified in previous *mob* mutants were removed from the analysis as allelism tests suggested different mutations in *mob7* compared to other *mob* mutants. The web application CandiSNP (Etherington et al., 2014) was used to plot the genomic positions of unique SNPs identified in *bak1-5 mob7* with an allele frequency over 60 %. Non-synonymous SNPs were identified with high-allele frequency at the top arm of chromosome 4 (Figure 4.5), in agreement with the region of strongest Col-0 genome enrichment from map-based cloning. Most of the SNPs were in transposable element genes except two non-synonymous SNPs, which were located around 0.5 Mbp in the genes *AT4G01290* (0.54 Mbp) and *AT4G01000* (0.43 Mbp) with an allele frequency of 1 and 0.875, respectively (Figure 4.5). Sanger sequencing of these SNPs in independent $F_{2:3}$ families confirmed the allele frequency of each SNP. Similarly, SNPs with high-allele frequency were analysed on other chromosomes. Several SNPs presented also high-allele frequency at the bottom arm of chromosome 4. Surprisingly, most SNPs at the bottom arm of chromosome 4 showed an allele frequency of 100 % indicating that they did not segregate with the backcross (Figure 4.5). One hypothesis to explain this observation is that the *bak1-5* plant used for backcrossing *bak1-5 mob7* and the plants used for whole-genome resequencing were different. As *bak1-5* is an EMS mutant, various SNPs might be still present and segregate across generation. Hence, these SNPs would appear with high-allele frequency as they were present in the plant used for crossing but not in the *bak1-5* plants, which was sequenced. The SNP in *AT4G01290* disrupts a splicing site between exon 3 and the following intron (Figure 4.6 A). Importantly, this SNP was present in all the F_2 plants associated with high ROS that were used for map-based cloning (Figure 4.3, Table 4.1).

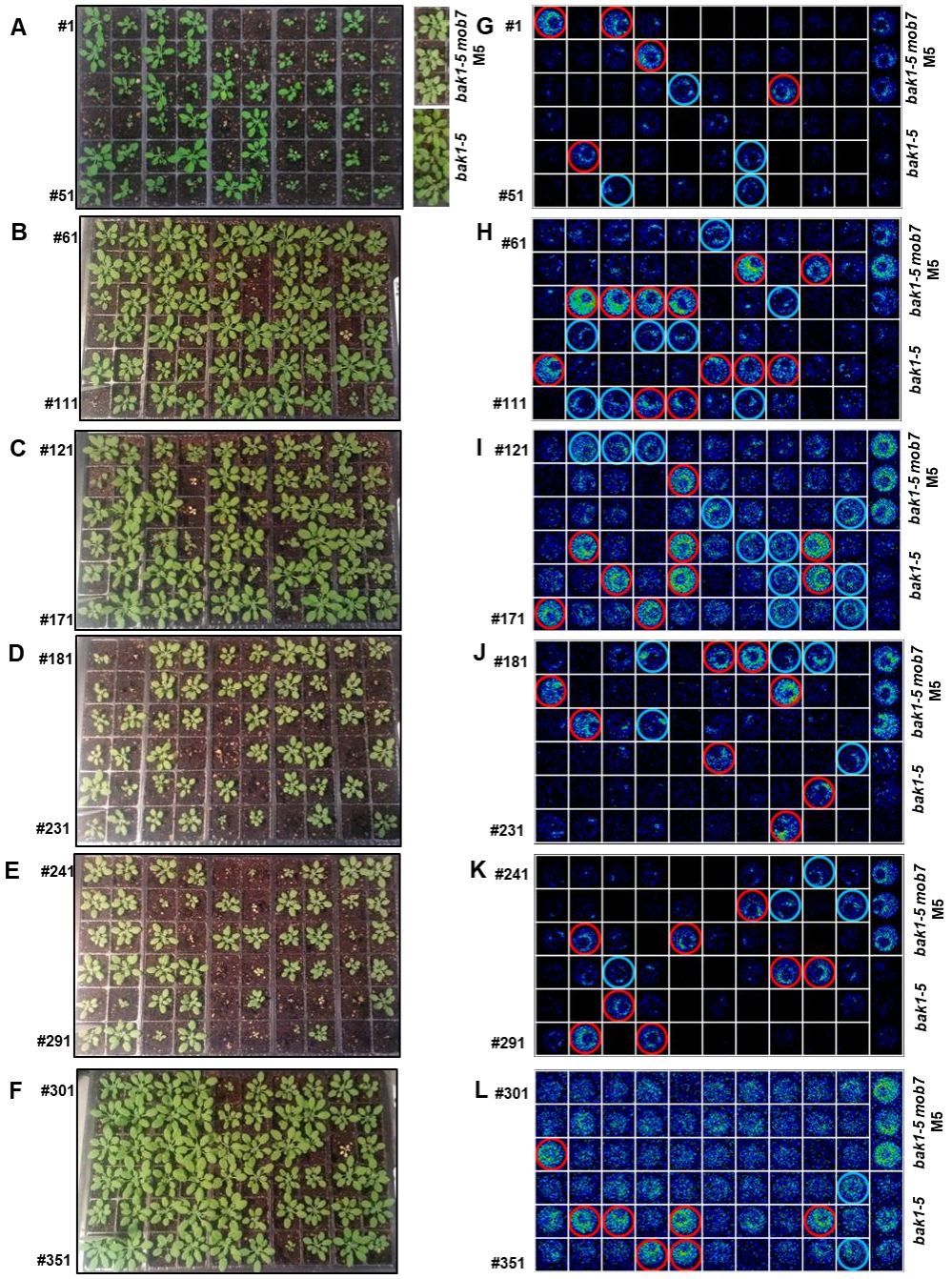

Figure 4.4 Screen of F_2 plants from *bak1-5 mob7* back-crossed to *bak1-5*.

(A-F) Pictures of F_2 plants from *bak1-5 mob7* back-crossed to *bak1-5* at 5-week old. Numbers on the left correspond to the plant number counted from left to right, top to bottom. (A) Pictures of tray1 including F_2 plants 1-60 and *bak1-5 mob7* M_5 and *bak1-5*. (G-L) Images of 66 wells from 96-well plates containing 1 leaf disc per F_2 plants and 3 leaf discs from 3 *bak1-5 mob7* M5 and *bak1-5* after elicitation with 2 mg/mL chitin. Images are on a false colour scale representing the integration of photon counts on a logarithmic scale over 56 min (G), 63 min (H), 61 min (I), 89 min (J), 82 min (K), 58 min (L). Wells with high (ROS ++) and moderate (ROS +) photon counts compared to *bak1-5 mob7* were encircled in red and blue, respectively. Pictures and corresponding ROS assay of F_2 plants 1-60 (A,G), 61-120 (B,H), 121-180 (C,I), 181-240 (D,J), 241-300 (E,K), 301-360 (F,L). These pictures were taken by Martin Stegmann.

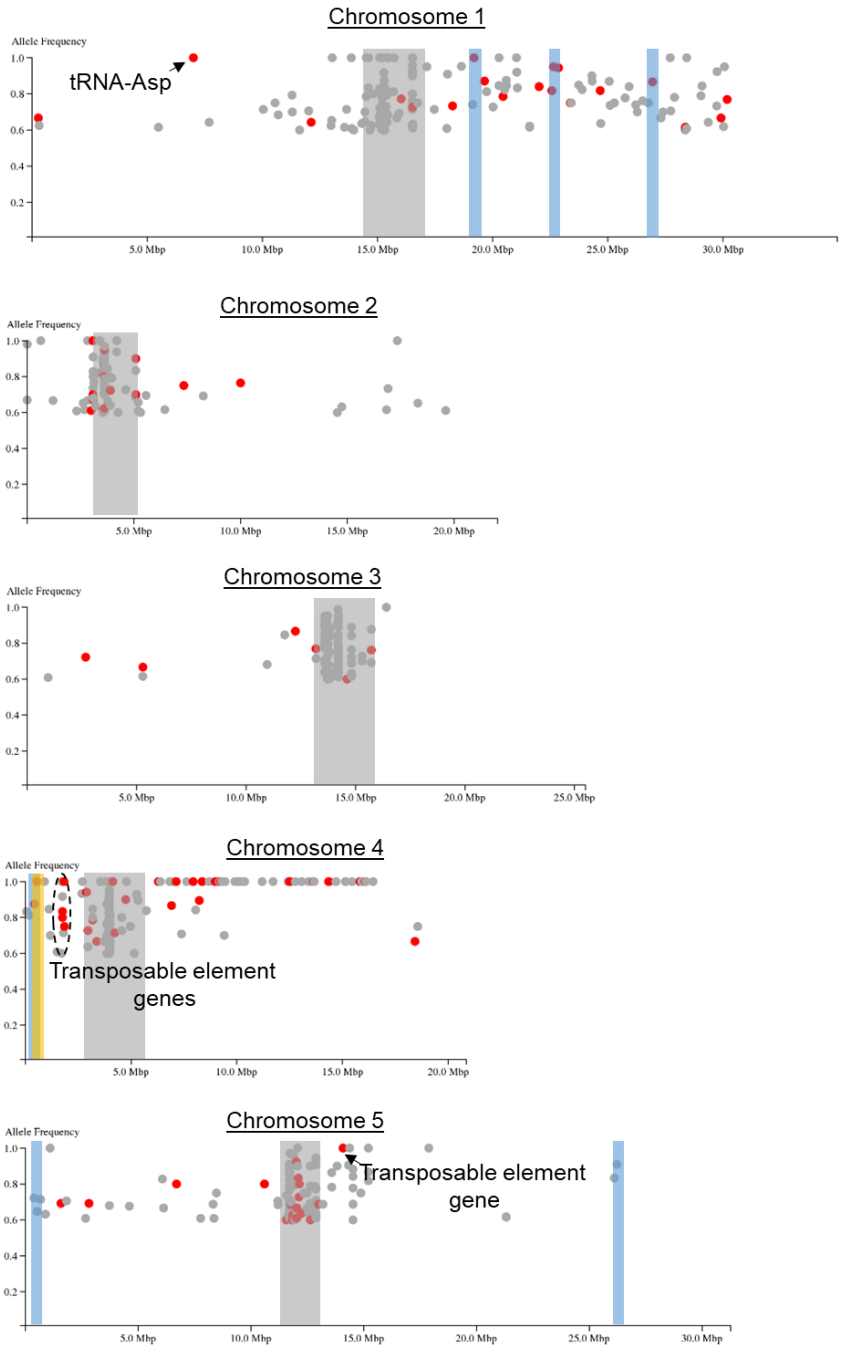

Figure 4.5 Whole-genome resequencing from $F_{2:3}$ family of *bak1-5 mob7* back-crossed to *bak1-5*. Density plot of SNPs using CandiSNP software. SNP with an allele frequency below 60 % were removed from the plots. Non synonymous SNP are shown in red and other in grey. Grey rectangles indicate the centromeres of each chromosome. Yellow rectangles delimit SNPs verified by Sanger sequencing in each $F_{2:3}$ family and where all alleles had the mutation/SNP. Blue rectangles delimit a SNP where both wild-type and *mob7* alleles were detected. The dash area delimits several non-synonymous SNPs in transposable element genes. Mbp, mega base pairs. Samples for sequencing were prepared Martin Stegmann and analysed by myself.

Taken together this data made the SNP in *AT4G01290* the strongest candidate for the causal mutation. Interestingly, *AT4G01290* encodes a RNA-binding protein, named CONSERVED BINDING OF EIF4E1 (CBE1) (Patrick et al., 2018). Analysis of cDNA generated from RNA of *bak1-5 mob7* shows the retention of the intron following exon 3 (Figure 4.6A). *In silico* prediction demonstrated that the SNP in *AT4G01290* could result in a premature stop codon in-frame with the start codon (Figure 4.6A). Transient expression of *AT4G01290* cDNA from Col-0 or *bak1-5 mob7* under the control of the 35S CaMV (cauliflower mosaic virus) overexpressing promoter followed by an N-terminal eGFP tag, confirmed a truncated protein of 16 kDa in *mob7* compared to 109 kDa for wild-type CBE1 (Figure 4.6B).

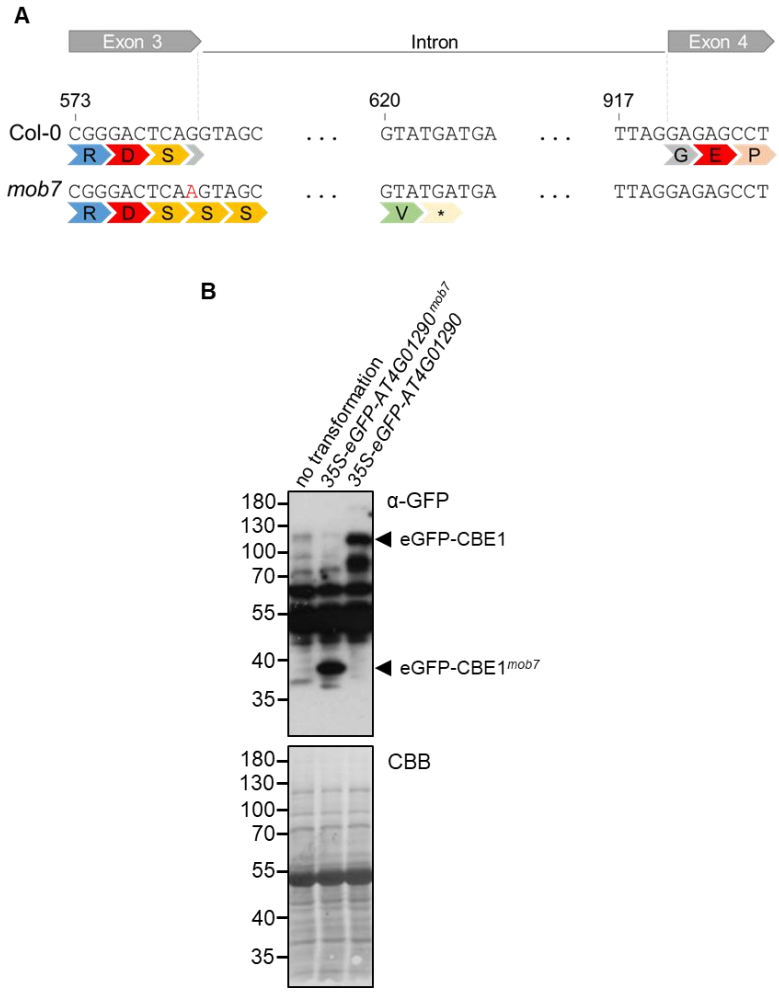

Figure 4.6 *mob7* mutation leads to the expression of a truncated protein.
(A) *mob7* mutation leads to a premature stop codon within the intron following exon 3. First line shows nucleotides from exons 3, 4 and intron in between of *AT4G01290*. The number indicates the nucleotide position relative to the adenosine of start codon. The second line shows amino acids corresponding to codons above. EMS-induced SNP in *mob7* is indicated in red. Star indicates a stop codon. (B) Western blot from transient expression at 3 days post-infiltration in *Nicotiana benthamiana*. Membranes were stained with CBB as loading control.

4.2.2. SNP in *CBE1* is responsible for *mob7* phenotypes

To confirm that the SNP isolated in *CBE1* is responsible for *mob7* phenotypes, T-DNA insertion lines were compared to a *mob7* single mutant. The *mob7* single mutant was obtained by crossing *bak1-5 mob7* to Col-0 and selecting F_2 plants that segregated out the *bak1-5* mutation and showed higher chitin-induced ROS production compared to *bak1-5* (Figure 4.1) (cross and F_2 screen was performed by Martin Stegmann and analysed by myself). In agreement with the mapping results, all the F_3 plants with higher ROS production possessed the *mob7* SNP in *CBE1*. Three different T-DNA insertion lines in *CBE1* were analysed. The allele *cbe1-1* (WiscDsLoxHs188_10F) has a T-DNA insert within exon 6 and is a knock-out mutant of *CBE1* (Patrick et al., 2018). Two other T-DNA insertion lines were identified, SALK_038452 and GK_150_H09, which have insertions in exon 9 and the intron following exon 9

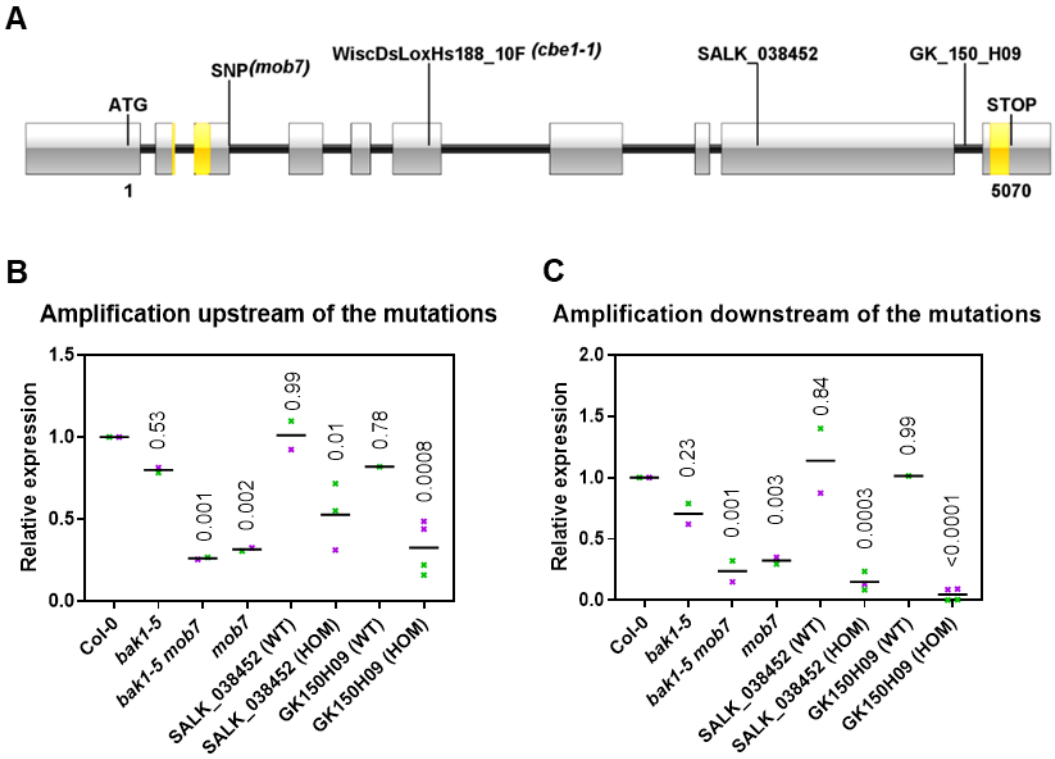

Figure 4.7 *CBE1* transcript accumulation in *mob7* and T-DNA lines.
(A) Gene structure of *AT4G01290*. Exons are shown as grey boxes. T-DNA insertion and SNP in *mob7* are indicated with the name above. Fragments amplified by RT-qCPR are indicated in yellow Bp, base pairs. (B, C) Quantitative reverse-transcription polymerase chain reaction of *AT4G01290* upstream of the T-DNA insertions/*mob7* mutation (B) or downstream of the insertions/mutation (C). (B,C) Expression values relative to the *U-BOX* housekeeping gene are shown. Horizontal lines represent the means from 1-2 independent experiments (n≥1) (B,C) The symbol colours indicate the different experiments. Numbers above symbols are p-values from Dunnett's multiple comparison test between corresponding genotype and Col-0.

respectively (Figure 4.7 A). Both T-DNA lines were genotyped and homozygous lines were isolated and compared to their respective wild-type, noted "HOM" and "WT", respectively. Analysis of these T-DNA lines revealed that the line SALK_038452 and GK_150_H09 are knock-down for *CBE1*, as some transcripts could be detected by RT-qPCR upstream, and downstream of the T-DNA insertions (Figure 4.7 B,C). Interestingly, transcripts in all *CBE1* mutants showed reduced level upstream of the mutation/insertion compared to Col-0, including *bak1-5 mob7* and *mob7* (Figure 4.7 B,C). One hypothesis to explain this observation is that the transcripts are degraded by nonsense-mediated RNA decay (NMD), which degrades mRNA with premature stop codon (Shaul, 2015).

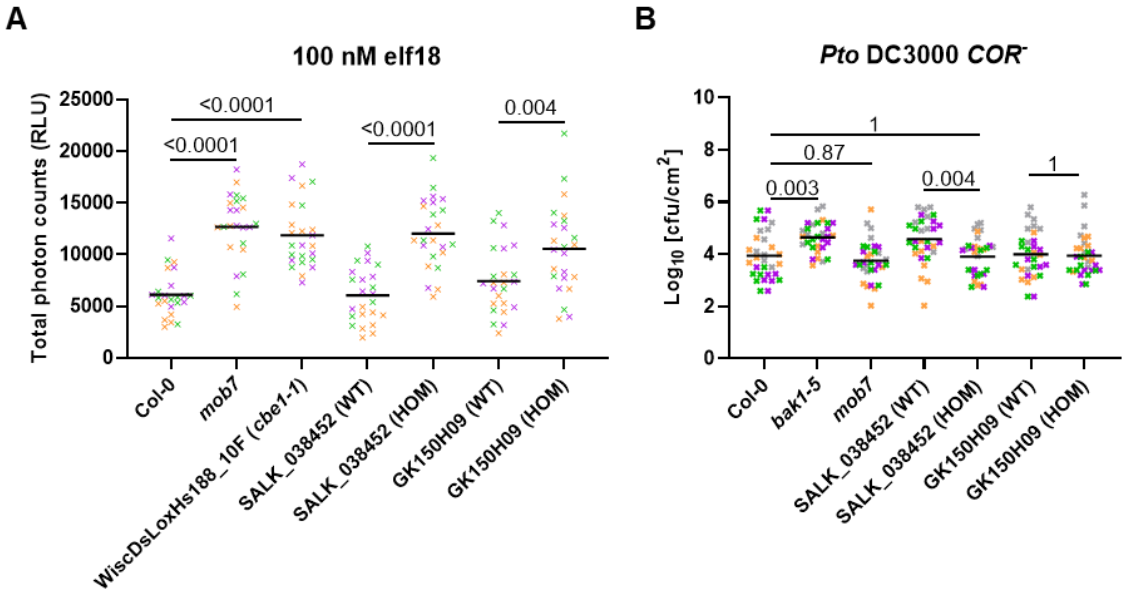

Figure 4.8 CBE1 negatively regulates elicitor-induced ROS production.
(A) Total ROS accumulation over 60 min expressed as RLU after treatment with 100 nM elf18. Horizontal lines represent the means from three independent experiments (n=8). (B) Bacterial growth (cfu/cm^2) in leaves spray inoculated with 10^7 cfu/mL (O.D. 0.2) *P. syringae* pv. *tomato* (*Pto*) DC3000 *COR*$^-$ and sampled at 3 dpi. Horizontal lines represent the means from 4 independent experiments (n≥7) (A,B) The symbol colours indicate the different experiments. Numbers above symbols are p-values from Sidak's multiple comparison test between corresponding genotypes.

Importantly, all T-DNA lines show higher elf18-induced ROS production compared to Col-0 or their respective wild-type, similar to *mob7* single mutant (Figure 4.8A). However, despite reduced susceptibility in *bak1-5 mob7* relative to *bak1-5*, susceptibility to *Pseudomonas syringae* pathovar *tomato* (*Pto*) DC3000 *COR*$^-$ was similar between *mob7* single mutants and Col-0 (Figure 4.8B). Although a decrease bacterial titer was observed in the T-DNA line SALK_038452 compared to the WT of this line, no difference was observed compared to Col-0 (Figure 4.8B). Altogether these results suggest that CBE1 acts as a negative regulator of elicitor-induced ROS production.

As a final confirmation that the SNP isolated in *CBE1* is responsible for *mob7* phenotypes, stable transformation in *bak1-5 mob7* with constructs overexpressing *CBE1* were generated, but silencing of the constructs was unfortunately consistently observed. Similarly, no stable transformants could be isolated in *bak1*-5 expressing $CBE1^{mob7}$ for phenotype recapitulation. Transformations with other constructs under different promoters are currently in progress. To test all potential variables, constructs were generated using different binary vectors, either genomic DNA or cDNA, and different tags.

4.3. Discussion

The SNP responsible for *mob7* phenotypes was identified as a semi-dominant mutation in the gene *CBE1*. A splice site mutation in *mob7* mutation leads to the retention of the intron following exon 3, a premature stop codon, and the expression of a truncated protein.

4.3.1. *MOB7* encodes the RNA-binding protein CBE1.

Although CBE1 has not been linked to plant immunity previously, CBE1 was shown to be linked to RNA dynamic. CBE1 binds the translation factor EUKARYOTIC INITIATION FACTOR 4E1 (eIF4E1) through its eIF4E1-binding motif (Patrick et al., 2018). Similar to eIF4E1, CBE1 is part of the 5' cap complex, which associates with the 7-methylguanylate cap of mRNAs (Bush et al., 2009). Moreover, CBE1 has been shown to directly bind mRNAs in large proteomic analysis of RNA-binding proteins (RBPs) in Arabidopsis (Reichel et al., 2016; Bach-Pages et al., 2020).

4.3.2. RNA-binding proteins in plant immunity.

RBPs have diverse roles in post-transcriptional gene expression, including regulation of alternative splicing, RNA export and localisation, RNA stability and translation (Iadevaia and Gerber, 2015). In addition to their role in normal cellular functions, RBPs are emerging as a class of proteins involved in a wide range of post-transcriptional regulatory events that are important in providing plants with the ability to respond rapidly to changes in environmental conditions (Woloshen et al., 2011; Ambrosone et al., 2012; Marondedze et al., 2016). Recently, several RBPs have been shown to be regulated upon immune elicitation (Bach-Pages et al., 2020). In addition, pathogens manipulate RBPs in order to create an infection favourable environment, as exemplified by GLYCINE RICH PROTEIN 7 (GRP7), which is hijacked by the *Pseudomonas* effector HopU1 (Nicaise et al., 2013).

4.3.2.1. Splicing factors

In Arabidopsis, 61 % of mRNA molecules have at least two isoforms, which increases the transcriptome and proteome complexity and allows a fine control of developmental programs and responses to the environment (Marquez et al., 2012). Splicing factors have been linked to transcripts involved in

immunity (Rigo et al., 2019). For example, IMMUNOREGULATORY RNA-BINDING PROTEIN (IRR) is a splicing factor associating with the transcripts of the negative regulator of immunity CPK28 (Dressano et al., 2020). In addition, SERINE/ARGININE-RICH 45 (SR45) was also shown to be a splicing regulator and a suppressor of innate immunity in Arabidopsis (Zhang et al., 2017a). Interestingly, IRR and SR45 are both negative regulator of elicitor-induced ROS production, like CBE1.

4.3.2.2. RNA decay and storage

The 5'-cap provides protection for the mRNA until it is removed by the decapping machinery and subsequent degradation occurs in a 5' to 3' manner (Jiao et al., 2008). Similar to CBE1, the decapping enhancer ARABIDOPSIS HOMOLOG OF YEAST PAT1 (PAT1) is a RNA-binding protein, which associates with the 5' cap of mRNA, however, PAT1 is part of the mRNA decapping complex (Roux et al., 2015; Vindry et al., 2019). PAT1 is phosphorylated by MPK4 upon flg22 treatment, and is guarded by the nucleotide-binding domain leucine-rich repeat (NLR) SUPPRESSOR OF MKK1 MKK2 2 (SUMM2) suggesting that PAT1 is a target for pathogen manipulation (Roux et al., 2015). DECAPPING PROTEIN 1 (DCP1) is also a RNA-binding protein, which is part of the mRNA decapping complex (Xu et al., 2006; Yu et al., 2019a). DCP1 was shown to positively regulate PAMP-triggered responses and immunity against pathogenic bacteria in Arabidopsis by contributing to the degradation of transcripts encoding regulators involved in immunity (Yu et al., 2019a).

mRNA decapping is not the only mRNA regulatory pathway characterised by constitutive defence responses. Nonsense-mediated RNA decay (NMD) modulates immune receptor levels (Gloggnitzer et al., 2014), and mutants of NMD factor including *upf3-1*, *upf1-5* and *smg7* display autoimmune phenotypes (Jeong et al., 2011a; Rayson et al., 2012; Riehs-Kearnan et al., 2012; Shi et al., 2012). 5'–3' mRNA decay is also essential to maintain defence mRNAs at basal levels under normal conditions as the helicases RH6, RH8 and RH12 are involved in the negative control of immunity (Chantarachot et al., 2020). Moreover, TANDEM ZINC FINGER PROTEIN 9 (TZF9) is a RNA-binding protein, which fine-tunes defence gene expression at the post-transcriptional level (Tabassum et al., 2019). Similar to TZF9, POLY(A) BINDING PROTEIN 2 (PAB2) associates with RNA in stress granules and plays a negative role in basal translation, but a positive role in elf18-induced translation (Xu et al., 2017b).

4.3.2.3. Translation factors

Finally, RNA-binding proteins contribute to plant immunity against viruses as they rely on the host translation machinery. The translation factor eIF4E1, which interacts with CBE1, inhibits Cucumber mosaic virus (CMV) multiplication (Yoshii et al., 2004). Similarly, the translation factor eIF4G inhibits Turnip crinkle virus (TCV) multiplication in Arabidopsis (Yoshii et al., 2004).

4.4. Future perspectives

In order to better understand how the RBP CBE1 affects ROS production, functional characterisation of CBE1 will be investigated during immunity. In addition, immune responses of other RBP mutants and subcellular localisation of CBE1 with various RBPs will be conducted to further elucidate the role of CBE1. The impact of CBE1 on transcripts during elicitation will be also explored.

5. Roles of CBE1 in immunity

5.1. Introduction

Messenger RNAs (mRNA) convey genetic information from nuclear DNA to ribosomes for protein synthesis (Brenner et al., 1961). The molecular machinery for protein synthesis is highly similar between plants and other eukaryotes. Similarly, the correlation between mRNA transcript levels and protein levels across kingdoms is limited (Baerenfaller et al., 2008; Piques et al., 2009; Buccitelli, 2020; Zander et al., 2020). The dynamic interplay between mRNA translation, stabilisation, and turnover fine-tunes the differential regulation of genes to enable developmental plasticity and effective environmental responses (Chantarachot and Bailey-Serres, 2018).

5.1.1. mRNA dynamics

As the nascent pre-mRNA is being synthesized in the nucleus, a 5'-m7 GpppN-cap structure, consisting of a 7-methyl guanosine residue connected to mRNA via an unusual 5′ to 5′ triphosphate linkage, (hereafter, referred to as 5'cap) is added before the end of transcription and protects mRNA from degradation (Ramanathan et al., 2016). In addition, introns are excised from pre-mRNA by splicing (Lorković et al., 2000) and once the RNA is cleaved and detached from RNA polymerase, a poly(A) tail is added at the 3' end (Hunt, 2012). The poly(A) tail is important for the nuclear export, translation, stability of mRNA and acts as the binding site for poly(A)-binding proteins (PABPs) (Stewart, 2019). Similar to the poly(A) tail, the 5' cap acts as a binding site for the two subunits nuclear cap-binding complex (CBC) composed of CAP BINDING PROTEIN 20 (CBP20) and CBP80 (Gonatopoulos-Pournatzis and Cowling, 2014). After processing of the primary transcripts by splicing, capping, and polyadenylation has been completed in the nucleus, the mature mRNA is exported into the cytoplasm through the nuclear pore complex (Xu and Meier, 2008). The mRNAs are then translated either on ribosomes associated with the endoplasmic reticulum or on free cytosolic ribosomes (Browning and Bailey-Serres, 2015). After the first round of translation and replacement of CBP20 by EUKARYOTIC TRANSLATION INITIATION FACTOR 4E (eIF4E), only mRNAs that pass the quality-control check can enter into active translation as templates for bulk protein synthesis. The mRNAs with defects in translation are subjected to degradation via different pathways, and under cellular stress, mRNA can be sequestrated and stored (Chantarachot and Bailey-Serres, 2018). Translation, decay, and storage of cytoplasmic mRNAs involve three heterogeneous mRNA ribonucleoprotein (mRNP) complexes: polyribosomes (polysomes), processing bodies (p-bodies), and stress granules (SGs), respectively (Chantarachot and Bailey-Serres, 2018).

5.1.1.1. Translation and polysomes

Polysomes are cytoplasmic complexes of multiple 80S ribosomes and a 5'-capped and 3'-polyadenylated mRNA undergoing translation (Dever and Green, 2012; Chantarachot and Bailey-Serres, 2018). Translation involves the phases of initiation, elongation and termination that enable the ribosome to decode a transcript into a polypeptide (Dever and Green, 2012; Browning and Bailey-Serres, 2015). Initiation of translation of a cytosolic mRNA utilises both the 5'-cap and the 3'-poly(A) tail with initiation factors that specifically recognise these features to start the process of initiation. The eIF4E protein binds the 5' cap with its partner eIF4G to form the eIF4F complex (Keiper et al., 1999; Prévôt et al., 2003), which serves as a scaffold for the assembly of initiation factors eIF4A, eIF4B, eIF3, and poly(A)-binding protein (Pelletier and Sonenberg, 2019). This protein-mRNA complex then recruits the 40S ribosome prior to scanning for the initiator AUG codon (Asano, 2000; Pestova and Hellen, 2000; Sonenberg and Dever, 2003). Plants possess another distinct initiation protein complex for 5'-cap recognition, named eiIFiso4F, consisting of eIFiso4E and eIFiso4Gs (Patrick and Browning, 2012). The different isoforms lead to different translation efficiencies (Dennis and Browning, 2009; Kropiwnicka et al., 2015; Gallie, 2016; Khan and Goss, 2018). Cytoplasmic mRNAs within polysomes form a closed-loop, where PABP forms a physical bridge via eIF4G and eIF4E between the 5' and 3' ends of the mRNA (Browning and Bailey-Serres, 2015; Gallie, 2018). This physical circularisation of the polysome enhances primary initiation and subsequent ribosome-recycling events (Wells et al., 1998; Gallie, 2014; Browning and Bailey-Serres, 2015). At the end of the initiation step, the mRNA is positioned so that the next codon can be translated during the elongation stage of protein synthesis (Dever et al., 2018). Once the ribosome reaches a stop codon, it initiates the termination phase, which ends with the disengagement of the peptide from the ribosome (Dever and Green, 2012; Jackson et al., 2012).

5.1.1.2. Translation modulation

Among the three steps of translation, initiation is the most highly regulated and involves the largest number of factors (Browning and Bailey-Serres, 2015). The core translation initiation factors partner with a variety of accessory proteins that influence their activity. In mammals, protein synthesis can be regulated by modulating the ability of eIF4E to interact with eIF4G, which is carried out by a group of repressor proteins called 4E-binding proteins (4E-BPs) (Raught and Gingras, 1999; Pyronnet and Sonenberg, 2001). The 4E-BPs function by mimicking eIF4G and are able to bind and sequester eIF4E, blocking the formation of eIF4F complex. 4E-BPs are phosphoproteins and in their hypophosphorylated forms, strongly bind to eIF4E, and consequently repress translation (Gingras et al., 1999). Under favourable growth conditions, which promote translation, cell growth, and proliferation, 4E-BPs become phosphorylated mainly as a consequence of the activation of mammalian target of rapamycin (mTOR) (Gingras et al., 1998; Gingras, 2001). While clear homologs for 4E-BPs are missing in plant genomes,

different proteins interact with translation factors leaving possible the existence of analogues or completely new translational modulators in plants (Browning, 2004; Urquidi Camacho et al., 2020). For example, CONSERVED BINDING OF EIF4E1 (CBE1) interacts with eIF4E and eIFiso4E, but the effect of CBE1 and other proposed eIF4E-binding proteins on translation remains unknown (Wu et al., 2017b; Patrick et al., 2018). In addition, CERES is another plant-specific eIF4E and eIFiso4E-binding protein (Toribio et al., 2019). Unlike mammalian "canonical" 4E-BPs, CERES positively regulates translation. During the day, CERES specifically promotes the translation of light- and carbohydrate-related mRNAs (Toribio et al., 2019). Furthermore, similar to all eukaryotes, plants possess RIBOSOME-INACTIVATING PROTEINS (RIPs), which are toxic N-glycosidases that depurinate eukaryotic and prokaryotic rRNAs, thereby arresting protein synthesis during translation.

5.1.1.3. mRNA decay and processing bodies

Translation of mRNA is also regulated through stability of the transcript. Three major pathways for mRNA degradation in plants have been found: nonsense-mediated decay (NMD), non-stop decay (NSD), and no-go decay (NGD). The mRNAs containing an unusual sequence feature that causes premature translation termination (*e.g.* long 3' UTRs, spliced introns downstream of a stop codon, premature stop codons) are targeted for NMD (Shaul, 2015; Chantarachot and Bailey-Serres, 2018). In addition, mRNAs lacking an in-frame stop codon are degraded by NSD and mRNAs, which contain an elongation inhibitor structure are degraded through NGD (Szádeczky-Kardoss et al., 2018).

Translationally inactive mRNAs and proteins involved in translation repression and mRNA turnover processes assemble in dynamic cytoplasmic macromolecular assemblies named p-bodies (Chantarachot and Bailey-Serres, 2018). p-bodies are mobile mRNPs associated with the actin cytoskeleton (Steffens et al., 2014). In plants, p-bodies markers include DECAPPING 1 (DCP1), DCP2, VARICOSE (VCS), and EXORIBONUCLEASE 4 (XRN4) (Maldonado-Bonilla, 2014). Although p-bodies are generally associated with mRNA decay, these assemblies can be highly heterogeneous, and are regularly described in term of their specific proteins, transcripts, and biological activities studied. In fact, in many cases, mRNAs targeted to p-bodies in plant cells are stabilised rather than degraded despite the presence of mRNA decay factors (Li et al., 2015c; Merchante et al., 2015; Steffens et al., 2015; Scarpin et al., 2017; Jang et al., 2019). Interestingly, p-bodies numbers increase when *Arabidopsis thaliana* (hereafter Arabidopsis) was treated with the immune elicitor flg22, suggesting a link between p-body-mediated mRNA stability and immunity (Roux et al., 2015; Yu et al., 2019a).

5.1.1.4. Ribonucleoprotein storage and stress granules

In response to stress-induced inhibition of translation initiation, mRNPs can assemble into SGs (Protter and Parker, 2016). In plants, SGs were first observed in response to heat stress and also occur during hypoxia, darkness, salt, and other conditions (Weber et al., 2008; Sorenson and Bailey-Serres, 2014; Yan et al., 2014; Gutierrez-Beltran et al., 2015; Lokdarshi et al., 2016). SGs sequester intact mRNAs away from the 80S ribosome. SGs are transient structures which assembly requires microtubule dynamics (Gutierrez-Beltran et al., 2015). In Arabidopsis, numerous proteins associate with SGs including the OLIGOURIDYLATE-BINDING PROTEINs (UBPs) and the RNA-BINDING PROTEIN 45 (RBP45) and RBP47, which are absent from p-bodies (Weber et al., 2008; Sorenson and Bailey-Serres, 2014; Nguyen et al., 2016; Nguyen et al., 2017). Although not well characterised in plants, SGs with stabilised mRNAs can include translation initiation factors (*e.g*. eIF3, eIF4E, eIF4A) and the 40S ribosomal subunit, indicating that these complexes are in dynamic equilibrium with translating ribosomes (Urquidi Camacho et al., 2020). Typically, mRNAs stored in SGs are translationally competent and can re-enter the translational pool once released. Upon the release of the stress, SGs quickly disappear and mRNAs return to the polysomal pool (Branco-Price et al., 2008; Sorenson and Bailey-Serres, 2014). SGs exchange mRNAs with p-bodies, and SGs can be found associated with p-bodies (Hamada et al., 2018). Thus, SGs lie at the nexus of two post-transcriptional processes, translation and mRNA turnover (Chantarachot and Bailey-Serres, 2018; Urquidi Camacho et al., 2020).

5.1.2. Objectives

As part of a forward genetic screen to identify new regulators of immune signalling, an EMS-induced mutation was found in *CBE1* (Chapter 4). A single nucleotide polymorphism (SNP) in the mutant *modifier of bak1-5 7(mob7),* was found at the splicing site of exon 3 and 4, which prevents excision of the intron and leads to the expression of a truncated CBE1 protein (Chapter 4). Interestingly, the *mob7* mutant, as well as other knock-down alleles of CBE1, showed higher reactive oxygen species (ROS) production induced by the immune elicitors elf18 and chitin compared to wild-type (Chapter 3,4). Despite hypersensitivity to these elicitors, *CBE1* alleles had similar susceptibility to the pathogen *Pseudomonas syringae* DC3000 *COR*$^{-}$ as wild-type (Chapter 3,4). In order to understand how this eIF4E1-interacting protein affects ROS production, the impact of CBE1 on immune signalling was investigated. In addition, the effect of CBE1 on translation and mRNA during immune signalling was explored.

5.2. Results

5.2.1. CBE1, the putative plant 4E-BP

CBE1 is encoded in genomes across land plants and appears well-conserved; however, it is not found outside of plants or in green algae (Figure 5.1 A) (Patrick et al., 2018). Full-length CBE1 binds directly

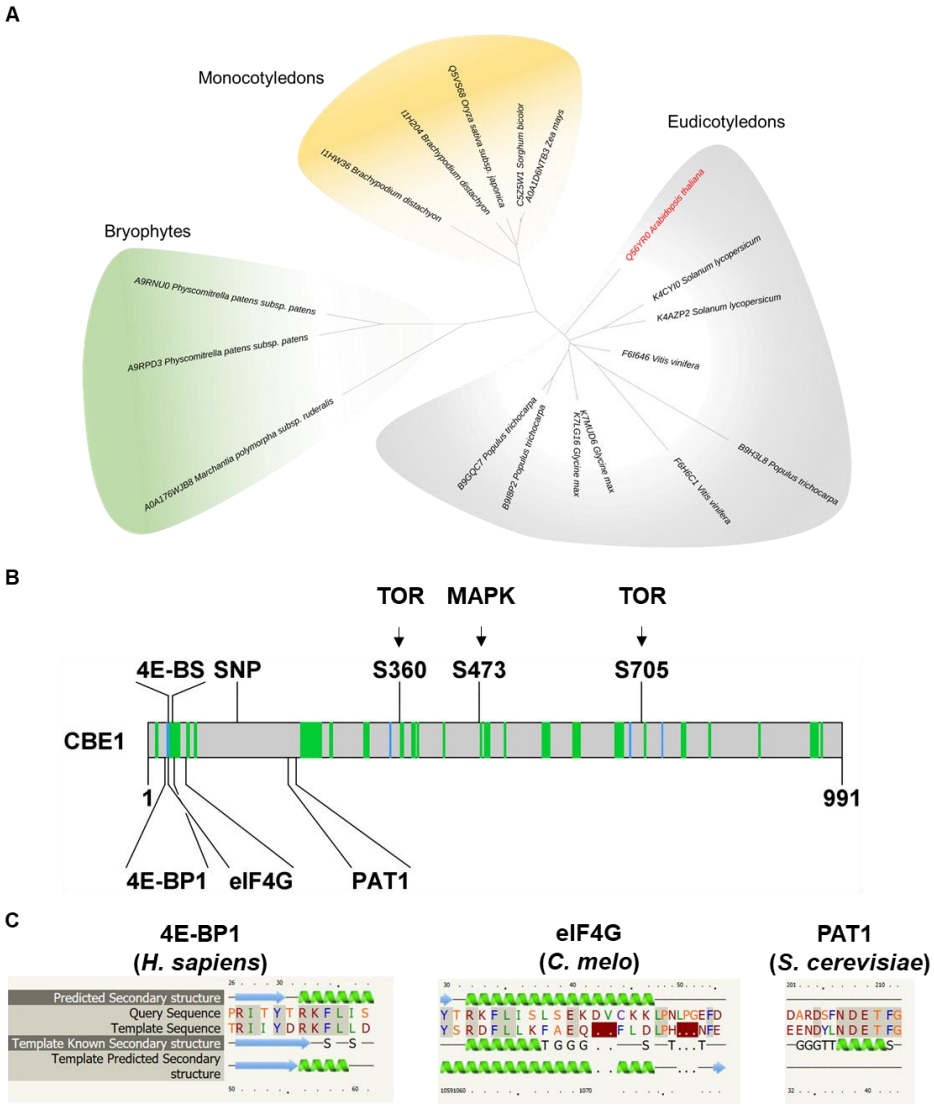

Figure 5.1 CBE1 is an eIF4E-interacting protein that evolved in land plant lineage.
(A) Phylogenetic tree generated from a protein distance matrix using PHYLIP neighbour joining methods and using the Jones-Taylor-Thornton model. The reference sequence is highlighted in red. (B) Schematic illustration of CBE1 amino acid sequence. Predicted α helix regions are highlighted in green, strands in blue and coils in grey. SNP indicates the mutation identified in *mob7* and 4E-BS, the binding site of eIF4E. Phosphorylation sites induced by TOR and MAPK are shown above the corresponding amino acids. Sequences with 3D homology to CBE1 are shown below with the corresponding protein. (C) 3D homology analysis of CBE1 protein using Phyre2. Phyre output of CBE1 sequence and structure (query) against the modelled structure (template) of 4E-BP1 from *Homo sapiens*, eIF4G from *Cucumis melo* and PAT1 from *Saccharomyces cerevisiae.* Only homologs with confidence above 60 % were represented.

to the eIF4E-family proteins of Arabidopsis, eIF4E, eIFiso4E, and 4E HOMOLOGOUS PROTEIN (4EHP; also known as nCBP), while the N-terminal of CBE1 only binds eIF4E and eIFiso4E (Patrick et al., 2018). Consistent with its interaction, CBE1 possesses the well-conserved eIF4E-binding site (4E-BS) in the N-terminus characterised by the minimal canonical sequence YXXXXLϕ (where X is any residue and ϕ is any hydrophobic amino acid) (Figure 5.1 B,C) (Peter et al., 2015). Furthermore, CBE1 is part of the mRNA cap-binding complex in an eIF4E-dependent manner (Bush et al., 2009; Patrick et al., 2018). Similar to mammalian 4E-BPs, CBE1 seems linked to TOR signalling, as phosphorylation sites in CBE1 are induced by sucrose and rapidly reduced by the TOR inhibitor AZD-8055 (Figure 5.1B) (Van Leene et al., 2019). In addition, MAPK4 and MAPK6 phosphorylation sites were also found in CBE1 (Rayapuram et al., 2018; Wang et al., 2020a). Three-dimensional homology analysis of CBE1 amino acid sequence revealed homology to different proteins involved in translation (Figure 5.1 B,C). Among the homologs detected with confidence above 60 %, sequence within N-terminus of CBE1 around the 4E-BS, are similar to the human protein 4E-BP1 but also to the melon protein eIF4G, consistent with mammalian 4E-BPs function as eIF4G mimics (Figure 5.1 B,C) (Van Leene et al., 2019). Despite some homology to eIF4G, CBE1 lacks HEAT domains, which direct the assembly of the translation initiation machinery, suggesting that CBE1 would not act as a positive initiation factor but more similar to mammalian 4E-BPs (Van Leene et al., 2019). Another sequence was found to be homologous to the yeast decapping factor PAT1. Altogether, these results suggest that CBE1 possesses a similar function as 4E-BPs, and, thus, acts as translational repressor although CBE1 and 4E-BPs have very limited structure homology. While the effect of CBE1 on translation remains open, CBE1 directly binds RNA and it was shown, in a directed test, to attenuate the expression of cell cycle genes (Patrick et al., 2018).

5.2.2. Mutations in the decapping factor *PAT1* and initiation factor *EIF4E* phenocopy the effect of mutations in *CBE1* on elicitor-induced ROS production

To further investigate the role of CBE1 on translation modulation, different mutants of RBPs, shown to be involved in plant immunity and implicated in mRNA dynamic at various stages, were analysed for elicitor-induced ROS production (Chapter 4) (Jeong et al., 2011b; Rayson et al., 2012; Shi et al., 2012; Roux et al., 2015). From the different mutants tested, the NMD factor mutant *upf1-5* shows different sensitivity to elicitor compared to *cbe1-1*; however, the decapping and mRNA decay factor mutant *pat1-1* shows hypersensitivity to elf18, similar to *cbe1-1* (Figure 5.2A). In plants, PAT1 is guarded by the NLR SUMM2 (Roux et al., 2015). Interestingly, while *summ2* mutant is statistically different from *cbe1-*

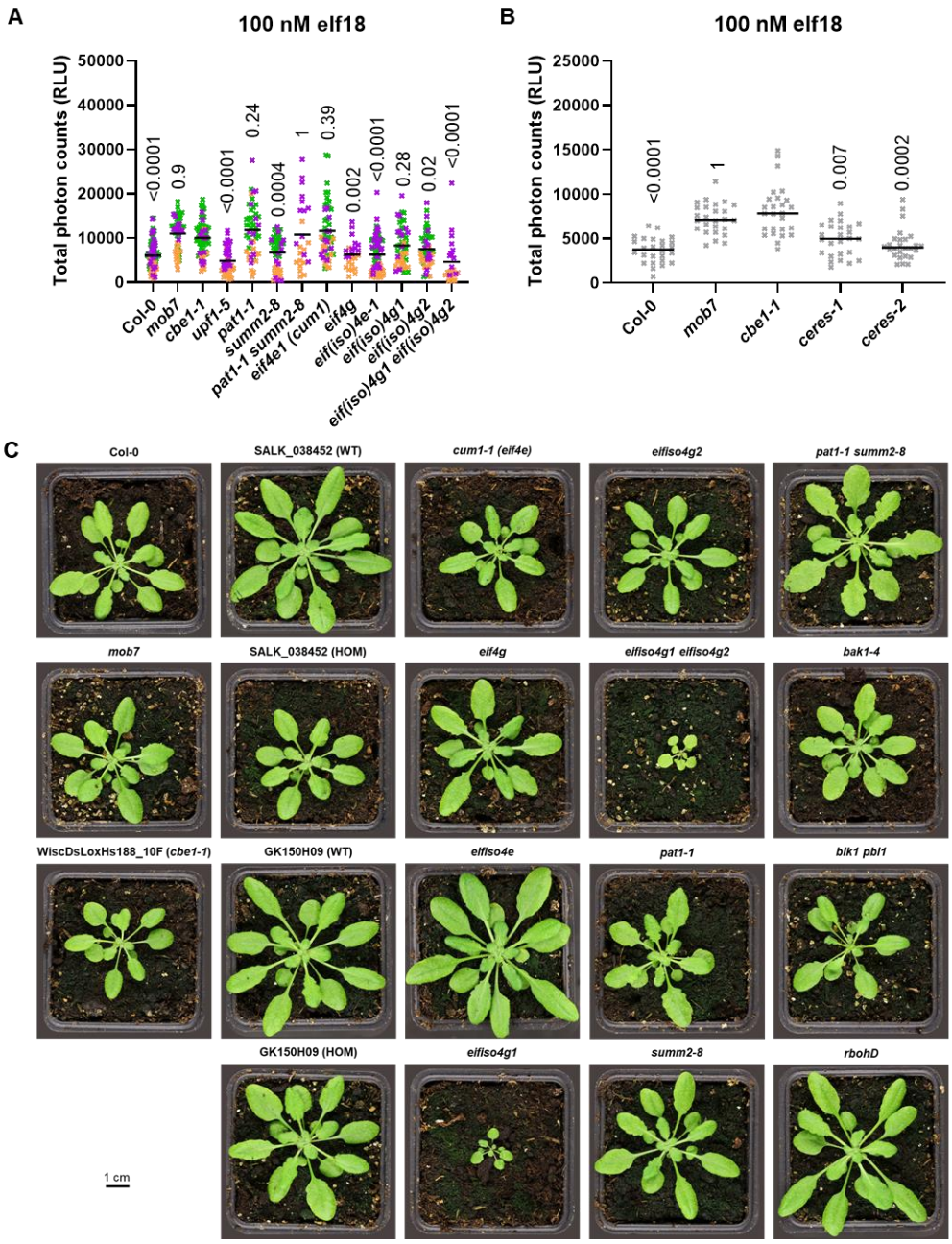

Figure 5.2 Decapping factor and initiation factors phenocopy the impact of CBE1 on elicitor-induced ROS production.

(A-B) Total ROS accumulation over 60 min expressed as RLU after treatment with 100 nM elf18. Numbers above symbols are p-values from Dunnett's multiple comparison test between corresponding genotype and *cbe1-1*. (A) Horizontal lines represent the means from 2-3 independent experiments (n>11) and the symbol colours indicate the different experiments. (B) Horizontal lines represent the means from 1 experiment (n>11) (C) Rosette morphology of 5-week-old plants of the corresponding genotype.

1, the double mutant *pat1-1 summ2-8*, showed similar sensitivity as *cbe1-1* in response to elf18 elicitation (Figure 5.2A). PAT1 thus impacts elicitor-induced ROS production independently of the NLR SUMM2.

As CBE1 interacts with the initiation factors eIF4E and eIFiso4E (Patrick et al., 2018), mutants from the eIF4F and eIFiso4F complexes were also analysed. The mutant *cum1-1* in the gene *eIF4E* and the mutant *eif4isog1* show comparable sensitivity to elf18 as *cbe1-1* mutant (Figure 5.2A). Similar to the SNP found in *mob7*, *cum1-1* is an allele of eIF4E with a truncated protein. Surprisingly, the mutant allele in the other eIFiso4G isoform, *eifiso4g2* had a different phenotype and similar to the single mutant, the double mutant *eifiso4g1 eifiso4g2* is statistically different from *cbe1-1* (Figure 5.2A). ROS production was also analysed in mutants of the initiation factor CERES; however, two mutant alleles did not phenocopy elf18 hypersensitivity of *cbe1* mutants (Figure 5.2B). Despite the importance of mRNA regulation, most of these mutants did not show growth phenotypes at the adult plant stage, suggesting high redundancy among these RBPs or specific roles in stress responses (Figure 5.2C).

5.2.3. CBE1 is nucleocytoplasmic and localises in p-bodies and stress granules

To know if CBE1 could be associated with one or more mRNPs, CBE1 was transiently expressed in *Nicotiana benthamiana* with markers of p-bodies and SGs (Figure 5. 2A). CBE1-N-terminal-tagged with GFP and RFP was observed in cytoplasmic foci and the nucleus (Figures 5.3A; 5.4C). Furthermore, CBE1 co-localised with the p-bodies markers UPF1 and DCP1 (Figure 5.3). In addition, CBE1 co-localised with the SG markers PAB2, UBP1B, EIF4E and RBP47C even in the absence of specific stresses (Figure 5.3). However, CBE1 did not co-localise with free RFP or GFP (Figure 5.3).

To investigate whether CBE1 localises predominantly with p-body markers, co-localisation was analysed by quantifying Pearson's correlation coefficient (PCC) in the region of interest (ROI). Five ROIs were placed per image on foci where CBE1 localisation was the highest. These ROIs were then reported to the other channels and the Pearson correlation coefficient calculated. Based on this quantification, the correlation coefficient (R) was measured between -0.05 and 0.84 (Figure 5.4A,B). On average the highest correlation was observed between GFP-tagged and RFP-tagged CBE1, while the lowest correlation was observed with the co-localisation of CBE1 and free GFP or RFP (Figure 5.4A,B). PCCs were distinguishable between the two co-localisations, indicating that CBE1 localisation in foci could be clearly separated from free cytoplasmic RFP or GFP (Figure 5.4A,B). A threshold was then selected with a PCC of 0.38 to distinguish between random cytoplasmic co-localisation and co-localisation within CBE1-localised foci (Figure 5.4A,B). The percentage of PCC values above the threshold, symbolising co-localisation was then calculated for each samples. Interestingly, the highest percentages were observed with p-bodies markers, especially with the decapping factor DCP1 (Figure 5.4A). Among SG markers, only PAB2 and UBP1B showed a percentage of co-localisation within foci above 50% (Figure 5.4B). CBE1 thus appears to localise predominantly with p-bodies. In addition, only full-length CBE1 localises to foci as the truncated CBE1^{mob7} protein did not show this localisation pattern (Figures 5.4B,C; 4.6B).

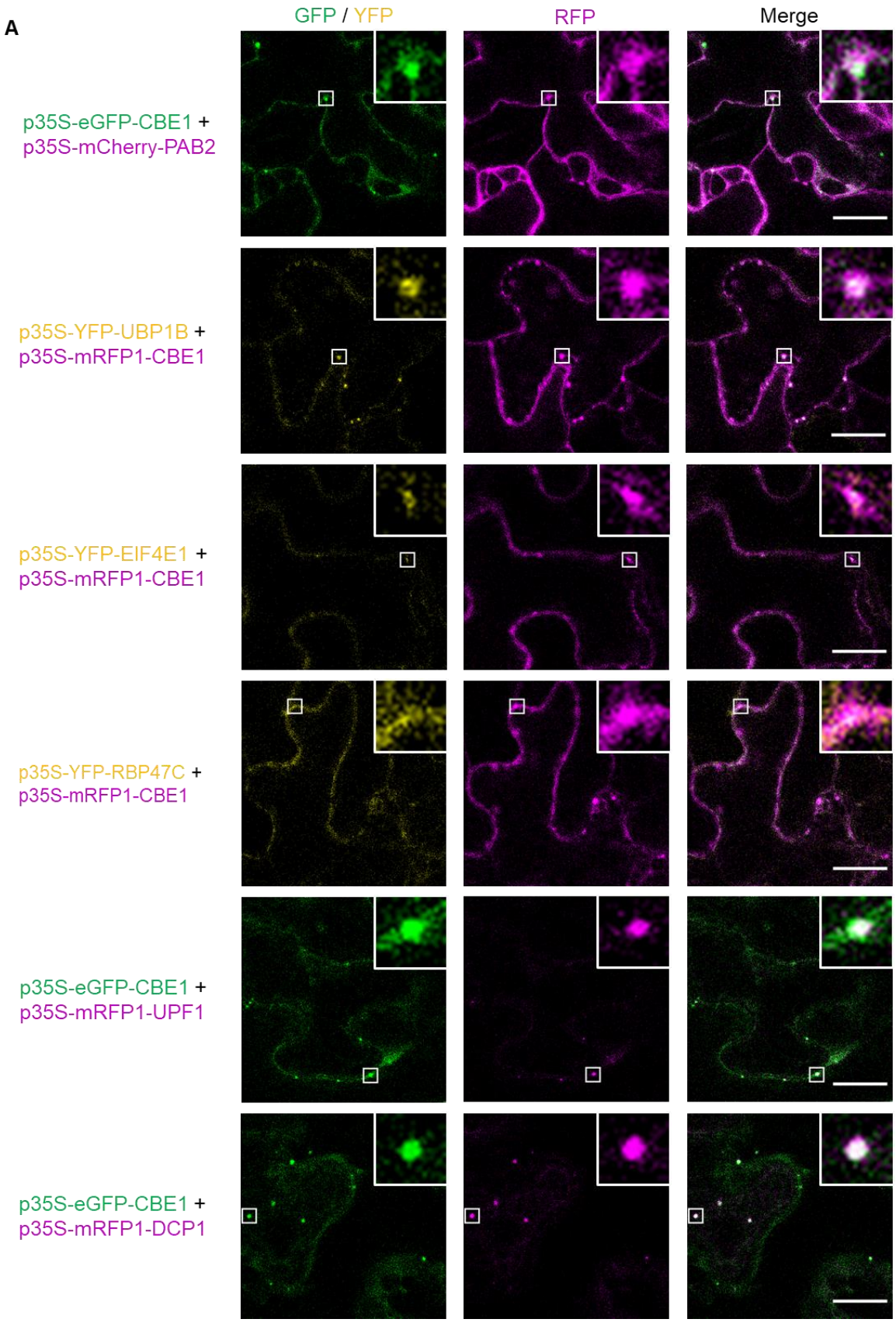
A
GFP / YFP
RFP
Merge
p35S-eGFP-CBE1 +
p35S-mCherry-PAB2
p35S-YFP-UBP1B +
p35S-mRFP1-CBE1
p35S-YFP-EIF4E1 +
p35S-mRFP1-CBE1
p35S-YFP-RBP47C +
p35S-mRFP1-CBE1
p35S-eGFP-CBE1 +
p35S-mRFP1-UPF1
p35S-eGFP-CBE1 +
p35S-mRFP1-DCP1

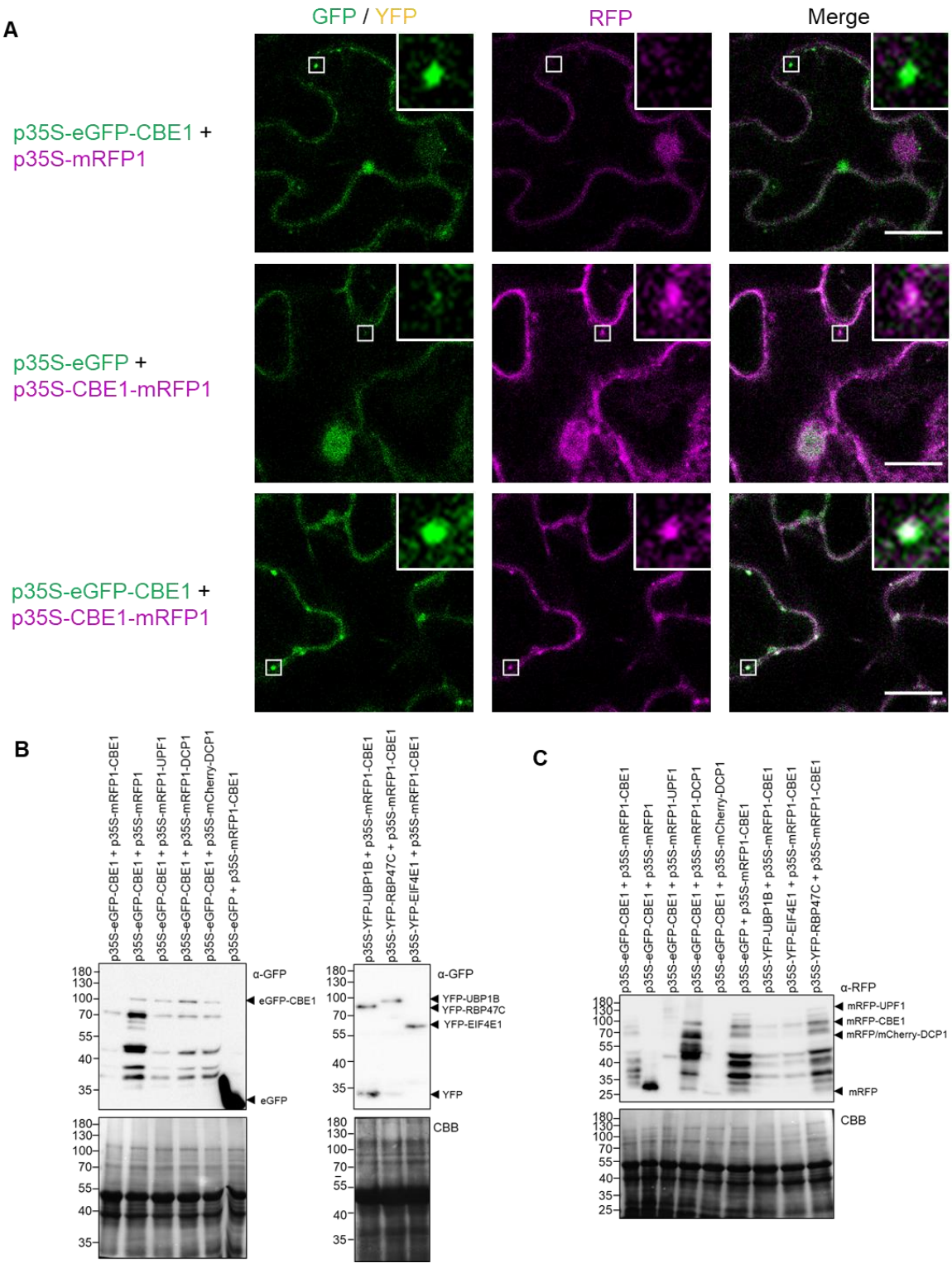

Figure 5.3 CBE1 co-localises with p-bodies and stress granules markers.
(A) Confocal images of green, yellow and red fluorescent proteins. The proteins were transiently co-expressed in *N. benthamiana*. Confocal microscopy on leaf discs was conducted 3 days post-infiltration. Merged pictures show overlay of GFP/YFP and RFP. The scale bar corresponds to 20 µm. An ROI of 25 μm^2 is shown by white square and enlarged in on the top right of the images. (B-C) Respective immunoblots from co-localisation shown in (A) using GFP antibody (A) or RFP antibody (B).

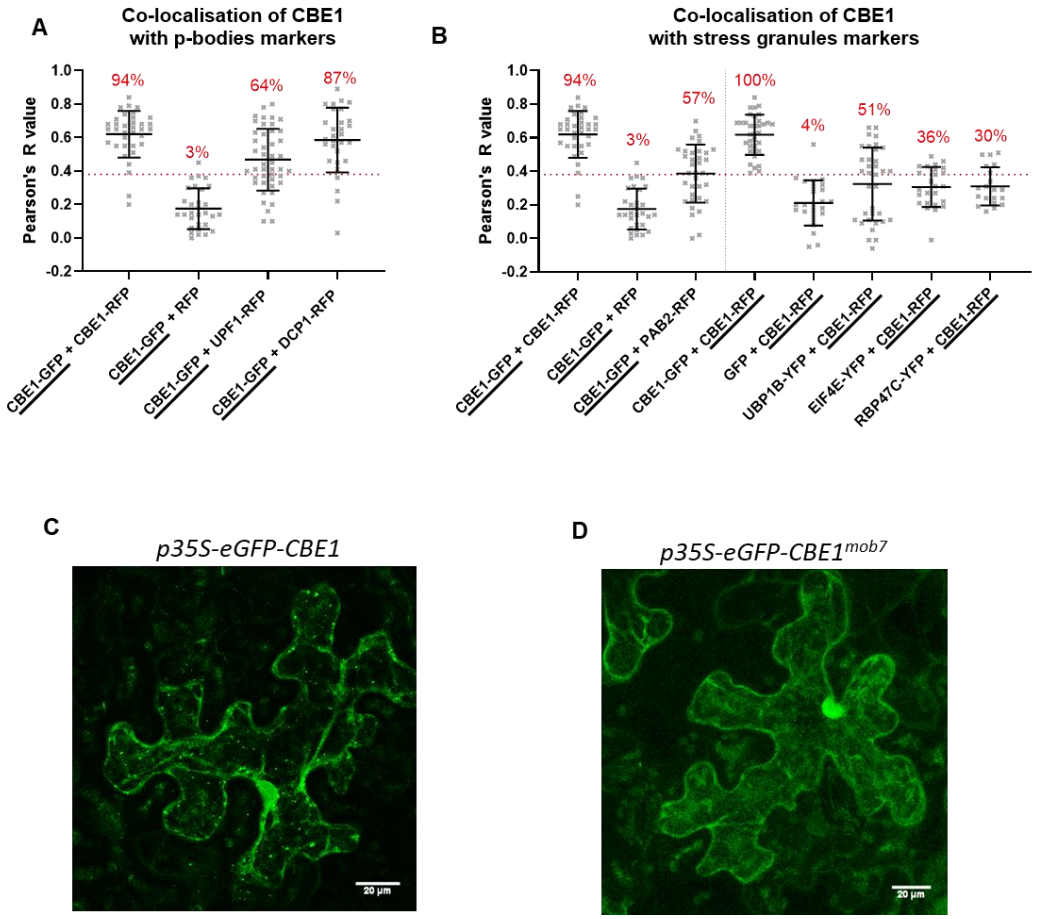

Figure 5.4 CBE1 co-localises predominantly with p-bodies rather than stress granules markers.
(A-B) Quantitative co-localisation analysis for CBE1 with p-bodies (A) and stress granules markers (B) after transient co-expression in *N. benthamiana*. The Pearson correlation coefficient (R) was calculated with five ROIs (25 µm^2) per image (n>3, images) and the proteins underlined refers to the channel of the protein used to draw the ROIs. Numbers above scatter plots are the percentage of values above 0.38. Horizontal lines represent the means and the errors bars, the standard deviations. (C-D) Confocal images of CBE1-GFP (C) or CBE1^{mob7}-GFP (D) after transient expression in *N. benthamiana*. Each picture is a projection of a z-stack of images. Confocal microscopy on leaf discs was conducted 3 days post-infiltration. The scale bar corresponds to 20 µm.

5.2.4. Role of CBE1 on immune signalling

Upon elicitation, pattern recognition receptors (PRRs) heterodimerise with the receptor BRI1-ASSOCIATED RECEPTOR KINASE 1 (BAK1). Activated PRR complexes phosphorylate the receptor-like cytoplasmic kinase (RLCK) BOTRYTIS-INDUCED KINASE1 (BIK1), which in turns phosphorylates the NADPH oxidase RESPIRATORY BURST OXIDASE HOMOLOG D (RBOHD) (Liang et al., 2018; Wang et al., 2020b). In parallel, PRR activation triggers MAPK phosphorylation cascades (Mithoe and Menke, 2018). In order to investigate whether CBE1 and other initiation factors impact these signalling components, their protein levels and activation was verified in *cbe1* and *cum1-1* mutants in 5-week-old Arabidopsis plants.

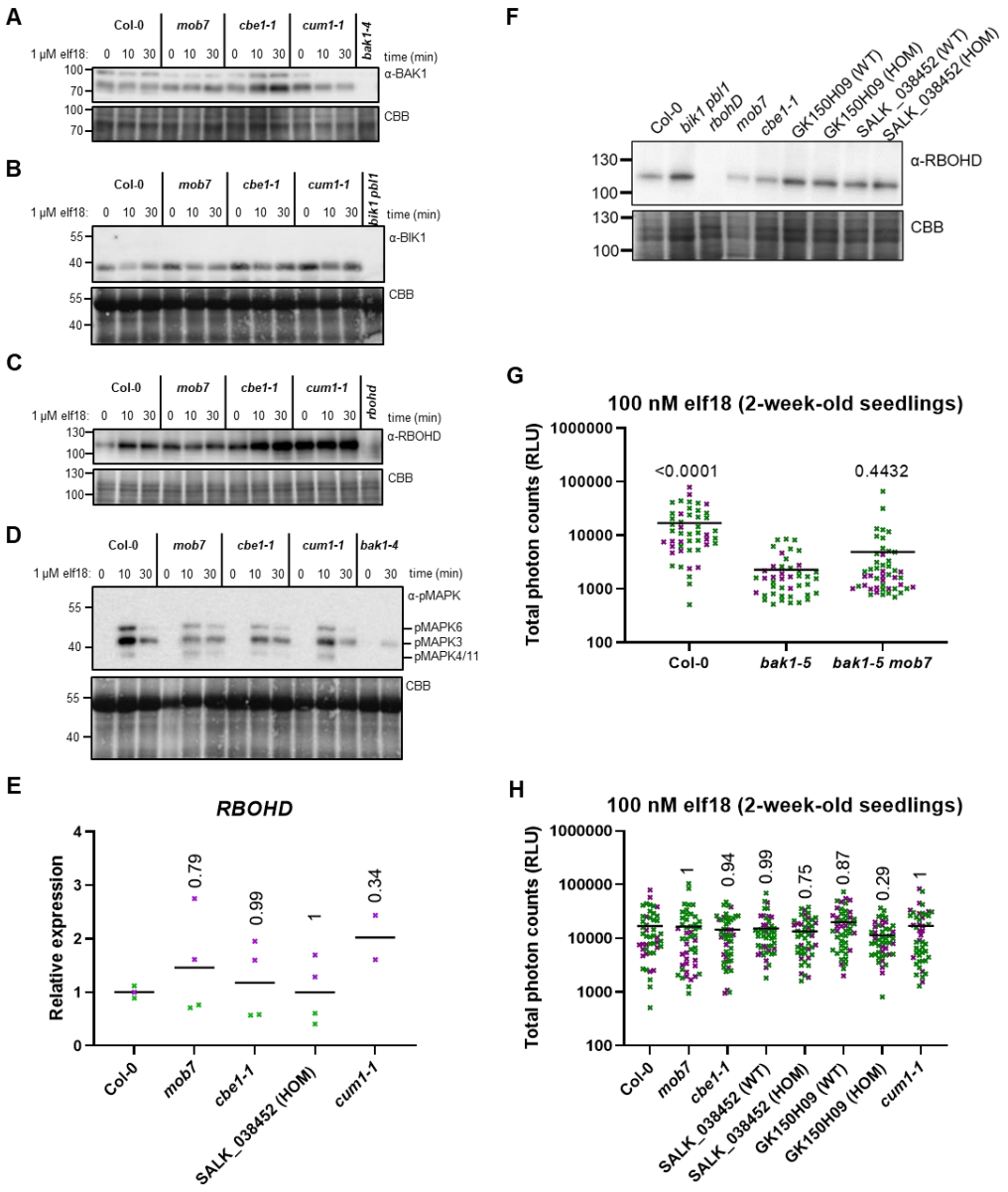

Figure 5.5 CBE1 negatively affects RBOHD protein level in adult Arabidopsis.

(A-D) Immunoblots of proteins extracted from leaf discs of 5-week-old Arabidopsis with anti-pMAPKs (A), anti-BAK1 (B), anti-BIK1 (C), anti-RBOHD (D) antibodies treated over a time course with elf18. Coomassie brilliant blue (CBB)-stained PVDF loading control are shown below immunoblots. (A) For MAPK activation, the expected identities of the respective bands are marked on the right. (E) *RBOHD* gene expression values relative to the U-BOX housekeeping gene. Horizontal lines represent the means from 1-2 independent experiments (n=1-2) Numbers above symbols are p-values from Dunnett's multiple comparison test between corresponding genotype and Col-0. (F) Immunoblots of proteins extracted from 2-week-old Arabidopsis with anti-RBOHD. Coomassie brilliant blue (CBB)-stained PVDF loading control is shown below immunoblot. (G-H) Total ROS accumulation over 60 min expressed as RLU after treatment with 100 nM elf18 on 2-week-old Arabidopsis. Horizontal lines represent the means from different seedlings (n≥16). Numbers above symbols are p-values from Dunnett's multiple comparison test between corresponding genotype and *bak1-5* (G) or Col-0 (H). (E,G,H) The symbol colours indicate the different experiments.

No consistent differences were observed for BAK1 protein level in *mob7* and *cum1-1* mutants compared to Col-0 (Figure 5.5A). Although *cbe1-1* mutants showed slightly higher BAK1 protein levels, loading control showed also higher amount of proteins (Figure 5.5A). Concerning BIK1 protein level, a slightly higher amount of BIK1 was detected in *cbe1* and *cum1-1* mutants compared to Col-0 at time 0, before elicitation with elf18 (Figure 5.5B). Similarly, the RBOHD protein level was higher in *cbe1* and *cum1-1* mutants at time 0, compared to Col-0 (Figure 5.5C). However, after elicitation the levels of both proteins BIK1 and RBOHD, seem variable among the different mutants and difficult to draw conclusions (Figure 5.5B,C). For MAPK activation, phosphorylation seems reduced in *cbe1* and *cum1-1* mutants (Figure 5.5D). These differences are nevertheless less important than the impact of *bak1-4* allele, which is a knock-out mutant of BAK1, and thus has reduced immune activation upon elicitation (Figure 5.5D). However, phosphorylation of MAPK6 and MAPK4/11 seems to sustain longer in *cbe1* and *cum1-1* mutants compared to Col-0 (Figure 5.5D). While the difference in RBOHD protein level in *cbe1* seems clear, additional repeats will be required and other differences in protein level and phosphorylation need further investigation.

CBE1 colocalises with p-bodies, which are generally associated with mRNA decay. In order to investigate whether enhanced RBOHD protein level in the *cbe1* mutant may be due to enhanced RBOHD transcript stability, the transcript level was verified in these mutants but no difference was observed (Figure 5.5E). As all these observations were in adult plants, RBOHD protein level was also verified at younger stage, especially in seedlings. Interestingly, the protein level of RBOHD was not different in *cbe1* mutants compared to Col-0 (Figure 5.5F). Accordingly, no difference was observed in elicitor-induced ROS production in seedlings for the different *cbe1* mutants but also in *bak1-5 mob7* compared to *bak1-5* (Figure 5.5 G,H).

5.2.5. Impact of CBE1 on translation during elicitation

In order to investigate the role of CBE1 on RBOHD protein level – and more generally on immunity –, and on translation regulation, transcripts regulated by CBE1 must be identified. As CBE1 is a RNA-binding protein (Reichel et al., 2016), transcripts bound to CBE1 can be investigated by RNA-immunoprecipitation. However, no antibodies for CBE1 currently exist, and silencing of *CBE1* was observed in transgenic lines expressing tagged CBE1 (Chapter 3). Instead, the translatome of *cbe1* mutant during immunity was investigated by translating ribosome affinity purification (TRAP) followed by RNA sequencing (TRAP-SEQ), which is based on the immunoprecipitation of associated transcripts to a His_6-FLAG-tagged cytoplasmic ribosomal protein (HF-RPL18) (Mustroph et al., 2009). Total mRNAs were also extracted from the same samples for transcriptome analysis in order to compare all ribosome-associated mRNAs to all the transcribed mRNAs in Col-0 and *cbe1-1* in normal condition and after elicitation. Hence, the *cbe1-1* T-DNA mutant was crossed to the plant overexpressing HF-RPL18

(Figure 5.6A). F_2 plants were genotyped to obtain homozygous mutant plants, and were compared to wild-type plants, from the same cross, which did not have the T-DNA insertion (Figure 5.6A).

Five-week-old rosettes were then subjected to elicitation with 1 µM elf18 or water treatment (Mock) for 30 minutes (Figure 5.6A). Affinity purification was then performed using FLAG antibodies and total mRNAs were also extracted from the same samples. Immunoblots revealed that ribosomal proteins were enriched after immunoprecipitation compared to the input (Figure 5.6B). Expression of tagged RPL18 was also verified in the wild-type and *cbe1-1* F_2 lines for each condition, and all expressed the ribosomal protein (Figure 5.6C). To confirm that the rosettes were elicited by elf18, the transcript level of the elf18-induced marker gene *ETHYLENE RESPONSE FACTOR 105 (ERF105)* (Bjornson et al, unpublished) was verified by RT-qPCR. Even though the strength of elicitation was different among the different experiments, all showed a higher level of expression after elicitation compared to the mock control (Figure 5.6D). The T-DNA insertion in the genotyped F_2 lines was verified by RT-qPCR with primers spanning the T-DNA insertion; as expected, only *cbe1-1* lines showed no transcript expression (Figure 5.6E). Samples are currently analysed and in parallel different approaches are investigated to identify the transcripts bound directly to CBE1.

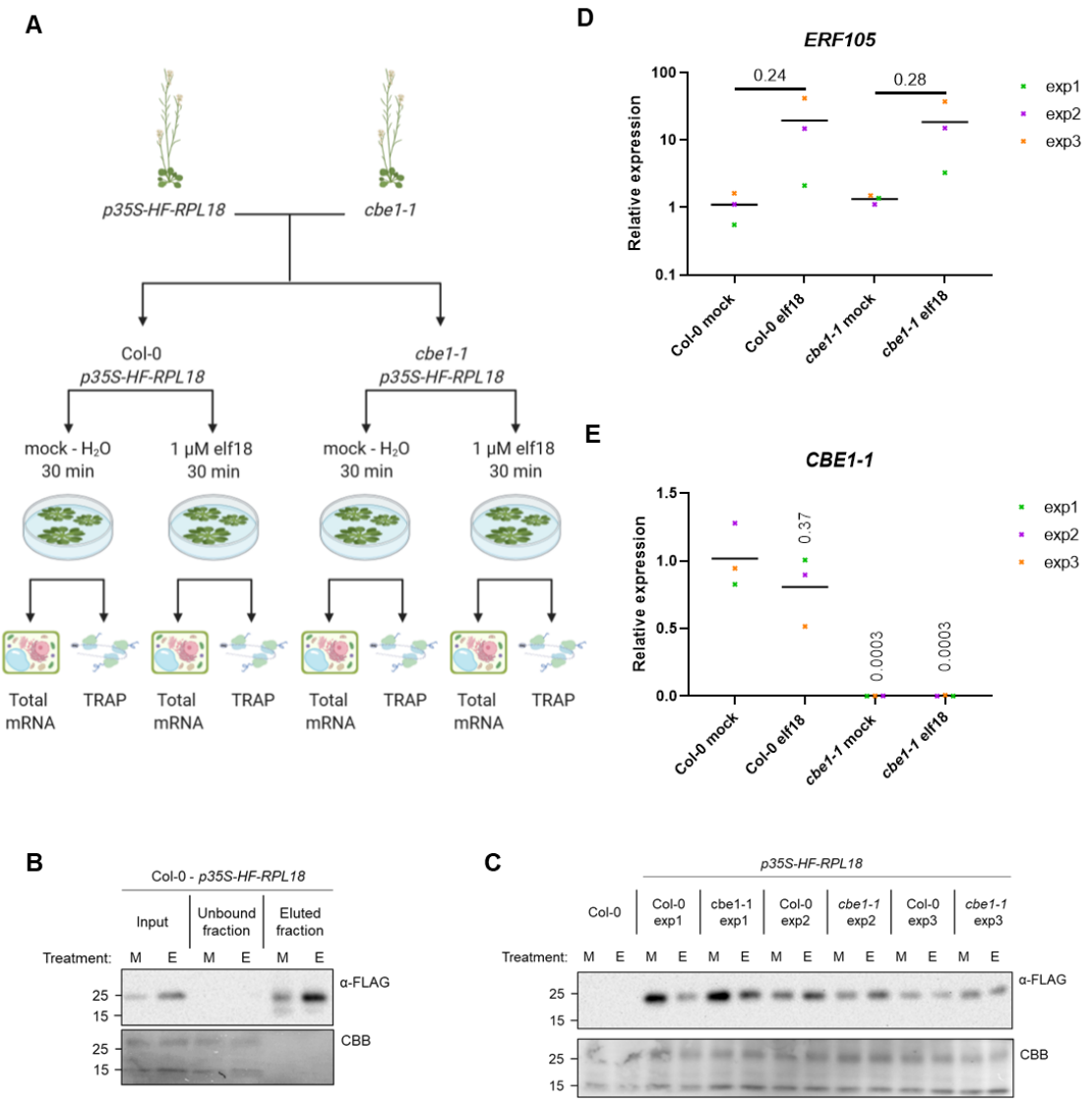

Figure 5.6 Strategy to analyse the impact of CBE1 on the transcriptome and translatome during elicitation.

(A) Schematic representation of experimental set-up for transcriptome and translatome analyses. Rosettes of 5-week-old F2 plants from cross between plants overexpressing His-FLAG-tagged RIBOSOMAL PROTEIN 18 (p35S-HF-RPL18) and *cbe1-1* mutant were treated for 30 min with 1 µM elf18 or water (mock). Ribosome-associated RNAs (TRAP) and total RNA were isolated from the same tissue. (B) Efficiency of the TRAP procedure. Total, unbound and eluted/immunopurified fractions were extracted from F_0 plants overexpressing HF-RPL18 treated with water "M" or elf18 "E" and were analysed by immunoblot using anti-FLAG antibody. Coomassie brilliant blue (CBB)-stained PVDF loading control is shown below immunoblot. (C) Immunoblots using anti-FLAG of immunopurified proteins from F2 or negative control (Col-0) rosettes treated with water "M" or elf18 "E". Coomassie brilliant blue (CBB)-stained PVDF loading control is shown below immunoblot. (D-E) Gene expression values from F_2 samples relative to the U-BOX housekeeping gene. Horizontal lines represent the means from 3 independent experiments. Numbers above symbols are p-values from Sidak's multiple comparison test between corresponding genotypes (D) or from Dunnett's multiple comparison test between corresponding genotype and Col-0 mock (E). The symbol colours indicate the different experiments.

5.3. Discussion

5.3.1. CBE1 features hallmarks of 4E-BP

Assembly of the eIF4F complex is highly regulated in eukaryotic cells. One prominent mechanism is the binding of 4E-BPs to eIF4E, which blocks the eIF4E-eIF4G association and subsequent initiation of translation. While no clear homolog of 4E-BPs was found in plants, CBE1 present features of 4E-BPs, suggesting a similar function. CBE1 is part of the 5' cap complex, and binds the initiation factors eIF4E and eIFiso4E through the well-conserved 4E-BS (Bush et al., 2009; Patrick et al., 2018). In addition, the CBE1 N-terminus, which carries the 4E-BS, shares structural homology with 4E-BP1 and eIF4G. Similar to 4E-BPs in other organisms, CBE1 bears phosphosites induced by sucrose and rapidly repressed by TOR inhibitor. CBE1 also lacks HEAT domains, which are found in eIF4G and normally directs assembly of the translation initiation machinery. In addition, although CBE1 is a much larger protein than 4E-BP1, 4E-BPs vary in sizes among organisms; for example, in *Drosophila melanogaster*, CUP (1117 aa; 126 kDa) is a 4E-BP of similar size as CBE1 (991 aa; 109 kDa) (Wilhelm et al., 2003).

5.3.2. mRNA regulator mutants phenocopy *cbe1*

CBE1 was found to regulate negatively ROS production upon elicitation and to potentially regulate RBOHD protein level. Similarly, mutants of the decapping factor PAT1 and the initiation factors eIF4E and eIFiso4G1 were found to be hypersensitive to elf18 in term of ROS production. In addition, the eIF4E mutant *cum1-1* showed higher RBOHD protein level, in preliminary results. Interestingly CBE1 shares multiple similarities with PAT1, including a partial structure homology to the yeast PAT1. Moreover, PAT1 is phosphorylated by MPK4, and residues within CBE1 sequence were found to be putative MAPK phosphosites (Roux et al., 2015; Rayapuram et al., 2018; Wang et al., 2020a). PAT1 also localises within p-bodies, and has higher accumulation upon elicitation (Roux et al., 2015). Although CBE1 localisation was not tested upon elicitation, CBE1 localised within p-bodies. It will be interesting to investigate CBE1 and PAT1 co-localisation after elicitation, and to elucidate whether the role of PAT1 is linked to the impact of the *cbe1* and *pat1* mutants on ROS production. Interestingly, PAT1 is guarded by the NLR SUMM2 (Roux et al., 2015). However, the role of PAT1 in ROS production seems independent of SUMM2, as the double mutant displays the same phenotype as *pat1*, indicating that the mutant phenotype is not due to autoimmunity linked to SUMM2 activation.

Although *eifiso4g1* showed similar sensitivity to elf18 as *cbe1*, *eifiso4g2* and *eifiso4g1 eifiso4g2* did not show a similar phenotype. Interestingly, eIFiso4G1 also controls the translation of an array of genes under hypoxia, while *eifiso4g2* mutant has normal submergence tolerance, suggesting that eIFiso4G2 displays only a certain degree of redundancy with eIFiso4G1 (Cho et al., 2019). Further investigation is

thus required to elucidate the difference between these two isoforms, and to understand how the initiation factor eIFiso4G1 could phenocopy a putative repressor of translation, CBE1.

Surprisingly, the *eif4e1* mutant *cum1-1* phenocopied also *cbe1-1*, although their protein functions are predicted to be antagonistic. As the current model proposes that eIF4E and eIFiso4E act redundantly as translation initiation factors, there must be specificities in their functions linked to ROS production and CBE1. One hypothesis is that the function of the 4E-BP CBE1 is strictly eIF4E dependent. Further investigation is thus required to study this hypothesis and investigate the reported CBE1 interaction with eIFiso4E (Patrick et al., 2018).

5.3.3. CBE1, the plant homolog of human 4E-T: a working model

While 4E-BP1-3 in human are associated with translation repression, the 4E-BP named 4E-TRANSPORTER (4E-T) is a component of the mRNA decay machinery (Nishimura et al., 2015). 4E-T is a shuttling protein that imports eIF4E to the nucleus and recruits eIF4E to cytoplasmic p-bodies (Dostie et al., 2000a; Ferraiuolo et al., 2005). Similar to CBE1, 4E-T is a large (985-aa) protein with no characterised regions, except for the short eIF4E-binding motif at its N-terminus. Although eIF4E1 is predominantly localised to the cytoplasm, a substantial fraction of eIF4E1 can move to the nucleus where it is thought to export a subset of mRNA (Dostie et al., 2000b). Similarly, CBE1 was found to be present in p-bodies and the nucleus. However, further work is required to confirm that CBE1 localisation is not biased by its overexpression in *N. benthamiana.* Similar to 4E-T, CBE1 carries predicted nuclear localisation and export signals, which also require further confirmation. In p-bodies, 4E-T promotes mRNA turnover by physically linking the 3'-terminal mRNA decay machinery to the 5' cap via its interaction with eIF4E. In fact, 4E-T associates not only with the decay factors DDX6, LSM14 and the LSM1-7-PAT1 complex, but also with the decapping factor DCP1 (Nishimura et al., 2015). Interestingly, this model could explain why *cbe1* phenocopied *pat1* and *eif4e*, and also the co-localisation of CBE1 with the decapping factor DCP1. To further speculate on this model and the current results, CBE1 could potentially promote mRNA turnover of a positive regulator of immunity. Hence, TOR and MAPK pathways would fine-tune the role CBE1 by phosphorylating it, which would then lead to the activation or inhibition of CBE1. The identification of CBE1-associated mRNAs or mRNAs which translation depends on CBE1 will shed light on the identity of this/theses regulator(s).

5.4. Future perspectives

Future work will aim to confirm preliminary results and the role of CBE1 as the putative plant 4E-T. In addition, the impact of CBE1 on transcripts will be analysed to further understand the impact of CBE1 on immune signalling and especially ROS production.

6. General discussion and future perspectives

6.1. Introduction

Immune signalling relies on tight regulation to allow a proportionate and timely response. Through the suppressor screen *modifier of bak1-5 (mob),* novel regulators of immune signalling have been discovered. *MOB1* and *MOB2* encode CALCIUM-DEPENDENT PROTEIN KINASE 28 (CPK28), which negatively regulates immune signalling by controlling the accumulation of the receptor-like cytoplasmic kinase (RLCK) BOTRYTIS-INDUCED KINASE 1 (BIK1) (Monaghan et al., 2014; Monaghan et al., 2015; Wang et al., 2018b). *MOB4* was mapped and encode CONSTITUTIVE ACTIVE CELL DEATH 1 (CAD1) (Monaghan *et al.*, unpublished results). CAD1 is involved in immunity at different levels by controlling programmed cell death and regulating the phyllosphere microbial community (Morita-Yamamuro et al., 2005; Chen et al., 2020). *mob6* was found to be a mutant of the gene encoding SITE-1 PROTEASE (S1P) that controls the cleavage of the endogenous peptide RAPID ALKALINIZATION FACTOR 23 (RALF23) to regulate PTI signalling (Stegmann et al., 2017). Hence, the success of the *mob* screen in uncovering new pathways in immunity regulation makes the identity of the remaining MOB mutants of paramount interest as it could lead to more knowledge on the specificity of the response for each elicitor and unravel novel mechanisms of immune signalling regulation.

My project was concentrated on the uncharacterised mutants *mob7*, *mob8*, *mob9* and *mob10.* The first objective was to characterise these mutants in their immune responses. While *bak1-5 mob7*, *8*, *9* and *10* show a restoration of elicitor-induced signalling; interestingly, *bak1-5 mob*s showed some specificities in their response to the different elicitors tested (Chapter 3). The objective was then to identify and confirm the mutations responsible for their phenotypes. Through map-based cloning and whole-genome resequencing, the *mob7* causative mutation was mapped to *CONSERVED BINDING OF EIF4E1* (*CBE1*) (Chapter 4). Three independent T-DNA lines phenocopied the phenotype of *mob7* mutant and thus confirmed that the mutation within the RNA-binding protein (RBP)-encoding gene *CBE1* is responsible for *mob7* phenotypes (Chapter 4). The last objective of this project was then to functionally characterise the role of MOB7 in immunity. Although limited information was available on CBE1 function when identified, this project led to the hypothesis that CBE1 is a functional ortholog of the human EIF4E-TRANSPORTER (4E-T) (Chapter 5). In addition, CBE1 negatively regulates elicitor-induced ROS production and potentially RESPIRATORY BURST OXIDASE HOMOLOG D (RBOHD) protein level, which suggest that CBE1 regulates transcript turnover of important factor(s) involved in PTI signalling (Chapter 5).

6.2. CBE1 and 4E-T share similarities

While little information is known on translation regulation in plants and especially on eIF4E-binding proteins (4E-BPs), convergent information suggest that CBE1 acts as a repressor of translation, similar to the human 4E-T.

6.2.1. eIF4E-TRANSPORTER

4E-T is a nucleocytoplasmic shuttling protein required for the localisation of eIF4E to the nucleus (Dostie et al., 2000b). However, in cells, 4E-T is predominantly located to processing (p)-bodies, which are mRNA ribonucleoprotein (mRNP) complexes associated with translation repression and mRNA turnover processes (Andrei et al., 2005; Ferraiuolo et al., 2005). 4E-T represses translation by displacing the initiation factors to p-bodies and promoting mRNA turnover (Ferraiuolo et al., 2005; Kubacka et al.,

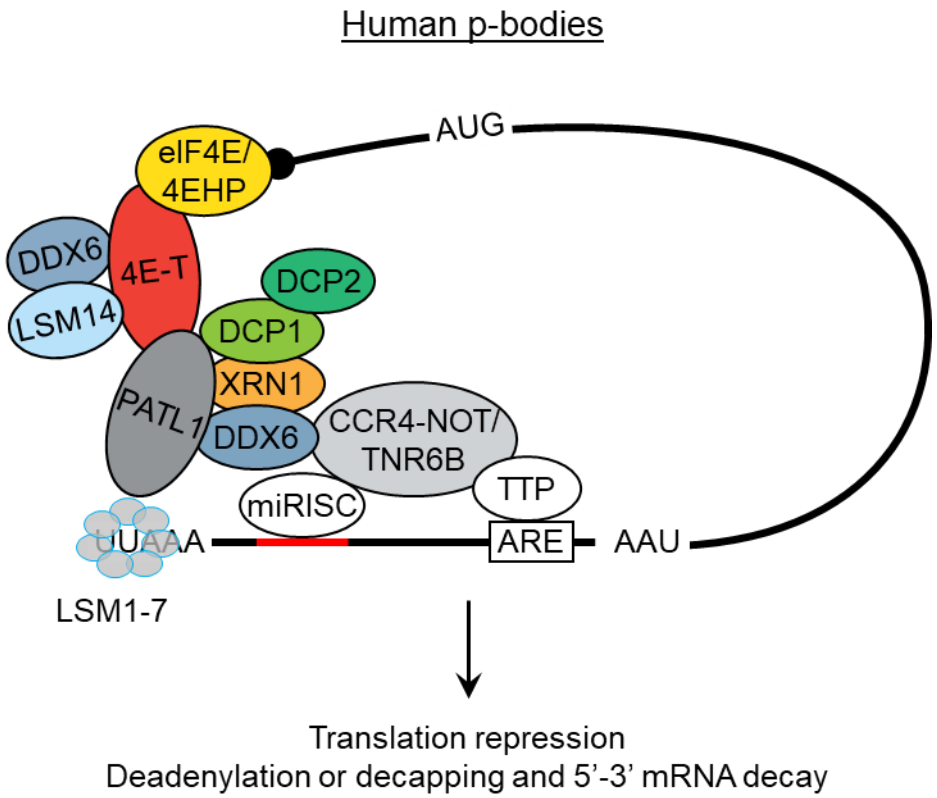

Figure 6.1 Model for the role of 4E-T in mediating mRNA turnover in human p-bodies.
Regulation of deadenylation and decapping by 4E-T relies on specific protein partners. The mRNA deadenylation is a consequence of the interaction of 4E-T's Mid region with the CCR4–NOT complex, whereas inhibition of decapping and subsequent degradation requires interaction with the cap-binding proteins eIF4E/4EHP. This figure has been adapted with permission from one published by Nishimura et al., 2015.

2013; Kamenska et al., 2014) (Figure 6.1). 4E-T regulates the decay of mRNAs destabilised by adenine and uracil (AU)-rich elements and microRNAs (miRNAs) (Räsch et al., 2020)

In p-bodies, 4E-T acts as a scaffold protein connecting translation, deadenylation, and decapping factors (Kamenska et al., 2016). Depending on the 4E-T-associated complex, transcripts undergo different fates. When 4E-T is associated with the CARBON CATABOLITE REPRESSOR4-NEGATIVE ON TATA (CCR4-NOT), transcripts are decapped and degraded (Nishimura et al., 2015). In contrast, association with EIF4E HOMOLOGOUS PROTEIN (4EHP) (Chapat et al., 2017) or TRINUCLEOTIDE REPEAT-CONTAINING GENE 6B (TNRC6B) (Räsch et al., 2020), leads to deadenylation and storage of mRNAs in a repressed form (Chapat et al., 2017; Räsch et al., 2020).

In addition, the interaction of 4E-T with DEAD BOX PROTEIN 6 (DDX6) is required for p-body assembly and translational repression (Kamenska et al., 2016).

6.2.2. Putative CBE1 interactors

Similar to 4E-T, CBE1 is a large (991-aa) protein interacting with eIF4E, 4EHP and the plant-specific eIFiso4E (Patrick et al., 2018). Also similar to 4E-T, CBE1 localises predominantly within p-bodies, while also being present in stress granules and the nucleus (Figures 5.3, 5.4). Although biochemical assays are required to confirm that CBE1 interacts within p-bodies with similar factors as 4E-T, preliminary results from this project point towards conservation of these interactions and 4E-T function. CBE1 acts as a negative regulator of elicitor-induced ROS production, and, accordingly, RBOHD protein level showed a higher level in *cbe1-1* mutants (Figure 5.2, 5.5). Mutant alleles of ARABIDOPSIS HOMOLOG OF YEAST PAT1 (PAT1) and eIF4E proteins phenocopied hypersensitivity phenotypes to elicitors of *cbe1* mutants (Figure 5.2). Both orthologous proteins in human were reported to interact within p-bodies with 4E-T (Nishimura et al., 2015), which suggest that similar interactions happen within p-bodies to regulate transcripts important for RBOHD accumulation. AtPAT1 acts as well as a decapping factor, like human PAT1-LIKE PROTEIN 1 (HsPATL1) (Ozgur et al., 2010; Roux et al., 2015). Altogether, these observations suggest that CBE1 and PAT1 act jointly in Arabidopsis (Figure 6.2).

HsPAT1 also plays the role of a scaffold in p-bodies and interacts notably with HsDCP1 (Ozgur et al., 2010). Remarkably, CBE1 and AtDCP1 were the factors that showed the strongest co-localisation (Figure 5.4). However, DCP1 and DCP2 were recently found to act as a positive regulators of immune signalling (Yu et al., 2019a). To clarify potential interaction or similarity with CBE1's role, it would be necessary to verify whether DCP1 and DCP2, similar to CBE1, regulate elicitor-induced ROS production. Human 4E-T, depending on the complex bound, either stabilises some translationally repressed mRNA or degrade them; it is thus possible that CBE1 acts similarly and this may explain differing phenotypes of CBE1 and potential interacting partners. However, the conditions for these different mechanisms are still unclear even for 4E-T (Räsch et al., 2020).

Another decapping factor, HsDDX6 directly interacts with 4E-T (Nishimura et al., 2015), and recently the DDX6-like proteins RNA HELICASE 6 (RH6), RH8 and RH12 were shown in Arabidopsis to mediate decay of stress-responsive mRNAs under non-stress conditions (Chantarachot et al., 2020). Analysing their interactions with CBE1 and the mRNAs regulated by these proteins and CBE1 will be required to elucidate whether these proteins play a similar function.

To summarise, CBE1's homology to 4E-T allowed to suggest a list of putative interactors and associated proteins of CBE1. Future work will aim to confirm these associations and their role in immune signalling.

6.2.3. Regulation of CBE1 localisation

Interestingly, CBE1^{mob7} did not localise within cytoplasmic foci, suggesting that factors downstream of the premature stop codon within *CBE1*^{mob7} control its sub-cellular localisation. Among known factors controlling 4E-T localisation are the nuclear localisation signal (NLS), nuclear export signal (NES) and interactors present in p-bodies (Dostie et al., 2000a). In addition, post-translation modification of 4E-BPs was reported to impact also sub-cellular localisation of these factors (Dostie et al., 2000a). Hypophosphorylated forms bind strongly to eIF4E and consequently repress translation (Gingras et al., 1999). Under favourable growth conditions, which promote translation, cell growth, and proliferation, 4E-BPs become phosphorylated mainly as a consequence of the activation of mammalian target of rapamycin (mTOR) (Gingras et al., 1998; Gingras, 2001). Although *in silico* analysis predicted NLS and NES within CBE1, further characterisation of these motifs will be required to determine whether they have an impact on CBE1 localisation.

As known post-translational modifications of CBE1 are also downstream of the mutation in *CBE1*^{mob7}, they could also be responsible for the mislocalisation of the mutant protein (Figure 5.1, 6.2). For example, CBE1 bears hallmarks of TOR signalling, given that phosphorylation sites were identified to be induced by sucrose and rapidly supressed by the TOR inhibitor AZD-8055 (Figure 5.1, 6.2) (Van Leene et al., 2019). In addition, CBE1 possesses phosphosites induced by MAPK4 and MAPK6 (Rayapuram et al., 2018; Wang et al., 2020a), which might also regulate its localisation. MAPK4 and MAPK6 belong to the MAPK cascade activated upon elicitors (Mithoe and Menke, 2018), and have diverse effects on proposed CBE1-interacting proteins: PAT1 is phosphorylated by MAPK4, and PAT1 localisation in p-bodies increased upon elicitor treatment (Roux et al., 2015). Inversely, MAPK3 and MAPK6 phosphorylate DCP1, which leads to the degradation of decapped mRNAs and p-body disassembly (Yu et al., 2019a). However, the difference of the impact of MAPK phosphorylation on p-bodies assembly might be due to the different tissues used and subsequent permeability of these tissues to elicitors as DCP1 localisation was observed in protoplasts, while PAT1 was observed in seedlings (Roux et al., 2015; Yu et al., 2019a). Further investigation will be required to know the spatiotemporal regulation of p-bodies during immunity. More specifically, it will be interesting to know whether CBE1

accumulates within p-bodies or contributes to the disassembly of these mRNPs; which will contribute to elucidating the mechanism underlying CBE1's function.

Among factors that might recruit CBE1 to p-bodies, AtRHs might also be good candidates as HsDDX6 is essential for p-body formation and interacts with Hs4E-T and HsPATL1 (Tritschler et al., 2009; Nishimura et al., 2015). Thus, CBE1 might associate with RHs through the sequence which shows 3D homology to PAT1 orthologs and is situated downstream of the mutation in *CBE1*^{mob7}. Besides elucidating the reasons for CBE1^{mob7} localisation, this truncated protein represents an important tool to identify the interaction domains of CBE1 and also the role of CBE1 within the nucleus. Moreover, it will allow understanding the semi-dominant effect of this mutation observed in *bak1*-5 (Figure 4.2, 4.6).

6.2.4. CBE1, a plant-specific 4E-T?

All eukaryotes rely on a similar model of transcription and translation machinery; despite this, there are specificities between organisms, such as exemplified by CBE1. Indeed, CBE1 has evolved specifically in land plants with little 3D homology to non-plant organisms and functional homology to 4E-BP (Figure 5.1). This study thus contributes to solving a long-standing question on the presence of 4E-BPs in plants. Analysis of CBE1 impact on translation will settle this controversy. As 4E-T in human is different from other 4E-BP1-3 (Dostie et al., 2000a) and no paralogs of CBE1 were found in Arabidopsis (Figure 5.1), further analysis of the domains required for CBE1 function and their structures has the potential to reveal other 4E-BPs in Arabidopsis.

6.3. CBE1 acts as a translation repressor and negative regulator of elicitor-induced ROS production

Altogether, current knowledge on CBE1 with the results from this project leads to the current working model in which CBE1 acts as translation repressor within p-bodies by controlling mRNA turnover (Figure 6.2). Upon elicitation, PRRs are activated and lead to activation of MAPKs. MAPKs then might phosphorylate CBE1 and the decapping machinery components DCP1 and PAT1, which would lead to their accumulation in p-bodies (Figure 6.2A). CBE1 will bring the initiation factors eIF4E and the decapping machinery with the decapping activators DHH1/DDX6-like RHs in close proximity to the 5'cap (Figure 6.2A). Once decapped, mRNA would be then degraded, which could lead to disassembly of p-bodies. Among the mRNAs regulated, turnover of *RBOHD* transcripts or regulators of RBOHD protein level will thus allow fine-tuning of immune signalling. Once p-bodies are disassembled, eIF4E could interact with eIF4G and protein synthesis restart; thus, allowing transcriptional reprogramming to take place with new transcripts generated and translated (Figure 6.2B). In growth condition or without

elicitor, TOR phosphorylates CBE1 and inhibits CBE1 displacing eIF4E from initiating translation and thus preventing translation repression (Figure 6.2B).

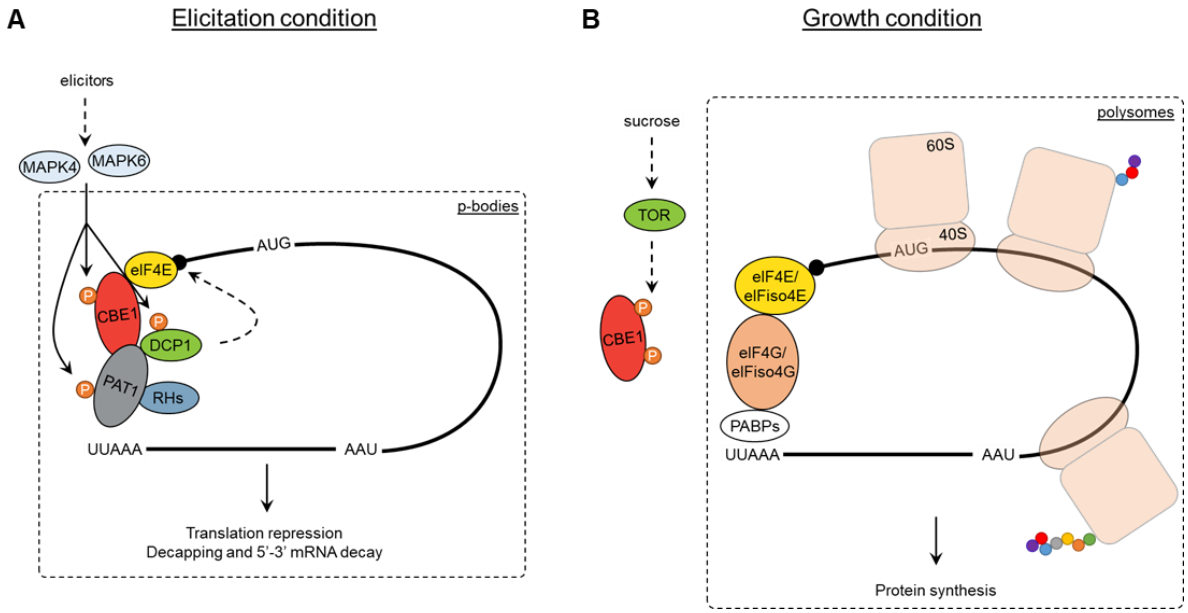

Figure 6.2 Working model for the role of CBE1 in mediating mRNA turnover in Arabidopsis.
(A) Regulation of decapping and translation by CBE1 and associated proteins during immunity in p-bodies. (B) Translation and inhibition of CBE1 under growth condition.

As human 4E-T associates also with the deadenylation complex to repress temporarily mRNAs, a similar mechanism might take place also in plants, although none of these proteins were found until now, to be linked to CBE1. However, the machinery of uridylation and poly(A)-binding proteins, which cooperate to restore a defined tail length and control the extent of mRNA deadenylation was shown to be functional in plants (Zuber et al., 2016). The specificity of transcripts regulated by 4E-T depends on AU-rich elements, and miRNAs (Ferraiuolo et al., 2005; Kamenska et al., 2014; Nishimura et al., 2015). Such mechanisms for CBE1 in plants remains unknown, but it will be interesting to investigate how the specificity of transcripts bound to CBE1 is achieved. Interestingly, although CBE1 was identified as a RNA-binding protein, no known RNA-binding domain was found in its sequence, which seems to indicate that a similar mechanism as in humans take place for CBE1.

6.4. Post-transcriptional regulation of immune signalling in plants

Post-transcriptional regulation represents one mechanism to quickly remodel signalling pathways and the resultant cellular outputs (Gassmann, 2008; Staiger et al., 2013; Yang et al., 2014; Urquidi Camacho et al., 2020). Elicitor perception induces global translational reprogramming (Meteignier et al., 2017; Xu et al., 2017b; Yoo et al., 2020) and remodelling of the cellular RBPome (Bach-Pages et al., 2020), and these RBPs control transcripts of important immune signalling components. For example, alternative

splicing (AS) targets PRRs, kinases, transcription factors and nucleotide-binding domain leucine-rich repeat proteins (NLRs) (Dinesh-Kumar and Baker, 2000; Zhang and Gassmann, 2007; Gassmann, 2008; Yang et al., 2014; Zhang et al., 2014; Liu et al., 2016; Bazin et al., 2020; Dressano et al., 2020). In addition, the decapping and deadenylation protein complex, but also nonsense mRNA decay (NMD) factors associated with p-bodies or stress granules have been shown to regulate stress-responsive mRNAs (Liang et al., 2009; Walley et al., 2010; Gloggnitzer et al., 2014; Tabassum et al., 2019; Yu et al., 2019a; Chantarachot et al., 2020). Accordingly, these changes at the level of RBPs and transcripts contribute to plant resistance to not only viruses but also other pathogens (Yu et al., 2019a; Bach-Pages et al., 2020; Chantarachot et al., 2020). CBE1 represents a novel RBP involved in immune signalling regulating elicitor-induced ROS production by potentially controlling RBOHD protein level. Despite further work needed to understand CBE1's function in immunity, it will be critical to continue characterising the role of CBE1 on the regulation of RBOHD protein level. In addition, other immune outputs need to be characterised in cbe1 mutants to understand the specificity of CBE1 on immune signalling.

During immunity, MAPKs play a key role and several RBPs were shown to be phosphorylated and regulated by MAPKs (Roux et al., 2015; Tabassum et al., 2019; Yu et al., 2019a; Bazin et al., 2020). For example, *mpk4* mutant is compromised in more than 40 % of AS upon PAMP treatment (Bazin et al., 2020). As putative phosphorylation sites by MAPKs were also found in CBE1 sequences, MAPKs might regulate its function. The role of these phosphosites will be investigated by studying the impact of the different CBE1 phosphovariants on immune signalling and p-bodies dynamic.

6.5. Linking immune signalling and growth

Spatiotemporal regulation of mRNA decay is critical for the cellular transcriptome adjustment in response to both developmental and environmental cues in plants (Chantarachot and Bailey-Serres, 2018; Chantarachot et al., 2020; Urquidi Camacho et al., 2020). Dysfunction in decapping due to loss of function of non-redundant components results in post-embryonic lethality (*e.g.* DCP1, DCP2, VCS and DCP5) or severe growth alterations (LSM1 and PAT1) (Xu et al., 2006; Goeres et al., 2007; Xu and Chua, 2009; Perea-Resa et al., 2012; Roux et al., 2015). The cause of the developmental defects in certain decapping mutants is associated with disruption of mRNA quality control and small interfering RNA (siRNA) production (Martínez de Alba et al., 2015). Several of these factors are also implicated in immune signalling corroborating with the antagonistic relation between growth and defence appearing to be the result of incompatible molecular pathways or sharing of signalling components between the programs (Kliebenstein, 2016). In addition, among the endogenous RALF peptides, which cause growth inhibition in seedlings (Pearce et al., 2001; Stegmann et al., 2017), RALF1 promotes FERONIA-mediated phosphorylation of eIF4E1 (Zhu et al., 2020). As most of these factors represent putative interactors of CBE1, it will be thus interesting to investigate to which extent CBE1 is involved in the

balance between growth and immunity. TOR signalling, which drives and optimize plant growth might thereby contribute to this antagonism by phosphorylating CBE1. On the other hand, CBE1 might control growth by regulating ROS, as ROS was shown to impact TOR signalling (Mhamdi and Van Breusegem, 2018).

6.6. Conclusion

Overall in this project, *MOB7* was found to encode the RBP CBE1. The mutation in *mob7*, identified as semi-dominant, leads to the retention of an intron and premature stop codon, which provoke the expression of a truncated protein. Like CPK28 (MOB1/MOB2) or S1P (MOB6), CBE1 acts as a negative regulator of immune signalling. CBE1 impacts elicitor-induced ROS production through the potential regulation of the protein level of components of immune signalling, similar to CPK28. Current knowledge on CBE1 with the results from this project leads to the working model in which CBE1 acts as translation repressor within p-bodies by controlling mRNA turnover. Among the possible mRNAs regulated, transcripts of *RBOHD* or positive regulators of RBOHD protein level will thus allow fine-tuning of immune signalling and explain how CBE1 negatively regulate elicitor-induced ROS production. Further work will characterise the role of CBE1 on the adjustment of RBOHD protein level and regulation of CBE1 upon PRR activation, which would unravel a novel mechanism of immune signalling regulation.

Bibliography

Adams JA (2003) Activation loop phosphorylation and catalysis in protein kinases: is there functional evidence for the autoinhibitor model? Biochemistry **42**: 601–607

Adler J, Parmryd I (2010) Quantifying colocalization by correlation: The Pearson correlation coefficient is superior to the Mander's overlap coefficient. Cytom Part A **77A**: 733–742

Ahmed H, Howton TC, Sun Y, Weinberger N, Belkhadir Y, Mukhtar MS (2018) Network biology discovers pathogen contact points in host protein-protein interactomes. Nat Commun **9**: 1–13

Ahuja I, Kissen R, Bones AM (2012) Phytoalexins in defense against pathogens. Trends Plant Sci **17**: 73–90

Albert I, Böhm H, Albert M, Feiler CE, Imkampe J, Wallmeroth N, Brancato C, Raaymakers TM, Oome S, Zhang H, et al (2015) An RLP23–SOBIR1–BAK1 complex mediates NLP-triggered immunity. Nat Plants **1**: 15140

Albert I, Hua C, Nürnberger T, Pruitt RN, Zhang L (2020) Surface sensor systems in plant immunity. Plant Physiol **182**: 1582–1596

Albrecht C, Boutrot F, Segonzac C, Schwessinger B, Gimenez-Ibanez S, Chinchilla D, Rathjen JP, De Vries SC, Zipfel C (2012) Brassinosteroids inhibit pathogen-associated molecular pattern-triggered immune signaling independent of the receptor kinase BAK1. Proc Natl Acad Sci **109**: 303–308

Alonso JM, Ecker JR (2006) Moving forward in reverse: Genetic technologies to enable genome-wide phenomic screens in Arabidopsis. Nat Rev Genet **7**: 524–536

Amano Y, Tsubouchi H, Shinohara H, Ogawa M, Matsubayashi Y (2007) Tyrosine-sulfated glycopeptide involved in cellular proliferation and expansion in Arabidopsis. Proc Natl Acad Sci **104**: 18333–18338

Ambrosone A, Costa A, Leone A, Grillo S (2012) Beyond transcription: RNA-binding proteins as emerging regulators of plant response to environmental constraints. Plant Sci **182**: 12–18

Anderson JC, Bartels S, Besteiro MAG, Shahollari B, Ulm R, Peck SC (2011) Arabidopsis MAP Kinase Phosphatase 1 (AtMKP1) negatively regulates MPK6-mediated PAMP responses and resistance against bacteria. Plant J **67**: 258–268

Andrei MA, Ingelfinger D, Heintzmann R, Achsel T, Rivera-Pomar R, Lührmann R (2005) A role for eIF4E and eIF4E-transporter in targeting mRNPs to mammalian processing bodies. RNA

11: 717–27

Ao Y, Li Z, Feng D, Xiong F, Liu J, Li JF, Wang M, Wang J, Liu B, Wang H-B (2014) OsCERK1 and OsRLCK176 play important roles in peptidoglycan and chitin signaling in rice innate immunity. Plant J **80**: 1072–1084

Arciga-Reyes L, Wootton L, Kieffer M, Davies B (2006) UPF1 is required for nonsense-mediated mRNA decay (NMD) and RNAi in Arabidopsis. Plant J **47**: 480–489

Arnaud D, Hwang I (2015) A sophisticated network of signaling pathways regulates stomatal defenses to bacterial pathogens. Mol Plant **8**: 566–581

Arthur JSC, Ley SC (2013) Mitogen-activated protein kinases in innate immunity. Nat Rev Immunol **13**: 679–692

Asai T, Tena G, Plotnikova J, Willmann MR, Chiu W-LL, Gomez-Gomez L, Boller T, Ausubel FM, Sheen J (2002) MAP kinase signalling cascade in Arabidopsis innate immunity. Nature **415**: 977–83

Asano K (2000) A multifactor complex of eukaryotic initiation factors, eIF1, eIF2, eIF3, eIF5, and initiator tRNAMet is an important translation initiation intermediate in vivo. Genes Dev **14**: 2534–2546

Austin RS, Vidaurre D, Stamatiou G, Breit R, Provart NJ, Bonetta D, Zhang J, Fung P, Gong Y, Wang PW, et al (2011) Next-generation mapping of Arabidopsis genes. Plant J **67**: 715–725

Ausubel FM (2005) Are innate immune signaling pathways in plants and animals conserved? Nat Immunol **6**: 973–979

Bach-Pages M, Chen H, Sanguankiattichai N, Kaschani F, Kaiser M, Mohammed S, Hoorn AL Van Der, Castello A, Preston GM (2020) Proteome-wide profiling of RNA-binding protein responses to flg22 reveals novel components of plant immunity. bioRxiv. doi: 10.1101/2020.09.16.299701

Baerenfaller K, Grossmann J, Grobei M a, Hull R, Hirsch-Hoffmann M, Yalovsky S, Zimmermann P, Grossniklaus U, Gruissem W, Baginsky S (2008) Genome-scale proteomics reveals Arabidopsis thaliana gene models and proteome dynamics. Science (80-) **320**: 938–941

Bai M-Y, Fan M, Oh E, Wang Z-Y (2012) A triple helix-loop-helix/basic helix-loop-helix cascade controls cell elongation downstream of multiple hormonal and environmental signaling pathways in Arabidopsis. Plant Cell **24**: 4917–4929

Bartels S, Anderson JC, González Besteiro MA, Carreri A, Hirt H, Buchala A, Métraux JP, Peck

SC, Ulm R (2009) Map kinase phosphatase1 and protein tyrosine phosphatase1 are repressors of salicylic acid synthesis and SNC1 -mediated responses in Arabidopsis. Plant Cell **21**: 2884–2897

Bartels S, Boller T (2015) Quo vadis, Pep? Plant elicitor peptides at the crossroads of immunity, stress, and development. J Exp Bot **66**: 5183–5193

Bartels S, Lori M, Mbengue M, Verk M Van, Klauser D, Hander T, Böni R, Robatzek S, Boller T (2013) The family of peps and their precursors in arabidopsis: Differential expression and localization but similar induction of pattern-Triggered immune responses. J Exp Bot **64**: 5309–5321

Bazin J, Mariappan K, Jiang Y, Blein T, Voelz R, Crespi M, Hirt H (2020) Role of MPK4 in pathogen-associated molecular pattern-triggered alternative splicing in Arabidopsis. PLOS Pathog **16**: e1008401

Belkhadir Y, Jaillais Y, Epple P, Balsemao-Pires E, Dangl JL, Chory J (2012) Brassinosteroids modulate the efficiency of plant immune responses to microbe-associated molecular patterns. Proc Natl Acad Sci **109**: 297–302

Benschop JJ, Mohammed S, O'Flaherty M, Heck AJRR, Slijper M, Menke FLHH (2007) Quantitative phosphoproteomics of early elicitor signaling in Arabidopsis. Mol Cell Proteomics **6.7**: 1198–1214

Berridge MJ, Lipp P, Bootman MD (2000) The versatility and universality of calcium signalling. Nat Rev Mol Cell Biol **1**: 11–21

Bethke G, Pecher P, Eschen-Lippold L, Tsuda K, Katagiri F, Glazebrook J, Scheel D, Lee J (2012) Activation of the Arabidopsis thaliana mitogen-activated protein kinase MPK11 by the flagellin-derived elicitor peptide, flg22. Mol Plant-Microbe Interact **25**: 471–480

Bewell MA, Maathuis FJM, Allen GJ, Sanders D (1999) Calcium-induced calcium release mediated by a voltage-activated cation channel in vacuolar vesicles from red beet. FEBS Lett **458**: 41–44

Bhasin H, Hülskamp M (2017) ANGUSTIFOLIA, a Plant Homolog of CtBP/BARS Localizes to Stress Granules and Regulates Their Formation. Front Plant Sci **8**: 1–17

Bhuiyan NH, Selvaraj G, Wei Y, King J (2009) Gene expression profiling and silencing reveal that monolignol biosynthesis plays a critical role in penetration defence in wheat against powdery mildew invasion. J Exp Bot **60**: 509–521

Bi G, Zhou Z, Wang W, Li L, Rao S, Wu Y, Zhang X, Menke FLH, Chen S, Zhou J-M (2018) Receptor-like cytoplasmic kinases directly link diverse pattern recognition receptors to the

activation of mitogen-activated protein kinase cascades in Arabidopsis. Plant Cell **6**: tpc.00981.2017

Van Der Biezen EA, Jones JDG (1998) Plant disease-resistance proteins and the gene-for-gene concept. Trends Biochem Sci **23**: 454–456

Blaum BS, Mazzotta S, Nöldeke ER, Halter T, Madlung J, Kemmerling B, Stehle T (2014) Structure of the pseudokinase domain of BIR2, a regulator of BAK1-mediated immune signaling in Arabidopsis. J Struct Biol **186**: 112–121

Böhm H, Albert I, Fan L, Reinhard A, Nürnberger T (2014) Immune receptor complexes at the plant cell surface. Curr Opin Plant Biol **20**: 47–54

Bohman S, Staal J, Thomma BPHJ, Wang M, Dixelius C (2004) Characterisation of an Arabidopsis-Leptosphaeria maculans pathosystem: Resistance partially requires camalexin biosynthesis and is independent of salicylic acid, ethylene and jasmonic acid signalling. Plant J **37**: 9–20

Boller T, Felix G (2009) A renaissance of elicitors: perception of microbe-associated molecular patterns and danger signals by pattern-recognition receptors. Annu Rev Plant Biol **60**: 379–406

Borner GHH, Sherrier DJ, Stevens TJ, Arkin IT, Dupree P (2002) Prediction of glycosylphosphatidylinositol-anchored proteins in Arabidopsis. A genomic analysis. Plant Physiol **129**: 486–499

Bosch L, Kraal B, Van der Meide PH, Duisterwinkel FJ, Van Noort JM (1983) The elongation factor EF-Tu and its two encoding genes. Prog. Nucleic Acid Res. Mol. Biol. pp 91–126

Boschi F, Schvartzman C, Murchio S, Ferreira V, Siri MI, Galván GA, Smoker M, Stransfeld L, Zipfel C, Vilaró FL, et al (2017) Enhanced bacterial wilt resistance in potato through expression of arabidopsis efr and introgression of quantitative resistance from solanum commersonii. Front Plant Sci **8**: 1–11

Boudsocq M, Willmann MR, McCormack M, Lee H, Shan L, He P, Bush J, Cheng S-HH, Sheen J (2010) Differential innate immune signalling via Ca 2+ sensor protein kinases. Nature **464**: 418–422

Boutrot F, Segonzac C, Chang KN, Qiao H, Ecker JR, Zipfel C, Rathjen JP (2010) Direct transcriptional control of the Arabidopsis immune receptor FLS2 by the ethylene-dependent transcription factors EIN3 and EIL1. Proc Natl Acad Sci **107**: 14502–14507

Boutrot F, Zipfel C (2017) Function, Discovery, and Exploitation of Plant Pattern Recognition

Receptors for Broad-Spectrum Disease Resistance. Annu Rev Phytopathol **55**: 257–286

Bouwmeester K, de Sain M, Weide R, Gouget A, Klamer S, Canut H, Govers F (2011) The lectin receptor kinase LecRK-I.9 is a novel Phytophthora resistance component and a potential host target for a RXLR effector. PLoS Pathog. doi: 10.1371/journal.ppat.1001327

Branco-Price C, Kaiser KA, Jang CJH, Larive CK, Bailey-Serres J (2008) Selective mRNA translation coordinates energetic and metabolic adjustments to cellular oxygen deprivation and reoxygenation in Arabidopsis thaliana. Plant J **56**: 743–755

Brandizzi F, Wasteneys GO (2013) Cytoskeleton-dependent endomembrane organization in plant cells: An emerging role for microtubules. Plant J **75**: 339–349

Brauer EK, Ahsan N, Dale R, Kato N, Coluccio AE, Piñeros MA, Kochian L V., Thelen JJ, Popescu SC (2016) The Raf-like kinase ILK1 and the high affinity K+ transporter HAK5 are required for innate immunity and abiotic stress response. Plant Physiol **171**: 1470–1484

Brenner S, Jacob F, Meselson M (1961) An Unstable Intermediate Carrying Information from Genes to Ribosomes for Protein Synthesis. Nature **190**: 576–581

Brock AK, Willmann R, Kolb D, Grefen L, Lajunen HM, Bethke G, Lee J, Nürnberger T, Gust AA (2010) The arabidopsis mitogen-activated protein kinase phosphatase PP2C5 affects seed germination, stomatal aperture, and abscisic acid-inducible gene expression. Plant Physiol **153**: 1098–1111

Browning KS (2004) Plant translation initiation factors: it is not easy to be green. Biochem Soc Trans **32**: 589–591

Browning KS, Bailey-Serres J (2015) Mechanism of Cytoplasmic mRNA Translation. Arab B **13**: e0176

Brückner A, Polge C, Lentze N, Auerbach D, Schlattner U (2009) Yeast two-hybrid, a powerful tool for systems biology. Int J Mol Sci **10**: 2763–2788

Brutus A, Sicilia F, Macone A, Cervone F, De Lorenzo G (2010) A domain swap approach reveals a role of the plant wall-associated kinase 1 (WAK1) as a receptor of oligogalacturonides. Proc Natl Acad Sci **107**: 9452–9457

Buccitelli C (2020) mRNAs , proteins and the emerging principles of gene expression control. Nat Rev Genet **21**: 630–644

Bucherl CA, Jarsch IK, Schudoma C, Segonzac C, Mbengue M, Robatze S, MacLean D, Ott T, Zipfel C (2017) Plant immune and growth receptors share common signalling components but

localise to distinct plasma membrane nanodomains. Elife **6**: 1–28

Buscaill P, Chandrasekar B, Sanguankiattichai N, Kourelis J, Kaschani F, Thomas EL, Morimoto K, Kaiser M, Preston GM, Ichinose Y, et al (2019) Glycosidase and glycan polymorphism control hydrolytic release of immunogenic flagellin peptides. Science (80-). doi: 10.1126/science.aav0748

Buscaill P, Rivas S (2014) Transcriptional control of plant defence responses. Curr Opin Plant Biol **20**: 35–46

Bush MS, Hutchins AP, Jones AME, Naldrett MJ, Jarmolowski A, Lloyd CW, Doonan JH (2009) Selective recruitment of proteins to 5′ cap complexes during the growth cycle in Arabidopsis. Plant J **59**: 400–412

Caillaud MC, Wirthmueller L, Sklenar J, Findlay K, Piquerez SJM, Jones AME, Robatzek S, Jones JDG, Faulkner C (2014) The Plasmodesmal Protein PDLP1 Localises to Haustoria-Associated Membranes during Downy Mildew Infection and Regulates Callose Deposition. PLoS Pathog **10**: 1–13

Cao Y, Liang Y, Tanaka K, Nguyen CT, Jedrzejczak RP, Joachimiak A, Stacey G (2014a) The kinase LYK5 is a major chitin receptor in Arabidopsis and forms a chitin-induced complex with related kinase CERK1. Elife **3**: 1–19

Cao Y, Tanaka K, Nguyen CT, Stacey G (2014b) Extracellular ATP is a central signaling molecule in plant stress responses. Curr Opin Plant Biol **20**: 82–87

Castells E, Casacuberta JM (2007) Signalling through kinase-defective domains: The prevalence of atypical receptor-like kinases in plants. J Exp Bot **58**: 3503–3511

Caunt CJ, Keyse SM (2013) Dual-specificity MAP kinase phosphatases (MKPs): Shaping the outcome of MAP kinase signalling. FEBS J **280**: 489–504

Chan C, Panzeri D, Okuma E, Tõldsepp K, Wang Y, Louh G-Y, Chin T-C, Yeh Y-H, Yeh H-L, Yekondi S, et al (2020) STRESS INDUCED FACTOR 2 Regulates Arabidopsis Stomatal Immunity Through Phosphorylation of the Anion Channel SLAC1. Plant Cell **2**: tpc.00578.2019

Chandra S, Low PS (1995) Role of phosphorylation in elicitation of the oxidative burst in cultured soybean cells. Proc Natl Acad Sci **92**: 4120–4123

Chantarachot T, Bailey-Serres J (2018) Polysomes, Stress Granules, and Processing Bodies: A Dynamic Triumvirate Controlling Cytoplasmic mRNA Fate and Function. Plant Physiol **176**: 254–269

Chantarachot T, Sorenson RS, Hummel M, Ke H, Kettenburg AT, Chen D, Aiyetiwa K, Dehesh K, Eulgem T, Sieburth LE, et al (2020) DHH1/DDX6-like RNA helicases maintain ephemeral half-lives of stress-response mRNAs. Nat Plants **6**: 772087

Chapat C, Jafarnejad SM, Matta-Camacho E, Hesketh GG, Gelbart IA, Attig J, Gkogkas CG, Alain T, Stern-Ginossar N, Fabian MR, et al (2017) Cap-binding protein 4EHP effects translation silencing by microRNAs. Proc Natl Acad Sci **114**: 5425–5430

Chen T, Nomura K, Wang X, Sohrabi R, Xu J, Yao L, Paasch BC, Ma L, Kremer J, Cheng Y, et al (2020) A plant genetic network for preventing dysbiosis in the phyllosphere. Nature. doi: 10.1038/s41586-020-2185-0

Chen YL, Lee CY, Cheng KT, Chang WH, Huang RN, Nam HG, Chen YR (2014) Quantitative peptidomics study reveals that a wound-induced peptide from PR-1 regulates immune signaling in tomato. Plant Cell **26**: 4135–4148

Cheval C, Faulkner C (2018) Plasmodesmal regulation during plant-pathogen interactions. New Phytol **217**: 62–67

Cheval C, Samwald S, Johnston MG, de Keijzer J, Breakspear A, Liu X, Bellandi A, Kadota Y, Zipfel C, Faulkner C (2020) Chitin perception in plasmodesmata characterizes submembrane immune-signaling specificity in plants. Proc Natl Acad Sci **117**: 9621–9629

Chezem WR, Clay NK (2016) Regulation of plant secondary metabolism and associated specialized cell development by MYBs and bHLHs. Phytochemistry **131**: 26–43

Chezem WR, Memon A, Li FS, Weng JK, Clay NK (2017) SG2-type R2R3-MYB transcription factor MYB15 controls defense-induced lignification and basal immunity in arabidopsis. Plant Cell **29**: 1907–1926

Chinchilla D, Bauer Z, Regenass M, Boller T, Felix G (2006) The Arabidopsis Receptor Kinase FLS2 Binds flg22 and Determines the Specificity of Flagellin Perception. Plant Cell **18**: 465–476

Chinchilla D, Shan L, He P, de Vries S, Kemmerling B (2009) One for all: the receptor-associated kinase BAK1. Trends Plant Sci **14**: 535–541

Chinchilla D, Zipfel C, Robatzek S, Kemmerling B, Nürnberger T, Jones JDG, Felix G, Boller T (2007) A flagellin-induced complex of the receptor FLS2 and BAK1 initiates plant defence. Nature **448**: 497–500

Chisholm ST, Coaker G, Day B, Staskawicz BJ (2006) Host-microbe interactions: Shaping the evolution of the plant immune response. Cell **124**: 803–814

Cho HY, Lu MYJ, Shih MC (2019) The SnRK1-eIFiso4G1 signaling relay regulates the translation of specific mRNAs in Arabidopsis under submergence. New Phytol **222**: 366–381

Cho MH, Lee SW (2015) Phenolic phytoalexins in rice: Biological functions and Biosynthesis. Int J Mol Sci **16**: 29120–29133

Choi HW, Klessig DF (2016) DAMPs, MAMPs, and NAMPs in plant innate immunity. BMC Plant Biol **16**: 232

Choi HW, Manohar M, Manosalva P, Tian M, Moreau M, Klessig DF (2016) Activation of Plant Innate Immunity by Extracellular High Mobility Group Box 3 and Its Inhibition by Salicylic Acid. PLoS Pathog **12**: 1–21

Choi J, Tanaka K, Cao Y, Qi Y, Qiu J, Liang Y, Lee SY, Stacey G (2014) Identification of a plant receptor for extracellular ATP. Science (80-) **343**: 290–294

Choi WG, Miller G, Wallace I, Harper J, Mittler R, Gilroy S (2017) Orchestrating rapid long-distance signaling in plants with Ca2+, ROS and electrical signals. Plant J **90**: 698–707

Clay NK, Adio AM, Denoux C, Jander G, Ausubel FM (2009) Glucosinolate Metabolites Required for an Arabidopsis Innate Immune Response. Science (80-) **323**: 95–101

Clough SJ, Bent AF (1998) Floral dip: A simplified method for Agrobacterium-mediated transformation of Arabidopsis thaliana. Plant J **16**: 735–743

Collins CA, LaMontagne ED, Anderson JC, Ekanayake G, Clarke AS, Bond LN, Salamango DJ, Cornish P V, Peck SC, Heese A (2020) EPSIN1 modulates the plasma membrane abundance of FLAGELLIN SENSING2 for effective immune responses. Plant Physiol **182**: pp.01172.2019

Côté F, Hahn MG (1994) Oligosaccharins: structures and signal transduction. Plant Mol Biol **26**: 1379–1411

Couto D, Niebergall R, Liang X, Bücherl CA, Sklenar J, Macho AP, Ntoukakis V, Derbyshire P, Altenbach D, Maclean D, et al (2016) The Arabidopsis Protein Phosphatase PP2C38 Negatively Regulates the Central Immune Kinase BIK1. PLoS Pathog **12**: 1–24

Couto D, Zipfel C (2016) Regulation of pattern recognition receptor signalling in plants. Nat Rev Immunol **16**: 537–552

Cui H, Tsuda K, Parker JE (2015) Effector-Triggered Immunity: From Pathogen Perception to Robust Defense. Annu Rev Plant Biol **66**: 487–511

Cui W, Lee JY (2016) Arabidopsis callose synthases CalS1/8 regulate plasmodesmal permeability

during stress. Nat Plants. doi: 10.1038/NPLANTS.2016.34

D'Ovidio R, Mattei B, Roberti S, Bellincampi D (2004) Polygalacturonases, polygalacturonase-inhibiting proteins and pectic oligomers in plant-pathogen interactions. Biochim Biophys Acta - Proteins Proteomics **1696**: 237–244

Danial NN, Korsmeyer SJ (2004) Cell Death: Critical Control Points. Cell **116**: 205–219

Dardick C, Schwessinger B, Ronald P (2012) Non-arginine-aspartate (non-RD) kinases are associated with innate immune receptors that recognize conserved microbial signatures. Curr Opin Plant Biol **15**: 358–366

Daudi A, Cheng Z, O'Brien JA, Mammarella N, Khan S, Ausubel FM, Bolwell GP (2012) The Apoplastic Oxidative Burst Peroxidase in Arabidopsis Is a Major Component of Pattern-Triggered Immunity. Plant Cell **24**: 275–287

Day B, Dahlbeck D, Staskawicz BJ (2006) NDR1 interaction with RIN4 mediates the differential activation of multiple disease resistance pathways in Arabidopsis. Plant Cell **18**: 2782–2791

DeFalco TA, Bender KW, Snedden WA (2010) Breaking the code: Ca2+ sensors in plant signalling. Biochem J **425**: 27–40

Deger AG, Scherzer S, Nuhkat M, Kedzierska J, Kollist H, Brosché M, Unyayar S, Boudsocq M, Hedrich R, Roelfsema MRG (2015) Guard cell SLAC1-type anion channels mediate flagellin-induced stomatal closure. New Phytol **208**: 162–173

Dennis MD, Browning KS (2009) Differential Phosphorylation of Plant Translation Initiation Factors by Arabidopsis thaliana CK2 Holoenzymes. J Biol Chem **284**: 20602–20614

Desaki Y, Kohari M, Shibuya N, Kaku H (2019) MAMP-triggered plant immunity mediated by the LysM-receptor kinase CERK1. J Gen Plant Pathol **85**: 1–11

Desaki Y, Miyata K, Suzuki M, Shibuya N, Kaku H (2018) Plant immunity and symbiosis signaling mediated by LysM receptors. Innate Immun **24**: 92–100

Dever TE, Dinman JD, Green R (2018) Translation elongation and recoding in eukaryotes. Cold Spring Harb Perspect Biol **10**: 1–19

Dever TE, Green R (2012) Phases of Translation in Eukaryotes. Cold Spring Harb Perspect Biol Perspect Biol **4**: 1–16

Dievart A, Gottin C, Périn C, Ranwez V, Chantret N (2020) Origin and Diversity of Plant Receptor-Like Kinases. Annu Rev Plant Biol **71**: annurev-arplant-073019-025927

Dinesh-Kumar SP, Baker BJ (2000) Alternatively spliced N resistance gene transcripts: Their possible role in tobacco mosaic virus resistance. Proc Natl Acad Sci U S A **97**: 1908–1913

Ding Z, Wang H, Liang X, Morris ER, Gallazzi F, Pandit S, Skolnick J, Walker JC, Van Doren SR (2007) Phosphoprotein and phosphopeptide interactions with the FHA domain from arabidopsis kinase-associated protein phosphatase. Biochemistry **46**: 2684–2696

Dinh TT, Luscher E, Li S, Liu X, Won SY, Chen X (2014) Genetic Screens for Floral Mutants in Arabidopsis thaliana: Enhancers and Suppressors. Methods Mol. Biol. pp 127–156

Dixon MS, Golstein C, Thomas CM, van der Biezen EA, Jones JDG (2000) Genetic complexity of pathogen perception by plants: The example of Rcr3, a tomato gene required specifically by Cf-2. Proc Natl Acad Sci **97**: 8807–8814

Dostie J, Ferraiuolo M, Pause A, Adam SA, Sonenberg N (2000a) A novel shuttling protein, 4E-T, mediates the nuclear import of the mRNA 5' cap-binding protein, eIF4E. EMBO J **19**: 3142–3156

Dostie J, Lejbkowicz F, Sonenberg N (2000b) Nuclear eukaryotic initiation factor 4E (eIF4E) colocalizes with splicing factors in speckles. J Cell Biol **148**: 239–245

Dressano K, Weckwerth PR, Poretsky E, Takahashi Y, Villarreal C, Shen Z, Schroeder JI, Briggs SP, Huffaker A (2020) Dynamic regulation of Pep-induced immunity through post-translational control of defence transcript splicing. Nat Plants. doi: 10.1038/s41477-020-0724-1

Du J, Verzaux E, Chaparro-Garcia A, Bijsterbosch G, Keizer LCP, Zhou J, Liebrand TWH, Xie C, Govers F, Robatzek S, et al (2015) Elicitin recognition confers enhanced resistance to Phytophthora infestans in potato. Nat Plants **1**: 1–5

Dubiella U, Seybold H, Durian G, Komander E, Lassig R, Witte C-PC-P, Schulze WX, Romeis T (2013) Calcium-dependent protein kinase/NADPH oxidase activation circuit is required for rapid defense signal propagation. Proc Natl Acad Sci **110**: 8744–9

Dunn KW, Kamocka MM, McDonald JH (2011) A practical guide to evaluating colocalization in biological microscopy. Am J Physiol Physiol **300**: C723–C742

Duprat A, Caranta C, Revers F, Menand B, Browning KS, Robaglia C, Duprat A, Caranta C (2002) The Arabidopsis eukaryotic initiation factor (iso)4E is dispensable for plant growth but required for susceptibility to potyviruses. Plant J **32**: 927–934

Duran-Flores D, Heil M (2016) Sources of specificity in plant damaged-self recognition. Curr Opin Plant Biol **32**: 77–87

Durrant WE, Dong X (2004) Systemic Acquired Resistance. Annu Rev Phytopathol **42**: 185–209

Duxbury Z, Ma Y, Furzer OJ, Huh SU, Cevik V, Jones JDG, Sarris PF (2016) Pathogen perception by NLRs in plants and animals: Parallel worlds. BioEssays **38**: 769–781

Edel KH, Kudla J (2015) Increasing complexity and versatility: How the calcium signaling toolkit was shaped during plant land colonization. Cell Calcium **57**: 231–246

Edwards K, Johnstone C, Thompson C (1991) A simple and rapid method for the preparation of plant genomic DNA for PCR analysis. Nucleic Acids Res **19**: 1349

Eichmann R, Schäfer P (2015) Growth versus immunity-a redirection of the cell cycle? Curr Opin Plant Biol **26**: 106–112

Elmore JM, Coaker G (2011) The role of the plasma membrane H+-ATPase in plant-microbe interactions. Mol Plant **4**: 416–427

Epple P, Apel K, Bohlmann H (1995) An Arabidopsis thaliana thionin gene is inducible via a signal transduction pathway different from that for pathogenesis-related proteins. Plant Physiol **109**: 813–820

Etherington GJ, Monaghan J, Zipfel C, MacLean D (2014) Mapping mutations in plant genomes with the user-friendly web application CandiSNP. Plant Methods **10**: 41

Evans MJ, Choi WG, Gilroy S, Morris RJ (2016) A ROS-assisted calcium wave dependent on the AtRBOHD NADPH oxidase and TPC1 cation channel propagates the systemic response to salt stress. Plant Physiol **171**: 1771–1784

Fan M, Bai MY, Kim JG, Wang T, Oh E, Chen L, Park CH, Son SH, Kim SK, Mudgett MB, et al (2014) The bHLH transcription factor HBI1 mediates the trade-off between growth and pathogen-associated molecular pattern-triggered immunity in Arabidopsis. Plant Cell **26**: 828–841

Faulkner C, Petutschnig E, Benitez-Alfonso Y, Beck M, Robatzek S, Lipka V, Maule AJ (2013) LYM2-dependent chitin perception limits molecular flux via plasmodesmata. Proc Natl Acad Sci **110**: 9166–9170

Felix G, Boller T (2003) Molecular sensing of bacteria in plants: The highly conserved RNA-binding motif RNP-1 of bacterial cold shock proteins is recognized as an elicitor signal in tobacco. J Biol Chem **278**: 6201–6208

Felix G, Duran JD, Volko S, Boller T, Miescher-institute F, Basel C- (1999) Plants have a sensitive perception system for the most conserved domain of bacterial flagellin. Plant J **18**: 265–276

Felix G, Regenass M, Boller T (1993) Specific perception of subnanomolar concentrations of chitin fragments by tomato cells: induction of extracellular alkalinization, changes in protein

phosphorylation, and establishment of a refractory state. Plant J **4**: 307–316

Felix G, Regenass M, Spanu P, Boller T (1994) The protein phosphatase inhibitor calyculin A mimics elicitor action in plant cells and induces rapid hyperphosphorylation of specific proteins as revealed by pulse labeling with [33P]phosphate. Proc Natl Acad Sci **91**: 952–956

Feng B, Liu C, de Oliveira MVV, Intorne AC, Li B, Babilonia K, de Souza Filho GA, Shan L, He P (2015) Protein Poly(ADP-ribosyl)ation Regulates Arabidopsis Immune Gene Expression and Defense Responses. PLoS Genet. doi: 10.1371/journal.pgen.1004936

Feng B, Ma S, Chen S, Zhu N, Zhang S, Yu B, Yu Y, Le B, Chen X, Dinesh-Kumar SP, et al (2016) PARylation of the forkhead-associated domain protein DAWDLE regulates plant immunity. EMBO Rep **17**: 1799–1813

Feng F, Yang F, Rong W, Wu X, Zhang J, Chen S, He C, Zhou J-M (2012) A Xanthomonas uridine 5′-monophosphate transferase inhibits plant immune kinases. Nature **485**: 114–118

Ferraiuolo MA, Basak S, Dostie J, Murray EL, Schoenberg DR, Sonenberg N (2005) A role for the eIF4E-binding protein 4E-T in P-body formation and mRNA decay. J Cell Biol **170**: 913–924

Ferrari S, Plotnikova JM, De Lorenzo G, Ausubel FM (2003) Arabidopsis local resistance to Botrytis cinerea involves salicylic acid and camalexin and requires EDS4 and PAD2, but not SID2, EDS5 or PAD4. Plant J **35**: 193–205

Ferrari S, Savatin D V., Sicilia F, Gramegna G, Cervone F, De Lorenzo G (2013) Oligogalacturonides: Plant damage-associated molecular patterns and regulators of growth and development. Front Plant Sci **4**: 1–9

Feys BJ, Wiermer M, Bhat RA, Moisan LJ, Medina-Escobar N, Neu C, Cabral A, Parker JE (2005) Arabidopsis SENESCENCE-ASSOCIATED GENE101 Stabilizes and Signals within an ENHANCED DISEASE SUSCEPTIBILITY1 Complex in Plant Innate Immunity. Plant Cell **17**: 2601–2613

Fischer I, Diévart A, Droc G, Dufayard JF, Chantret N (2016) Evolutionary dynamics of the leucine-rich repeat receptor-like kinase (LRR-RLK) subfamily in angiosperms. Plant Physiol **170**: 1595–1610

Flor HH (1942) Inheritance of pathogenicity in Melampsora lini. Phytopathology **32**: 653–669

Flor HH (1971) Current Status of the Gene-For-Gene Concept. Annu Rev Phytopathol **9**: 275–296

Flury P, Klauser D, Boller T, Bartels S (2013a) MAPK Phosphorylation Assay with Leaf Disks of Arabidopsis. BIO-PROTOCOL **3**: 3–6

Flury P, Klauser D, Schulze B, Boller T, Bartels S (2013b) The anticipation of danger: Microbe-associated molecular pattern perception enhances AtPep-triggered oxidative burst. Plant Physiol **161**: 2023–2035

Foresi NP, Laxalt AM, Tonón C V., Casalongué CA, Lamattina L (2007) Extracellular ATP induces nitric oxide production in tomato cell suspensions. Plant Physiol **145**: 589–592

Fritz-Laylin LK, Krishnamurthy N, Tor M, Sjolander K V., Jones JDG (2005) Phylogenomic Analysis of the Receptor-Like Proteins of. Plant Physiol **138**: 611–623

Fu ZQ, Guo M, Jeong BR, Tian F, Elthon TE, Cerny RL, Staiger D, Alfano JR (2007) A type III effector ADP-ribosylates RNA-binding proteins and quells plant immunity. Nature **447**: 284–288

Fürst U, Zeng Y, Albert M, Witte AK, Fliegmann J, Felix G (2020) Perception of Agrobacterium tumefaciens flagellin by FLS2XL confers resistance to crown gall disease. Nat Plants **6**: 22–27

Furukawa S, Taniai K, Yang J, Shono T, Yamakawa M (1999) Induction of gene expression of antibacterial proteins by chitin oligomers in the silkworm, Bombyx mori. Insect Mol Biol **8**: 145–148

Furukawa T, Inagaki H, Takai R, Hirai H, Che FS (2014) Two distinct EF-Tu epitopes induce immune responses in rice and Arabidopsis. Mol Plant-Microbe Interact **27**: 113–124

Galletti R, Denoux C, Gambetta S, Dewdney J, Ausubel FM, De Lorenzo G, Ferrari S (2008) The AtrbohD-mediated oxidative burst elicited by oligogalacturonides in Arabidopsis is dispensable for the activation of defense responses effective against Botrytis cinerea. Plant Physiol **148**: 1695–1706

Galletti R, Ferrari S, de Lorenzo G (2011) Arabidopsis MPK3 and MPK6 play different roles in basal and oligogalacturonide-or flagellin-induced resistance against Botrytis cinerea. Plant Physiol **157**: 804–814

Gallie DR (2016) Eukaryotic initiation factor eIFiso4G1 and eIFiso4G2 are isoforms exhibiting distinct functional differences in supporting translation in arabidopsis. J Biol Chem **291**: 1501–1513

Gallie DR (2018) Plant growth and fertility requires functional interactions between specific PABP and eIF4G gene family members. PLoS One **13**: e0191474

Gallie DR (2014) The role of the poly(A) binding protein in the assembly of the Cap-binding complex during translation initiation in plants. Translation **2**: e959378

Gamir J, Darwiche R, van't Hof P, Choudhary V, Stumpe M, Schneiter R, Mauch F (2017) The

sterol-binding activity of PATHOGENESIS-RELATED PROTEIN 1 reveals the mode of action of an antimicrobial protein. Plant J **89**: 502–509

Gangappa SN, Berriri S, Kumar SV (2017) PIF4 Coordinates Thermosensory Growth and Immunity in Arabidopsis. Curr Biol **27**: 243–249

Gao M, Wang X, Wang D, Xu F, Ding X, Zhang Z, Bi D, Cheng YT, Chen S, Li X, et al (2009) Regulation of Cell Death and Innate Immunity by Two Receptor-like Kinases in Arabidopsis. Cell Host Microbe **6**: 34–44

Gao X, Ruan X, Sun Y, Wang X, Feng B (2018) BAKing up to survive a battle: Functional dynamics of BAK1 in plant programmed cell death. Front Plant Sci **9**: 1–14

Gassmann W (2008) Alternative splicing in plant defense. Curr Top Microbiol Immunol **326**: 219–233

Geng X, Jin L, Shimada M, Kim MG, Mackey D (2014) The phytotoxin coronatine is a multifunctional component of the virulence armament of Pseudomonas syringae. Planta **240**: 1149–1165

Gimenez-Ibanez S, Hann DR, Ntoukakis V, Petutschnig EK, Lipka V, Rathjen JP (2009a) AvrPtoB Targets the LysM Receptor Kinase CERK1 to Promote Bacterial Virulence on Plants. Curr Biol **19**: 423–429

Gimenez-Ibanez S, Ntoukakis V, Rathjen JP (2009b) The LysM receptor kinase CERK1 mediates bacterial perception in Arabidopsis. Plant Signal Behav **4**: 539–541

Gingras A-C (2001) Regulation of translation initiation by FRAP/mTOR. Genes Dev **15**: 807–826

Gingras A-C, Kennedy SG, O'Leary MA, Sonenberg N, Hay N (1998) 4E-BP1, a repressor of mRNA translation, is phosphorylated and inactivated by the Akt(PKB) signaling pathway. Genes Dev **12**: 502–513

Gingras A-C, Raught B, Sonenberg N (1999) eIF4 Initiation Factors: Effectors of mRNA Recruitment to Ribosomes and Regulators of Translation. Annu Rev Biochem **68**: 913–963

Glazebrook J (2005) Contrasting Mechanisms of Defense Against Biotrophic and Necrotrophic Pathogens. Annu Rev Phytopathol **43**: 205–227

Gloggnitzer J, Akimcheva S, Srinivasan A, Kusenda B, Riehs N, Stampfl H, Bautor J, Dekrout B, Jonak C, Jiménez-Gómez JM, et al (2014) Nonsense-Mediated mRNA Decay Modulates Immune Receptor Levels to Regulate Plant Antibacterial Defense. Cell Host Microbe **16**: 376–390

Goeres DC, Van Norman JM, Zhang W, Fauver NA, Spencer M Lou, Sieburth LE (2007) Components of the Arabidopsis mRNA Decapping Complex Are Required for Early Seedling Development. Plant Cell **19**: 1549–1564

Göhre V, Spallek T, Häweker H, Mersmann S, Mentzel T, Boller T, de Torres M, Mansfield JW, Robatzek S (2008) Plant Pattern-Recognition Receptor FLS2 Is Directed for Degradation by the Bacterial Ubiquitin Ligase AvrPtoB. Curr Biol **18**: 1824–1832

Gómez-Gómez L, Bauer Z, Boller T (2001) Both the Extracellular Leucine-Rich Repeat Domain and the Kinase Activity of FLS2 Are Required for Flagellin Binding and Signaling in Arabidopsis. Plant Cell **13**: 1155–1163

Gómez-Gómez L, Boller T (2000) FLS2: An LRR Receptor–like Kinase Involved in the Perception of the Bacterial Elicitor Flagellin in Arabidopsis. Mol Cell **5**: 1003–1011

Gómez-Gómez L, Felix G, Boller T (1999) A single locus determines sensitivity to bacterial flagellin in Arabidopsis thaliana. Plant J **18**: 277–284

Gonatopoulos-Pournatzis T, Cowling VH (2014) Cap-binding complex (CBC). Biochem J **457**: 231–242

Gong BQ, Xue J, Zhang N, Xu L, Yao X, Yang QJ, Yu Y, Wang H Bin, Zhang D, Li JF (2017) Rice Chitin Receptor OsCEBiP Is Not a Transmembrane Protein but Targets the Plasma Membrane via a GPI Anchor. Mol Plant **10**: 767–770

Gough C, Cullimore J (2011) Lipo-chitooligosaccharide signaling in endosymbiotic plant-microbe interactions. Mol Plant-Microbe Interact **24**: 867–878

Griebel T, Maekawa T, Parker JE (2014) NOD-like receptor cooperativity in effector-triggered immunity. Trends Immunol **35**: 562–570

Gubaeva E, Gubaev A, Melcher RLJ, Cord-Landwehr S, Singh R, El Gueddari NE, Moerschbacher BM (2018) 'Slipped Sandwich' Model for Chitin and Chitosan Perception in Arabidopsis. Mol Plant-Microbe Interact **31**: MPMI-04-18-0098

Gully K, Pelletier S, Guillou M-CC, Ferrand M, Aligon S, Pokotylo I, Perrin A, Vergne E, Fagard M, Ruelland E, et al (2019) The SCOOP12 peptide regulates defense response and root elongation in Arabidopsis thaliana. J Exp Bot **70**: 1349–1365

Gust AA, Biswas R, Lenz HD, Rauhut T, Ranf S, Kemmerling B, Götz F, Glawischnig E, Lee J, Felix G, et al (2007) Bacteria-derived Peptidoglycans Constitute Pathogen-associated Molecular Patterns Triggering Innate Immunity in Arabidopsis. J Biol Chem **282**: 32338–32348

Gust AA, Felix G (2014) Receptor like proteins associate with SOBIR1-type of adaptors to form bimolecular receptor kinases. Curr Opin Plant Biol **21**: 104–111

Gust AA, Pruitt R, Nürnberger T (2017) Sensing Danger: Key to Activating Plant Immunity. Trends Plant Sci **22**: 779–791

Gutierrez-Beltran E, Moschou PN, Smertenko AP, Bozhkov P V. (2015) Tudor Staphylococcal Nuclease Links Formation of Stress Granules and Processing Bodies with mRNA Catabolism in Arabidopsis. Plant Cell **27**: 926–943

Halim VA, Altmann S, Ellinger D, Eschen-Lippold L, Miersch O, Scheel D, Rosahl S (2009) PAMP-induced defense responses in potato require both salicylic acid and jasmonic acid. Plant J **57**: 230–242

Halter T, Imkampe J, Mazzotta S, Wierzba M, Postel S, Bücherl C, Kiefer C, Stahl M, Chinchilla D, Wang X, et al (2014) The leucine-rich repeat receptor kinase BIR2 is a negative regulator of BAK1 in plant immunity. Curr Biol **24**: 134–143

Hamada T, Yako M, Minegishi M, Sato M, Kamei Y, Yanagawa Y, Toyooka K, Watanabe Y, Hara-Nishimura I (2018) Stress granule formation is induced by a threshold temperature rather than a temperature difference in Arabidopsis. J Cell Sci. doi: 10.1242/jcs.216051

Hander T, Fernandez-Fernandez AD, Kumpf RP, Schatowitz H, Pottie R, Rombaut D, Staes A, Nolf J, Boller T, Gevaert K, et al (2019) Damage activates calcium-dependent metacaspases for release of plant immunomodulatory peptides. Science (80-). doi: 10.1126/science.aar7486

Hardtke CS, Müller J, Berleth T (1996) Genetic similarity among Arabidopsis thaliana ecotypes estimated by DNA sequence comparison. Plant Mol Biol **32**: 915–922

Haruta M, Sabat G, Stecker K, Minkoff BB, Sussman MR (2014) A Peptide Hormone and Its Receptor Protein Kinase Regulate Plant Cell Expansion. Science (80-) **343**: 408–411

Harvey KL, Jarocki VM, Charles IG, Djordjevic SP (2019) The diverse functional roles of elongation factor tu (Ef-tu) in microbial pathogenesis. Front Microbiol **10**: 1–19

Hayafune M, Berisio R, Marchetti R, Silipo A, Kayama M, Desaki Y, Arima S, Squeglia F, Ruggiero A, Tokuyasu K, et al (2014) Chitin-induced activation of immune signaling by the rice receptor CEBiP relies on a unique sandwich-type dimerization. Proc Natl Acad Sci **111**: E404–E413

Hayashi F, Smith KD, Ozinsky A, Hawn TR, Yi EC, Goodlett DR, Eng JK, Akira S, Underhill DM, Aderem A (2001) The innate immune response to bacterial flagellin is mediated by Toll-

like receptor 5. Nature **410**: 1099–1103

He K, Gou X, Yuan T, Lin H, Asami T, Yoshida S, Russell SD, Li J (2007) BAK1 and BKK1 Regulate Brassinosteroid-Dependent Growth and Brassinosteroid-Independent Cell-Death Pathways. Curr Biol **17**: 1109–1115

Heese A, Hann DR, Gimenez-Ibanez S, Jones AME, He K, Li J, Schroeder JI, Peck SC, Rathjen JP (2007) The receptor-like kinase SERK3/BAK1 is a central regulator of innate immunity in plants. Proc Natl Acad Sci **104**: 12217–12222

Heil M, Land WG (2014) Danger signals - damaged-self recognition across the tree of life. Front Plant Sci **5**: 1–16

Henty-Ridilla JL, Li J, Day B, Staiger CJ (2014) ACTIN DEPOLYMERIZING FACTOR4 regulates actin dynamics during innate immune signaling in arabidopsis. Plant Cell **26**: 340–352

Henty-Ridilla JL, Shimono M, Li J, Chang JH, Day B, Staiger CJ (2013) The Plant Actin Cytoskeleton Responds to Signals from Microbe-Associated Molecular Patterns. PLoS Pathog. doi: 10.1371/journal.ppat.1003290

Heride C, Urbé S, Clague MJ (2014) Ubiquitin code assembly and disassembly. Curr Biol **24**: R215–R220

Hind SR, Strickler SR, Boyle PC, Dunham DM, Bao Z, O'Doherty IM, Baccile JA, Hoki JS, Viox EG, Clarke CR, et al (2016) Tomato receptor FLAGELLIN-SENSING 3 binds flgII-28 and activates the plant immune system. Nat Plants **2**: 1–8

Hogenhout SA, Bos JIB (2011) Effector proteins that modulate plant-insect interactions. Curr Opin Plant Biol **14**: 422–428

Hohmann U, Lau K, Hothorn M (2017) The Structural Basis of Ligand Perception and Signal Activation by Receptor Kinases. Annu Rev Plant Biol **68**: 109–137

Hohmann U, Nicolet J, Moretti A, Hothorn LA, Hothorn M (2018) The SERK3 elongated allele defines a role for BIR ectodomains in brassinosteroid signalling. Nat Plants. doi: 10.1038/s41477-018-0150-9

Hok S, Danchin EGJ, Allasia V, Panabières F, Attard A, Keller H (2011) An Arabidopsis (malectin-like) leucine-rich repeat receptor-like kinase contributes to downy mildew disease. Plant Cell Environ **34**: 1944–57

Holmes DR, Grubb LE, Monaghan J (2018) The jasmonate receptor COI1 is required for AtPep1-induced immune responses in Arabidopsis thaliana. BMC Res Notes **11**: 555

Holton N, Nekrasov V, Ronald PC, Zipfel C (2015) The Phylogenetically-Related Pattern Recognition Receptors EFR and XA21 Recruit Similar Immune Signaling Components in Monocots and Dicots. PLoS Pathog **11**: 1–22

Van Der Hoorn RAL, Wulff BBH, Rivas S, Durrant MC, Van Der Ploeg A, De Wit PJGM, Jones JDG (2005) Structure-function analysis of Cf-9, a receptor-like protein with extracytoplasmic leucine-rich repeats. Plant Cell **17**: 1000–1015

Horbach R, Navarro-Quesada AR, Knogge W, Deising HB (2011) When and how to kill a plant cell: Infection strategies of plant pathogenic fungi. J Plant Physiol **168**: 51–62

Horsefield S, Burdett H, Zhang X, Manik MK, Shi Y, Chen J, Qi T, Gilley J, Lai JS, Rank MX, et al (2019) NAD+ cleavage activity by animal and plant TIR domains in cell death pathways. Science (80-) **365**: 793–799

Hosseini S, Schmidt EDL, Bakker FT (2020) LRR-Receptor Like Kinase II phylogenetics reveals five main clades throughout the plant kingdom. Plant J 1–14

Hou S, Liu Z, Shen H, Wu D (2019) Damage-Associated Molecular Pattern-Triggered Immunity in Plants. Front Plant Sci. doi: 10.3389/fpls.2019.00646

Hou S, Wang X, Chen D, Yang X, Wang M, Turrà D, Di Pietro A, Zhang W (2014) The Secreted Peptide PIP1 Amplifies Immunity through Receptor-Like Kinase 7. PLoS Pathog **10**: e1004331

Hou X, Li L, Peng Z, Wei B, Tang S, Ding M, Liu J, Zhang F, Zhao Y, Gu H, et al (2010) A platform of high-density INDEL/CAPS markers for map-based cloning in Arabidopsis. Plant J **63**: 880–888

Houston K, Tucker MR, Chowdhury J, Shirley N, Little A (2016) The plant cell wall: A complex and dynamic structure as revealed by the responses of genes under stress conditions. Front Plant Sci **7**: 1–18

Hruz T, Laule O, Szabo G, Wessendorp F, Bleuler S, Oertle L, Widmayer P, Gruissem W, Zimmermann P (2008) Genevestigator V3: A Reference Expression Database for the Meta-Analysis of Transcriptomes. Adv Bioinformatics **2008**: 1–5

Hu L, Yang L (2019) Time to fight: Molecular mechanisms of age-related resistance. Phytopathology **109**: 1500–1508

Hu Y, Hewezi T (2018) Nematode-secreted peptides and host factor mimicry. J Exp Bot **69**: 2866–2868

Hu Z, Yan C, Liu P, Huang Z, Ma R, Zhang C, Wang R, Zhang Y, Martinon F, Miao D, et al

(2013) Crystal structure of NLRC4 reveals its autoinhibition mechanism. Science (80-) **341**: 172–175

Huang PY, Catinot J, Zimmerli L (2016) Ethylene response factors in Arabidopsis immunity. J Exp Bot **67**: 1231–1241

Hückelhoven R (2007) Cell Wall–Associated Mechanisms of Disease Resistance and Susceptibility. Annu Rev Phytopathol **45**: 101–127

Huffaker A, Pearce G, Ryan C a (2006) An endogenous peptide signal in Arabidopsis activates components of the innate immune response. Proc Natl Acad Sci **103**: 10098–10103

Hunt AG (2012) RNA regulatory elements and polyadenylation in plants. Front Plant Sci **2**: 1–5

Huot B, Yao J, Montgomery BL, He SY (2014) Growth-defense tradeoffs in plants: A balancing act to optimize fitness. Mol Plant **7**: 1267–1287

Hyun Y, Richter R, Vincent C, Martinez-Gallegos R, Porri A, Coupland G (2016) Multi-layered Regulation of SPL15 and Cooperation with SOC1 Integrate Endogenous Flowering Pathways at the Arabidopsis Shoot Meristem. Dev Cell **37**: 254–266

Iadevaia V, Gerber AP (2015) Combinatorial control of mRNA fates by RNA-binding proteins and non-coding RNAs. Biomolecules **5**: 2207–2222

Igarashi D, Tsuda K, Katagiri F (2012) The peptide growth factor, phytosulfokine, attenuates pattern-triggered immunity. Plant J **71**: 194–204

Imkampe J, Halter T, Huang S, Schulze S, Mazzotta S, Schmidt N, Manstretta R, Postel S, Wierzba M, Yang Y, et al (2017) The Arabidopsis Leucine-rich Repeat Receptor Kinase BIR3 Negatively Regulates BAK1 Receptor Complex Formation and Stabilizes BAK1. Plant Cell **29**: tpc.00376.2017

Irieda H, Inoue Y, Mori M, Yamada K, Oshikawa Y, Saitoh H, Uemura A, Terauchi R, Kitakura S, Kosaka A, et al (2019) Conserved fungal effector suppresses PAMP-triggered immunity by targeting plant immune kinases. Proc Natl Acad Sci 201807297

Jabs T, Tschope M, Colling C, Hahlbrock K, Scheel D (1997) Elicitor-stimulated ion fluxes and O2- from the oxidative burst are essential components in triggering defense gene activation and phytoalexin synthesis in parsley. Proc Natl Acad Sci **94**: 4800–4805

Jackson RJ, Hellen CUT, Pestova T V. (2012) Termination and post-termination events in eukaryotic translation. Adv. Protein Chem. Struct. Biol., 1st ed. pp 45–93

James GV, Patel V, Nordström KJ, Klasen JR, Salomé PA, Weigel D, Schneeberger K (2013) User guide for mapping-by-sequencing in Arabidopsis. Genome Biol **14**: R61

Jamieson PA, Shan L, He P (2018) Plant cell surface molecular cypher: Receptor-like proteins and their roles in immunity and development. Plant Sci **274**: 242–251

Jang G-J, Yang J-Y, Hsieh H-L, Wu S-H (2019) Processing bodies control the selective translation for optimal development of Arabidopsis young seedlings. Proc Natl Acad Sci **116**: 6451–6456

Jeong BR, Lin Y, Joe A, Guo M, Korneli C, Yang H, Wang P, Yu M, Cerny RL, Staiger D, et al (2011a) Structure function analysis of an ADP-ribosyltransferase type III effector and its RNA-binding target in plant immunity. J Biol Chem **286**: 43272–43281

Jeong H-J, Kim YJ, Kim SH, Kim Y-H, Lee I-J, Kim YK, Shin JS (2011b) Nonsense-Mediated mRNA Decay Factors, UPF1 and UPF3, Contribute to Plant Defense. Plant Cell Physiol **52**: 2147–2156

Jeong YJ, Shang Y, Kim BH, Kim SY, Song JH, Lee JS, Lee MM, Li J, Nam KH (2010) BAK7 displays unequal genetic redundancy with BAK1 in brassinosteroid signaling and early senescence in arabidopsis. Mol Cells **29**: 259–266

Jeworutzki E, Roelfsema MRG, Anschütz U, Krol E, Elzenga JTM, Felix G, Boller T, Hedrich R, Becker D (2010) Early signaling through the arabidopsis pattern recognition receptors FLS2 and EFR involves Ca2+-associated opening of plasma membrane anion channels. Plant J **62**: 367–378

Jia Y, McAdams SA, Bryan GT, Hershey HP, Valent B (2000) Direct interaction of resistance gene and avirulence gene products confers rice blast resistance. EMBO J **19**: 4004–4014

Jiang Y, Han B, Zhang H, Mariappan KG, Bigeard J, Colcombet J, Hirt H, Dac PD, Dac PD (2019) MAP4K4 associates with BIK1 to regulate plant innate immunity. EMBO Rep **1**: e47965

Jiao Y, Riechmann JL, Meyerowitz EM (2008) Transcriptome-wide analysis of uncapped mRNAs in Arabidopsis reveals regulation of mRNA degradation. Plant Cell **20**: 2571–2585

Jiménez-Góngora T, Kim SK, Lozano-Durán R, Zipfel C (2015) Flg22-triggered immunity negatively regulates key BR biosynthetic genes. Front Plant Sci **6**: 1–7

Jogawat A, Meena MK, Kundu A, Varma M, Vadassery J (2020) Calcium channel CNGC19 mediates basal defense signaling to regulate colonization by Piriformospora indica on Arabidopsis roots. J Exp Bot. doi: 10.1093/jxb/eraa028

Johnson JM, Thürich J, Petutschnig EK, Altschmied L, Meichsner D, Sherameti I, Dindas J, Mrozinska A, Paetz C, Scholz SS, et al (2018) A Poly(A) Ribonuclease Controls the

Cellotriose-Based Interaction between Piriformospora indica and Its Host Arabidopsis. Plant Physiol **176**: 2496–2514

Johnson LN, Noble MEM, Owen DJ (1996) Active and inactive protein kinases: Structural basis for regulation. Cell **85**: 149–158

Jones JDG, Dangl JL (2006) The plant immune system. Nature **444**: 323–329

Jones JDG, Vance RE, Dangl JL (2016) Intracellular innate immune surveillance devices in plants and animals. Science (80-) **354**: aaf6395

Kadota Y, Sklenar J, Derbyshire P, Stransfeld L, Asai S, Ntoukakis V, Jones JDG, Shirasu K, Menke FLH, Jones AME, et al (2014) Direct Regulation of the NADPH Oxidase RBOHD by the PRR-Associated Kinase BIK1 during Plant Immunity. Mol Cell **54**: 43–55

Kaku H, Nishizawa Y, Ishii-Minami N, Akimoto-Tomiyama C, Dohmae N, Takio K, Minami E, Shibuya N (2006) Plant cells recognize chitin fragments for defense signaling through a plasma membrane receptor. Proc Natl Acad Sci **103**: 11086–11091

Kamenska A, Lu W-T, Kubacka D, Broomhead H, Minshall N, Bushell M, Standart N (2014) Human 4E-T represses translation of bound mRNAs and enhances microRNA-mediated silencing. Nucleic Acids Res **42**: 3298–3313

Kamenska A, Simpson C, Vindry C, Broomhead H, Bénard M, Ernoult-Lange M, Lee BP, Harries LW, Weil D, Standart N (2016) The DDX6–4E-T interaction mediates translational repression and P-body assembly. Nucleic Acids Res **44**: 6318–6334

Kanellos G, Frame MC (2016) Cellular functions of the ADF/cofilin family at a glance. J Cell Sci **129**: 3211–3218

Kang S, Yang F, Li L, Chen H, Chen S, Zhang J (2015) The arabidopsis transcription factor brassinosteroid insensitive1-ethyl methanesulfonate-suppressor1 is a direct substrate of mitogen-activated protein kinase6 and regulates immunity. Plant Physiol **167**: 1076–1086

Katagiri F, Thilmony R, He SY (2002) The Arabidopsis Thaliana-Pseudomonas Syringae Interaction. Arab B **1**: e0039

Kato H, Onai K, Abe A, Shimizu M, Takagi H, Tateda C, Utsushi H, Singkarabanit-Ogawa S, Kitakura S, Ono E, et al (2020) Lumi-Map, a real-time luciferase bioluminescence screen of mutants combined with MutMap, reveals Arabidopsis genes involved in PAMP-triggered immunity. Mol Plant-Microbe Interact MPMI-05-20-0118-TA

Katsuragi Y, Takai R, Furukawa T, Hirai H, Morimoto T, Katayama T, Murakami T, Che F-S

(2015) CD2-1, the C-Terminal Region of Flagellin, Modulates the Induction of Immune Responses in Rice. Mol Plant-Microbe Interact **28**: 648–658

Keinath NF, Waadt R, Brugman R, Schroeder JI, Grossmann G, Schumacher K, Krebs M (2015) Live Cell Imaging with R-GECO1 Sheds Light on flg22- and Chitin-Induced Transient [Ca2+]cyt Patterns in Arabidopsis. Mol Plant **8**: 1188–1200

Keiper BD, Gan W, Rhoads RE (1999) Protein synthesis initiation factor 4G. Int J Biochem Cell Biol **31**: 37–41

Kemmerling B, Schwedt A, Rodriguez P, Mazzotta S, Frank M, Qamar SA, Mengiste T, Betsuyaku S, Parker JE, Müssig C, et al (2007) The BRI1-Associated Kinase 1, BAK1, Has a Brassinolide-Independent Role in Plant Cell-Death Control. Curr Biol **17**: 1116–1122

Kesten C, Gámez-Arjona FM, Menna A, Scholl S, Dora S, Huerta AI, Huang H, Tintor N, Kinoshita T, Rep M, et al (2019) Pathogen-induced pH changes regulate the growth-defense balance in plants. EMBO J **38**: 1–20

Ben Khaled S, Postma J, Robatzek S (2015) A Moving View: Subcellular Trafficking Processes in Pattern Recognition Receptor–Triggered Plant Immunity. Annu Rev Phytopathol **53**: 379–402

Khan MA, Goss DJ (2018) Kinetic analyses of phosphorylated and non-phosphorylated eIFiso4E binding to mRNA cap analogues. Int J Biol Macromol **106**: 387–395

Kim SY, Sivaguru M, Stacey G (2006) Extracellular ATP in plants. Visualization, localization, and analysis of physiological significance in growth and signaling. Plant Physiol **142**: 984–992

Kimura S, Hunter K, Vaahtera L, Tran HC, Citterico M, Vaattovaara A, Rokka A, Stolze SC, Harzen A, Meißner L, et al (2020) CRK2 and C-terminal Phosphorylation of NADPH Oxidase RBOHD Regulate Reactive Oxygen Species Production in Arabidopsis. Plant Cell **32**: 1063–1080

Kliebenstein DJ (2016) False idolatry of the mythical growth versus immunity tradeoff in molecular systems plant pathology. Physiol Mol Plant Pathol **95**: 55–59

Kliebenstein DJ, Kroymann J, Mitchell-Olds T (2005) The glucosinolate-myrosinase system in an ecological and evolutionary context. Curr Opin Plant Biol **8**: 264–271

Klune JR, Dhupar R, Cardinal J, Billiar TR, Tsung A (2008) HMGB1: Endogenous danger signaling. Mol Med **14**: 476–484

Knepper C, Savory EA, Day B (2011) Arabidopsis NDR1 is an integrin-like protein with a role in fluid loss and plasma membrane-cell wall adhesion. Plant Physiol **156**: 286–300

Kobayashi I, Kobayashi Y, Yamaoka N, Kunoh H (1992) Recognition of a pathogen and a nonpathogen by barley coleoptile cells. III. Responses of microtubules and actin filaments in barley coleoptile cells to penetration attempts. Can J Bot **70**: 1815–1823

Kohorn BD (2016) Cell wall-associated kinases and pectin perception. J Exp Bot **67**: 489–494

Komori R, Amano Y, Ogawa-Ohnishi M, Matsubayashi Y (2009) Identification of tyrosylprotein sulfotransferase in Arabidopsis. Proc Natl Acad Sci **106**: 15067–15072

Kondo T, Kawai T, Akira S (2012) Dissecting negative regulation of Toll-like receptor signaling. Trends Immunol **33**: 449–458

Kong Q, Qu N, Gao M, Zhang Z, Ding X, Yang F, Li Y, Dong OX, Chen S, Li X, et al (2012) The MEKK1-MKK1/MKK2-MPK4 kinase cascade negatively regulates immunity mediated by a mitogen-activated protein kinase kinase kinase in Arabidopsis. Plant Cell **24**: 2225–2236

Kong Q, Sun T, Qu N, Ma J, Li M, Cheng YT, Zhang Q, Wu D, Zhang Z, Zhang Y (2016) Two redundant receptor-like cytoplasmic kinases function downstream of pattern recognition receptors to regulate activation of SA biosynthesis. Plant Physiol **171**: 1344–1354

Krasileva K V., Dahlbeck D, Staskawicz BJ (2010) Activation of an Arabidopsis resistance protein is specified by the in planta association of its leucine-rich repeat domain with the cognate oomycete effector. Plant Cell **22**: 2444–2458

Krieg DR (1963) Ethyl methanesulfonate-induced reversion of bacteriophage T4rII mutants. Genetics **48**: 561–80

Krol E, Mentzel T, Chinchilla D, Boller T, Felix G, Kemmerling B, Postel S, Arents M, Jeworutzki E, Al-Rasheid KAS, et al (2010) Perception of the Arabidopsis danger signal peptide 1 involves the pattern recognition receptor AtPEPR1 and its close homologue AtPEPR2. J Biol Chem **285**: 13471–13479

Kropiwnicka A, Kuchta K, Lukaszewicz M, Kowalska J, Jemielity J, Ginalski K, Darzynkiewicz E, Zuberek J (2015) Five eIF4E isoforms from Arabidopsis thaliana are characterized by distinct features of cap analogs binding. Biochem Biophys Res Commun **456**: 47–52

Krupa A, Preethi G, Srinivasan N (2004) Structural modes of stabilization of permissive phosphorylation sites in protein kinases: Distinct strategies in Ser/Thr and Tyr kinases. J Mol Biol **339**: 1025–1039

Kubacka D, Kamenska A, Broomhead H, Minshall N, Darzynkiewicz E, Standart N (2013) Investigating the Consequences of eIF4E2 (4EHP) Interaction with 4E-Transporter on Its Cellular

Distribution in HeLa Cells. PLoS One **8**: e72761

Kumar V, Van Staden J (2019) Multi-tasking of SERK-like kinases in plant embryogenesis, growth, and development: current advances and biotechnological applications. Acta Physiol Plant **41**: 31

Kunwar S, Iriarte F, Fan Q, Da Silva EE, Ritchie L, Nguyen NS, Freeman JH, Stall RE, Jones JB, Minsavage G V., et al (2018) Transgenic expression of EFR and Bs2 genes for field management of bacterial wilt and bacterial spot of tomato. Phytopathology **108**: 1402–1411

Kunze G, Zipfel C, Robatzek S, Niehaus K, Boller T, Felix G (2004) The N Terminus of Bacterial Elongation Factor Tu Elicits Innate Immunity in Arabidopsis Plants. Plant Cell **16**: 3496–3507

Lacombe S, Rougon-Cardoso A, Sherwood E, Peeters N, Dahlbeck D, van Esse HP, Smoker M, Rallapalli G, Thomma BPHJ, Staskawicz B, et al (2010) Interfamily transfer of a plant pattern-recognition receptor confers broad-spectrum bacterial resistance. Nat Biotechnol **28**: 365–369

Ladwig F, Dahlke RI, Stührwohldt N, Hartmann J, Harter K, Sauter M (2015) Phytosulfokine Regulates Growth in Arabidopsis through a Response Module at the Plasma Membrane That Includes CYCLIC NUCLEOTIDE-GATED CHANNEL17, H + -ATPase, and BAK1. Plant Cell **27**: 1718–1729

Laemmli UK (1970) Cleavage of structural proteins during the assembly of the head of bacteriophage T4. Nature **227**: 680–5

Lal NK, Nagalakshmi U, Hurlburt NK, Flores R, Bak A, Sone P, Ma X, Song G, Walley J, Shan L, et al (2018) The Receptor-like Cytoplasmic Kinase BIK1 Localizes to the Nucleus and Regulates Defense Hormone Expression during Plant Innate Immunity. Cell Host Microbe **23**: 485-497.e5

Lannoo N, Van Damme EJM (2014) Lectin domains at the frontiers of plant defense. Front Plant Sci **5**: 1–16

Laxalt AM, Raho N, Ten Have A, Lamattina L (2007) Nitric oxide is critical for inducing phosphatidic acid accumulation in xylanase-elicited tomato cells. J Biol Chem **282**: 21160–21168

Lee AHY, Hurley B, Felsensteiner C, Yea C, Ckurshumova W, Bartetzko V, Wang PW, Quach V, Lewis JD, Liu YC, et al (2012) A bacterial acetyltransferase destroys plant microtubule networks and blocks secretion. PLoS Pathog. doi: 10.1371/journal.ppat.1002523

Lee D, Lal NK, Lin ZD, Ma S, Liu J, Castro B, Toruño T, Dinesh-Kumar SP, Coaker G (2020) Regulation of reactive oxygen species during plant immunity through phosphorylation and ubiquitination of RBOHD. Nat Commun **11**: 1838

Lee J, Eschen-Lippold L, Lassowskat I, Böttcher C, Scheel D (2015) Cellular reprogramming through mitogen-activated protein kinases. Front Plant Sci **6**: 940

Lee JY, Lu H (2011) Plasmodesmata: The battleground against intruders. Trends Plant Sci **16**: 201–210

Lee JY, Wang X, Cui W, Sager R, Modla S, Czymmek K, Zybaliov B, Van Wijk K, Zhang C, Lu H, et al (2011) A plasmodesmata-localized protein mediates crosstalk between cell-to-cell communication and innate immunity in arabidopsis. Plant Cell **23**: 3353–3373

Lee M, Jeon HS, Kim SH, Chung JH, Roppolo D, Lee H, Cho HJ, Tobimatsu Y, Ralph J, Park OK (2019) Lignin-based barrier restricts pathogens to the infection site and confers resistance in plants. EMBO J **38**: 1–17

Van Leene J, Han C, Gadeyne A, Eeckhout D, Matthijs C, Cannoot B, De Winne N, Persiau G, Van De Slijke E, Van de Cotte B, et al (2019) Capturing the phosphorylation and protein interaction landscape of the plant TOR kinase. Nat Plants **5**: 316–327

Lehti-Shiu MD, Zou C, Hanada K, Shiu S (2009) Evolutionary History and Stress Regulation of Plant Receptor-Like Kinase/Pelle Genes. Plant Physiol **150**: 12–26

Lemtiri-Chlieh F, MacRobbie EAC, Webb AAR, Manison NF, Brownlee C, Skepper JN, Chen J, Prestwich GD, Brearley CA (2003) Inositol hexakisphosphate mobilizes an endomembrane store of calcium in guard cells. Proc Natl Acad Sci **100**: 10091–10095

Lenzoni G, Liu J, Knight MR (2018) Predicting plant immunity gene expression by identifying the decoding mechanism of calcium signatures. New Phytol **217**: 1598–1609

Li B, Ferreira MA, Huang M, Camargos LF, Yu X, Teixeira RM, Carpinetti PA, Mendes GC, Gouveia-Mageste BC, Liu C, et al (2019) The receptor-like kinase NIK1 targets FLS2/BAK1 immune complex and inversely modulates antiviral and antibacterial immunity. Nat Commun **10**: 1–14

Li B, Jiang S, Yu X, Cheng C, Chen S, Cheng Y, Yuan JS, Jiang D, He P, Shan L (2015a) Phosphorylation of trihelix transcriptional repressor ASR3 by MAP KINASE4 negatively regulates arabidopsis immunity. Plant Cell **27**: 839–856

Li B, Meng X, Shan L, He P (2016a) Transcriptional Regulation of Pattern-Triggered Immunity in Plants. Cell Host Microbe **19**: 641–650

Li C, Wu HM, Cheung AY (2016b) FERONIA and her pals: Functions and mechanisms. Plant Physiol **171**: 2379–2392

Li F, Cheng C, Cui F, de Oliveira MVV, Yu X, Meng X, Intorne AC, Babilonia K, Li M, Li B, et al (2014a) Modulation of RNA Polymerase II Phosphorylation Downstream of Pathogen Perception Orchestrates Plant Immunity. Cell Host Microbe **16**: 748–758

Li H, Durbin R (2009) Fast and accurate short read alignment with Burrows-Wheeler transform. Bioinformatics **25**: 1754–1760

Li J, Cao L, Staiger CJ (2017) Capping protein modulates actin remodeling in response to reactive Oxygen species during plant innate immunity. Plant Physiol **173**: 1125–1136

Li J, Chory J (1997) A putative leucine-rich repeat receptor kinase involved in brassinosteroid signal transduction. Cell **90**: 929–938

Li J, Henty-Ridilla JL, Staiger BH, Day B, Staiger CJ (2015b) Capping protein integrates multiple MAMP signalling pathways to modulate actin dynamics during plant innate immunity. Nat Commun **6**: 1–13

Li J, Wen J, Lease KA, Doke JT, Tax FE, Walker JC (2002) BAK1, an Arabidopsis LRR receptor-like protein kinase, interacts with BRI1 and modulates brassinosteroid signaling. Cell **110**: 213–222

Li J, Zhao-Hui C, Batoux M, Nekrasov V, Roux M, Chinchilla D, Zipfel C, Jones JDG (2009) Specific ER quality control components required for biogenesis of the plant innate immune receptor EFR. Proc Natl Acad Sci **106**: 15973–15978

Li L, Kim P, Yu L, Cai G, Chen S, Alfano JR, Zhou J-M (2016c) Activation-Dependent Destruction of a Co-receptor by a Pseudomonas syringae Effector Dampens Plant Immunity. Cell Host Microbe **20**: 504–514

Li L, Li M, Yu L, Zhou Z, Liang X, Liu Z, Cai G, Gao L, Zhang X, Wang Y, et al (2014b) The FLS2-Associated Kinase BIK1 Directly Phosphorylates the NADPH Oxidase RbohD to Control Plant Immunity. Cell Host Microbe **15**: 329–338

Li L, Yu Y, Zhou Z, Zhou JM (2016d) Plant pattern-recognition receptors controlling innate immunity. Sci China Life Sci **59**: 878–888

Li P, Day B (2019) Battlefield cytoskeleton: Turning the tide on plant immunity. Mol Plant-Microbe Interact **32**: 25–34

Li W, Ma M, Feng Y, Li H, Wang Y, Ma Y, Li M, An F, Guo H (2015c) EIN2-Directed Translational Regulation of Ethylene Signaling in Arabidopsis. Cell **163**: 670–683

Liang W, Li C, Liu F, Jiang H, Li S, Sun J, Wu X, Li C (2009) The Arabidopsis homologs of

CCR4-associated factor 1 show mRNA deadenylation activity and play a role in plant defence responses. Cell Res **19**: 307–316

Liang X, Ma M, Zhou Z, Wang J, Yang X, Rao S, Bi G, Li L, Zhang X, Chai J, et al (2018) Ligand-triggered de-repression of Arabidopsis heterotrimeric G proteins coupled to immune receptor kinases. Cell Res **28**: 529–543

Liebrand TWH, van den Berg GCM, Zhang Z, Smit P, Cordewener JHG, America AHP, Sklenar J, Jones AME, Tameling WIL, Robatzek S, et al (2013) Receptor-like kinase SOBIR1/EVR interacts with receptor-like proteins in plant immunity against fungal infection. Proc Natl Acad Sci **110**: 10010–10015

Liebrand TWH, van den Burg HA, Joosten MHAJ (2014) Two for all: Receptor-associated kinases SOBIR1 and BAK1. Trends Plant Sci **19**: 123–132

Lin W, Li B, Lu D, Chen S, Zhu N, He P, Shan L (2014) Tyrosine phosphorylation of protein kinase complex BAK1/BIK1 mediates Arabidopsis innate immunity. Proc Natl Acad Sci **111**: 3632–3637

Lindner H, Müller LM, Boisson-Dernier A, Grossniklaus U (2012) CrRLK1L receptor-like kinases: Not just another brick in the wall. Curr Opin Plant Biol **15**: 659–669

Liu B, Li J, Ao Y, Qu J, Li Z, Su J, Zhang Y, Liu J, Feng D, Qi K, et al (2012a) Lysin Motif-Containing Proteins LYP4 and LYP6 Play Dual Roles in Peptidoglycan and Chitin Perception in Rice Innate Immunity. Plant Cell **24**: 3406–3419

Liu J, Chen X, Liang X, Zhou X, Yang F, Liu J, He SY, Guo Z (2016) Alternative splicing of rice WRKY62 and WRKY76 transcription factor genes in pathogen defense. Plant Physiol **171**: 1427–1442

Liu J, Li J, Shan L (2020) SERKs. Curr Biol **30**: R293–R294

Liu J, Liu B, Chen S, Gong B-Q, Chen L, Zhou Q, Xiong F, Wang M, Feng D, Li J-F, et al (2018) A Tyrosine Phosphorylation Cycle Regulates Fungal Activation of a Plant Receptor Ser/Thr Kinase. Cell Host Microbe **23**: 241-253.e6

Liu T, Liu Z, Song C, Hu Y, Han Z, She J, Fan F, Wang J, Jin C, Chang J, et al (2012b) Chitin-Induced Dimerization Activates a Plant Immune Receptor. Science (80-) **336**: 1160–1164

Liu Y, Maierhofer T, Rybak K, Sklenar J, Breakspear A, Johnston MG, Fliegmann J, Huang S, Roelfsema MRG, Felix G, et al (2019) Anion channel SLAH3 is a regulatory target of chitin receptor-associated kinase PBL27 in microbial stomatal closure. Elife **8**: 1–23

Liu Y, Zhang S (2004) Phosphorylation of 1-Aminocyclopropane-1-Carboxylic Acid Synthase by MPK6, a Stress-Responsive Mitogen-Activated Protein Kinase, Induces Ethylene Biosynthesis in Arabidopsis. Plant Cell **16**: 3386–3399

Liu Z, Wu Y, Yang F, Zhang Y, Chen S, Xie Q, Tian X, Zhou J-M (2013) BIK1 interacts with PEPRs to mediate ethylene-induced immunity. Proc Natl Acad Sci **110**: 6205–6210

Livak KJ, Schmittgen TD (2001) Analysis of Relative Gene Expression Data Using Real-Time Quantitative PCR and the 2−ΔΔCT Method. Methods **25**: 402–408

Lokdarshi A, Conner WC, McClintock C, Li T, Roberts DM (2016) Arabidopsis CML38, a Calcium Sensor That Localizes to Ribonucleoprotein Complexes under Hypoxia Stress. Plant Physiol **170**: 1046–1059

Lolle S, Stevens D, Coaker G (2020) Plant NLR-triggered immunity: from receptor activation to downstream signaling. Curr Opin Immunol **62**: 99–105

van Loon LC, Rep M, Pieterse CMJ (2006) Significance of Inducible Defense-related Proteins in Infected Plants. Annu Rev Phytopathol **44**: 135–162

De Lorenzo G, D'Ovidio R, Cervone F (2001) The Role of Polygalacturonase-Inhibiting Proteins (PGIPS) in Defense Against Pathogenic Fungi. Annu Rev Phytopathol **39**: 313–335

Lorković ZJ, Wieczorek Kirk DA, Lambermon MHL, Filipowicz W (2000) Pre-mRNA splicing in higher plants. Trends Plant Sci **5**: 160–167

Lozano-Durán R, Macho AP, Boutrot F, Segonzac C, Somssich IE, Zipfel C (2013) The transcriptional regulator BZR1 mediates trade-off between plant innate immunity and growth. Elife **2013**: 1–15

Lozano-Durán R, Zipfel C (2015) Trade-off between growth and immunity: Role of brassinosteroids. Trends Plant Sci **20**: 12–19

Lozano-Torres JL, Wilbers RHP, Gawronski P, Boshoven JC, Finkers-Tomczak A, Cordewener JHG, America AHP, Overmars HA, Van 't Klooster JW, Baranowski L, et al (2012) Dual disease resistance mediated by the immune receptor Cf-2 in tomato requires a common virulence target of a fungus and a nematode. Proc Natl Acad Sci **109**: 10119–10124

Lu D, Lin W, Gao X, Wu S, Cheng C, Avila J, Heese A, Devarenne TP, He P, Shan L (2011) Direct Ubiquitination of Pattern Recognition Receptor FLS2 Attenuates Plant Innate Immunity. Science (80-) **332**: 1439–1442

Lu D, Wang T, Persson S, Mueller-Roeber B, Schippers JHM (2014) Transcriptional control of

ROS homeostasis by KUODA1 regulates cell expansion during leaf development. Nat Commun. doi: 10.1038/ncomms4767

Lu D, Wu S, Gao X, Zhang Y, Shan L, He P (2010) A receptor-like cytoplasmic kinase, BIK1, associates with a flagellin receptor complex to initiate plant innate immunity. Proc Natl Acad Sci **107**: 496–501

Lu F, Wang H, Wang S, Jiang W, Shan C, Li B, Yang J, Zhang S, Sun W (2015) Enhancement of innate immune system in monocot rice by transferring the dicotyledonous elongation factor Tu receptor EFR. J Integr Plant Biol **57**: 641–652

Lu X, Tintor N, Mentzel T, Kombrink E, Boller T, Robatzek S, Schulze-Lefert P, Saijo Y (2009) Uncoupling of sustained MAMP receptor signaling from early outputs in an Arabidopsis endoplasmic reticulum glucosidase II allele. Proc Natl Acad Sci **106**: 22522–22527

van der Luit AH, Piatti T, van Doorn A, Musgrave A, Felix G, Boller T, Munnik T (2000) Elicitation of Suspension-Cultured Tomato Cells Triggers the Formation of Phosphatidic Acid and Diacylglycerol Pyrophosphate. Plant Physiol **123**: 1507–1516

Lukowitz W, Gillmor CSS, Scheible W-RR (2000) Positional cloning in Arabidopsis. Why it feels good to have a genome initiative working for you. Plant Physiol **123**: 795–805

Lumbreras V, Vilela B, Irar S, Solé M, Capellades M, Valls M, Coca M, Pagès M (2010) MAPK phosphatase MKP2 mediates disease responses in Arabidopsis and functionally interacts with MPK3 and MPK6. Plant J **63**: 1017–1030

Luna E, Pastor V, Robert J, Flors V, Mauch-Mani B, Ton J (2011) Callose deposition: A multifaceted plant defense response. Mol Plant-Microbe Interact **24**: 183–193

Ma C, Liu Y, Bai B, Han Z, Tang J, Zhang H, Yaghmaiean H, Zhang Y, Chai J (2017) Structural basis for BIR1-mediated negative regulation of plant immunity. Cell Res **27**: 1521–1524

Ma W (2014) From pathogen recognition to plant immunity: BIK1 crosses the divide. Cell Host Microbe **15**: 253–254

Ma W, Smigel A, Tsai YC, Braam J, Berkowitz GA (2008) Innate immunity signaling: Cytosolic Ca2+ elevation is linked to downstream nitric oxide generation through the action of calmodulin or a calmodulin-like protein. Plant Physiol **148**: 818–828

Ma X, Xu G, He P, Shan L (2016) SERKing Coreceptors for Receptors. Trends Plant Sci **21**: 1017–1033

Ma Y, Walker RK, Zhao Y, Berkowitz GA (2012) Linking ligand perception by PEPR pattern

recognition receptors to cytosolic Ca2+ elevation and downstream immune signaling in plants. Proc Natl Acad Sci **109**: 19852–19857

Ma Y, Zhao Y, Walker RK, Berkowitz GA (2013) Molecular Steps in the Immune Signaling Pathway Evoked by Plant Elicitor Peptides: Ca 2+ -Dependent Protein Kinases, Nitric Oxide, and Reactive Oxygen Species Are Downstream from the Early Ca 2+ Signal. Plant Physiol **163**: 1459–1471

Machado JPB, Brustolini OJB, Mendes GC, Santos AA, Fontes EPB (2015) NIK1, a host factor specialized in antiviral defense or a novel general regulator of plant immunity? BioEssays **37**: 1236–1242

Macho AP, Boutrot F, Rathjen JP, Zipfel C (2012) ASPARTATE OXIDASE plays an important role in Arabidopsis stomatal immunity. Plant Physiol **159**: 1845–1856

Macho AP, Lozano-Durán R, Zipfel C (2015) Importance of tyrosine phosphorylation in receptor kinase complexes. Trends Plant Sci **20**: 269–272

Macho AP, Schwessinger B, Ntoukakis V, Brutus A, Segonzac C, Roy S, Kadota Y, Oh M-H, Sklenar J, Derbyshire P, et al (2014) A Bacterial Tyrosine Phosphatase Inhibits Plant Pattern Recognition Receptor Activation. Science (80-) **343**: 1509–1512

Maekawa T, Kufer TA, Schulze-Lefert P (2011) NLR functions in plant and animal immune systems: so far and yet so close. Nat Immunol **12**: 817–826

Majhi BB, Sreeramulu S, Sessa G (2019) BRASSINOSTEROID-SIGNALING KINASE5 Associates with Immune Receptors and Is Required for Immune Responses. Plant Physiol **180**: 1166–1184

Malinovsky FG, Batoux M, Schwessinger B, Youn JH, Stransfeld L, Win J, Kim SK, Zipfel C (2014) Antagonistic regulation of growth and immunity by the arabidopsis basic helix-loop-helix transcription factor HOMOLOG OF BRASSINOSTEROID ENHANCED EXPRESSION2 INTERACTING WITH INCREASED LEAF INCLINATION1 BINDING bHLH1. Plant Physiol **164**: 1443–1455

Man J, Gallagher JP, Bartlett M (2020) Structural evolution drives diversification of the large LRR-RLK gene family. New Phytol. doi: 10.1111/nph.16455

Mang H, Feng B, Hu Z, Boisson-Dernier A, Franck CM, Meng X, Huang Y, Zhou J, Xu G, Wang T, et al (2017) Differential Regulation of Two-Tiered Plant Immunity and Sexual Reproduction by ANXUR Receptor-Like Kinases. Plant Cell **29**: 3140–3156

Mao G, Meng X, Liu Y, Zheng Z, Chen Z, Zhang S (2011) Phosphorylation of a WRKY

transcription factor by two pathogen-responsive MAPKs drives phytoalexin biosynthesis in Arabidopsis. Plant Cell **23**: 1639–1653

Marondedze C, Thomas L, Serrano NL, Lilley KS, Gehring C (2016) The RNA-binding protein repertoire of Arabidopsis thaliana. Sci Rep **6**: 1–13

Marquez Y, Brown JWS, Simpson C, Barta A, Kalyna M (2012) Transcriptome survey reveals increased complexity of the alternative splicing landscape in Arabidopsis. Genome Res **22**: 1184–1195

Martínez de Alba AE, Moreno AB, Gabriel M, Mallory AC, Christ A, Bounon R, Balzergue S, Aubourg S, Gautheret D, Crespi MD, et al (2015) In plants, decapping prevents RDR6-dependent production of small interfering RNAs from endogenous mRNAs. Nucleic Acids Res **43**: 2902–2913

Masachis S, Segorbe D, Turrà D, Leon-Ruiz M, Fürst U, El Ghalid M, Leonard G, López-Berges MS, Richards TA, Felix G, et al (2016) A fungal pathogen secretes plant alkalinizing peptides to increase infection. Nat Microbiol. doi: 10.1038/nmicrobiol.2016.43

Matsubayashi Y, Ogawa M, Kihara H, Niwa M, Sakagami Y (2006) Disruption and overexpression of Arabidopsis phytosulfokine receptor gene affects cellular longevity and potential for growth. Plant Physiol **142**: 45–53

Matsubayashi Y, Sakagami Y (1996) Phytosulfokine, sulfated peptides that induce the proliferation of single mesophyll cells of Asparagus officinalis L. Proc Natl Acad Sci **93**: 7623–7627

Mbengue M, Bourdais G, Gervasi F, Beck M, Zhou J, Spallek T, Bartels S, Boller T, Ueda T, Kuhn H, et al (2016) Clathrin-dependent endocytosis is required for immunity mediated by pattern recognition receptor kinases. Proc Natl Acad Sci **113**: 11034–11039

McGurl B, Pearce G, Orozco-Cardenas M, Ryan C (1992) Structure, expression, and antisense inhibition of the systemin precursor gene. Science (80-) **255**: 1570–1573

Meena MK, Prajapati R, Krishna D, Divakaran K, Pandey Y, Reichelt M, Mathew MK, Boland W, Mithöfer A, Vadassery J (2019) The Ca2+ channel CNGC19 regulates arabidopsis defense against spodoptera herbivory. Plant Cell **31**: 1539–1562

Mejias J, Truong NM, Abad P, Favery B, Quentin M (2019) Plant Proteins and Processes Targeted by Parasitic Nematode Effectors. Front Plant Sci. doi: 10.3389/fpls.2019.00970

Melotto M, Underwood W, Koczan J, Nomura K, He SY (2006) Plant stomata function in innate immunity against bacterial invasion. Cell **126**: 969–80

Meng X, Chen X, Mang H, Liu C, Yu X, Gao X, Torii KU, He P, Shan L (2015) Differential Function of Arabidopsis SERK Family Receptor-like Kinases in Stomatal Patterning. Curr Biol **25**: 2361–2372

Meng X, Xu J, He Y, Yang K-Y, Mordorski B, Liu Y, Zhang S (2013) Phosphorylation of an ERF Transcription Factor by Arabidopsis MPK3/MPK6 Regulates Plant Defense Gene Induction and Fungal Resistance. Plant Cell **25**: 1126–1142

Meng X, Zhang S (2013) MAPK Cascades in Plant Disease Resistance Signaling. Annu Rev Phytopathol **51**: 245–266

Meng X, Zhou J, Tang J, Li B, de Oliveira MV V., Chai J, He P, Shan L (2016) Ligand-Induced Receptor-like Kinase Complex Regulates Floral Organ Abscission in Arabidopsis. Cell Rep **14**: 1330–1338

Merchante C, Brumos J, Yun J, Hu Q, Spencer KR, Enríquez P, Binder BM, Heber S, Stepanova AN, Alonso JM (2015) Gene-Specific Translation Regulation Mediated by the Hormone-Signaling Molecule EIN2. Cell **163**: 684–697

Mermigka G, Amprazi M, Mentzelopoulou A, Amartolou A, Sarris PF (2020) Plant and Animal Innate Immunity Complexes: Fighting Different Enemies with Similar Weapons. Trends Plant Sci **25**: 80–91

Meteignier L-V, El Oirdi M, Cohen M, Barff T, Matteau D, Lucier J-F, Rodrigue S, Jacques P-E, Yoshioka K, Moffett P (2017) Translatome analysis of an NB-LRR immune response identifies important contributors to plant immunity in Arabidopsis. J Exp Bot **68**: 2333–2344

Mhamdi A, Van Breusegem F (2018) Reactive oxygen species in plant development. Development **145**: dev164376

Miedes E, Vanholme R, Boerjan W, Molina A (2014) The role of the secondary cell wall in plant resistance to pathogens. Front Plant Sci **5**: 1–13

Miklis M, Consonni C, Bhat RA, Lipka V, Schulze-Lefert P, Panstruga R (2007) Barley MLO modulates actin-dependent and actin-independent antifungal defense pathways at the cell periphery. Plant Physiol **144**: 1132–1143

Millet YA, Danna CH, Clay NK, Songnuan W, Simon MD, Werck-Reichhart D, Ausubel FM (2010) Innate immune responses activated in Arabidopsis roots by microbe-associated molecular patterns. Plant Cell **22**: 973–990

Mishina TE, Zeier J (2007) Pathogen-associated molecular pattern recognition rather than

development of tissue necrosis contributes to bacterial induction of systemic acquired resistance in Arabidopsis. Plant J **50**: 500–513

Mithoe SC, Ludwig C, Pel MJ, Cucinotta M, Casartelli A, Mbengue M, Sklenar J, Derbyshire P, Robatzek S, Pieterse CMJ, et al (2016) Attenuation of pattern recognition receptor signaling is mediated by a MAP kinase kinase kinase. EMBO Rep **17**: 441–454

Mithoe SC, Menke FLH (2018) Regulation of pattern recognition receptor signalling by phosphorylation and ubiquitination. Curr Opin Plant Biol **45**: 162–170

Miya A, Albert P, Shinya T, Desaki Y, Ichimura K, Shirasu K, Narusaka Y, Kawakami N, Kaku H, Shibuya N (2007) CERK1, a LysM receptor kinase, is essential for chitin elicitor signaling in Arabidopsis. Proc Natl Acad Sci **104**: 19613–19618

Monaghan J, Matschi S, Romeis T, Zipfel C (2015) The calcium-dependent protein kinase CPK28 negatively regulates the BIK1-mediated PAMP-induced calcium burst. Plant Signal Behav **10**: e1018497

Monaghan J, Matschi S, Shorinola O, Rovenich H, Matei A, Segonzac C, Malinovsky FG, Rathjen JP, MacLean D, Romeis T, et al (2014) The Calcium-Dependent Protein Kinase CPK28 Buffers Plant Immunity and Regulates BIK1 Turnover. Cell Host Microbe **16**: 605–615

Moore JW, Loake GJ, Spoel SH (2011) Transcription dynamics in plant immunity. Plant Cell **23**: 2809–2820

Moreno AB, Martínez de Alba AE, Bardou F, Crespi MD, Vaucheret H, Maizel A, Mallory AC (2013) Cytoplasmic and nuclear quality control and turnover of single-stranded RNA modulate post-transcriptional gene silencing in plants. Nucleic Acids Res **41**: 4699–4708

Morita-Yamamuro C, Tsutsui T, Sato M, Yoshioka H, Tamaoki M, Ogawa D, Matsuura H, Yoshihara T, Ikeda A, Uyeda I, et al (2005) The Arabidopsis gene CAD1 controls programmed cell death in the plant immune system and encodes a protein containing a MACPF domain. Plant Cell Physiol **46**: 902–912

Mosher S, Seybold H, Rodriguez P, Stahl M, Davies KA, Dayaratne S, Morillo SA, Wierzba M, Favery B, Keller H, et al (2013) The tyrosine-sulfated peptide receptors PSKR1 and PSY1R modify the immunity of Arabidopsis to biotrophic and necrotrophic pathogens in an antagonistic manner. Plant J **73**: 469–482

Moussu S, Santiago J (2019) Structural biology of cell surface receptor–ligand interactions. Curr Opin Plant Biol **52**: 38–45

Müller DB, Vogel C, Bai Y, Vorholt JA (2016) The Plant Microbiota: Systems-Level Insights and Perspectives. Annu Rev Genet **50**: 211–234

Mustroph A, Juntawong P, Bailey-Serres J (2009) Isolation of Plant Polysomal mRNA by Differential Centrifugation and Ribosome Immunopurification Methods. Plant Syst. Biol. pp 109–126

Nafisi M, Goregaoker S, Botanga CJ, Glawischnig E, Olsen CE, Halkier BA, Glazebrook J (2007) Arabidopsis cytochrome P450 monooxygenase 71A13 catalyzes the conversion of indole-3-acetaldoxime in camalexin synthesis. Plant Cell **19**: 2039–2052

Nam KH, Li J (2002) BRI1/BAK1, a receptor kinase pair mediating brassinosteroid signaling. Cell **110**: 203–212

Navarro L, Dunoyer P, Jay F, Arnold B, Dharmasiri N, Estelle M, Voinnet O, Jones JDG (2006) A Plant miRNA Contributes to Antibacterial Resistance by Repressing Auxin Signaling. Science (80-) **312**: 436–439

Navarro L, Zipfel C, Rowland O, Keller I, Robatzek S, Boller T, Jones JDG (2004) The Transcriptional Innate Immune Response to flg22..pdf. Plant Physiol **135**: 1113–1128

Navazio L, Bewell MA, Siddiqua A, Dickinson GD, Galione A, Sanders D (2000) Calcium release from the endoplasmic reticulum of higher plants elicited by the NADP metabolite nicotinic acid adenine dinucleotide phosphate. Proc Natl Acad Sci **97**: 8693–8698

Neff MM, Turk E, Kalishman M (2002) Web-based primer design for single nucleotide polymorphism analysis. Trends Genet **18**: 613–615

Nekrasov V, Li J, Batoux M, Roux M, Chu ZH, Lacombe S, Rougon A, Bittel P, Kiss-Papp M, Chinchilla D, et al (2009) Control of the pattern-recognition receptor EFR by an ER protein complex in plant immunity. EMBO J **28**: 3428–3438

Neuser J, Metzen CC, Dreyer BH, Feulner C, van Dongen JT, Schmidt RR, Schippers JHM (2019) HBI1 Mediates the Trade-off between Growth and Immunity through Its Impact on Apoplastic ROS Homeostasis. Cell Rep **28**: 1670-1678.e3

Ng CKY, Carr K, McAinsh MR, Powell B, Hetherington AM (2001) Drought-induced guard cell signal transduction involves sphingosine-1-phosphate. Nature **410**: 596–599

Ngou BPM, Ahn H, Ding P, Jones JDG (2020) Mutual Potentiation of Plant Immunity by Cell-surface and Intracellular Receptors. bioRxiv 1–29

Nguyen CC, Nakaminami K, Matsui A, Kobayashi S, Kurihara Y, Toyooka K, Tanaka M, Seki

M (2016) Oligouridylate binding protein 1b plays an integral role in plant heat stress tolerance. Front Plant Sci **7**: 1–9

Nguyen CC, Nakaminami K, Matsui A, Watanabe S, Kanno Y, Seo M, Seki M (2017) Overexpression of oligouridylate binding protein 1b results in ABA hypersensitivity. Plant Signal Behav **12**: e1282591

Nicaise V, Gallois J-L, Chafiai F, Allen LM, Schurdi-Levraud V, Browning KS, Candresse T, Caranta C, Le Gall O, German-Retana S (2007) Coordinated and selective recruitment of eIF4E and eIF4G factors for potyvirus infection in Arabidopsis thaliana. FEBS Lett **581**: 1041–1046

Nicaise V, Joe A, Jeong BR, Korneli C, Boutrot F, Westedt I, Staiger D, Alfano JR, Zipfel C (2013) Pseudomonas HopU1 modulates plant immune receptor levels by blocking the interaction of their mRNAs with GRP7. EMBO J **32**: 701–712

Nishimura T, Padamsi Z, Fakim H, Milette S, Dunham WH, Gingras AC, Fabian MR (2015) The eIF4E-Binding Protein 4E-T Is a Component of the mRNA Decay Machinery that Bridges the 5' and 3' Termini of Target mRNAs. Cell Rep **11**: 1425–1436

Nissen KS, Willats WGT, Malinovsky FG (2016) Understanding CrRLK1L Function: Cell Walls and Growth Control. Trends Plant Sci **21**: 516–527

Noman A, Liu Z, Aqeel M, Zainab M, Khan MI, Hussain A, Ashraf MF, Li X, Weng Y, He S (2017) Basic leucine zipper domain transcription factors: the vanguards in plant immunity. Biotechnol Lett **39**: 1779–1791

Nühse TS, Bottrill AR, Jones AME, Peck SC (2007) Quantitative phosphoproteomic analysis of plasma membrane proteins reveals regulatory mechanisms of plant innate immune responses. Plant J **51**: 931–940

Nühse TS, Peck SC, Hirt H, Boller T (2000) Microbial elicitors induce activation and dual phosphorylation of the Arabidopsis thaliana MAPK 6. J Biol Chem **275**: 7521–7526

Nuruzzaman M, Sharoni AM, Kikuchi S (2013) Roles of NAC transcription factors in the regulation of biotic and abiotic stress responses in plants. Front Microbiol **4**: 1–16

Obayashi T, Aoki Y, Tadaka S, Kagaya Y, Kinoshita K (2018) ATTED-II in 2018: A Plant Coexpression Database Based on Investigation of the Statistical Property of the Mutual Rank Index. Plant Cell Physiol **59**: e3–e3

Oh M-H, Wang X, Kota U, Goshe MB, Clouse SD, Huber SC (2009) Tyrosine phosphorylation of

the BRI1 receptor kinase emerges as a component of brassinosteroid signaling in Arabidopsis. Proc Natl Acad Sci **106**: 658–663

Okamura Y, Obayashi T, Kinoshita K (2015) Comparison of gene coexpression profiles and construction of conserved gene networks to find functional modules. PLoS One **10**: 1–17

Opalski KS, Schultheiss H, Kogel KH, Hückelhoven R (2005) The receptor-like MLO protein and the RAC/ROP family G-protein RACB modulate actin reorganization in barley attacked by the biotrophic powdery mildew fungus Blumeria graminis f.sp. hordei. Plant J **41**: 291–303

Ossowski S, Schneeberger K, Lucas-Lledó JI, Warthmann N, Clark RM, Shaw RG, Weigel D, Lynch M (2010) The rate and molecular spectrum of spontaneous mutations in arabidopsis thaliana. Science (80-) **327**: 92–94

Ozgur S, Chekulaeva M, Stoecklin G (2010) Human PAT1B connects deadenylation with mRNA decapping and controls the assembly of processing bodies. Mol Cell Biol **30**: 4308–4323

Păcurar DI, Păcurar ML, Street N, Bussell JD, Pop TI, Gutierrez L, Bellini C (2012) A collection of INDEL markers for map-based cloning in seven Arabidopsis accessions. J Exp Bot **63**: 2491–2501

Page DR, Grossniklaus U (2002) the Art and Design of Genetic Screens: Arabidopsis Thaliana. Nat Rev Genet **3**: 124–136

Park C-J, Peng Y, Chen X, Dardick C, Ruan D, Bart R, Canlas PE, Ronald PC (2008) Rice XB15, a Protein Phosphatase 2C, Negatively Regulates Cell Death and XA21-Mediated Innate Immunity. PLoS Biol **6**: e231

Passardi F, Penel C, Dunand C (2004) Performing the paradoxical: How plant peroxidases modify the cell wall. Trends Plant Sci **9**: 534–540

Patrick RM, Browning KS (2012) The eIF4F and eIFiso4F Complexes of Plants: An Evolutionary Perspective. Comp Funct Genomics **2012**: 287814

Patrick RM, Lee JCH, Teetsel JRJ, Yang S, Choy GS, Browning KS (2018) Discovery and characterization of conserved binding of eIF4E 1 (CBE1), a eukaryotic translation initiation factor 4E–binding plant protein. J Biol Chem **293**: 17240–17247

Pearce G, Moura DS, Stratmann J, Ryan CA (2001) RALF, a 5-kDa ubiquitous polypeptide in plants, arrests root growth and development. Proc Natl Acad Sci **98**: 12843–12847

Pearce G, Strydom D, Johnson S, Ryan CA (1991) A polypeptide from tomato leaves induces wound-inducible proteinase inhibitor proteins. Science (80-) **253**: 895–7

Pearce G, Yamaguchi Y, Munske G, Ryan CA (2010) Structure-activity studies of RALF, Rapid Alkalinization Factor, reveal an essential - YISY - motif. Peptides **31**: 1973–1977

Pecher P, Eschen-Lippold L, Herklotz S, Kuhle K, Naumann K, Bethke G, Uhrig J, Weyhe M, Scheel D, Lee J (2014) The Arabidopsis thaliana mitogen-activated protein kinases MPK3 and MPK6 target a subclass of 'VQ-motif'-containing proteins to regulate immune responses. New Phytol **203**: 592–606

Pelletier J, Sonenberg N (2019) The Organizing Principles of Eukaryotic Ribosome Recruitment. Annu Rev Biochem **88**: 307–335

Penninckx IAMA, Thomma BPHJ, Buchala A, Métraux JP, Broekaert WF (1998) Concomitant activation of jasmonate and ethylene response pathways is required for induction of a plant defensin gene in Arabidopsis. Plant Cell **10**: 2103–2113

Perea-Resa C, Hernández-Verdeja T, López-Cobollo R, Castellano M del M, Salinas J (2012) LSM Proteins Provide Accurate Splicing and Decay of Selected Transcripts to Ensure Normal Arabidopsis Development. Plant Cell **24**: 4930–4947

Perraki A, DeFalco TA, Derbyshire P, Avila J, Séré D, Sklenar J, Qi X, Stransfeld L, Schwessinger B, Kadota Y, et al (2018) Phosphocode-dependent functional dichotomy of a common co-receptor in plant signalling. Nature. doi: 10.1038/s41586-018-0471-x

Pestova T V., Hellen CUT (2000) The structure and function of initiation factors in eukaryotic protein synthesis. Cell Mol Life Sci **57**: 651–674

Peter D, Igreja C, Weber R, Wohlbold L, Weiler C, Ebertsch L, Weichenrieder O, Izaurralde E (2015) Molecular Architecture of 4E-BP Translational Inhibitors Bound to eIF4E. Mol Cell **57**: 1074–1087

Petutschnig EK, Jones AME, Serazetdinova L, Lipka U, Lipka V (2010) The Lysin Motif Receptor-like Kinase (LysM-RLK) CERK1 is a major chitin-binding protein in Arabidopsis thaliana and subject to chitin-induced phosphorylation. J Biol Chem **285**: 28902–28911

Pfeilmeier S, George J, Morel A, Roy S, Smoker M, Stransfeld L, Downie JA, Peeters N, Malone JG, Zipfel C (2019) Expression of the Arabidopsis thaliana immune receptor EFR in Medicago truncatula reduces infection by a root pathogenic bacterium, but not nitrogen-fixing rhizobial symbiosis. Plant Biotechnol J **17**: 569–579

Pfund C, Tans-Kersten J, Dunning FM, Alonso JM, Ecker JR, Allen C, Bent AF (2004) Flagellin is not a major defense elicitor in Ralstonia solanacearum cells or extracts applied to Arabidopsis

thaliana. Mol Plant-Microbe Interact **17**: 696–706

Pham AQ, Cho S-H, Nguyen CT, Stacey G (2020) Arabidopsis Lectin Receptor Kinase P2K2 Is a Second Plant Receptor for Extracellular ATP and Contributes to Innate Immunity. Plant Physiol **183**: 1364–1375

Phukan UJ, Jeena GS, Shukla RK (2016) WRKY transcription factors: Molecular regulation and stress responses in plants. Front Plant Sci **7**: 1–14

Pieterse CMJ, Van der Does D, Zamioudis C, Leon-Reyes A, Van Wees SCM (2012) Hormonal Modulation of Plant Immunity. Annu Rev Cell Dev Biol **28**: 489–521

Pieterse CMJJ, Zamioudis C, Berendsen RL, Weller DM, Van Wees SCMM, Bakker PAHMHM (2014) Induced Systemic Resistance by Beneficial Microbes. Annu Rev Phytopathol **52**: 347–375

Piques M, Schulze WX, Höhne M, Usadel B, Gibon Y, Rohwer J, Stitt M (2009) Ribosome and transcript copy numbers, polysome occupancy and enzyme dynamics in Arabidopsis. Mol Syst Biol **5**: 314

Postma J, Liebrand TWH, Bi G, Evrard A, Bye RR, Mbengue M, Kuhn H, Joosten MHAJ, Robatzek S (2016) Avr4 promotes Cf-4 receptor-like protein association with the BAK1/SERK3 receptor-like kinase to initiate receptor endocytosis and plant immunity. New Phytol **210**: 627–642

Prévôt D, Darlix JL, Ohlmann T (2003) Conducting the initiation of protein synthesis: The role of eIF4G. Biol Cell **95**: 141–156

Protter DSW, Parker R (2016) Principles and Properties of Stress Granules. Trends Cell Biol **26**: 668–679

Pyronnet S, Sonenberg N (2001) Cell-cycle-dependent translational control. Curr Opin Genet Dev **11**: 13–18

Qi J, Wang J, Gong Z, Zhou J-M (2017) Apoplastic ROS signaling in plant immunity. Curr Opin Plant Biol **38**: 92–100

Qiu J-L, Fiil BK, Petersen K, Nielsen HB, Botanga CJ, Thorgrimsen S, Palma K, Suarez-Rodriguez MC, Sandbech-Clausen S, Lichota J, et al (2008) Arabidopsis MAP kinase 4 regulates gene expression through transcription factor release in the nucleus. EMBO J **27**: 2214–21

Qu L, Qin G (2014) Generation and Identification of Arabidopsis EMS Mutants. Arab. Protoc. Methods Mol. Biol. pp 225–239

Qutob D, Kemmerling B, Brunner F, Küfner I, Engelhardt S, Gust AA, Luberacki B, Seitz HU, Stahl D, Rauhut T, et al (2006) Phytotoxicity and innate immune responses induced by Nep1-like proteins. Plant Cell **18**: 3721–3744

Rajniak J, Barco B, Clay NK, Sattely ES (2015) A new cyanogenic metabolite in Arabidopsis required for inducible pathogen defence. Nature **525**: 375–379

Rallapalli G, Kemen EM, Robert-Seilaniantz A, Segonzac C, Etherington GJ, Sohn KH, MacLean D, Jones JDG (2014) EXPRSS: An Illumina based high-throughput expression-profiling method to reveal transcriptional dynamics. BMC Genomics **15**: 1–18

Ramanathan A, Robb GB, Chan SH (2016) mRNA capping: Biological functions and applications. Nucleic Acids Res **44**: 7511–7526

Ramos HC, Rumbo M, Sirard JC (2004) Bacterial flagellins: Mediators of pathogenicity and host immune responses in mucosa. Trends Microbiol **12**: 509–517

Ranf S, Eschen-Lippold L, Fröhlich K, Westphal L, Scheel D, Lee J (2014) Microbe-associated molecular pattern-induced calcium signaling requires the receptor-like cytoplasmic kinases, PBL1 and BIK1. BMC Plant Biol **14**: 374

Ranf S, Eschen-Lippold L, Pecher P, Lee J, Scheel D (2011) Interplay between calcium signalling and early signalling elements during defence responses to microbe- or damage-associated molecular patterns. Plant J **68**: 100–113

Rao S, Zhou Z, Miao P, Bi G, Hu M, Wu Y, Feng F, Zhang X, Zhou J-M (2018) Roles of receptor-like cytoplasmic kinase VII members in pattern-triggered immune signaling. Plant Physiol **177**: 1679–1690

Räsch F, Weber R, Izaurralde E, Igreja C (2020) 4E-T-bound mRNAs are stored in a silenced and deadenylated form. Genes Dev **34**: 847–860

Rasmussen MW, Roux M, Petersen M, Mundy J (2012) MAP kinase cascades in arabidopsis innate immunity. Front Plant Sci **3**: 169

Raught B, Gingras AC (1999) eIF4E activity is regulated at multiple levels. Int J Biochem Cell Biol **31**: 43–57

Rayapuram N, Bigeard J, Alhoraibi H, Bonhomme L, Hesse A-M, Vinh J, Hirt H, Pflieger D (2018) Quantitative Phosphoproteomic Analysis Reveals Shared and Specific Targets of Arabidopsis Mitogen-Activated Protein Kinases (MAPKs) MPK3, MPK4, and MPK6. Mol Cell Proteomics **17**: 61–80

Rayson S, Arciga-Reyes L, Wootton L, De Torres Zabala M, Truman W, Graham N, Grant M, Davies B (2012) A Role for Nonsense-Mediated mRNA Decay in Plants: Pathogen Responses Are Induced in Arabidopsis thaliana NMD Mutants. PLoS One **7**: e31917

Reichel M, Liao Y, Rettel M, Ragan C, Evers M, Alleaume A-M, Horos R, Hentze MW, Preiss T, Millar AA (2016) In Planta Determination of the mRNA-Binding Proteome of Arabidopsis Etiolated Seedlings. Plant Cell **28**: 2435–2452

Reina-Pinto JJ, Yephremov A (2009) Surface lipids and plant defenses. Plant Physiol Biochem **47**: 540–549

Reynoso MA, Juntawong P, Lancia M, Blanco FA, Bailey-Serres J, Zanetti ME (2015) Translating Ribosome Affinity Purification (TRAP) Followed by RNA Sequencing Technology (TRAP-SEQ) for Quantitative Assessment of Plant Translatomes. *In* JM Alonso, AN Stepanova, eds, Plant Funct. Genomics Methods Protoc. Second Ed. Springer New York, New York, NY, pp 185–207

Ricci P, Bonnet P, Huet J-C, Sallantin M, Beauvais-Canté F, Bruneteau M, Billard V, Michel G, Pernollet J-C (1989) Structure and activity of proteins from pathogenic fungi Phytophthora eliciting necrosis and acquired resistance in tobacco. Eur J Biochem **183**: 555–563

Rieder B, Neuhaus HE (2011) Identification of an Arabidopsis plasma memrane-located ATP transporter important for anther development. Plant Cell **23**: 1932–1944

Riehs-Kearnan N, Gloggnitzer J, Dekrout B, Jonak C, Riha K (2012) Aberrant growth and lethality of Arabidopsis deficient in nonsense-mediated RNA decay factors is caused by autoimmune-like response. Nucleic Acids Res **40**: 5615–5624

Rietz S, Stamm A, Malonek S, Wagner S, Becker D, Medina-Escobar N, Corina Vlot A, Feys BJ, Niefind K, Parker JE (2011) Different roles of Enhanced Disease Susceptibility1 (EDS1) bound to and dissociated from Phytoalexin Deficient4 (PAD4) in Arabidopsis immunity. New Phytol **191**: 107–119

Rigo R, Bazin J, Crespi M, Charon C (2019) Alternative Splicing in the Regulation of Plant–Microbe Interactions. Plant Cell Physiol **60**: 1906–1916

Robatzek S, Chinchilla D, Boller T (2006) Ligand-induced endocytosis of the pattern recognition receptor FLS2 in Arabidopsis service Ligand-induced endocytosis of the pattern recognition receptor FLS2 in Arabidopsis. Genes Dev 537–542

Robert-Seilaniantz A, Grant M, Jones JDG (2011) Hormone Crosstalk in Plant Disease and Defense: More Than Just JASMONATE-SALICYLATE Antagonism. Annu Rev Phytopathol **49**:

317–343

Ron M, Avni A (2004) The Receptor for the Fungal Elicitor Ethylene-Inducing Xylanase Is a Member of a Resistance-Like Gene Family in Tomato. Plant Cell **16**: 1604–1615

Rooney HCE, Van&#039 JW, t Klooster, van der Hoorn RAL, Joosten MHAJ, Jones JDG, de Wit PJGM (2005) Cladosporium Avr2 Inhibits Tomato Rcr3 Protease Required for Cf-2-Dependent Disease Resistance. Science (80-) **308**: 1783 LP – 1786

Le Roux C, Huet G, Jauneau A, Camborde L, Trémousaygue D, Kraut A, Zhou B, Levaillant M, Adachi H, Yoshioka H, et al (2015) A receptor pair with an integrated decoy converts pathogen disabling of transcription factors to immunity. Cell **161**: 1074–1088

Roux M, Schwessinger B, Albrecht C, Chinchilla D, Jones A, Holton N, Malinovsky FG, Tör M, de Vries S, Zipfel C (2011) The Arabidopsis Leucine-Rich Repeat Receptor–Like Kinases BAK1/SERK3 and BKK1/SERK4 Are Required for Innate Immunity to Hemibiotrophic and Biotrophic Pathogens. Plant Cell **23**: 2440–2455

Roux ME, Rasmussen MW, Palma K, Lolle S, Regué ÀM, Bethke G, Glazebrook J, Zhang W, Sieburth L, Larsen MR, et al (2015) The mRNA decay factor PAT1 functions in a pathway including MAP kinase 4 and immune receptor SUMM2. EMBO J **34**: 593–608

Saijo Y, Tintor N, Lu X, Rauf P, Pajerowska-Mukhtar K, Häweker H, Dong X, Robatzek S, Schulze-Lefert P (2009) Receptor quality control in the endoplasmic reticulum for plant innate immunity. EMBO J **28**: 3439–3449

Sakamoto T, Deguchi M, Brustolini OJB, Santos AA, Silva FF, Fontes EPB (2012) The tomato RLK superfamily: Phylogeny and functional predictions about the role of the LRRII-RLK subfamily in antiviral defense. BMC Plant Biol. doi: 10.1186/1471-2229-12-229

Sanabria NM, Dubery IA (2016) Alternative splicing of the receptor-like kinase Nt-Sd-RLK in tobacco cells responding to lipopolysaccharides: suggestive of a role in pathogen surveillance and perception? FEBS Lett **590**: 3628–3638

Santiago J, Brandt B, Wildhagen M, Hohmann U, Hothorn LA, Butenko MA, Hothorn M (2016) Mechanistic insight into a peptide hormone signaling complex mediating floral organ abscission. Elife **5**: 1–19

Sarris PF, Duxbury Z, Huh SU, Ma Y, Segonzac C, Sklenar J, Derbyshire P, Cevik V, Rallapalli G, Saucet SB, et al (2015) A plant immune receptor detects pathogen effectors that target WRKY transcription factors. Cell **161**: 1089–1100

Scarpin MR, Sigaut L, Temprana SG, Boccaccio GL, Pietrasanta LI, Muschietti JP (2017) Two Arabidopsis late pollen transcripts are detected in cytoplasmic granules. Plant Direct. doi: 10.1002/pld3.12

Schäffer C, Messner P (2017) Emerging facets of prokaryotic glycosylation. FEMS Microbiol Rev **41**: 49–91

Schallus T, Jaeckh C, Fehér K, Palma AS, Liu Y, Simpson JC, Mackeen M, Stier G, Gibson TJ, Feizi T, et al (2008) Malectin: A Novel Carbohydrate-binding Protein of the Endoplasmic Reticulum and a Candidate Player in the Early Steps of Protein N -Glycosylation. Mol Biol Cell **19**: 3404–3414

Scheler C, Durner J, Astier J (2013) Nitric oxide and reactive oxygen species in plant biotic interactions. Curr Opin Plant Biol **16**: 534–539

SCHENKE D, BÖTTCHER C, SCHEEL D (2011) Crosstalk between abiotic ultraviolet-B stress and biotic (flg22) stress signalling in Arabidopsis prevents flavonol accumulation in favor of pathogen defence compound production. Plant Cell Environ **34**: 1849–1864

Schilmiller AL, Howe GA (2005) Systemic signaling in the wound response. Curr Opin Plant Biol **8**: 369–377

Schlaeppi K, Abou-Mansour E, Buchala A, Mauch F (2010) Disease resistance of Arabidopsis to Phytophthora brassicae is established by the sequential action of indole glucosinolates and camalexin. Plant J **62**: 840–851

Schlaeppi K, Bulgarelli D (2015) The plant microbiome at work. Mol Plant-Microbe Interact **28**: 212–217

Schmelz EA, Huffaker A, Sims JW, Christensen SA, Lu X, Okada K, Peters RJ (2014) Biosynthesis, elicitation and roles of monocot terpenoid phytoalexins. Plant J **79**: 659–678

Schmidt R, Kunkowska AB, Schippers JHM (2016) Role of reactive oxygen species during cell expansion in leaves. Plant Physiol **172**: 2098–2106

Schneeberger K (2014) Using next-generation sequencing to isolate mutant genes from forward genetic screens. Nat Rev Genet **15**: 662–76

Schneeberger K, Ossowski S, Lanz C, Juul T, Høgh A, Petersen AH, Nielsen KL, Jørgensen J-E, Weigel D, Andersen SU (2009) SHOREmap: simultaneous mapping and mutation identification by deep sequencing. Nat Methods **6**: 550–551

Schneeberger K, Weigel D (2011) Fast-forward genetics enabled by new sequencing technologies.

Trends Plant Sci **16**: 282–288

Schoonbeek H, Wang H, Stefanato FL, Craze M, Bowden S, Wallington E, Zipfel C, Ridout CJ (2015) Arabidopsis EF-Tu receptor enhances bacterial disease resistance in transgenic wheat. New Phytol **206**: 606–13

Schöpfer P (1996) Hydrogen peroxide-mediated cell-wall stiffening in vitro in maize coleoptiles. Planta **199**: 43–49

Schreiber L (2010) Transport barriers made of cutin, suberin and associated waxes. Trends Plant Sci **15**: 546–553

Schulze B, Mentzel T, Jehle AK, Mueller K, Beeler S, Boller T, Felix G, Chinchilla D (2010) Rapid heteromerization and phosphorylation of ligand-activated plant transmembrane receptors and their associated kinase BAK1. J Biol Chem **285**: 9444–9451

Schweighofer A, Kazanaviciute V, Scheikl E, Teige M, Doczi R, Hirt H, Schwanninger M, Kant M, Schuurink R, Mauch F, et al (2007) The PP2C-type phosphatase AP2C1, which negatively regulates MPK4 and MPK6, modulates innate immunity, jasmonic acid, and ethylene levels in Arabidopsis. Plant Cell **19**: 2213–2224

Schwessinger B, Bahar O, Thomas N, Holton N, Nekrasov V, Ruan D, Canlas PE, Daudi A, Petzold CJ, Singan VR, et al (2015) Transgenic Expression of the Dicotyledonous Pattern Recognition Receptor EFR in Rice Leads to Ligand-Dependent Activation of Defense Responses. PLoS Pathog **11**: 1–34

Schwessinger B, Roux M, Kadota Y, Ntoukakis V, Sklenar J, Jones A, Zipfel C (2011) Phosphorylation-Dependent Differential Regulation of Plant Growth, Cell Death, and Innate Immunity by the Regulatory Receptor-Like Kinase BAK1. PLoS Genet **7**: e1002046

Segonzac C, Feike D, Gimenez-Ibanez S, Hann DR, Zipfel C, Rathjen JP (2011) Hierarchy and roles of pathogen-associated molecular pattern-induced responses in nicotiana benthamiana. Plant Physiol **156**: 687–699

Segonzac C, Macho AP, Sanmartin M, Ntoukakis V, Sanchez-Serrano JJ, Zipfel C (2014) Negative control of BAK1 by protein phosphatase 2A during plant innate immunity. EMBO J **33**: 2069–2079

Segonzac C, Monaghan J (2019) Modulation of plant innate immune signaling by small peptides. Curr Opin Plant Biol **51**: 22–28

Sels J, Mathys J, De Coninck BMA, Cammue BPA, De Bolle MFC (2008) Plant pathogenesis-

related (PR) proteins: A focus on PR peptides. Plant Physiol Biochem **46**: 941–950

Seo JS, Diloknawarit P, Park BS, Chua NH (2019) ELF18-INDUCED LONG NONCODING RNA 1 evicts fibrillarin from mediator subunit to enhance PATHOGENESIS-RELATED GENE 1 (PR1) expression. New Phytol **221**: 2067–2079

Seo JS, Sun H-X, Park BS, Huang C-H, Yeh S-D, Jung C, Chua N-H (2017) ELF18-INDUCED LONG-NONCODING RNA associates with mediator to enhance expression of innate immune response genes in Arabidopsis. Plant Cell **29**: 1024–1038

Serrano M, Kanehara K, Torres M, Yamada K, Tintor N, Kombrink E, Schulze-Lefert P, Saijo Y (2012) Repression of sucrose/ultraviolet B light-induced flavonoid accumulation in microbe-associated molecular pattern-triggered immunity in Arabidopsis. Plant Physiol **158**: 408–422

Seybold H, Trempel F, Ranf S, Scheel D, Romeis T, Lee J (2014) Ca2+ signalling in plant immune response: from pattern recognition receptors to Ca2+ decoding mechanisms. New Phytol **204**: 782–90

Shan L, He P, Li J, Heese A, Peck SC, Nürnberger T, Martin GB, Sheen J (2008) Bacterial Effectors Target the Common Signaling Partner BAK1 to Disrupt Multiple MAMP Receptor-Signaling Complexes and Impede Plant Immunity. Cell Host Microbe **4**: 17–27

Shang Y, Dai C, Lee MM, Kwak JM, Nam KH (2016) BRI1-Associated Receptor Kinase 1 Regulates Guard Cell ABA Signaling Mediated by Open Stomata 1 in Arabidopsis. Mol Plant **9**: 447–460

Shaul O (2015) Unique Aspects of Plant Nonsense-Mediated mRNA Decay. Trends Plant Sci **20**: 767–779

Shaw AS, Kornev AP, Hu J, Ahuja LG, Taylor SS (2014) Kinases and Pseudokinases: Lessons from RAF. Mol Cell Biol **34**: 1538–1546

Shi C, Baldwin IT, Wu J (2012) Arabidopsis Plants Having Defects in Nonsense-mediated mRNA Decay Factors UPF1, UPF2, and UPF3 Show Photoperiod-dependent Phenotypes in Development and Stress Responses. J Integr Plant Biol **54**: 99–114

Shi H, Bressan R (2006) RNA Extraction. Arab. Protoc. Humana Press, New Jersey, pp 345–348

Shi H, Shen Q, Qi Y, Yan H, Nie H, Chen Y, Zhao T, Katagiri F, Tang D (2013) BR-SIGNALING KINASE1 Physically Associates with FLAGELLIN SENSING2 and Regulates Plant Innate Immunity in Arabidopsis. Plant Cell **25**: 1143–1157

Shibuya N, Minami E (2001) Oligosaccharide signalling for defence responses in plant. Physiol Mol

Plant Pathol **59**: 223–233

Shimizu T, Nakano T, Takamizawa D, Desaki Y, Ishii-Minami N, Nishizawa Y, Minami E, Okada K, Yamane H, Kaku H, et al (2010) Two LysM receptor molecules, CEBiP and OsCERK1, cooperatively regulate chitin elicitor signaling in rice. Plant J **64**: 204–214

Shimono M, Higaki T, Kaku H, Shibuya N, Hasezawa S, Day B (2016) Quantitative evaluation of stomatal cytoskeletal patterns during the activation of immune signaling in arabidopsis thaliana. PLoS One **11**: 1–17

Shinya T, Motoyama N, Ikeda A, Wada M, Kamiya K, Hayafune M, Kaku H, Shibuya N (2012) Functional characterization of CEBiP and CERK1 homologs in arabidopsis and rice reveals the presence of different chitin receptor systems in plants. Plant Cell Physiol **53**: 1696–1706

Shinya T, Nakagawa T, Kaku H, Shibuya N (2015) Chitin-mediated plant–fungal interactions: catching, hiding and handshaking. Curr Opin Plant Biol **26**: 64–71

Shiu S-H, Bleecker AB (2001a) Plant Receptor-Like Kinase Gene Family: Diversity, Function, and Signaling. Sci Signal. doi: 10.1126/stke.2001.113.re22

Shiu S, Bleecker AB (2001b) Receptor-like kinases from Arabidopsis form a monophyletic gene family related to animal receptor kinases. Proc Natl Acad Sci **98**: 10763–10768

Shiu S, Bleecker AB (2003) Expansion of the Receptor-Like Kinase / Pelle Gene Family and Receptor-Like Proteins in Arabidopsis. Plant Physiol **132**: 530–543

Shiu S, Karlowski WM, Pan R, Tzeng Y-H, Mayer KFX, Li W-H (2004) Comparative Analysis of the Receptor-Like Kinase Family in Arabidopsis and Rice. Plant Cell **16**: 1220–1234

Siddique MI, Back S, Lee JH, Jo J, Jang S, Han K, Venkatesh J, Kwon JK, Jo YD, Kang BC (2020) Development and characterization of an ethyl methane sulfonate (Ems) induced mutant population in capsicum annuum l. Plants **9**: 1–16

Smakowska-Luzan E, Mott GA, Parys K, Stegmann M, Howton TC, Layeghifard M, Neuhold J, Lehner A, Kong J, Grünwald K, et al (2018) An extracellular network of Arabidopsis leucine-rich repeat receptor kinases. Nature **553**: 342–346

Smakowska E, Kong J, Busch W, Belkhadir Y (2016) Organ-specific regulation of growth-defense tradeoffs by plants. Curr Opin Plant Biol **29**: 129–137

Smith JM, Leslie ME, Robinson SJ, Korasick DA, Zhang T, Backues SK, Cornish P V., Koo AJ, Bednarek SY, Heese A (2014) Loss of Arabidopsis thaliana Dynamin-Related Protein 2B Reveals Separation of Innate Immune Signaling Pathways. PLoS Pathog. doi:

10.1371/journal.ppat.1004578

Smith KD, Andersen-Nissen E, Hayashi F, Strobe K, Bergman MA, Rassoulian Barrett SL, Cookson BT, Aderem A (2003) Toll-like receptor 5 recognizes a conserved site on flagellin required for protofilament formation and bacterial motility. Nat Immunol **4**: 1247–1253

Smith SE, Smith FA (2011) Roles of Arbuscular Mycorrhizas in Plant Nutrition and Growth: New Paradigms from Cellular to Ecosystem Scales. Annu Rev Plant Biol **62**: 227–250

Sonenberg N, Dever TE (2003) Eukaryotic translation initiation factors and regulators. Curr Opin Struct Biol **13**: 56–63

Sorenson R, Bailey-Serres J (2014) Selective mRNA sequestration by OLIGOURIDYLATE-BINDING PROTEIN 1 contributes to translational control during hypoxia in Arabidopsis. Proc Natl Acad Sci **111**: 2373–2378

Souza C de A, Li S, Lin AZ, Boutrot F, Grossmann G, Zipfel C, Somerville SC (2017) Cellulose-Derived Oligomers Act as Damage-Associated Molecular Patterns and Trigger Defense-Like Responses. Plant Physiol **173**: 2383–2398

Sprinzl M (1994) Elongation factor Tu: a regulatory GTPase with an integrated effector. Trends Biochem Sci **19**: 245–250

Sreekanta S, Bethke G, Hatsugai N, Tsuda K, Thao A, Wang L, Katagiri F, Glazebrook J (2015) The receptor-like cytoplasmic kinase PCRK1 contributes to pattern-triggered immunity against Pseudomonas syringae in Arabidopsis thaliana. New Phytol **207**: 78–90

Srivastava R, Liu JX, Guo H, Yin Y, Howell SH (2009) Regulation and processing of a plant peptide hormone, AtRALF23, in Arabidopsis. Plant J **59**: 930–939

Staal J, Kaliff M, Bohman S, Dixelius C (2006) Transgressive segregation reveals two Arabidopsis TIR-NB-LRR resistance genes effective against Leptosphaeria maculans, causal agent of blackleg disease. Plant J **46**: 218–230

Staiger D, Korneli C, Lummer M, Navarro L (2013) Emerging role for RNA-based regulation in plant immunity. New Phytol **197**: 394–404

Steffens A, Bräutigam A, Jakoby M, Hülskamp M (2015) The beach domain protein spirrig is essential for arabidopsis salt stress tolerance and functions as a regulator of transcript stabilization and localization. PLoS Biol **13**: 1–31

Steffens A, Jaegle B, Tresch A, Hülskamp M, Jakoby M (2014) Processing-body movement in arabidopsis depends on an interaction between myosins and decapping protein1. Plant Physiol

164: 1879–1892

Stegmann M, Anderson RG, Ichimura K, Pecenkova T, Reuter P, Žárský V, McDowell JM, Shirasu K, Trujillo M (2012) The ubiquitin ligase PUB22 targets a subunit of the exocyst complex required for PAMP-triggered responses in arabidopsis c w. Plant Cell **24**: 4703–4716

Stegmann M, Monaghan J, Smakowska-Luzan E, Rovenich H, Lehner A, Holton N, Belkhadir Y, Zipfel C (2017) The receptor kinase FER is a RALF-regulated scaffold controlling plant immune signaling. Science (80-) **355**: 287–289

Stewart M (2019) Polyadenylation and nuclear export of mRNAs. J Biol Chem **294**: 2977–2987

Stotz HU, Jikumaru Y, Shimada Y, Sasaki E, Stingl N, Mueller MJ, Kamiya Y (2011) Jasmonate-dependent and COI1-independent defense responses against sclerotinia sclerotiorum in arabidopsis thaliana: Auxin is part of COI1-independent defense signaling. Plant Cell Physiol **52**: 1941–1956

Stuart JM, Segal E, Koller D, Kim SK (2003) A Gene-Coexpression Network for Global Discovery of Conserved Genetic Modules. Science (80-) **302**: 249–255

Su SH, Bush SM, Zaman N, Stecker K, Sussman MR, Krysan P (2013) Deletion of a tandem gene family in Arabidopsis: Increased MEKK2 abundance triggers autoimmunity when the MEKK1-MKK1/2-MPK4 signaling cascade is disrupted. Plant Cell **25**: 1895–1910

Sun H, Qiao Z, Chua KP, Tursic A, Liu X, Gao YG, Mu Y, Hou X, Miao Y (2018) Profilin Negatively Regulates Formin-Mediated Actin Assembly to Modulate PAMP-Triggered Plant Immunity. Curr Biol **28**: 1882-1895.e7

Sun J, Cardoza V, Mitchell DM, Bright L, Oldroyd GED, Harris JM, Biology S, Centre JI, Biochemistry A (2006) Crosstalk between jasmonic acid, ethylene and Nod factor signaling allows integration of diverse inputs for regulation of nodulation. Plant J **46**: 961–970

Sun T, Zhang Y, Li Y, Zhang Q, Ding Y, Zhang Y (2015) ChIP-seq reveals broad roles of SARD1 and CBP60g in regulating plant immunity. Nat Commun **6**: 10159

Sun Y, Li L, Macho AP, Han Z, Hu Z, Zipfel C, Zhou J-M, Chai J (2013) Structural basis for flg22-induced activation of the Arabidopsis FLS2-BAK1 immune complex. Science (80-) **342**: 624–8

Suzuki M, Shibuya M, Shimada H, Motoyama N, Nakashima M, Takahashi S, Suto K, Yoshida I, Matsui S, Tsujimoto N, et al (2016) Autophosphorylation of specific threonine and tyrosine residues in arabidopsis CERK1 is essential for the activation of chitin-induced immune signaling.

Plant Cell Physiol **57**: 2312–2322

Szádeczky-Kardoss I, Gál L, Auber A, Taller J, Silhavy D (2018) The No-go decay system degrades plant mRNAs that contain a long A-stretch in the coding region. Plant Sci **275**: 19–27

Szklarczyk D, Gable AL, Lyon D, Junge A, Wyder S, Huerta-Cepas J, Simonovic M, Doncheva NT, Morris JH, Bork P, et al (2019) STRING v11: Protein-protein association networks with increased coverage, supporting functional discovery in genome-wide experimental datasets. Nucleic Acids Res **47**: D607–D613

Tabassum N, Eschen-Lippold L, Athmer B, Baruah M, Brode M, Maldonado-Bonilla LD, Hoehenwarter W, Hause G, Scheel D, Lee J (2019) Phosphorylation-dependent control of an RNA granule-localized protein that fine-tunes defence gene expression at a post-transcriptional level. Plant J 1–17

Taguchi F, Shimizu R, Nakajima R, Toyoda K, Shiraishi T, Ichinose Y (2003) Differential effects of flagellins from Pseudomonas syringae pv. tabaci, tomato and glycinea on plant defense response. Plant Physiol Biochem **41**: 165–174

Takken FLW, Goverse A (2012) How to build a pathogen detector: Structural basis of NB-LRR function. Curr Opin Plant Biol **15**: 375–384

Tamborski J, Krasileva K V. (2020) Evolution of Plant NLRs: From Natural History to Precise Modifications. Annu Rev Plant Biol **71**: 1–24

Tang D, Wang G, Zhou J-M (2017) Receptor Kinases in Plant-Pathogen Interactions: More Than Pattern Recognition. Plant Cell **29**: 618–637

Tang J, Han Z, Sun Y, Zhang H, Gong X, Chai J (2015) Structural basis for recognition of an endogenous peptide by the plant receptor kinase PEPR1. Cell Res **25**: 110–120

Tateda C, Zhang Z, Shrestha J, Jelenska J, Chinchilla D, Greenberg JT (2014) Salicylic acid regulates Arabidopsis microbial pattern receptor kinase levels and signaling. Plant Cell **26**: 4171–4187

Testerink C, Munnik T (2011) Molecular, cellular, and physiological responses to phosphatidic acid formation in plants. J Exp Bot **62**: 2349–2361

Thomma BPHJ, Nelissen I, Eggermont K, Broekaert WF (1999) Deficiency in phytoalexin production causes enhanced susceptibility of Arabidopsis thaliana to the fungus Alternaria brassicicola. Plant J **19**: 163–171

Thompson JN, Burdon JJ (1992) Gene-for-gene coevolution between plants and parasites. Nature

360: 121–125

Thor K, Jiang S, Michard E, George J, Scherzer S, Huang S, Dindas J, Derbyshire P, Leitão N, DeFalco TA, et al (2020) The calcium-permeable channel OSCA1.3 regulates plant stomatal immunity. Nature **585**: 569–573

Thynne E, Saur IML, Simbaqueba J, Ogilvie HA, Gonzalez-Cendales Y, Mead O, Taranto A, Catanzariti AM, McDonald MC, Schwessinger B, et al (2017) Fungal phytopathogens encode functional homologues of plant rapid alkalinization factor (RALF) peptides. Mol Plant Pathol **18**: 811–824

Tian W, Hou C, Ren Z, Wang C, Zhao F, Dahlbeck D, Hu S, Zhang L, Niu Q, Li L, et al (2019) A calmodulin-gated calcium channel links pathogen patterns to plant immunity. Nature. doi: 10.1038/s41586-019-1413-y

Tiku AR (2020) Antimicrobial Compounds (Phytoanticipins and Phytoalexins) and Their Role in Plant Defense. Co-Evolution Second. Metab. pp 845–868

Tilsner J, Nicolas W, Rosado A, Bayer EM (2016) Staying Tight: Plasmodesmal Membrane Contact Sites and the Control of Cell-to-Cell Connectivity in Plants. Annu Rev Plant Biol **67**: 337–364

Tintor N, Ross A, Kanehara K, Yamada K, Fan L, Kemmerling B, Nurnberger T, Tsuda K, Saijo Y (2013) Layered pattern receptor signaling via ethylene and endogenous elicitor peptides during Arabidopsis immunity to bacterial infection. Proc Natl Acad Sci **110**: 6211–6216

Tintor N, Saijo Y (2014) ER-mediated control for abundance, quality, and signaling of transmembrane immune receptors in plants. Front Plant Sci **5**: 2008–2013

Toribio R, Muñoz A, Castro-Sanz AB, Merchante C, Castellano MM (2019) A novel eIF4E-interacting protein that forms non-canonical translation initiation complexes. Nat Plants **5**: 1283–1296

Torres MA, Dangl JL, Jones JDG (2002) Arabidopsis gp91phox homologues AtrbohD and AtrbohF are required for accumulation of reactive oxygen intermediates in the plant defense response. Proc Natl Acad Sci **99**: 517–522

Torres MA, Jones JDG, Dangl JL (2006) Reactive oxygen species signaling in response to pathogens. Plant Physiol **141**: 373–378

Tritschler F, Braun JE, Eulalio A, Truffault V, Izaurralde E, Weichenrieder O (2009) Structural Basis for the Mutually Exclusive Anchoring of P Body Components EDC3 and Tral to the DEAD Box Protein DDX6/Me31B. Mol Cell **33**: 661–668

Truchet G, Roche P, Lerouge P, Vasse J, Camut S, De Billy F, Promé JC, Dénarié J (1991) Sulphated lipo-oligosaccharide signals of Rhizobium meliloti elicit root nodule organogenesis in alfalfa. Nature **351**: 670–673

Trujillo M, Ichimura K, Casais C, Shirasu K (2008) Negative Regulation of PAMP-Triggered Immunity by an E3 Ubiquitin Ligase Triplet in Arabidopsis. Curr Biol **18**: 1396–1401

Tsuda K, Sato M, Glazebrook J, Cohen JD, Katagiri F (2008) Interplay between MAMP-triggered and SA-mediated defense responses. Plant J **53**: 763–775

Tsuda K, Sato M, Stoddard T, Glazebrook J, Katagiri F (2009) Network properties of robust immunity in plants. PLoS Genet. doi: 10.1371/journal.pgen.1000772

Tsuda K, Somssich IE (2015) Transcriptional networks in plant immunity. New Phytol **206**: 932–947

Tsuji J, Jackson EP, Gage DA, Hammerschmidt R, Somerville SC (1992) Phytoalexin accumulation in arabidopsis thaliana during the hypersensitive reaction to Pseudomonas syringae pv syringae. Plant Physiol **98**: 1304–1309

Udvardi M, Poole PS (2013) Transport and Metabolism in Legume-Rhizobia Symbioses. Annu Rev Plant Biol **64**: 781–805

Underwood W, Melotto M, He SY (2007) Role of plant stomata in bacterial invasion. Cell Microbiol **9**: 1621–1629

Urquidi Camacho RA, Lokdarshi A, Arnim AG (2020) Translational gene regulation in plants: A green new deal. WIREs RNA 1–40

USADEL B, OBAYASHI T, MUTWIL M, GIORGI FM, BASSEL GW, TANIMOTO M, CHOW A, STEINHAUSER D, PERSSON S, PROVART NJ (2009) Co-expression tools for plant biology: opportunities for hypothesis generation and caveats. Plant Cell Environ **32**: 1633–1651

VanEtten HD, Mansfield JW, Bailey JA, Farmer EE (1994) Two Classes of Plant Antibiotics: Phytoalexins versus “Phytoanticipins.” Plant Cell 1191–1192

Vindry C, Weil D, Standart N (2019) Pat1 RNA-binding proteins: Multitasking shuttling proteins. Wiley Interdiscip Rev RNA **10**: 1–17

Walley JW, Kelley DR, Savchenko T, Dehesh K (2010) Investigating the function of CAF1 deadenylases during plant stress responses. Plant Signal Behav **5**: 802–805

Wan J, Tanaka K, Zhang X, Son GH, Brechenmacher L, Nguyen THN, Stacey G (2012) LYK4, a Lysin Motif Receptor-Like Kinase, Is Important for Chitin Signaling and Plant Innate Immunity

in Arabidopsis. Plant Physiol **160**: 396–406

Wan J, Zhang X-C, Neece D, Ramonell KM, Clough S, Kim S, Stacey MG, Stacey G (2008) A LysM Receptor-Like Kinase Plays a Critical Role in Chitin Signaling and Fungal Resistance in Arabidopsis. Plant Cell **20**: 471–481

Wan L, Essuman K, Anderson RG, Sasaki Y, Monteiro F, Chung EH, Nishimura EO, DiAntonio A, Milbrandt J, Dangl JL, et al (2019a) TIR domains of plant immune receptors are NAD+-cleaving enzymes that promote cell death. Science (80-) **365**: 799–803

Wan W, Zhang L, Pruitt R, Zaidem M, Brugman R, Ma X, Krol E, Perraki A, Kilian J, Grossmann G, et al (2019b) Comparing Arabidopsis receptor kinase and receptor protein-mediated immune signaling reveals BIK1-dependent differences. New Phytol **221**: 2080–2095

Wang C, Huang X, Li Q, Zhang Y, Li JL, Mou Z (2019a) Extracellular pyridine nucleotides trigger plant systemic immunity through a lectin receptor kinase/BAK1 complex. Nat Commun. doi: 10.1038/s41467-019-12781-7

Wang C, Liu R, Lim GH, De Lorenzo L, Yu K, Zhang K, Hunt AG, Kachroo A, Kachroo P (2018a) Pipecolic acid confers systemic immunity by regulating free radicals. Sci Adv **4**: 1–12

Wang C, Zhou M, Zhang X, Yao J, Zhang Y, Mou Z (2017) A lectin receptor kinase as a potential sensor for extracellular nicotinamide adenine dinucleotide in arabidopsis thaliana. Elife **6**: 1–23

Wang G, Ellendorff U, Kemp B, Mansfield JW, Forsyth A, Mitchell K, Bastas K, Liu CM, Woods-Tör A, Zipfel C, et al (2008a) A genome-wide functional investigation into the roles of receptor-like proteins in arabidopsis. Plant Physiol **147**: 503–517

Wang J, Hu M, Wang J, Qi J, Han Z, Wang G, Qi Y, Wang H-W, Zhou J-M, Chai J (2019b) Reconstitution and structure of a plant NLR resistosome conferring immunity. Science (80-) **364**: eaav5870

Wang J, Wang J, Hu M, Wu S, Qi J, Wang G, Han Z, Qi Y, Gao N, Wang H-W, et al (2019c) Ligand-triggered allosteric ADP release primes a plant NLR complex. Science (80-) **364**: eaav5868

Wang JJ, Grubb LE, Wang JJ, Liang X, Li LL, Gao C, Ma M, Feng F, Li M, Li LL, et al (2018b) A Regulatory Module Controlling Homeostasis of a Plant Immune Kinase. Mol Cell **69**: 493-504.e6

Wang L, Einig E, Almeida-Trapp M, Albert M, Fliegmann J, Mithöfer A, Kalbacher H, Felix G (2018c) The systemin receptor SYR1 enhances resistance of tomato against herbivorous insects.

Nat Plants **4**: 152–156

Wang L, Tsuda K, Truman W, Sato M, Nguyen L V., Katagiri F, Glazebrook J (2011) CBP60g and SARD1 play partially redundant critical roles in salicylic acid signaling. Plant J **67**: 1029–1041

Wang P, Hsu C-C, Du Y, Zhu P, Zhao C, Fu X, Zhang C, Paez JS, Macho AP, Tao WA, et al (2020a) Mapping proteome-wide targets of protein kinases in plant stress responses. Proc Natl Acad Sci **117**: 3270–3280

Wang R, He F, Ning Y, Wang G (2020b) Fine-Tuning of RBOH-Mediated ROS Signaling in Plant Immunity. Trends Plant Sci. doi: 10.1016/j.tplants.2020.08.001

Wang X, Kota U, He K, Blackburn K, Li J, Goshe MB, Huber SC, Clouse SD (2008b) Sequential Transphosphorylation of the BRI1/BAK1 Receptor Kinase Complex Impacts Early Events in Brassinosteroid Signaling. Dev Cell **15**: 220–235

Wang X, Sager R, Cui W, Zhang C, Lu H, Lee J-Y (2013) Salicylic Acid Regulates Plasmodesmata Closure during Innate Immune Responses in Arabidopsis. Plant Cell **25**: 2315–2329

Wang Y, Li Z, Liu D, Xu J, Wei X, Yan L, Yang C, Lou Z, Shui W (2014) Assessment of BAK1 activity in different plant receptor-like kinase complexes by quantitative profiling of phosphorylation patterns. J Proteomics **108**: 484–493

Wang Y, Tyler BM, Wang Y (2019d) Defense and Counterdefense During Plant-Pathogenic Oomycete Infection. Annu Rev Microbiol **73**: 667–696

Wang YH, Wang YH (2008) How effective is T-DNA insertional mutagenesis in Arabidopsis? J Biochem Technol **1**: 11–20

Weber C, Nover L, Fauth M (2008) Plant stress granules and mRNA processing bodies are distinct from heat stress granules. Plant J **56**: 517–530

Wells SE, Hillner PE, Vale RD, Sachs AB (1998) Circularization of mRNA by eukaryotic translation initiation factors. Mol Cell **2**: 135–140

Wiermer M, Feys BJ, Parker JE (2005) Plant immunity: The EDS1 regulatory node. Curr Opin Plant Biol **8**: 383–389

Wilhelm JE, Hilton M, Amos Q, Henzel WJ (2003) Cup is an eIF4E binding protein required for both the translational repression of oskar and the recruitment of Barentsz. J Cell Biol **163**: 1197–1204

Willmann R, Lajunen HM, Erbs G, Newman M, Kolb D, Tsuda K (2011) Mediate Bacterial Peptidoglycan Sensing and Immunity To Bacterial Infection. Proc Natl Acad Sci **108**: 19824–19829

Win J, Chaparro-Garcia A, Belhaj K, Saunders DGO, Yoshida K, Dong S, Schornack S, Zipfel C, Robatzek S, Hogenhout SA, et al (2012) Effector biology of plant-associated organisms: Concepts and perspectives. Cold Spring Harb Symp Quant Biol **77**: 235–247

Woloshen V, Huang S, Li X (2011) RNA-Binding Proteins in Plant Immunity. J Pathog **2011**: 1–11

Wu C-H, Abd-El-Haliem A, Bozkurt TO, Belhaj K, Terauchi R, Vossen JH, Kamoun S (2017a) NLR network mediates immunity to diverse plant pathogens. Proc Natl Acad Sci **114**: 8113–8118

Wu F, Chi Y, Jiang Z, Xu Y, Xie L, Huang F, Wan D, Ni J, Yuan F, Wu X, et al (2020) Hydrogen peroxide sensor HPCA1 is an LRR receptor kinase in Arabidopsis. Nature **578**: 577–581

Wu G, Park MY, Conway SR, Wang JW, Weigel D, Poethig RS (2009) The Sequential Action of miR156 and miR172 Regulates Developmental Timing in Arabidopsis. Cell **138**: 750–759

Wu Z, Huang S, Zhang X, Wu D, Xia S, Li X (2017b) Regulation of plant immune receptor accumulation through translational repression by a glycine-tyrosine-phenylalanine (GYF) domain protein. Elife. doi: 10.7554/eLife.23684

Xiang T, Zong N, Zou Y, Wu Y, Zhang J, Xing W, Li Y, Tang X, Zhu L, Chai J, et al (2008) Pseudomonas syringae Effector AvrPto Blocks Innate Immunity by Targeting Receptor Kinases. Curr Biol **18**: 74–80

Xiao Y, Stegmann M, Han Z, DeFalco TA, Parys K, Xu L, Belkhadir Y, Zipfel C, Chai J (2019) Mechanisms of RALF peptide perception by a heterotypic receptor complex. Nature **572**: 270–274

Xing S, Wallmeroth N, Berendzen KW, Grefen C (2016) Techniques for the analysis of protein-protein interactions in vivo. Plant Physiol **171**: pp.00470.2016

Xu B, Cheval C, Laohavisit A, Hocking B, Chiasson D, Olsson TSG, Shirasu K, Faulkner C, Gilliham M (2017a) A calmodulin-like protein regulates plasmodesmal closure during bacterial immune responses. New Phytol **215**: 77–84

Xu G, Greene GH, Yoo H, Liu L, Marqués J, Motley J, Dong X (2017b) Global translational reprogramming is a fundamental layer of immune regulation in plants. Nature **545**: 487–490

Xu J, Chua N-H (2009) Arabidopsis Decapping 5 Is Required for mRNA Decapping, P-Body Formation, and Translational Repression during Postembryonic Development. Plant Cell **21**:

3270–3279

Xu J, Yang J-Y, Niu Q-W, Chua N-H (2006) Arabidopsis DCP2, DCP1, and VARICOSE Form a Decapping Complex Required for Postembryonic Development. Plant Cell **18**: 3386–3398

Xu XM, Meier I (2008) The nuclear pore comes to the fore. Trends Plant Sci **13**: 20–27

Yamada K, Yamaguchi K, Shirakawa T, Nakagami H, Mine A, Ishikawa K, Fujiwara M, Narusaka M, Narusaka Y, Ichimura K, et al (2016a) The Arabidopsis CERK 1 -associated kinase PBL 27 connects chitin perception to MAPK activation. Embo J **35**: 1–16

Yamada K, Yamashita-yamada M, Hirase T, Fujiwara T, Tsuda K, Hiruma K, Saijo Y (2016b) Danger peptide receptor signaling in plants ensures basal immunity upon pathogen-induced depletion of BAK1. EMBO J **35**: 46–61

Yamaguchi K, Yamada K, Ishikawa K, Yoshimura S, Hayashi N, Uchihashi K, Ishihama N, Kishi-Kaboshi M, Takahashi A, Tsuge S, et al (2013) A Receptor-like Cytoplasmic Kinase Targeted by a Plant Pathogen Effector Is Directly Phosphorylated by the Chitin Receptor and Mediates Rice Immunity. Cell Host Microbe **13**: 347–357

Yamaguchi T, Minami E, Shibuya N (2003) Activation of phospholipases by N-acetylchitooligosaccharide elicitor in suspension-cultured rice cells mediates reactive oxygen generation. Physiol Plant **118**: 361–370

Yamaguchi Y, Huffaker A (2011) Endogenous peptide elicitors in higher plants. Curr Opin Plant Biol **14**: 351–357

Yamaguchi Y, Huffaker A, Bryan AC, Tax FE, Ryan CA (2010) PEPR2 Is a Second Receptor for the Pep1 and Pep2 Peptides and Contributes to Defense Responses in Arabidopsis. Plant Cell **22**: 508–522

Yamaguchi Y, Pearce G, Ryan CA (2006) The cell surface leucine-rich repeat receptor for AtPep1, an endogenous peptide elicitor in Arabidopsis, is functional in transgenic tobacco cells. Proc Natl Acad Sci **103**: 10104–10109

Yan C, Yan Z, Wang Y, Yan X, Han Y (2014) Tudor-SN, a component of stress granules, regulates growth under salt stress by modulating GA20ox3 mRNA levels in Arabidopsis. J Exp Bot **65**: 5933–5944

Yan H, Zhao Y, Shi H, Li J, Wang Y, Tang D (2018) BRASSINOSTEROID-SIGNALING kinase1 phosphorylates MAPKKK5 to regulate immunity in arabidopsis. Plant Physiol **176**: 2991–3002

Yang H, Matsubayashi Y, Nakamura K, Sakagami Y (2001) Diversity of Arabidopsis genes

encoding precursors for phytosulfokine, a peptide growth factor. Plant Physiol **127**: 842–851

Yang H, Matsubayashi Y, Nakamura K, Sakagami Y (1999) Oryza sativa PSK gene encodes a precursor of phytosulfokine-alpha , a sulfated peptide growth factor found in plants. Proc Natl Acad Sci **96**: 13560–13565

Yang S, Tang F, Zhu H (2014) Alternative splicing in plant immunity. Int J Mol Sci **15**: 10424–10445

Yang Y, Liu J, Yin C, de Souza Vespoli L, Ge D, Huang Y, Feng B, Xu G, de Manhães AMEA, Dou S, et al (2020) RNA interference-based screen reveals concerted functions of MEKK2 and CrCK3 in plant cell death regulation. Plant Physiol **183**: 331–344

Yasuda S, Okada K, Saijo Y (2017) A look at plant immunity through the window of the multitasking coreceptor BAK1. Curr Opin Plant Biol **38**: 10–18

Yeh Y-H, Panzeri D, Kadota Y, Huang Y-C, Huang P-Y, Tao C-N, Roux M, Chien H-C, Chin T-C, Chu P-W, et al (2016) The Arabidopsis Malectin-Like/LRR-RLK IOS1 is Critical for BAK1-Dependent and BAK1-Independent Pattern-Triggered Immunity. Plant Cell **28**: tpc.00313.2016

Yi SY, Shirasu K, Moon JS, Lee SG, Kwon SY (2014) The activated SA and JA signaling pathways have an influence on flg22-triggered oxidative burst and callose deposition. PLoS One. doi: 10.1371/journal.pone.0088951

Yip Delormel T, Boudsocq M (2019) Properties and functions of calcium-dependent protein kinases and their relatives in *Arabidopsis thaliana*. New Phytol nph.16088

Yoo H, Greene GH, Yuan M, Xu G, Burton D, Liu L, Marqués J, Dong X (2020) Translational Regulation of Metabolic Dynamics during Effector-Triggered Immunity. Mol Plant **13**: 88–98

Yoshii M, Nishikiori M, Tomita K, Yoshioka N, Kozuka R, Naito S, Ishikawa M (2004) The Arabidopsis Cucumovirus Multiplication 1 and 2 Loci Encode Translation Initiation Factors 4E and 4G. J Virol **78**: 6102–6111

Yoshii M, Yoshioka N, Ishikawa M, Naito S (1998) Isolation of an Arabidopsis thaliana mutant in which accumulation of cucumber mosaic virus coat protein is delayed. Plant J **13**: 211–219

Yu X, Li B, Jang G-JJ, Jiang S, Jiang D, Jang JC, Wu SH, Shan L, He P (2019a) Orchestration of Processing Body Dynamics and mRNA Decay in Arabidopsis Immunity. Cell Rep **28**: 2194-2205.e6

Yu X, Xu G, Li B, de Souza Vespoli L, Liu H, Moeder W, Chen S, de Oliveira MVV, Ariádina de Souza S, Shao W, et al (2019b) The Receptor Kinases BAK1/SERK4 Regulate Ca2+ Channel-Mediated Cellular Homeostasis for Cell Death Containment. Curr Biol **29**: 3778-3790.e8

Yuan AM, Jiang Z, Bi G, Liu M, He SY (2020) Pattern-recognition receptors are required for NLR-mediated plant immunity. bioRxiv

Zander M, Lewsey MG, Clark NM, Yin L, Bartlett A, Saldierna Guzmán JP, Hann E, Langford AE, Jow B, Wise A, et al (2020) Integrated multi-omics framework of the plant response to jasmonic acid. Nat Plants **6**: 290–302

Zanetti ME, Rípodas C, Niebel A (2017) Plant NF-Y transcription factors: Key players in plant-microbe interactions, root development and adaptation to stress. Biochim Biophys Acta - Gene Regul Mech **1860**: 645–654

Zeidler D, Zahringer U, Gerber I, Dubery I, Hartung T, Bors W, Hutzler P, Durner J (2004) From The Cover: Innate immunity in Arabidopsis thaliana: Lipopolysaccharides activate nitric oxide synthase (NOS) and induce defense genes. Proc Natl Acad Sci **101**: 15811–15816

Zeqiraj E, van Aalten DMF (2010) Pseudokinases-remnants of evolution or key allosteric regulators? Curr Opin Struct Biol **20**: 772–781

Zhang H, Hu Z, Lei C, Zheng C, Wang J, Shao S, Li X, Xia X, Cai X, Zhou J, et al (2018a) A plant phytosulfokine peptide initiates auxin-dependent immunity through cytosolic Ca2+ signaling in tomato. Plant Cell **30**: 652–667

Zhang J, Li W, Xiang T, Liu Z, Laluk K, Ding X, Zou Y, Gao M, Zhang X, Chen S, et al (2010a) Receptor-like Cytoplasmic Kinases Integrate Signaling from Multiple Plant Immune Receptors and Are Targeted by a Pseudomonas syringae Effector. Cell Host Microbe **7**: 290–301

Zhang M, Chiang Y-H, Toruño TY, Lee D, Ma M, Liang X, Lal NK, Lemos M, Lu Y-J, Ma S, et al (2018b) The MAP4 Kinase SIK1 Ensures Robust Extracellular ROS Burst and Antibacterial Immunity in Plants. Cell Host Microbe **24**: 379-391.e5

Zhang N, Pombo MA, Rosli HG, Martin GB (2020) Tomato wall-associated kinase SlWak1 acts in an Fls2- and Fls3-dependent manner to promote apoplastic immune responses to Pseudomonas syringae. bioRxiv

Zhang W, He SY, Assmann SM (2008) The plant innate immunity response in stomatal guard cells invokes G-protein-dependent ion channel regulation. Plant J **56**: 984–996

Zhang X, Mou Z (2009) Extracellular pyridine nucleotides induce PR gene expression and disease resistance in Arabidopsis. Plant J **57**: 302–312

Zhang XC, Gassmann W (2007) Alternative splicing and mRNA levels of the disease resistance gene RPS4 are induced during defense responses. Plant Physiol **145**: 1577–1587

Zhang XN, Shi Y, Powers JJ, Gowda NB, Zhang C, Ibrahim HMM, Ball HB, Chen SL, Lu H, Mount SM (2017a) Transcriptome analyses reveal SR45 to be a neutral splicing regulator and a suppressor of innate immunity in Arabidopsis thaliana. BMC Genomics **18**: 1–17

Zhang XS, Choi JH, Heinz J, Chetty CS (2006) Domain-specific positive selection contributes to the evolution of arabidopsis leucine-rich repeat receptor-like kinase (LRR RLK) genes. J Mol Evol **63**: 612–621

Zhang Y, Xu S, Ding P, Wang D, Cheng YT, He J, Gao M, Xu F, Li Y, Zhu Z, et al (2010b) Control of salicylic acid synthesis and systemic acquired resistance by two members of a plant-specific family of transcription factors. Proc Natl Acad Sci **107**: 18220–18225

Zhang Z, Liu Y, Ding P, Li Y, Kong Q, Zhang Y (2014) Splicing of receptor-like kinase-encoding SNC4 and CERK1 is regulated by two conserved splicing factors that are required for plant immunity. Mol Plant **7**: 1766–1775

Zhang Z, Liu Y, Huang H, Gao M, Wu D, Kong Q, Zhang Y (2017b) The NLR protein SUMM 2 senses the disruption of an immune signaling MAP kinase cascade via CRCK 3 . EMBO Rep **18**: 292–302

Zhang Z, Wu Y, Gao M, Zhang J, Kong Q, Liu Y, Ba H, Zhou J-M, Zhang Y (2012) Disruption of PAMP-Induced MAP Kinase Cascade by a Pseudomonas syringae Effector Activates Plant Immunity Mediated by the NB-LRR Protein SUMM2. Cell Host Microbe **11**: 253–263

Zheng X, McLellan H, Fraiture M, Liu X, Boevink PC, Gilroy EM, Chen Y, Kandel K, Sessa G, Birch PRJ, et al (2014) Functionally Redundant RXLR Effectors from Phytophthora infestans Act at Different Steps to Suppress Early flg22-Triggered Immunity. PLoS Pathog **10**: e1004057

Zheng X, Wagener N, McLellan H, Boevink PC, Hua C, Birch PRJ, Brunner F (2018) Phytophthora infestans RXLR effector SFI5 requires association with calmodulin for PTI/MTI suppressing activity. New Phytol **219**: 1433–1446

Zhu S, Estévez JM, Liao H, Zhu Y, Yang T, Li C, Wang Y, Li L, Liu X, Pacheco JM, et al (2020) The RALF1–FERONIA Complex Phosphorylates eIF4E1 to Promote Protein Synthesis and Polar Root Hair Growth. Mol Plant 1–19

Zhu X, Dunand C, Snedden W, Galaud JP (2015) CaM and CML emergence in the green lineage. Trends Plant Sci **20**: 483–489

Zipfel C, Kunze G, Chinchilla D, Caniard A, Jones JDG, Boller T, Felix G (2006) Perception of the Bacterial PAMP EF-Tu by the Receptor EFR Restricts Agrobacterium-Mediated

Transformation. Cell **125**: 749–760

Zipfel C, Oldroyd GED (2017) Plant signalling in symbiosis and immunity. Nature **543**: 328–336

Zipfel C, Robatzek S, Navarro L, Oakeley EJ, Jones JDG, Felix G, Boller T (2004) Bacterial disease resistance in Arabidopsis through flagellin perception. Nature **428**: 764–767

Zou Y, Wang S, Zhou Y, Bai J, Huang G, Liu X, Zhang Y, Tang D, Lu D (2018) Transcriptional Regulation of the Immune Receptor FLS2 Controls the Ontogeny of Plant Innate Immunity. Plant Cell **30**: 2779–2794

Zuber H, Scheer H, Ferrier E, Sement FM, Mercier P, Stupfler B, Gagliardi D (2016) Uridylation and PABP Cooperate to Repair mRNA Deadenylated Ends in Arabidopsis. Cell Rep **14**: 2707–2717